Assessing the Effects of Radiotherapy on Head and Neck Squamous Cell Carcinoma using Microfluidic Techniques

Simon David Carr

BSc (Hons) MBChB MRCS DOHNS

Submitted for MD by Thesis

At the University of Hull and the University of York

Hull York Medical School

September 2013

Abstract

Objective

The aim of this study was to investigate how HNSCC tissue biopsies maintained in a pseudo *in vivo* environment within a bespoke microfluidic device, respond to radiation treatment.

Materials and Methods

35 patients with HNSCC were recruited; in addition liver tissue from 5 Wistar rats was used. A glass microfluidic device was used to maintain the tissue biopsy samples in a viable state. Rat liver was used to optimise the methodology. HNSCC was obtained from patients with T1-T3 laryngeal or oropharyngeal SCC; N1-N2 metastatic cervical lymph nodes were also obtained. Irradiation consisted of single doses of between 2 Gy and 40 Gy and a fractionated course of 5x2 Gy. Cell death was assessed in the tissue effluent using the soluble markers LDH and cytochrome c, and in the tissue by immunohistochemical detection of cleaved cytokeratin18 (M30 antibody). Radiation-induced DNA strand breaks were detected using the TUNEL assay.

Results

A significant surge in LDH release was demonstrated in the rat liver after a single dose of 20 Gy; in HNSCC it was seen after 40 Gy, compared to the control. There was no significant difference in cytochrome c release after 5 Gy or 10 Gy. M30 demonstrated a dose-dependent increase in apoptotic index for a given increase in single dose radiation. There was a significant increase in apoptotic index between the non-irradiated HNSCC tissue and irradiated tissue and between the tissue irradiated with 1x2 Gy and 5x2 Gy. As with the apoptotic index, there was a significant increase in radiation-induced DNA breaks between the non-irradiated and the irradiated tissue and between the tissue irradiated with 1x2 Gy and 5x2 Gy.

Conclusion

This microfluidic technique can be used to study the effects of radiation on HNSCC tissue. The device was capable of maintaining the HNSCC in a viable state, without it undergoing significant apoptosis or DNA damage and can be used to demonstrate the relationship between radiotherapy dose and radiation-induced cell death using tissue-based cell death markers.

This study is a significant step towards achieving the ultimate goal of developing this device as a tool, capable of predicting a patient's response to radiotherapy prior to the commencement of treatment.

Contents

Chapter 1 – Introduction

Tables

Figures

Glossary

ADH	Alcohol dehydrogenase
ALDH	Aldehyde dehydrogenase
APAF1	Apoptotic protease activating factor
ATM	Ataxia-mutated telangiectasia
ATR	Ataxia-telangiectasia and rad3-related
BAX	B-cell lymphoma associated X-protein
BCL	B-cell lymphoma
BID	BH3-interacting domain
CDK	Cyclin-dependent kinase
CSC	Cancer stem cell
DNA-PK	DNA-dependent protein kinase
EGFR	Epidermal growth factor receptor
FADD	Fas-associated protein with death domain
FHIT	Fragile histidine triad gene
HIF	Hypoxia inducible factor
HRR	Homologous recombination repair
HNSCC	Head and neck squamous cell carcinoma
LDH	Lactate dehydrogenase
MMP	Matrix metalloproteinase
MOMP	Mitochondrial outer membrane permeabilisation
MRN	Mre11 Rad50 Nbs1
NHEJ	Non-homologous end-joining
OPSCC	Oropharyngeal squamous cell carcinoma
PARP1	Poly (ADP-ribose) polymerase 1

P53	Tumour protein 53
PIDD	p53 inducible death domain
PPIB	Cyclophilin B
Rb	Retinoblastoma gene
TUNEL	Terminal deoxynucleotidyl transferase dUTP nick end labelling
UICC	Union International Cancer Control
XRCC	X-ray repair cross-complementary protein

Acknowledgements

The author would like to thank Prof. J. Greenman and Prof. N. Stafford for their excellent supervision. Dr. V. Green for her expertise and assistance in the laboratory. Mr. J. Jose, Consultant Head and Neck Surgeon and the rest of the surgical team at Castle Hill Hospital, Hull for providing us with the tissue samples. Prof. A Beavis, Consultant Medical Physicist and Head of Radiation Physics for the Hull and East Yorkshire Hospitals NHS Trust, and Dr. G. Liney, Senior Radiotherapy Physicist for their expertise and assistance with the radiation treatments. Dr. L. Karsai, Consultant Histopathologist, Castle Hill Hospital, Hull for his assistance in assessing the sectioned tissue specimens.

Publications and Presentations

Publication

Carr S, Green VL, Stafford ND, Greenman J. Analysis of radiation induced cell death in HNSCC and rat liver maintained in microfluidic devices. *Otolaryngology Head and Neck Surgery* 2014; 150:73-80

Presentations

Sep 2012 Employing microfluidic techniques to study the effect of radiotherapy on HNSCC.
Carr S, Green VL, Stafford ND, Greenman J.
North of England ENT meeting, Hull
Awarded prize for best oral presentation

Sep 2012 Microfluidic techniques to assess radiosensitivity of HNSCC
Carr S, Green VL, Stafford ND, Greenman J
American Academy of Otolaryngology-Head and Neck Surgery Foundation Conference (AAO-HNSF), Washington DC

July 2012 Assessing radiosensitivity of HNSCC using microfluidic techniques
Carr S, Green VL, Stafford ND, Greenman J
British Academic Conference in Otolaryngology (BACO), Glasgow

Author's declaration

'I confirm that this work is original and that if any passage(s) or diagram(s) have been copied from academic papers, books, the internet or any other sources these are clearly identified by the use of quotation marks and the reference(s) is fully cited. I certify that, other than where indicated, this is my own work and does not breach the regulations of HYMS, the University of Hull or the University of York regarding plagiarism or academic conduct in examinations. I have read the HYMS Code of Practice on Academic Misconduct, and state that this piece of work is my own and does not contain any unacknowledged work from any other sources. I confirm that any patient information obtained to produce this piece of work has been appropriately anonymised'.

Chapter 1

Introduction

1.1 Epidemiology of head and neck squamous cell carcinoma

Head and neck squamous cell carcinoma (HNSCC) encompasses malignancies of the oral cavity, nasopharynx, oropharynx, larynx and hypopharynx. In 2011, it accounted for 2.8/100,000 of all cancers in the UK and represents the seventh most common cancer in Europe *(Jemal et al., 2011).* HNSCC is the sixth most common form of cancer in the world with a global incidence of 700,000 cases per year *(Parkin et al., 2001).* In the UK, laryngeal cancer is the largest subgroup of HNSCC, accounting for 50% of new cases; 2300 new cases of laryngeal cancer were diagnosed in 2008 with 1890 males and 402 females giving a male: female ratio of 5:1. The incidence rises sharply after the sixth decade of life with the zenith at 75-79 years, resulting in 75% of cases being in those aged over 60 years *(CRUK, 2009).*

An increased ratio of laryngeal cancer in males compared with females is reflected throughout Europe and Worldwide. In the UK, the male to female ratio is 5:1 compared to an average figure of 9:1 in the countries making up the European Union. The variation in incidence rates both between countries, and between men and women, are likely to reflect the variations in the prevalence of smoking and to a slightly lesser extent alcohol consumption *(CRUK, 2009).*

The most common laryngeal subsite for SCC, with 73% of cases, is the glottis, followed by the supraglottis with 24% and thirdly, the subglottis with 3% *(Ellis et al., 2011).* In the largest epidemiological study of laryngeal cancer in the UK with 8987 patients, Coupland et al. *(Coupland et al., 2009)* found that a higher proportion of men presented with glottic cancer 42.4% vs 26.4% whereas supraglottic cancer was more common in women 24.4% vs 14.2%.

Oropharyngeal SCC represents 10-15% of all head and neck tumours. In 2004, there were 67,000 new cases of oropharyngeal cancer in the European Union. The incidence rates are higher in Western Europe, compared with Northern or Southern Europe. However, the highest mortality rates are reported in Eastern Europe with 22 cases per 100,000 (CRUK, 2012). In the UK, there were 1346 new cases diagnosed in 2009 with numbers increasing since the late 1980s, particularly in men aged between 35 and 64. European age-standardised

incidence rates have increased for men and women by 25% and 28% respectively *(CRUK, 2012)*, a trend that has become increasingly apparent in young adults *(Llewellyn et al., 2001)*. Rates in Scotland are higher than in other parts of the UK for both men and women with a lifetime risk of 1.84% in males and 0.74% in females in Scotland compared to 1.06% and 0.48% respectively, in the rest of the UK *(Conway et al., 2006)*, possibly reflecting the increased tobacco and alcohol consumption amongst its population.

1.2 Anatomy of the head and neck region

The head and neck region encompasses the oral cavity, nasopharynx, oropharynx, larynx and hypopharynx (**Figure 1**).

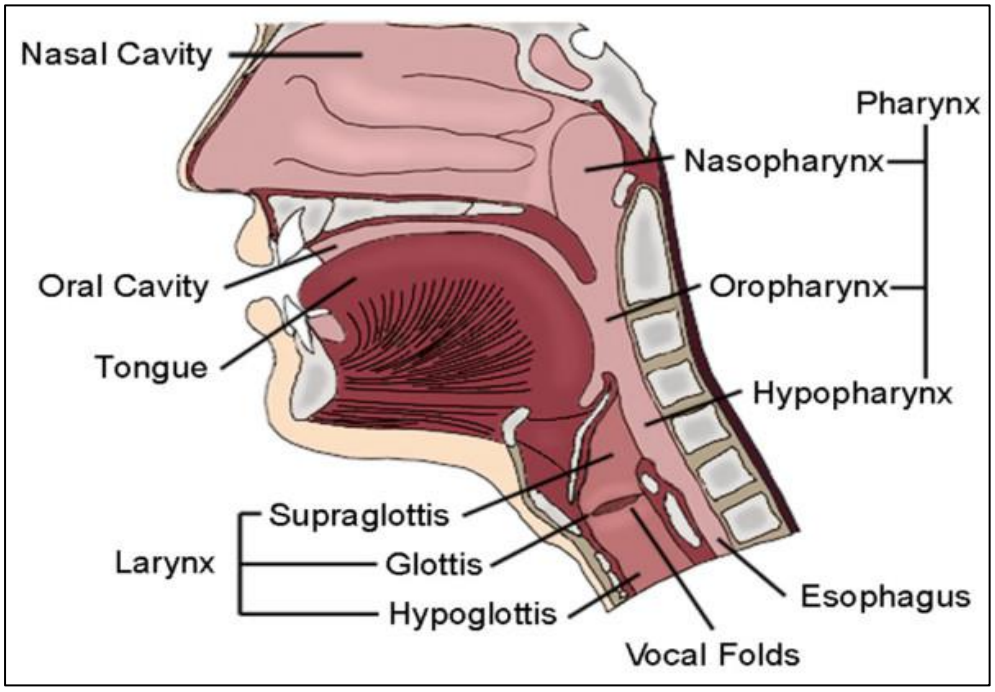

Figure 1. Schematic diagram of tumour subsites within the head and neck *(Liebertz et al., 2010)*.

The larynx develops from the laryngo-tracheal groove, which appears on the ventral aspect of the lower end of the embryonic pharynx in the region of the fourth and sixth pharyngeal arches during the fourth week of life. The endoderm of the groove forms the epithelium and glands of the larynx and trachea whilst the surrounding mesenchyme forms the connective tissue, muscle and cartilage *(MacKinnon, 2005)*.

The larynx extends from the laryngeal inlet to the inferior border of the cricoid cartilage, situated opposite the third to sixth cervical vertebrae. It is divided anatomically by the false and true vocal cords into three distinct regions: supraglottis, glottis and subglottis. The supraglottis consists superiorly of the epiglottis and aryepiglottic folds, which sweep posteroinferiorly to the arytenoids. Inferiorly, it is bordered by the false cords, which form the superior border of the glottis. The glottis consists of the true vocal cords, anterior and posterior commissures and extends from the undersurface of the false cords to 5-10mm below the true cords. The subglottis describes the region from the inferior aspect of the glottis to the undersurface of the cricoid cartilage, whereupon it becomes the trachea. The framework of the larynx consists of the hyoid bone, thyroid cartilage, cricoid cartilage and the trachea. A series of interconnecting membranes, ligaments and muscles join the structures of the larynx together and all are covered by an overlying epithelium, which is pseudostratified columnar and squamous in patches *(Beasley, 2008a).*

The pharynx is formed embryologically from the primitive gut. At the cephalic end, a blind ending tube is formed, namely the foregut, which is separated from the ectodermally lined stomatodaeum by the buccopharyngeal membrane. This membrane subsequently ruptures and the stomatodaeum becomes continuous with the foregut. The endodermal lining of the foregut differentiates to form many parts of the aerodigestive tract including the pharynx and oesophagus.

The pharyngeal arches develop in the fifth week of embryonic life. They consist of a core of mesoderm covered by ectoderm externally and endoderm internally. Each arch is separated externally by deep pharyngeal clefts and internally by the pharyngeal pouches, of which there are five pairs. The mesoderm of each differentiates into the cartilage, muscle and vascular structures of that arch. Each arch receives an afferent and efferent nerve supply for the skin, muscles and endodermal lining of that arch (post-trematic nerve) and an additional nerve from the next arch (pre-trematic nerve).

The oropharynx extends from the junction of the hard and soft palates to the floor of the vallecula. Anteriorly, it starts at the palatoglossal folds formed by the underlying palatoglossus muscle passing from the undersurface of the palate to the side of the tongue. Posterior to this, the palatopharyngeal fold passes posteroinferiorly from the lower border of the soft palate to the side wall of the pharynx. Beneath this is the palatopharyngeus muscle. The palatine tonsils lie in the space between these two folds. The posterior wall is formed by

the constrictor muscles and overlying mucous membrane. The superior wall is formed by the inferior surface of the soft palate and uvula. The anterior wall is formed by the tongue base, behind the vallate papillae *(Homer J, 2012)*.

1.2.1 Sensory and motor innervation

Sensory and motor innervation to the larynx is supplied by the vagus nerve. The internal branch of the superior laryngeal nerve provides sensation above the vocal cords, whilst the recurrent laryngeal nerve provides it below. Motor innervation to all the laryngeal musculature is provided by the recurrent laryngeal nerve except cricothyroid, which is innervated by the external branch of the superior laryngeal nerve.

The oropharynx is supplied via the glossopharyngeal and vagal nerves. The hypoglossal nerve supplies motor innervation to the base of tongue and the maxillary and mandibular divisions of the trigeminal nerve provide the motor and sensory innervation to the soft palate *(Beasley, 2008a)*.

1.2.2 Blood supply

The superior laryngeal branch of the superior thyroid artery supplies the upper half of the larynx, which originates from the external carotid artery, whilst the lower half is supplied by the inferior laryngeal artery, which is a branch of the inferior thyroid artery from the thyrocervical trunk which arises from the subclavian artery *(Dhillon, 2004)*. The ascending pharyngeal artery arises from the external carotid artery, from which branches supply the pharynx and the tonsil. The palatine branch supplies the inner aspect of the pharynx and soft palate. Further supply is received from the ascending palatine and tonsillar branches of the facial artery and the greater palatine and pterygoid branches of the maxillary artery *(Beasley, 2008b)*.

1.2.3 Lymph drainage

Regional HNSCC metastases spread via the lymphatic drainage pathways (**Figure 2**). In the larynx, the supraglottis is drained by vessels that accompany the superior laryngeal vein, which empty into the upper deep cervical nodes. The subglottis drains to the lower deep

cervical chain, often through prelaryngeal and pretracheal nodes. Due to the tight binding of the vocal cords to the underlying vocal ligament, no lymphatics are present, therefore, no metastatic spread is associated with tumours of the glottis *(Beasley, 2008a)*.

The lymphatic drainage from the oropharynx is mainly to levels II, III and IV with the addition of V if there is tongue base involvement *(Lim et al., 2006).* Central structures such as the tongue base, soft palate and the posterior pharyngeal wall drain bilaterally. The posterior pharyngeal wall and the tonsillar region also drain to the retropharyngeal nodes *(Bradley, 2008)*.

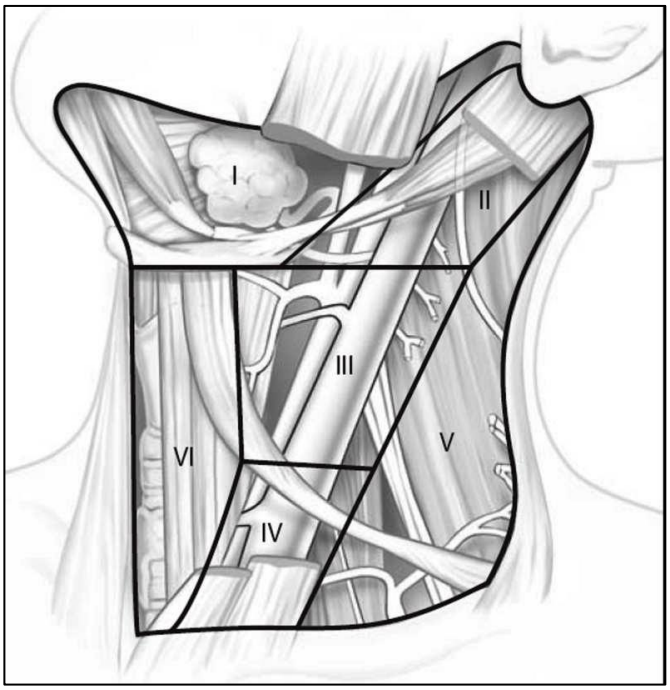

Figure 2. Levels in the neck in which lymph nodes are located *(Cummings, 2005).*

Level I – Submandibular triangle
Level II – Upper jugular chain
Level III – Middle jugular chain
Level IV – Lower jugular chain
Level V – Posterior triangle
Level VI – Anterior cervical chain

1.3 Functions of the larynx and oropharynx

1.3.1 Larynx

The larynx has three main functions: phonation, protection of the lower respiratory tract and generation of a high intrathoracic pressure for coughing and lifting.
At the commencement of phonation, air pressure within the subglottis builds until the 'phonation threshold' is achieved, which causes the vocal cords to be blown apart. The voice is generated by this exhaled air being forced between the adducted cords, which create a wave along the mucosal edge of the vocal cord.

During swallowing, the primary function of the larynx is to prevent food and liquid from entering the airway. After the oral phase, the food bolus is manoeuvred backwards towards the oropharynx. As it reaches the base of the tongue, the pharyngeal phase of swallowing is automatically initiated. During this, the laryngeal aditus narrows, the vocal cords adduct and the larynx is elevated to meet the epiglottis, covering the entrance to the larynx.

Raised intrathroacic pressure is created by forced expiration against a closed glottis. Adduction of the vocal cords following inspiration prevents expulsion of air, which fixes the chest wall and provides anchorage for the muscles of the arm and shoulder. This function of the larynx plays an important role during heavy lifting and coughing and also during childbirth and defaecation when abdominal muscles are used for forceful expulsion *(Beasley, 2008a).*

1.3.2 Oropharynx

There are three main functions of the oropharynx: hosting the immune response, swallowing and taste. The palatine and lingual tonsils and the adenoids are all composed of lymphoid tissue, which form Waldeyer's ring and act as a primary immunological barrier to inhaled and ingested pathogens. Swallowing has three distinct phases: an oral phase, a pharyngeal phase and an oesophageal phase. As a food bolus enters the oropharynx, a reflex is initiated in which the constrictors relax to dilate the pharynx, while the pharynx and larynx are raised by the longitudinal muscles. The bolus is manoeuvred over the epiglottis by the action of the constrictors contracting in sequence. On the surface of the base of tongue, there are situated between eight and twelve dome shaped structures known as the circumvallate papillae. These are innervated by the glossopharyngeal nerve and are responsible for sensation of taste *(Leslie, 2008).*

1.4 Clinical presentation of HNSCC

1.4.1 Laryngeal SCC

Symptoms caused by laryngeal carcinoma are dependent on which laryngeal subsite the tumour originates from. As normal voice production is dependent on a delicate six-cell thick epithelium and superficial lamina propria, an early glottis carcinoma will affect the mucosal wave along the vocal cord and, therefore, the patient's voice, which means that patients tend to present with early stage disease. A larger tumour may cause vocal cord fixation resulting in possible aspiration and stridor. As the tumour grows, the ultimate outcome will be complete airway obstruction. The risk of cervical metastatic disease in glottic cancer is approximately 10% due to the paucity of lymph drainage in this region *(Mackenzie K, 2012)*.

A supraglottic tumour will affect the voice, but with a characteristic 'hot potato' voice, which differs from tumours of glottic or subglottic (hypoglottic) origin. Small supraglottic lesions may present with a foreign body sensation in the throat or parasthesia. Lateral extension can cause odynophagia and true dyshpagia. If the tumour extends to the vocal cords, hoarseness will be caused as per glottic carcinoma. The probability of metastatic cervical disease increases with an increased primary tumour size. In a T1 tumour, the risk of N1 neck disease is 10% and 29% for N2-N3 disease, compared to 18% and 40% respectively with a T4 tumour *(Shah, 1990)*.

Subglottic carcinoma can also present with a foreign body sensation in the throat. Involvement of the glottis or recurrent laryngeal nerve may cause hoarseness. Circumferential progression leads to progressive dyspnoea and stridor with markedly shortened phonation times and rapid vocal fatigue *(Birchall, 2008)*.

1.4.2 Oropharyngeal SCC

Oropharyngeal squamous cell carcinoma (OPSCC) tends to present in one of three ways: firstly with symptoms, such as persistent sore throat, dysphagia or otalgia, from primary disease with or without lymph node metastases, secondly with lymph node metastasis with a clinically detectable OPSCC primary or lastly, with a lymph node metastasis from an unknown primary site. Lateral wall tumours account for 50% of OPSCC and usually involve the tonsil, whilst tongue base tumours account for 40%. Other sites involved are the soft palate and the posterior wall. Early stage tumours of lateral wall and tongue base are often

submucosal and difficult to detect, which leads to an increased number of patients, ranging from 50-80% presenting at an advanced stage (III to IV) of disease *(Zhen et al., 2004, Mackle and O'Dwyer, 2006, Lam et al., 2007, Homer J, 2012).* Lymph node metastases are common at presentation in OPSCC with over 50% having clinical or radiological evidence of cervical disease and with up to 30% presenting with metastases to the contralateral side *(Lim et al., 2006, Shimizu et al., 2006).*

1.5 Aetiology of HNSCC

1.5.1 Tobacco and alcohol

Tobacco smoking has been identified as the main causative agent in HNSCC cancer with up to 98% of patients being smokers *(Tuyns et al., 1988).* An increased duration and intensity of smoking has been shown to increase the risk of developing HNSCC. Wynder et al. *(Wynder et al., 1976)* showed that the relative risk of developing laryngeal cancer from smoking 10 cigarettes per day was 4.4 compared with 34.4 for those that smoked 40 per day. The method of smoking also plays an important role, with cigars associated with a 10-fold increase *(Shapiro et al., 2000)* and pipe smoking a 6 to 10-fold increase in cancer risk *(Lee et al., 2009)* of the larynx and oropharynx combined.

La Vecchia et al. *(La Vecchia et al., 1997)* estimated that between 25% and 68% of HNSCC were attributable to ethanol consumption. Ethanol is not a carcinogen itself, but functions as a tumour promoter or co-carcinogen *(Ketcham et al., 1963)* and when combined with tobacco has been shown to act in a synergistic manner. Multiple mechanisms are involved in alcohol-associated HNSCC development including its local effects, the effect of acetaldehyde (AA), the first metabolite of ethanol oxidation, the induction of cytochrome P-4502E1 (CYP2E1) leading to the generation of reactive oxygen species (ROS), and enhanced procarcinogen activation, as well as the modulation of cellular regeneration and nutritional deficiencies *(Poschl and Seitz, 2004).*

Locally, ethanol acts as a solvent that enhances the penetration of carcinogenic compounds into the mucosa. Chronic alcoholism causes atrophy and lipomatous metamorphosis of the salivary gland parenchyma leading to a reduction in saliva production. The mucosal surface is, therefore, inadequately rinsed and exposed to higher concentrations of locally acting carcinogens for a prolonged amount of time *(Maier et al., 1986).*

Hager et al. *(Hager et al., 2001)* demonstrated the mechanisms of increased cellular proliferation caused by alcohol in HNSCC cell lines that had been exposed to ethanol. They demonstrated an increase in hyperphosphorylated pRb, which is a tumour suppressor protein, and the downregulation of the cell cycle inhibitor p21, which accelerated the cell from G1 to S phase.

Studies have shown that AA is primarily responsible for the co-carcinogenic effect of ethanol. AA is formed during the metabolism of ethanol by alcohol dehydrogenase (ADH) and aldehyde dehydrogenase (ALDH). Numerous *in vitro* and *in vivo* experiments have shown that AA has a direct mutagenic and carcinogenic effect by inducing inflammation and metaplasia of tracheal epithelium, delaying cell cycle progression and enhancing cell injury associated with hyper-regeneration *(Seitz et al., 2001)*. When inhaled, AA has been shown to cause nasopharyngeal and laryngeal carcinoma in a rat model *(Woutersen et al., 1986)*. Genetic linkage studies in alcoholics have produced striking evidence about the causal role of AA and ethanol-associated HNSCC. Individuals who accumulate AA due to a polymorphism and/or a mutation in the gene coding for enzymes responsible for AA generation and detoxification have been shown to have an increased HNSCC risk. A comprehensive study of the ALDH2 genotype and cancer prevalence in a cohort of alcoholic patients in Japan showed that the frequency of inactive ALDH2 increased remarkably among alcoholics with HNSCC *(Yokoyama et al., 1998)*. These individuals also have high AA levels in their saliva and, therefore, deliver AA directly to the mucosal surface of the upper aerodigestive tract *(Vakevainen et al., 2000)*. ADH has also been implicated in the development of HNSCC with the isoforms ADH1C *(Visapaa et al., 2004)* and ADH1B *(Ji et al., 2011)* demonstrating an increased risk with odds ratios of 1.69 and 8.85 respectively.

Smoking and poor oral hygiene have been associated with an increase in AA levels in the oral cavity and pharynx. Smoking alters the flora from gram-negative to gram-positive bacteria and increases the levels of *Candida albicans*, both of which increase the levels of AA. Poor oral hygiene is associated with bacterial overgrowth, parodontitis and an increase in salivary AA levels *(Salaspuro, 2003)*.

Chronic alcohol consumption leads to an induction of cytochrome P-4502E1 (CYP2E1), which metabolises ethanol to AA. This cytochrome enzyme is also involved in the metabolism of various xenobiotics, including procarcinogens. Induction of CYP2E1 in the upper aerodigestive tract may be particularly relevant with respect to the procarcinogens

present in tobacco smoke and the established synergism between them. In a meta-analysis, Tang et al. *(Tang et al., 2010)* demonstrated an increased risk of developing HNSCC with the CYP2E1 polymorphisms PstI/RsaI (odds ratio1.96) and DraI (odds ratio 1.56).

The type of alcoholic beverage consumed affects the risk of developing cancer. In a population study of 28,180, Gronbak et al. *(Gronbaek et al., 1998)* found that, compared with non-drinkers, subjects who drank 7-21 units of alcohol per week of beer and/or spirits but no wine had an increased risk of developing oropharyngeal or oesophageal cancer (relative risk 3.0). However, subjects who drank a similar amount but who also drank wine, which accounted for over 30% of their total alcoholic intake had a reduced risk of developing cancer (relative risk 0.5). In those subjects that consumed over 21 units per week, their risk of developing cancer was higher compared to the group who drank 7-21 units in both the group that drank wine (relative risk 1.7) and those that did not (relative risk 5.2).

1.5.2 Viruses

Human Papilloma Virus (HPV) has been identified as a causative agent of HNSCC, in particular OPSCC *(Parkin, 2011)*. The expression of the proteins E6 and E7 by HPV bind and inactivate the tumour suppressor proteins p53 and pRB respectively, leading to malignant transformation *(Marur et al., 2010, Smeets et al., 2011).*

The virus infects epithelial cells of mucosal surfaces, matching its own life cycle to that of the epithelial cells and replicates to produce new virus particles just as the cells become squamous and reach the surface of the mucosa *(CRUK, 2011)*. Several subtypes are thought to be responsible and are stratified according to their risk: types 6, 11 (low risk), types 31, 33 (medium risk) and types 16, 18 (high risk) *(de Villiers, 1994).*

The prevalence of HPV varies within the subsites of the head and neck region. According to two meta-analyses, the prevalence for all subsites combined is 25-28% *(Ragin and Taioli, 2007, Torrente et al., 2011)*, but OPSCC the prevalence increases to approximately 40% *(Kreimer et al., 2005, Ragin and Taioli, 2007)* whilst the rates quoted for laryngeal SCC are between 25% and 60% *(Anwar et al., 1993, Clayman et al., 1994).*

1.5.3 Dietary factors

Case control studies have shown up to an 80% reduction in risk in people who eat the highest intakes of fruit and vegetables *(La Vecchia et al., 1990, De Stefani et al., 2000, Bosetti et al., 2002).* A high intake of red and processed meat has been associated with an increased risk of laryngeal cancer in case-control studies. Levi et al. *(Levi et al., 2004)* found that there was a three-fold increase in risk in those people who ate processed meat three or more times per week compared to those who ate it less than once a week. De Stefani et al. *(De Stefani et al., 2007)* found that people who consumed a western-style diet, high in fried, barbecued and processed meat, had an odds ratio of 3.2 of developing HNSCC.

Many patients with HNSCC have a poor nutritional status, which may be due to chronic alcoholism or as a direct result of the tumour. Poor nutritional status may contribute to alcohol associated carcinogenesis and is also associated with a poor prognosis *(Bianchini et al., 2012).* A diet deficient in vitamins A, C and E has been associated with an increased risk of developing HNSCC due to their action as scavengers of free radicals *(Esteve et al., 1996, McLaughlin et al., 1988).*

1.5.4 Occupational factors

Nickel and chromate refining workers have an increased incidence of laryngeal SCC *(Stafford, 2008).* Exposure to coal dust has been shown to give a risk ratio of 6 *(Bosetti et al., 2003)*; the risk increasing by 3.6 times if there has been greater than 50 years coal dust exposure *(Sapkota et al., 2008).*

There is no general consensus as to whether asbestos exposure causes laryngeal cancer. A meta-analysis carried out in 1999 of asbestos-exposed cohort showed a 33-57% increase in the risk of developing laryngeal cancer *(Goodman et al., 1999).* However, two subsequent studies did not agree with this. Magnani et al. *(Magnani et al., 2008)* found that in a cohort of 3434 people, 16 developed laryngeal cancer compared to an expected value of 12.2, a non-significant difference. Marchand et al. *(Marchand et al., 2000)* found that asbestos exposure resulted in a non-significant odds ratio of 1.24 of developing laryngeal cancer subsequent to asbestos exposure.

1.5.5 Laryngopharyngeal reflux

Several studies have demonstrated a causal relationship between laryngopharyngeal reflux and laryngeal cancer *(Lewin et al., 2003, Tae et al., 2011, Johnston et al., 2012, Cekin et al., 2012)* including a meta-analysis by Qadeer et al. *(Qadeer et al., 2005),* whilst others have refuted this *(Nurgalieva et al., 2005, Ozlugedik et al., 2006).* Currently, there is no consensus as to whether a link exists.

1.5.6 Molecular factors

HNSCC arises from a common premalignant progenitor followed by outgrowth of clonal populations associated with cumulative genetic alterations and phenotypic progression to invasive malignancy *(Nawroz et al., 1994, Califano et al., 1996, Califano et al., 2000)* (**Figure 3**). These genetic alterations result in inactivation of tumour suppressor genes and activation of proto-oncogenes by deletions, point mutations, promoter methylation and gene amplification *(Perez-Ordonez et al., 2006).*

Epidermal growth factor receptor (EGFR) is the cell-surface receptor for members of the epidermal factor family. EGFR dimerization stimulates its intrinsic intracellular protein-tyrosine kinase activity, which, in turn, causes increased activity in the downstream pathway. As EGFR is an important activator of mitogenic signalling *(Kalyankrishna and Grandis, 2006),* its increased activation leads to cellular proliferation. Overactivation of EGFR is well recognised in HNSCC and premalignant mucosa and occurs in up to 90% of cases *(Grandis and Tweardy, 1993).*

The phosphatidylinositide 3-kinase (PI3K)/ protein kinase B (AKT) pathway is an important downstream effector of the EGFR and its activation occurs in up to 90% of cases of HNSCC *(Bussink et al., 2008).* PI3K/AKT signalling regulates cellular proliferation, apoptosis, invasiveness, and the upregulation of hypoxia-related proteins (*Bussink et al., 2008*). The tumour suppressor gene phosphatase and tensin homologue gene (PTEN) inhibits the PI3K/AKT pathway promoting G1 cell cycle arrest. Activation of the pathway may occur through several mechanisms including amplification of the PIK3CA locus (30-40% of cases), amplification of AKT (20-30% of cases) or methylation of the PTEN locus *(Pedrero et al., 2005).*

The most common genetic alterations are loss of heterozygosity (LOH) at chromosomal locations 9p, 3p and 17p, as well as 5q, 8p, 9q and 11p *(Ah-See et al., 1994)*. LOH at 9p21 is an early event in HNSCC development and is found in 70-80% of cases *(van der Riet et al., 1994, Califano et al., 1996, Mao et al., 1996b)*. The CDKN2A gene locus found in chromosome 9p21 encodes $p16^{INK4A}$ and $p14^{ARF}$. The role of $p16^{INK4A}$ is to prevent the progression through the cell cycle from G1 to S phase by disrupting the complex formed by cyclin D1 and the cyclin dependent kinases CDK4 and CDK6. $p14^{ARF}$ inhibits murine double minute 2 protein (mdm2), which promotes p53 and, in turn p21 activation, which then binds and inactivates the cyclin-CDK complexes, inhibiting the cell cycle.

The tumour suppressor genes fragile histidine triad gene (FHIT) *(Mao et al., 1996a, Kisielewski et al., 1998)* and ras-associated domain family member 1 (RASSF1A) *(Hogg et al., 2002, Dong et al., 2003)* are located at 3p14 and 3p21 respectively and are associated with the development of HNSCC. These genes are inactivated by a combination of LOH of 3p *(Rowley et al., 1996, Hogg et al., 2002, Garnis et al., 2003)*, which occurs in up to 70% of cases *(Perez-Ordonez et al., 2006)* and hypermethylation of the normally unmethylated CpG islands of the gene promoter regions. The mechanisms by which inactivation of each of these tumour suppressor genes causes HNSCC remains unclear *(Zheng et al., 2004b)*, but it has been proposed that RASSF1A interacts with and stabilises microtubule formation during mitosis *(Dallol et al., 2004, Vos et al., 2004)*.

LOH of 17p and point mutations of the p53 gene are seen in approximately 50% of cases *(Perez-Ordonez et al., 2006)*, occurring late in the progression from epithelial dysplasia to invasive carcinoma *(Boyle et al., 1993, Shahnavaz et al., 2000)*. Amplification of 11q13 is seen in 30-60% of HNSCC, which leads to overexpression of cyclin D1 which enables progression from G1 to S phase of the cell cycle through phosphorylation of the retinoblastoma (Rb) gene and is associated with an increased rate of lymph node metastases and poor prognosis *(Meredith et al., 1995, Michalides et al., 1995, Maruya et al., 2004)*. In addition to cyclin D1, FADD (Fas-associated protein with death domain), which regulates apoptosis is located at 11q13 and has been associated with HNSCC development *(Rasamny et al., 2012)*.

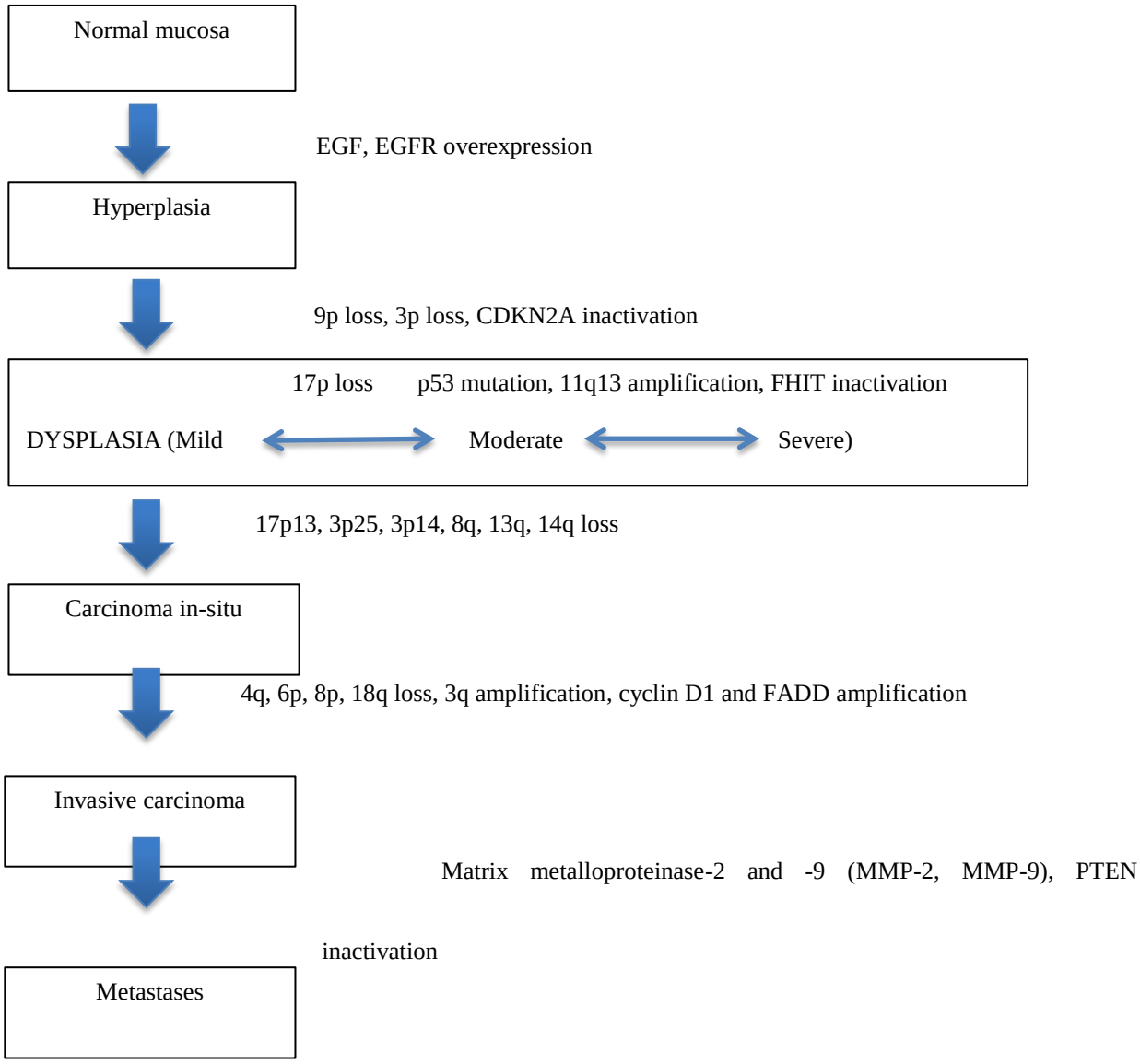

Figure 3. Progression of normal mucosa to invasive disease and metastatic HNSCC in association with genetic events *(Califano et al., 1996)*

1.6 Pathology of HNSCC

Squamous cell carcinoma (SCC) accounts for at least 90% of all primary malignant tumours of the larynx and oropharynx. Metastasis is typically by direct spread or via regional lymphatics in approximately 30-40% of advanced stage disease, whilst haematogenous spread, especially to the lungs, occurs in approximately 20-30% *(Forastiere et al., 2003)*. HNSCC, particularly originating from the oral cavity or larynx, typically begins as a non-invasive neoplastic epithelial precursor lesion (**Figure 3**). In its transition from normal tissue to invasive SCC, laryngeal mucosa undergoes dysplastic changes. Dysplasia refers to a pre-

malignant epithelial state, which demonstrates characteristic abnormal cytological and architectural features: anisocytosis, poikilocytosis, hyperchromatism and mitotic figures *(Cotran RS, 1997).* Dysplasia is classified as mild, moderate or severe depending on the extent to which the tissues are involved. Mild dysplasia refers to changes involving the outer third of the epithelium, moderate involves the middle third and severe involves the full thickness, also referred to as carcinoma-in-situ. Whilst the progression of a dysplastic lesion to invasive malignancy is not inevitable, the greater the severity of dysplasia, the more chance it has of becoming an invasive carcinoma *(Lakhani SR, 2003)* with approximately 11% of moderate to severe dysplastic lesions undergoing malignant transformation *(Thompson, 2006)*.

Macroscopically, SCC may be exophytic or endophytic, starting off as leukoplakia or erythroplakia, which progresses to an ulcerated mass with irregular indurated borders. Microscopically, mature squamous epithelial cells possess dense haematoxyphilic nuclei with a low nucleus-cytoplasmic ratio. The cytoplasm is densely eosinophilic and finely reticulated owing to keratin intermediate filaments. Well-differentiated HNSCC characteristically shows cytoplasmic and/or extracellular keratinisation plus intercellular prickles (spinous processes corresponding to desmosomes highlighted by cell shrinkage allowing separation between adjacent cell membranes) and keratin pearls *(Moorthy, 2012)* (**Figure 4**).

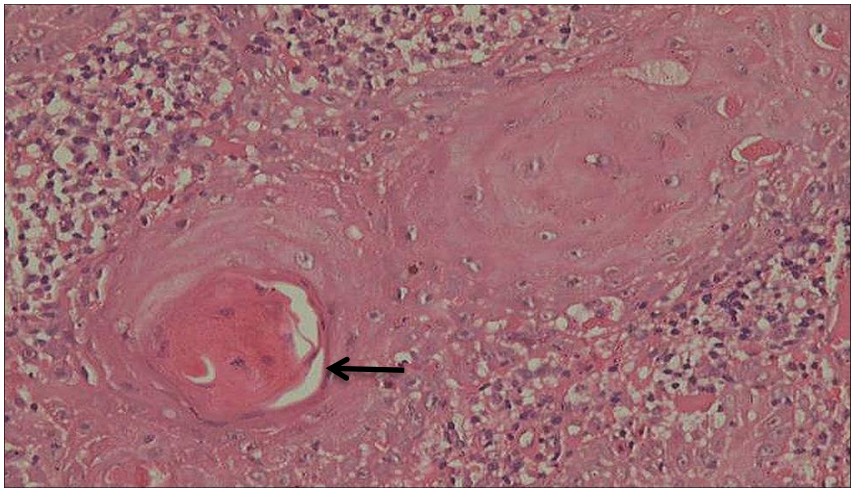

Figure 4. Haematoxylin and Eosin staining of laryngeal squamous cell carcinoma at 40x magnification showing keratin pearls (arrow) *(Singh, 2012).*

1.7 Staging of HNSCC

Table 1. TNM staging for malignant tumours of subsites of larynx and oropharynx according to the Union for International Cancer Control (UICC) *(Sobin, 2010).*

LARYNX

Supraglottis

T1	One subsite, normal vocal cord mobility
T2	Mucosa of more than one adjacent subsite of supraglottis or glottis or adjacent region outside the supraglottis; without fixation
T3	Cord fixation or invades postcricoid area, pre-epiglottic tissues, paraglottic space, thyroid cartilage erosion
T4a	Through thyroid cartilage; trachea, soft tissues of neck: deep/extrinsic muscle of tongue, strap muscles, thyroid, oesophagus
T4b	Prevertebral space, mediastinal structures, carotid artery

Glottis

T1	Limited to vocal cord(s), normal mobility. T1a One cord. T1b Both cords
T2	Supraglottis, subglottis, impaired cord mobility
T3	Cord fixation, paraglottic space, thyroid cartilage erosion
T4a/T4b	As per supraglottis

Subglottis

T1	Limited to subglottis
T2	Extends to vocal cord(s) with normal/impaired mobility
T3	Cord fixation
T4a/T4b	As per supraglottis

OROPHARYNX

T_x	Primary tumour cannot be assessed
T0	No evidence of primary tumour
T1	Tumour $\leq$ 2cm in greatest diameter
T2	Tumour 2 - 4cm in greatest diameter
T3	Tumour > 4cm in greatest diameter
T4	Tumour invades adjacent structures: pterygoid muscles, mandible, hard palate, deep muscle of the tongue, larynx

REGIONAL METASTASES

N0	No nodal metastases
N1	Single ipsilateral node $\leq$ 3cm
N2a	Single ipsilateral node 3-6cm
N2b	Mutliple ipsilateral nodes 3-6cm
N2c	Contralateral node 3-6cm
N3	Any node > 6cm

DISTANT METASTASES

M0	No distant metastases
M1	Distant metastases present

1.8 Prognosis of HNSCC

According to Cancer Research UK, the five and ten-year overall survival rates for laryngeal SCC, which accounts for 50% of HNSCC barely exceeded 60% in the period 1971-2001, despite advances in surgery and chemoradiotherapy (**Figure 5**) *(CRUK, 2009).* The prognosis of laryngeal SCC is poorer if associated with the following factors: advanced stage of disease at diagnosis, vocal cord fixation and massive local invasion, ulceration of the primary tumour, lymph node metastases at diagnosis, locoregional recurrences and male gender *(Eiband et al., 1989).* Eighty per cent of patients diagnosed with early stage cancer will live for at least five years. In T1 disease, the five-year survival rates are similar for both radiotherapy and trans-oral laser surgery at 90%. The overall five-year survival rate for T2 glottic carcinoma is 85%. The five-year survival rate for late stage laryngeal disease (stage III and IV) ranges from 25-60% depending on locoregional metastases *(CRUK, 2009).*

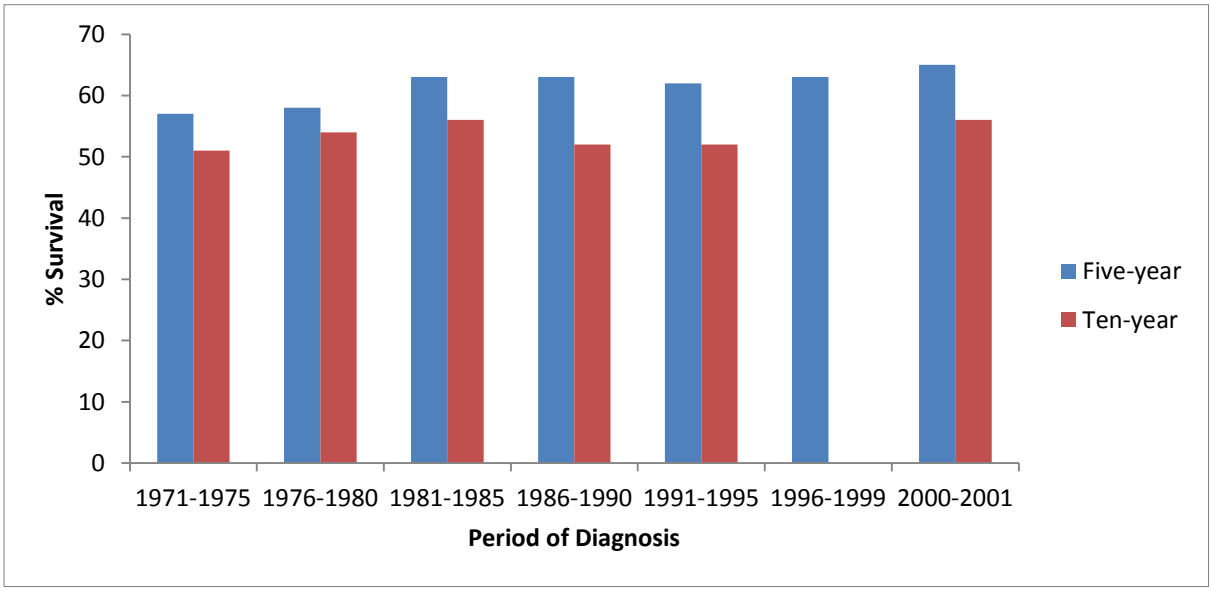

Figure 5. Five-year and ten-year age-standardised overall survival for laryngeal cancer for patients diagnosed in England and Wales during 1971-2001. No ten-year survival data for 1996-1999 available *(CRUK, 2009)*

In 2008, there were 1822 deaths from oral and oropharyngeal cancer. Whilst mortality rates for those aged over 75 have fallen since 1971, they have increased by 69% in men aged between 45 and 64. *(CRUK, 2010).* Using the improved Hart grouping system *(Hart et al.,*

1995), Ambrosch et al. demonstrated five year overall survival rates for OPSCC per stage: stage I 59%, stage II 31%, stage III 28% and stage IV 16% *(Ambrosch et al., 1998).*

1.9 Treatment of HNSCC

1.9.1 Treatment of laryngeal SCC

Early stage (T1 and T2) laryngeal cancer can be treated either surgically or non-surgically. The surgical options consist of trans-oral endoscopic laser surgery and open partial laryngectomy. Trans-oral laser has become the standard surgical treatment for T1, T2 and some selected T3 laryngeal cancers *(Silver et al., 2009)* over partial laryngectomy, whilst radiotherapy is the standard non-surgical treatment for T1 and T2. The five-year laryngectomy-free survival rates for each modality are comparable, with laser surgery being slightly higher. A Cochrane systematic review comparing radiotherapy, open surgery and trans-oral laser surgery for T1 and T2 cancers showed that all are accepted modalities of treatment, conferring similar survival advantages *(Dey et al., 2002).*

There are, however, disadvantages to both modalities. Laser surgery is associated with a poorer voice, although this is mild in most cases *(Kujath et al., 2011)*. Radiotherapy is a treatment that can only be performed once, compared to laser treatment which can be repeated, and many patients suffer from significant side effects such as mucositis, dysphagia, xerostomia, dermatitis and pain. Radiation-induced mucositis of the upper aerodigestive tract results in significant morbidity and altered quality of life *(Kelly et al., 2007).* The late radiation-induced toxicities include xerostomia (60-90% incidence) *(Wijers et al., 2002),* grade 3 dysphagia (15-30%), osteoradionecrosis of the mandible (5-15%) *(Mendenhall, 2004),* skin fibrosis and laryngeal cartilage necrosis *(Bhide et al., 2012).*

In a recent meta-analysis, Paleri et al. *(Paleri et al., 2011)* demonstrated that open partial laryngectomy, particularly for T1 and T2 tumours was an oncologically sound procedure with a high larynx preservation rate. However, it is not appropriate for recurrence of laryngeal carcinoma post-radiotherapy due to the associated complications of a longer hospital stay, soft tissue wound infection, chondritis, persistent laryngeal oedema and a higher rate of thoracic infections when compared to an endoscopic procedure *(Kooper et al., 1995).*

For advanced tumours (T3 and T4), the treatment options are total laryngectomy or chemoradiotherapy (CRT). Other less commonly used modalities include open partial laryngectomy, near total laryngectomy and transoral laser surgery, although these are not

appropriate for the majority of patients, given the high rate of complications *(Naudo et al., 1998).* Total laryngectomy provides excellent local and regional tumour control, however, it has a significant impact on a patient's ability to communicate and can severely affect their quality of life *(Terhaard et al., 1992).*

The development of laryngeal preservation CRT has been underway since the 1990s. Aisner et al. *(Aisner et al., 1994)* stated that in the treatment of more advanced (T3 and T4) laryngeal and oropharyngeal tumours, the combination of chemotherapy and radiotherapy has been proven to enhance HNSCC tumour control within the irradiated field. Forastiere et al. *(Forastiere et al., 2003)* demonstrated that in patients with laryngeal cancer, radiotherapy with concurrent administration of cisplatin is superior to induction chemotherapy followed by radiotherapy or radiotherapy alone for laryngeal preservation and locoregional control. Posner et al. *(Posner et al., 2007),* in a study of 501 patients, demonstrated significantly increased survival rates in patients with stage III or IV HNSCC disease using the TPF regimen (docetaxel, cisplatin and 5-fluorouracil) compared to the PF regimen (cisplatin and 5-fluorouracil) combined with radiotherapy. The overall three-year survival rate increased from 48% to 62% with improved locoregional control. However, there was no effect on the rate of the development of distant metastases.

1.9.2 Treatment of oropharyngeal SCC

There has been an increase in the use of chemoradiotherapy in the treatment of OPSCC with a decrease in radical surgery and adjuvant radiotherapy. Although it is not routinely tested for, HPV-induced tumours are strongly associated with improved therapeutic response and survival *(Fakhry et al., 2008).* Mellin et al. *(Mellin et al., 2000)* demonstrated a five-year survival for all tumour stages of 53.5% in the HPV-positive group compared to 31.5% in the HPV-negative group. They also showed that patients with HPV-positive tumours were more likely to remain disease-free over three years than HPV-negative, taking into account tumour stage (odds ratio 19.6) and lymph node status (odds ratio 7.33). Fakhry et al. *(Fakhry et al., 2008)* demonstrated an improved treatment response rate after induction chemotherapy 82% vs 55% and after CRT 84% vs 57%, better overall two-year survival 95% vs 62% and lower risk of progression (hazard ratio 0.27).

It has been shown that CRT results in a better rate of survival than radiotherapy alone *(Calais et al., 1999)* and has now become the standard of care for most patients with OPSCC *(Chen et al., 2007).* However, some studies have suggested that radiotherapy as a single modality treatment may offer comparable survival with better function *(Mendenhall et al., 2000, Parsons et al., 2002).* In their study of 48 patients, Nguyen et al. *(Nguyen et al., 2007)* demonstrated excellent results with CRT for early stage OPSCC with an overall survival of 84% for T1-T2, whilst the results for more advanced disease were disappointing with an overall survival of 27%. In their study of 226 patients with stage III/IV OPSCC treated with CRT, Denis et al. *(Denis et al., 2004)* demonstrated similar overall five-year survival rates of 22%.

However, acute and late-stage toxicity is a significant factor for patients receiving CRT treatment, with mucositis, haematological toxicity, long-term dysphagia and dependence on feeding tubes all being associated. These factors, together with the possible overtreatment of HPV associated OPSCC with conventional CRT has led to proposals for using cetuximab with radiotherapy alone, especially for HPV-induced tumours *(Eriksen et al., 2010).*

The use of trans-oral laser microsurgery with or without neck dissection with or without radiotherapy or CRT as adjuvant therapy has shown promising results for treatment of all stages of disease. Rich et al. *(Rich et al., 2009)* demonstrated an overall five-year survival of 88% in 84 patients over a ten-year period for all stages of disease, 93% of whom required adjuvant therapy. Only 3% required gastrostomy tubes at three years post-operatively. In their series, Camp et al. *(Camp et al., 2009)* demonstrated disease-free survival rates of 94% for T1, 51% for T2 and 21% for T3 with no patients requiring feeding tubes.

Currently in the UK, a post-CRT neck dissection is performed if there is evidence of residual neck disease, either clinically or radiologically, post-CRT *(Clayman et al., 2001).* This has led to the utilisation of the positron-emission tomography-computed tomography (PET-CT) after a patient has completed their CRT course in order to demonstrate residual disease, as it can be difficult to differentiate between tissue changes due to radiotherapy and residual disease on CT or MRI alone *(Homer J, 2012).*

1.9.3 Treatment of metastatic neck disease

The treatment of metastatic neck disease is usually determined by the stage of neck disease. In the N0 neck, there are two options: elective neck dissection or a ‘watch and wait’ policy to

see if the patient develops overt disease. Elective neck dissection is indicated if there is a 15-20% risk of subclinical neck disease e.g. supraglottic SCC *(Weiss et al., 1994),* if vigilant follow-up is not possible, if clinical evaluation of the neck is difficult or if access to the neck is required for reconstruction *(Paleri V, 2012).*

In the node-positive neck, the neck should receive the same treatment modality as the primary tumour, either surgery or CRT. If surgery is opted for, then adjuvant treatment with radiotherapy or CRT is required if there is extracapsular spread *(Bernier et al., 2004, Cooper et al., 2004, Bernier et al., 2005),* two or more positive nodes in the resection specimen, the neck disease is N2-3 or if there is residual disease. Adjuvant radiotherapy confers a 10% increase in five-year survival compared to surgery alone for the node-positive neck *(Lavaf et al., 2008).* If CRT is used, then the patient will require post-CRT imaging, preferably with CT-PET, performed at 8-12 weeks to assess for residual disease *(Yao et al., 2004, Porceddu et al., 2005, Isles et al., 2008).* If residual disease is present, which it is in 20-25% of patients *(Stenson et al., 2006, Sewall et al., 2007),* a salvage neck dissection is required, which is associated with significantly higher complication rates *(Paleri V, 2012).*

1.10 Rat liver

Rat liver was used in this study to optimise the microfluidic technique prior to it being used with the HNSCC tissue samples. There were several factors that made rat liver an ideal tissue for optimization. It was readily available as fresh tissue and had been previously maintained in an identical microfluidic device with consistent results *(Hattersley et al., 2008).* It was possible to measure liver metabolic products i.e. albumin and urea, as soluble biomarkers, as well as the cytotoxicity marker lactate dehydrogenase. It has properties that are similar to HNSCC in that it is a highly metabolic tissue and is moderately radiosensitive *(Stryker, 2007).*

1.10.1 Functions of rat liver

The liver is essential in regulating metabolism, storing vitamins and iron, degrading hormones and inactivating and excreting drugs and toxins. It also regulates the metabolism of carbohydrates, lipids and proteins and along with muscle is the main site of glycogen storage. The liver is also the major site of gluconeogenesis, the conversion of amino acids, lipids or simple carbohydrates into glucose.

The liver is the major organ involved in protein metabolism, breaking down ammonia to urea. Urea ($(NH_2)_2CO$) is produced as a result of protein metabolism and the breakdown of amino acids. All 20 amino acids can be converted to $CO_2 + H_2O$ after removal the amino group

($-NH_2$). Each traverses a specific degradative pathway; however, all these pathways converge into three general metabolic pathways: gluconeogenesis, ketogenesis and ureagenesis. The degradation of all amino acids will produce ammonia (NH_3), which, incorporated mainly into glutamine and alanine molecules, is then transported to the liver. Ammonia is highly neurotoxic and, therefore, undergoes conversion to urea, a metabolically inert molecule, in the liver via the Krebs-Henseleit urea cycle *(Genuth, 1998).*

The liver synthesizes all the major plasma proteins, including albumin, lipoproteins, globulins, fibrinogens and other proteins involved in blood clotting. Serum albumin is produced by the liver and is the most abundant protein in blood plasma, constituting about half of the blood serum protein and has a half-life of approximately 20 days. It transports fatty acids, hormones, buffers pH and maintains osmotic pressure. It is synthesised in the liver as preproalbumin, which has an N-terminal peptide that is removed before the nascent protein is released from the rough endoplasmic reticulum.

It transforms and excretes many hormones, drugs and toxins. The smooth endoplasmic reticulum of hepatocytes contains a variety of enzymes and cofactors that are responsible for the chemical transformation of many substances. Other enzymes in the endoplasmic reticulum catalyse the conjugation of many compounds with glucorinic acid, glycine or glutathione. The transformations that occur in the liver render many compounds more water soluble so that they are more readily excreted by the kidneys *(Kutchai, 1998).*

1.11 Radiotherapy

1.11.1 Radiation physics

The energy of X-ray beams that are used in the clinical setting are usually in the range of between 10 peak kilovoltage (kVp) and 50 megavolts (MV). They are produced when electrons, with kinetic energies of between 10 kiloelectronvolts (keV) and 50 megaelectronvolts (MeV), are decelerated in specialised metallic targets, which are usually made of tungsten. Most of the electron's energy is transformed into heat in the metallic target. A small fraction is emitted as X-ray photons, which are divided into two groups: characteristic X-rays and bremsstrahlung X-rays *(Podgorsak, 2005).*

Characteristic X-rays result from Coulomb interactions between the incident electrons and atomic orbital electrons of the target material (collision loss). In a Coulomb interaction between the incident electron and an orbital electron, the orbital electron is ejected from its shell and an electron from a higher level shell fills the resulting orbital vacancy. The energy difference between the two shells may either be emitted from the atom in the form of a characteristic photon (characteristic X-ray) or transferred to an orbital electron that is ejected from the atom as an Auger electron. The photons emitted through electronic shell transitions have discrete energies that are characteristic of the particular target atom in which the transitions have occurred, hence the term characteristic X-rays. Bremsstrahlung X-rays result from Coulomb interactions between the incident electron and the nuclei of the target material. During the Coulomb interaction between the incident electron and the nucleus, the incident electron is decelerated and loses part of its kinetic energy in the form of bremsstrahlung photons (radiative loss) *(Podgorsak, 2005).*

There are three types of X-rays that are used in the clinical setting:

- Superficial X-rays produced by electrons with kinetic energies between 10 and 100 keV produced by X-ray machines.
- Orthovoltage X-rays produced by electron kinetic energies between 100 and 500 keV produced by X-ray machines.
- Megavoltage X-rays produced by electron kinetic energies above 1 MeV produced by a linac, a cyclic particle accelerator, as used in the current study *(Podgorsak, 2005).*

A medical linac (**Figure 6**) accelerates electrons to kinetic energies from 4 to 25 MeV using non-conservative microwave radiofrequency (RF) fields. The electrons are accelerated following straight trajectories in special evacuated structures called waveguides. The high power RF fields used for electron acceleration in the acceleration waveguides are produced through the process of decelerating electrons in retarding potentials in evacuated devices called magnetrons and klystrons. They typically provide two photon energies, 6 and 18 MV *(Podgorsak, 2005),* with 6 MV being most suited to treating HNSCC *(Rowell, 2012).*

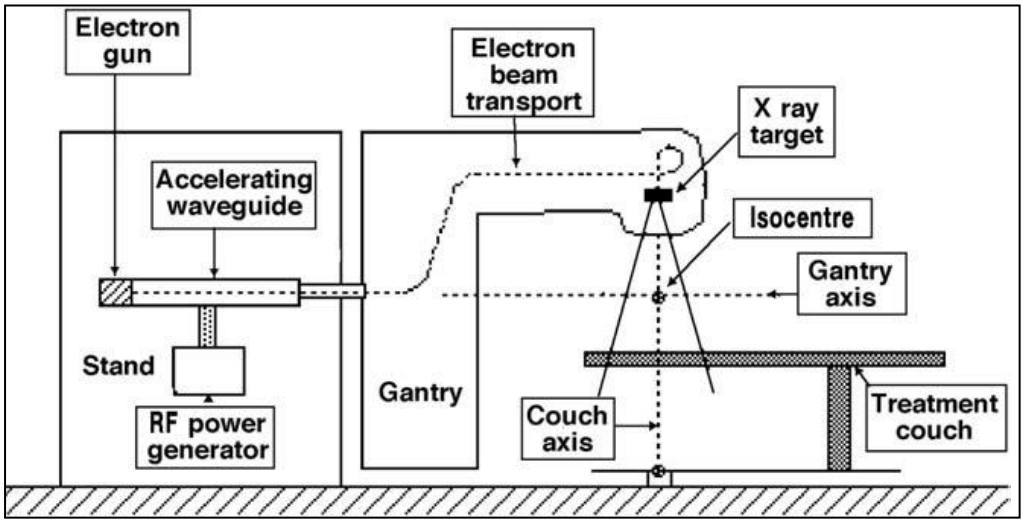

Figure 6. A schematic diagram showing the configuration of a medical linac *(Podgorsak, 2005).*

1.11.2 Dose-response relationships

Once the threshold dose, i.e. the minimum radiotherapy dose required to achieve a response in the tissue, has been reached, the relationship between the dose administered and the number of cells killed demonstrates a sigmoid curve. The gradient of the curve is given by the gamma value, which measures the increase in response as percentage points for a 1% increase in dose. In HNSCC, the gamma values are in the range 1.5 to 2.5 i.e. with a gamma value of two, a 10% increase in dose can be expected to increase the tumour cure probability by 20% *(Dische, 2002).*

The linear quadratic equation is the most widely accepted method of fitting the survival of cells following radiation to an equation:

Equation 1. The linear quadratic equation.

$$S(D)=e^{-(\alpha D+\beta D^2)}$$

S is the number of surviving cells following a radiation dose (D). α and β describe the linear and quadratic parts of the survival curve respectively. These vary between different tissue types and tumours.

As α relates to the linear component of the curve, cell death that results from this will increase linearly with the dose. As the dose increases, the cell death resulting from the β constant increases in proportion to the square of the dose. The α/β ratio relates to the dose in Gray (Gy) i.e. the amount of ionising radiation absorbed by one kilogram of tissue, when the number of cells killed by the linear component α is equal to the number of cells killed by the β component. The higher the α/β ratio is, the earlier responding tissues are, compared to a lower α/β ratio for later responding tissues (**Figure 7**). In HNSCC, the α/β ratio has been shown to be large at 10.5 Gy. The γ50 value indicates the increase in percentage tumour cell kill for an increase in dosage of 1 Gy at the intersection of the α and β lines *(Podgorsak, 2005).*

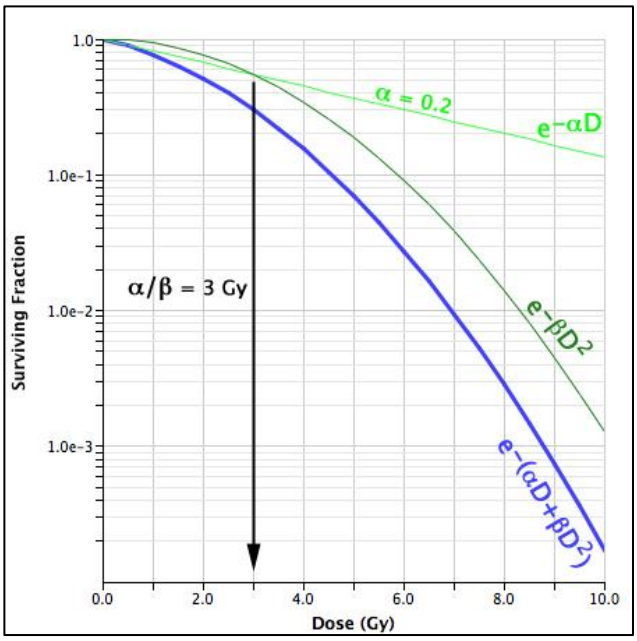

Figure 7. A survival curve using the standard LQ formula where α = 0.2 and α/β =3. The components of cell killing are equal where the curves e-αD and e-βD^2 intersect. This occurs at D = α/β i.e. 3 Gy *(Bartkowiak et al., 2001)*

1.11.3 Radioresistance

Approximately 5-10% of T1 and up to 25% of T2 laryngeal tumours are radioresistant *(Fernberg et al., 1989, Klintenberg et al., 1996, Johansen et al., 2002).* Nix et al. (*Nix, Cawkwell et al. 2005)* stated that there was no universally accepted definition of radioresistance in HNSCC, but defined it as shown in **Table 2**:

Table 2. Criteria used to determine radioresistance and radiosensitivity *(Nix et al., 2005).*

Radioresistance	• Radiotherapy given as a single modality treatment with curative intent for a biopsy proven SCC of the larynx • Biopsy proven recurrent SCC occurring at the original anatomical site within 12 months of finishing a course of radiotherapy
Radiosensitivity	• Radiotherapy given as a single modality treatment with curative intent for a biopsy proven SCC of the larynx • Minimum follow-up of three years after completion of radiotherapy with no evidence of recurrence at the original site of the tumour.

Radioresistance in HNSCC is due to a combination of clinical, both tumour- and patient-related, and biological factors. Tumour-related factors consist of tumour site, stage, volume, nodal status and grade *(Silva et al., 2007).* In demonstrating the effect of tumour site,

Dinshaw et al. *(Dinshaw et al., 2006)* showed that glottic tumours had a better response to radiotherapy than supraglottic tumours, which Snow et al. *(Snow et al., 1982)* proposed was due to the increased lymphatic drainage of the supraglottic region, usually resulting in a increased stage of supraglottic tumour at presentation.

When compared to an early stage HNSCC tumour, as defined by the TNM classification (T1 and T2), an advanced stage tumour (T3 and T4) is associated with poorer locoregional control and a shorter disease-free survival. Although a major drawback of the TNM system is that it does not assess tumour volume, a greater tumour volume is, again, associated with poorer local disease control and overall survival following radiotherapy *(Pameijer, 1997, Rudat et al., 1999)*. Despite the fact that tumour grading does not influence clinical decision making, it has been demonstrated to have an effect on the tumour's response to radiotherapy. Hansen et al. *(Hansen et al., 1997)* demonstrated that well or moderately differentiated carcinomas showed significantly reduced locoregional control compared to poorly differentiated tumours over prolonged radiotherapy schedules.

Silva et al. *(Silva et al., 2007)* described four patient-related factors that contribute to a tumour's radioresistance: patient age, gender, haemoglobin level and smoking status. They state that age is not an independent contributory factor after co-morbidity and physiological age is taken into account. Women demonstrated better locoregional control compared to men following radiotherapy, however, the reasons for this remain unclear. Low haemoglobin is a predictor of poor outcome in terms of local control and overall survival following radiotherapy *(Overgaard et al., 1986, Dubray et al., 1996)*. Other studies have shown that smoking during radiotherapy treatment reduce locoregional control (smokers 45% cf. non-smokers 74%) at 13 weeks post-treatment and survival (smokers 29 months cf. non-smokers 42 months) *(Browman et al., 1993, Browman et al., 2002)*.

It is not currently possible to predict which tumours will respond to radiotherapy prior to the patient commencing the treatment. If the patient's tumour proves to be radioresistant, then that patient will not only have undergone a non-beneficial treatment but will have also been exposed to all of its associated side effects, some of which are potentially serious. The duration of the treatment will have allowed the tumour to progress, thereby reducing the patient's chance of survival. As radiotherapy can only be performed once, failure of it to treat the tumour means that the only chance of cure for that patient is salvage surgery. Surgery is only appropriate if the patient is deemed fit enough, which a number are not; sometimes as a

result of the radiotherapy. Operating in a previously irradiated field is associated with higher complication rates, which affect swallowing, speech and cosmesis, all of which have a significant detrimental effect on the patient's quality of life *(McLaughlin et al., 1996)*.

1.11.4 Radiobiology

The interaction of an individual cell with radiotherapy ultimately determines the overall response of that tissue. Bussink et al. *(Bussink et al., 2008)* described three main biological factors relating to radioresistance in HNSCC tissue: tissue hypoxia, tumour cell proliferation and intrinsic cellular radioresistance. In addition to these there are five factors ('five R's') which influence the outcome of a course of fractionated radiotherapy: recovery, reoxygenation, repopulation, reassortment, and radiosensitivity. Recovery and repopulation are associated with decreased tumour cell killing, whilst reoxygenation and reassortment increase it *(McMillan, 2002)*.

Recovery refers to the cell's ability to repair damage caused by ionising radiation. There are three types of damage that ionising radiation can cause to a cell: lethal, sublethal and potentially lethal. Lethal damage is fatal, sublethal damage can be repaired before the administration of the next fraction and potentially lethal damage can be repaired under certain circumstances, usually when the cell is paused in the cell cycle. The repair of sublethal damage is dependent on a cell's ability to recognise the damage, activate repair pathways and initiate cell cycle arrest, during which a cell is more radiosensitive. Tumour cells have a reduced ability to repair this form of damage compared to normal cells due to impaired cell cycle arrest and DNA repair mechanisms *(McMillan, 2002)*.

Oxygen is a potent radiosensitiser, which acts to increase the effectiveness of a given dose of radiation by forming free radicals. Tumour cells in a hypoxic environment may be as much as two to three times more radioresistant than those in a normal oxygen environment *(Harrison et al., 2002)*. In solid tumours, such as HNSCC, there is an imbalance between oxygen delivery and consumption, leading to hypoxia. Low oxygen levels have been shown to be associated with poor local control and survival after radiotherapy *(Brizel et al., 1997, Kaanders et al., 2002, Nordsmark et al., 2005)*. Tumour hypoxia has also been shown to promote genetic instability, driving the tumour towards a more malignant phenotype by stimulating the invasion of tumour cells and, therefore, metastasis *(Harris, 2002)*. Mutations of key regulatory genes that are induced or promoted by hypoxia can select tumour cells with

an increased resistance to treatment, resulting in an overall adverse clinical outcome *(Koumenis, 2006)*. Hypoxia acts as a trigger for changes in gene expression to stimulate angiogenesis, glucose transport, pH regulation and erythopoiesis *(Semenza, 2003)*. Toustrup et al. *(Toustrup et al., 2011)* identified 15 genes that were upregulated in hypoxic conditions in HNSCC *in vivo.* Recently, Eustace et al. *(Eustace et al., 2013)*, in a study of 157 patients with T2-T4 laryngeal cancer, successfully used a 26-gene hypoxia signature to identify laryngeal tumours that would benefit from hypoxia-modifying therapy with carbogen and nicotinamide during the radiotherapy course. In those tumours that demonstrated increased expression of the hypoxic genes, the five-year regional control rates were 100% in those tumours treated with hypoxia modifying therapy compared to 81% in those treated with radiotherapy alone.

Radioresistance due to hypoxia can be reduced by fractionation of the radiotherapy dose, which enables reoxygenation to occur, i.e. the death of some tumour cells by a fraction of radiotherapy may lead to the improved oxygenation of other cells as they are brought closer to the oxygen supply, in time for the next fraction.

Tumour proliferation is an important factor in determining the outcome of radiotherapy as shown by studies that demonstrated a reduction in tumour control with an increase in overall treatment time *(Withers et al., 1988, Bentzen and Thames, 1991)*. HNSCC demonstrated an accelerated repopulation with an increase in doubling time and growth fraction at four to five weeks after commencing radiotherapy *(Withers et al., 1988)*. Dorr et al. *(Dorr et al., 2002)* demonstrated that accelerated repopulation in HNSCC commences as early as one week after the initiation of radiotherapy. Prolongation of radiotherapy treatment results in repopulation of stem cells that have survived the treatment. This is the justification for accelerated fractionation or hyperfractionation, which involves altering the fractionation regime so that the same total dose of radiotherapy is delivered, but that the overall treatment time is shortened.

Proliferation is dependent on a number of factors, such as differentiation status, cell-cycle gene regulation and microenvironmental factors, including oxygen and nutrient availability. As hypoxia delays progression of the tumour cell through the cell cycle, cells that retain proliferative capacity under hypoxic conditions might, therefore, represent an important clonogenic subpopulation of tumour cells that are responsible for treatment failure *(Hoogsteen et al., 2005)*.

A key marker of proliferation in HNSCC is EGFR (see section **1.5.6**), which is an important stimulator of cell growth and other key biological processes *(Silva et al., 2007)*. EGFR overexpression occurs in approximately 90% of HNSCC tumours (*Grandis and Tweardy, 1993)* and is associated with with a poor response to radiotherapy *(Gupta et al., 2002, Mendelsohn and Baselga, 2003, Eriksen et al., 2004).* Ang et al. *(Ang et al., 2002),* in a study of 155 HNSCC patients, demonstrated that EGFR overexpression was a strong prognostic indicator of reduced overall and disease-free survival and of locoregional relapse.

Reassortment refers to the point of the cell cycle that the cells are in when the fraction is given. The phase in mitosis at the time of radiotherapy is important in determining radiosensitivity *(Begg AC, 2002).* With ionising radiation, the maximum resistance is in S phase and the greatest sensitivity is in M and G_2. The effect of cells progressing through the cell cycle in between fractions is that cells that survived the first fraction due to being in a resistant phase of the cell cycle may be in a more sensitive phase at the next fraction.

The initial treatment in a fractionated course of radiotherapy may, after a period of mitotic arrest, lead to cell-cycle synchrony and, if the next treatment is given when the cells are in a sensitive phase of the cycle may lead to increased cell kill. However, although this has been demonstrated in research, in the clinical setting it is difficult to manipulate the cell cycle to improve results *(Goodhead, 1994).*

In HNSCC there is a discrepancy between the volume doubling time i.e. the time taken for the tumour to double in size and the median potential doubling time (i.e. the time within which the dimensions of a tumour would double if no cells were lost). The volume doubling time is between 40 and 80 days and the median potential doubling time for well-differentiated tumours is between 6.4 and 7.8 days *(Begg et al., 1999).* This discrepancy can be explained by cell loss due to desquamation; cell loss of around 95% is characteristic of HNSCC. This cell loss has important implications for treatment. A 1 cm diameter tumour contains approximately 10^9 cells; without cell loss, this size would be achieved in 30-35 generations. With cell loss, however, it could take up to 1000 generations to reach this size. The increased number of cellular divisions increases the chance of a mutation occurring, which could result in radioresistance.

Cell loss can, therefore, exaggerate the response to treatment. Modest reductions in the number of clonogenic cells present will, through the amplificatory effect of cell loss, produce rapid shrinkage of the tumour. The underlying problem, however, is the presence of

radioresistant cells, which will continue to grow throughout treatment, imperceptibly at first to ultimately dominate the tumour mass *(Munro AJ, 2008)*.

Several genetic factors have been implicated in determining the tumour tissue's intrinsic radiosensitivity i.e. the cellular response to radiation-induced DNA damage e.g. KU70, X-ray repair cross-complementing protein (XRCC5), DNA-dependent protein kinase (DNA-PK), ataxia-telangiectasia mutated (ATM), RAD51 and XRCC3 *(Silva et al., 2007)*. Radioresistance is also thought to be due, in part, to an imbalance in the expression and pro- and anti-apoptotic genes as well as the tumour suppressor gene p53. Promoters of apoptosis include B-cell lymphoma associated x-protein (bax), bak, bcl-X(S), bad and bid and inhibitors include B-cell lymphoma (bcl-2), bcl-X(L) and bcl-w, which is a member of the bcl-2 family *(Nikitakis, 2004)*. Nix et al *(Nix et al., 2005)* demonstrated that expression of the anti-apoptotic genes bcl-2 and bcl-X(L) and the downregulation of bax were associated with radioresistant laryngeal tumours.

Activation of the PI3K/AKT pathway (as in **Chapter 1.5.6**), which occurs in up to 90% of HNSCC cases, is associated with three major radioresistance mechanisms: intrinsic radioresistance, tumour cell proliferation and hypoxia *(Bussink et al., 2008)*. Activation of this pathway is due to several genetic alterations. In their study of 117 HNSCC tumours, Pedrero et al. *(Pedrero et al., 2005)* demonstrated amplification of the PIK3CA gene in 37% of specimens, AKT2 gene amplification (30%), PTEN downregulation (4%) and P110alpha downregulation (1%).

Other genes have been identified as causing radioresistance in HNSCC. Through the use of proteomics in radioresistant HNSCC cell lines, Lin et al. *(Lin et al., 2010)* identified 64 proteins and six genes that are potentially involved in radioresistance in HNSCC, with the upregulation of Gp96, Grp78, heat shock protein-60 (HSP60), Rab40B and growth differentiation factor-15 (GDF-15) and the downregulation of annexin V. Williams et al. *(Williams et al., 2011)* used a 41-gene model to identify genes implicated in radioresistance in a radioresistant cell line. They demonstrated that cyclophilin B (PPIB) had the strongest correlation with radioresistance and that it was associated with a significant decrease in overall five-year survival following radiotherapy (PPIB +ve tumours 50% cf. PPIB –ve tumours 100%). In addition to this, they also demonstrated correlation with several other genes that have previously been implicated in radioresistance: Harvey rat sarcoma (HRAS)

(McKenna et al., 1990a), myelocytomatosis (MYC) *(McKenna et al., 1990b)* and nuclear factor kappa beta (NFκB) *(Karin et al., 2004)*.

1.11.5 DNA repair mechanisms

Radiation-induced DNA damage is divided into direct, which is caused by high linear energy transfer (LET) radiation, and indirect effects. Indirect damage arises from energy deposited in water molecules surrounding the DNA, which forms free radicals, notably hydroxyl radicals, which, in turn, cause DNA damage. Most photon-induced damage is caused by free radical formation *(Goodhead, 1994).*

Many cellular structures are at risk of damage by radiotherapy including:

- Direct damage to the DNA base or sugar,
- DNA-protein crosslinks and DNA-DNA crosslinks,
- DNA single-strand break or DNA double-strand break, the latter of which is a lethal event for a cell.

DNA strand breaks may also have different types of DNA damage in their proximity e.g. DNA sugar or base damage, which are known as clustered damage and are a significant factor in radiation-induced cell death. An increase in the number and the complexity of these cluster damage events impairs a cell's ability to undergo DNA repair *(Goodhead, 1994).*

Following a DNA strand break, a cell will attempt repair. Initially the damaged termini undergo a cleansing process to leave clean ligatable ends, a process carried out by phosphodiesterase and kinase enzymes. In the event of a single-strand DNA break, the nuclear protein poly (ADP-ribose) polymerase-1 (PARP-1) interacts with XRCC1 which, in turn, interacts with the gap filling DNA polymerase B and DNA ligase III. These interact to perform base excision and to seal the resultant nick *(Lindahl et al., 1995).*

The repair process for a single-strand DNA break does not work in the event of a double-strand break as, after the cleaning of the termini, a straightforward ligation would lead to a change in the DNA sequence, as the damaged bases would have been removed, resulting in frameshift of the DNA. Therefore, in order to repair a double-strand break, a cell must utilise one of the two main pathways: non-homologous end joining (NHEJ) and homologous

recombination repair (HRR). NHEJ begins with the recognition of the DNA break by the Ku heterodimer, which subsequently binds to the broken ends. Once bound, the Ku heterodimer recruits the catalytic subunit of the DNA-PK_{CS} to the DNA ends, resulting in stimulation of the kinase activity. HRR can only take place if there is an undamaged copy of the DNA present, i.e. after DNA replication has taken place in late S phase, G_2 phase or in early mitosis. The DNA break is detected by ATM / ataxia-telangiectasia and Rad3-related (ATR) gene products as well as the Mre11, Rad50 and Nbs1 (MRN) complex *(Lee and Paull, 2004)*, which signal numerous other molecules, including p53, which to induces cell cycle arrest. The protein Rad52 binds to the broken ends which may then recruit proteins for homologous recombination, including Rad51 and possibly XRCC2 and XRCC3 *(Van Dyck et al., 1999)*. Rad51 can then catalyse pairing and strand exchange between homologous molecules to form heteroduplex DNA. The generation of intact DNA molecules is established through the action of a polymerase, a resolvase and a ligase which synthesise new DNA, unravel the complex and ligate the ends *(McMillan, 2002)*.

1.11.6 Cancer stem cell theory

Cancer stem cells (CSC) have previously been isolated in HNSCC *(Prince, 2008, Chen, 2009)* as well as other tumour types. They are defined as a small subpopulation of self-sustaining cancer cells with an ability to cause the heterogenous lineages of cancer cells via two main hypothesised methods: hierarchical and stochastic (**Figure 8**) *(Clarke et al., 2006)*. CSC demonstrate three main characteristics:

- The cell must demonstrate potent tumour initiation, capable of regenerating the tumour from a few cells. Prince et al. *(Prince et al., 2007)* reported that as few as 5000 $CD44^+$ HNSCC cells could generate tumours in knockout mice, whilst Chiou et al. *(Chiou et al., 2008)*, in their study using the marker $CD133^+$, stated that tumour regeneration could occur from as few as 1000 HNSCC cells.

- The cell must also be able to demonstrate self-renewal *in vivo*.

- The cell must demonstrate a differentiation capacity, enabling the production of heterogenous progeny, which represent a phenocopy of the original tumour *(Ward and Dirks, 2007, Chen, 2009)*. It was originally thought that CSC were normal endogenous tissue stem cells, however, Monroe et al. *(Monroe et al., 2011)* stated

that the accumulation of genetic mutations within a differentiated or progenitor cell could enable stem cell behaviour, providing an alternative source of CSC.

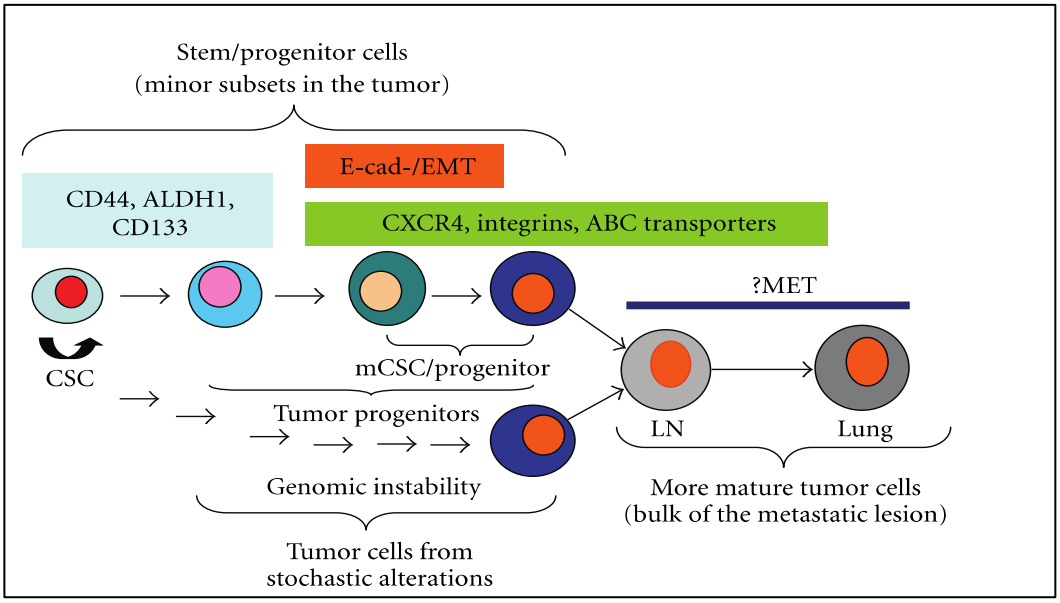

Figure 8. Hierarchical and stochastic models of CSC in progression of solid tumours *(Chen, 2009)*

CSC have also demonstrated significant radioresistance in several tumour types, including HNSCC *(Diehn and Clarke, 2006, Bao et al., 2006, Baumann et al., 2008, Al-Assar et al., 2009, McCord et al., 2009, Damek-Poprawa et al., 2011)*. This has significant implications in the treatment of HNSCC as current treatment modalities allow resistant CSC to reinitiate the tumour *(Frank et al., 2010)*. The number of CSC varies depending on the size of the tumour mass i.e. there will be 1000 times fewer clonogenic cells in a tumour 5 mm in diameter compared to a mass 5 cm in diameter *(Tubiana, 1988)*. Another factor, is the number of CSC that are killed for a given radiotherapy dose. A tumour mass measuring 20 mm treated with 66-70 Gy in 2 Gy fractions will provide 90% tumour cell kill. However, a similar dosage may only treat 50% of the cells in a mass measuring 5cm *(Munro AJ, 2008)*.

Various markers have been used for identification of CSC, including the biomarkers CD44, aldehyde dehydrogenase (ALDH), CD133 and c-Met, along with stemness markers, such as sex determining region Y-box 2 (SOX2) and B lymphoma Mo-MLV insertion region 1 homolog (Bmi-1) *(Major et al., 2013)*. As well as markers, the ability of CSC to form spheres *in vitro*, has been used to identify populations of cells containing CSC. In HNSCC, the markers CD44, Oct-4, Nanog, Nestin and CD133 have all been demonstrated on isolated

from spheres *(Chiou et al., 2008, Okamoto et al., 2009, Zhang et al., 2010).* The current gold standard for the identification of CSC as suggested by the American Association for Cancer Research (AACR) Workshop on Cancer Stem Cells in 2006 is the orthotopic xenograft assay. Cancer cells from either tumour cells or cell lines are initially sorted by specific cell surface markers. The selected cell population is then injected into experimental animals for tumorigenesis testing *(Clarke et al., 2006).*

Currently, no CSC markers are measured in the assessment of post-radiotherapy response in HNSCC; the current methods of assessment are based upon measuring tumour shrinkage through radiological imaging *(Dalerba et al., 2007, Sayed et al., 2011).* However, Rasheed et al. *(Rasheed et al., 2011)* proposed that, given the major role that CSC play in radioresistance, perhaps it is time to incorporate CSC measurement into the post-radiotherapy assessment.

1.11.7 Radiotherapy and chemotherapy

In the treatment of more advanced (T3 and T4) laryngeal and oropharyngeal tumours, the combination of chemotherapy and radiotherapy has been proven to enhance HNSCC tumour control within the irradiated field *(Aisner et al., 1994).* Chemotherapy can be used in conjunction with radiotherapy in one of three ways: neoadjuvant, concurrent or adjuvant. As a neoadjuvant therapy it can be used to reduce tumour size prior to radiotherapy and as an adjuvant therapy it can be used to treat micrometastatic disease after the primary has been treated with radiotherapy. Concurrent chemoradiotherapy involves treating patients with chemotherapy agents at the time of radiotherapy administration. Whilst this provides the greatest survival benefit, it is also associated with increased side effects, so can only be undertaken in fit patients *(Seiwert et al., 2007).*

The main chemotherapy agents used in the treatment of HNSCC are cisplatin, 5-fluorouracil and docetaxel. Cisplatin crosslinks with the DNA base guanine, which interferes with mitosis. Inhibition of the DNA repair mechanisms by cisplatin causes the cell to enter apoptosis *(Fuertes et al., 2003).* 5-fluorouracil (5-FU) acts primarily as a thymidylate synthase inhibitor, blocking thymidine, which is required for DNA replication, leading to cell cycle arrest and apoptosis *(Longley et al., 2003).* Docetaxel binds to microtubules, preventing their disassembly. This leads to a significant decrease in the levels of free tubulin, which is required for further microtubule formation, resulting in the inhibition of mitotic cell division

between metaphase and anaphase, preventing further cancer cell progeny *(Lyseng-Williamson and Fenton, 2005).*

In 2009, the Meta-analysis of Chemotherapy on Head and Neck Cancer (MACH-NC) *(Pignon et al., 2009)* collaborative published a meta-analysis of 93 randomised trials with 17,346 patients and demonstrated that concurrent chemoradiotherapy resulted in a 4.5% improvement in five-year overall survival rates compared to radiotherapy alone. In their study of different chemotherapy regimens, Posner et al. *(Posner et al., 2007),* in a study of 501 patients, demonstrated significantly increased survival rates in patients with stage III or IV HNSCC disease using the TPF regimen (docetaxel, cisplatin and 5-fluorouracil) compared to the PF regimen (cisplatin and 5-fluorouracil) combined with radiotherapy. The overall three-year survival rate increased from 48% to 62% with improved locoregional control.

EGFR has been demonstrated in up to 90% of HNSCC cases *(Grandis and Tweardy, 1993).* Cetuximab, a monoclonal antibody against EGFR, in conjunction with radiotherapy has shown improved overall five-year survival compared to treatment with radiotherapy alone (radiotherapy alone 35.6% cf. 45.6% cetuximab plus radiotherapy) *(Bonner et al., 2006, Bozec et al., 2013).*

1.11.8 Radiotherapy and surgery

Radiotherapy may be used as an adjuvant therapy in the treatment of HNSCC i.e. administered after surgery. This is indicated if there is residual disease near to the surgical margin or if there has been extracapsular spread of disease from lymph node metastases *(Mendenhall et al., 2006).* The interval between surgery and radiotherapy should be minimised as it has been shown that the growth factors in an operative field will stimulate tumour growth, making it more difficult to treat later on. There is a greater chance of post-radiotherapy morbidity as a result of the previous surgery and as evidence now suggests that these patients should receive combination therapy with chemotherapy, morbidity may be greater still *(Bernier et al., 2005).*

1.11.9 Intensity-modulated radiation therapy

Intensity-modulated radiation therapy (IMRT) is an advanced form of high-precision radiotherapy that has revolutionised the treatment of HNSCC. The use of computer-controlled linear accelerators allows for the radiation dose to conform more precisely to the three dimensional shape of the tumour by controlling the intensity of the radiation beam in multiple small volumes. Combinations of multiple-modulated fields coming from different beam directions produce a customised radiation dose that maximises tumour dose, whilst minimising the dose to adjacent normal tissues. As the radiotherapy dose to normal tissues is minimised, higher and more effective radiation doses can be safely delivered to the tumour with fewer side effects and reduced treatment toxicity *(Lee et al., 2007).*

1.12 Mechanisms of radiation-induced cell death

There are three methods of radiation-induced cell death: apoptosis, mitotic catastrophe and senescence *(Eriksson and Stigbrand, 2010).* In HNSCC, as with other solid tumours, mitotic catastrophe and senescence, a form of proliferative cell death, play a greater role than apoptosis in the response of the tumour to radiotherapy *(Ianzini et al., 2006).* The tumour suppressor gene tumour protein 53 (p53) plays an important role in determining the cellular response to radiation. As a transcription factor, it fulfils its tumour suppressor role by acting via four pathways: cell cycle arrest, DNA repair, apoptosis and senescence. Following irradiation, p53 activation promotes cell survival by growth arrest and DNA damage repair. If the DNA damage is deemed to be too severe to repair, p53 will initiate apoptosis or senescence *(Helton and Chen, 2007).* The outcome of the cell is governed by three factors in relation to p53: the amount of activated p53, the duration of its activation and the availability of p53 co-factors, which regulate the binding of p53 to specific target genes, *(Das et al., 2007, Tanaka et al., 2007, Das et al., 2008).* In the presence of increased levels of p53 and readily available apoptotic genes, a damaged cell will preferentially undergo apoptosis rather than senescence. Tumour cells that are classed as radiosensitive express increased levels of basal p53 mRNA compared to radioresistant cells, which promotes radiation-induced apoptosis *(Eriksson and Stigbrand, 2010).*

A cell with impaired activation of p53-dependent DNA damage checkpoints can undergo abnormal cell division following exposure to genotoxic damage. This may lead to aneuploidy

and subsequent tumour progression. However, these cells typically undergo mitotic catastrophe following irradiation *(Storchova and Pellman, 2004, Erenpreisa and Cragg, 2007, Ganem and Pellman, 2007, Ganem et al., 2007).*

1.12.1 Apoptosis

Apoptosis plays a role in the response of HNSCC tissue to radiotherapy, that role has been described as modest compared with haematological malignancies where it is the major mechanism of radiation-induced cell death (**Figure 9**) *(Radford et al., 1994, Jonathan et al., 1999).* This is due to the fact HNSCC tumours, as well as other solid tumours, lose their pro-apoptotic mechanisms during progression; p53 is impaired in over half of all human malignancies *(Hollstein et al., 1991, Soussi and Beroud, 2001, Soussi and Lozano, 2005).* Even if a tumour cell maintains a functional p53 pathway, the basic mechanisms required for apoptosis are often absent. In HNSCC, a tumour cell's ability to undergo apoptosis is further confounded by the overexpression of anti-apoptotic proteins, such as Bcl-2 and survivin, or the inactivation of pro-apoptotic proteins such as Bax and apoptotic protease activating factor 1 (Apaf1) *(Igney and Krammer, 2002).*

There are two apoptotic pathways, the intrinsic and extrinsic pathway, both of which can be initiated by exposure of a HNSCC cell to radiation. The intrinsic pathway, also known as the mitochondrial pathway, initially involves mitochondrial outer membrane permeabilisation (MOMP), which is controlled by members of the Bcl-2 family. This family is divided into pro-apoptotic and anti-apoptotic members. The pro-apoptotic members comprise two subfamilies, the Bax-like family (Bax, Bak, Bok) and the BH3-only proteins (Bid, Bad, Bim, Bik, Bmf, Noxa, Puma, Hrk). In order to form Bax-Bak pores in the mitochondrial outer membrane to enable MOMP to occur, both subfamilies need to be present *(Jin and El-Deiry, 2005).* Irradiation of a cell causes p53-mediated activation with the initiation of apoptosis mediated by Bax and members of the BH3-only subgroup *(Zhan et al., 1994, Findley et al., 1997, Kobayashi et al., 1998).* Genes encoding for proteins that localise to the cytoplasm including p53-inducible death domain (PIDD) can also be upregulated following irradiation *(Lin et al., 2000).* Genes that lower the threshold for apoptosis can act in conjunction in order to induce apoptosis: Apaf1, caspase-6 and BH3 interacting domain (Bid) *(Fei and El-Deiry, 2003).* Blockage of apoptosis occurs via the anti-apoptotic members of the Bcl-2 family (Bcl-2, BCl-XL, Bcl-W, Mc11, Bcl2A1, Bcl-B). Downregulation of the Bcl-2 gene *(Haldar et al.,*

1994, Miyashita et al., 1994) and inhibition of survivin *(Hoffman et al., 2002, Zhou et al., 2002)*, an apoptosis family member are mediated by p53 in order to promote apoptosis.

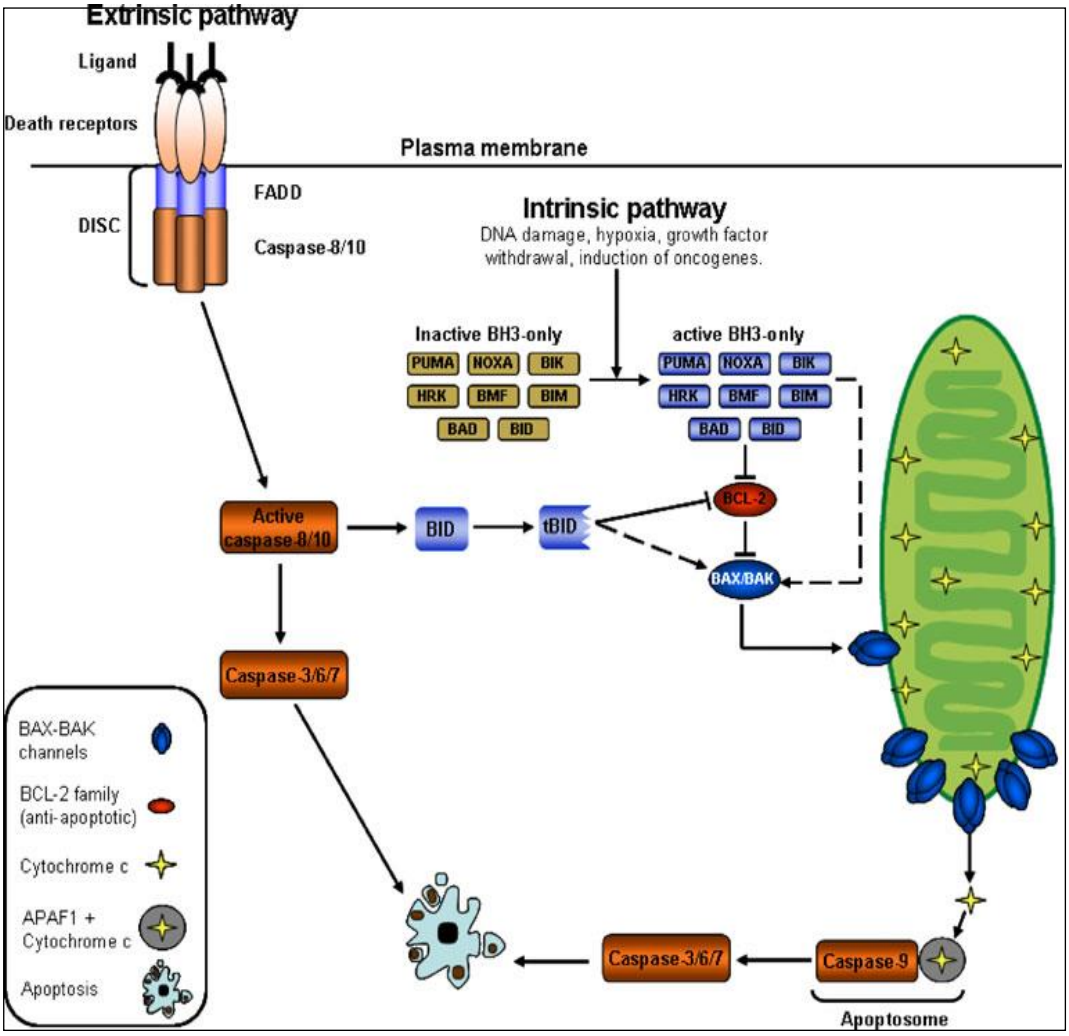

Figure 9. Schematic diagram illustrating the extrinsic (death-receptor-mediated) and intrinsic (mitochondria-mediated) pathways of apoptosis. Irradiation of a cell can activate both pathways *(Eriksson and Stigbrand, 2010).*

MOMP releases several potentially lethal proteins from the intermembrane space of the mitochondria into the cytoplasm *(Wang, 2001)* such as cytochrome c, second mitochondria-derived activator of caspases (SMAC/DIABLO), apoptosis-inducing factor (AIF), endonuclease G (EndoG) and OMI/HTRA2 *(Riedl and Shi, 2004)*. The most important of these is cytochrome c as it binds and activates Apaf1, enabling it to bind ATP/dATP *(Jiang and Wang, 2000)*, the resultant combination being known as the apoptosome, which activates the initiator caspase, caspase-9 *(Li et al., 1997, Rodriguez and Lazebnik, 1999).* Caspase-9 activates the effector caspases, caspase-3/6/7 *(Eriksson and Stigbrand, 2010).*

The extrinsic pathway, often referred to as the death receptor pathway requires ligand-dependent activation of plasma membrane receptors from the tumour necrosis factor (TNF) receptor superfamily. The expression of TNF death receptor family members Fas/CD95 *(Sheard et al., 1997, Kobayashi et al., 1998, Embree-Ku et al., 2002, Sheard et al., 2003)* and death receptor 5/TNF-related apoptosis-inducing ligand (DR5/TRAIL) receptor 2 *(Wu et al., 1997, Sheikh et al., 1998, Burns et al., 2001, Alvarez et al., 2006),* are upregulated by radiation, activating caspases by both mitochondria-dependent and independent mechanisms *(Kastan, 1997, Scaffidi et al., 1998).*

Interaction between specific ligands and the death receptor induces receptor-proximal recruitment of the death-inducing signalling complex resulting in activation of caspase-8/10 and subsequently effector caspases-3/6/7 *(Taylor et al., 2008).* In cells in which the initial level of caspase-8/10 activation is low, an amplification loop is triggered *(Scaffidi et al., 1998),* which results in the cleaving and activation of Bid by caspase 8/10. This, in turn, causes the release of cytochrome c from the mitochondria, which activates caspase-9 and -3, which significantly increases the initial apoptotic signal *(Luo et al., 1998).*

Caspases are a family of proteases that are involved in both the intrinsic and extrinsic apoptotic pathways, both of which can be activated by exposure of the cell to radiation *(Riedl and Shi, 2004, Timmer and Salvesen, 2007).* The activation of either apoptotic pathway results in the activation of the effector caspases-3/6/7, which are responsible for the demolition phase of apoptosis, targeting mediators and regulators of apoptosis, structural proteins, such as cytokeratins, cellular DNA repair proteins and cell-cycle-related proteins *(Jin and El-Deiry, 2005).*

1.12.2 Mitotic Catastrophe

Mitotic catastrophe (MC) is the main method of cell death in HNSCC and other solid tumours and occurs two to six days following irradiation *(Ruth and Roninson, 2000, Vakifahmetoglu et al., 2008).* Maalouf et al. *(Maalouf et al., 2009)* demonstrated MC in two HNSCC cell lines following irradiation. MC is defined in morphological terms as a mechanism of cell death which occurs during or after a cell's premature or incorrect entry into mitosis. This leads to atypical chromosome segregation and cell division, resulting in the formation of giant cells with aberrant nuclear morphology *(Eriksson et al., 2003, Castedo and Kroemer, 2004,*

Eriksson et al., 2007) multiple nuclei *(Erenpreisa et al., 2005, Eriksson et al., 2007),* or micronuclei and decondensed chromatin *(Roninson et al., 2001).* Cell death as a result of MC can be apoptotic, either caspase-dependent or caspase-independent, or necrotic (**Figure 10**) *(Vakifahmetoglu et al., 2008).*

There are two main theories as to the mechanisms by which MC occurs: Firstly, mitotic catastrophe occurs as a result of DNA damage and defective cell cycle checkpoints, which require p53-dependent and independent mechanisms to function. In order for radiation-induced DNA repair to occur, a cell must enter and maintain cell cycle arrest, which requires p53 (as in **Chapter 1.11.5**). The inactivation of p53, which is inherent in tumour cells, results in a deficiency in the cell cycle checkpoints, particularly the G2/M checkpoint, which allows the cell to enter mitosis prematurely with unrepaired DNA, which promotes MC *(Ianzini et al., 2006).*

The second mechanism is that MC occurs due to the hyperamplification *(Kawamura et al., 2004, Kawamura et al., 2006, Eriksson et al., 2007, Bourke et al., 2007, Dodson et al., 2007))* or overduplication *(Sato et al., 2000)* of centrosomes, which leads to multipolar mitosis, resulting in abnormal chromosomal segregation, which creates cells with multiple micronuclei or binucleated giant cells *(Eriksson et al., 2008, Wang et al., 2009),* which leads to MC *(Castedo et al., 2004).*

Once the cell has undergone MC, a delayed form of apoptosis ensues. During mitotic catastrophe, the cell enters a transient G2 arrest, but then progresses to mitosis prematurely. The mitotic checkpoint, known as the spindle assembly checkpoint, is subsequently activated and progression through mitosis is delayed *(Jallepalli and Lengauer, 2001).* This delay in mitosis may be permanent and fatal due to activation of the apoptotic pathways.

However, cells can adapt to the mitotic checkpoint and avoid death during metaphase. These cells exit cell cycle arrest, but fail cytokinesis and enter the next G1 phase with a tetraploid DNA content *(Weaver and Cleveland, 2005, Yamada and Gorbsky, 2006).* Although these cells can survive for days, they eventually die by delayed necrosis, delayed apoptosis or induced senescence *(Rieder and Maiato, 2004).* Apoptosis in G1 is largely dependent on activation of the Bax-dependent mitochondrial pathway by p53 *(Castedo et al., 2006).* P53 can also activate p21, which causes a post-mitotic G1 arrest causing the cells to become senescent *(Roninson et al., 2001, Klein et al., 2005, Blagosklonny et al., 2006).* Cells deficient in p53 will enter another round of DNA amplification, resulting in the cells becoming

aneuploid or polyploid *(Casenghi et al., 1999, Klein et al., 2005)*. These cells may continue through several cycles of division (endoreplication), but will eventually succumb to delayed apoptosis or necrosis *(Maalouf et al., 2009).*

The majority of evidence for the biology of MC is based on observations from monolayer cells and, although these function well as models, extrapolation to three-dimensional structures should be performed with caution *(Indovina et al., 2007)*. Vakifahmetoglu et al. *(Vakifahmetoglu et al., 2008)* stated that cell-cell and cell-matrix interactions may be as important as the genomic background for the MC response, but is often neglected, a factor that microfluidic techniques can address by maintaining the tumour microenvironment.

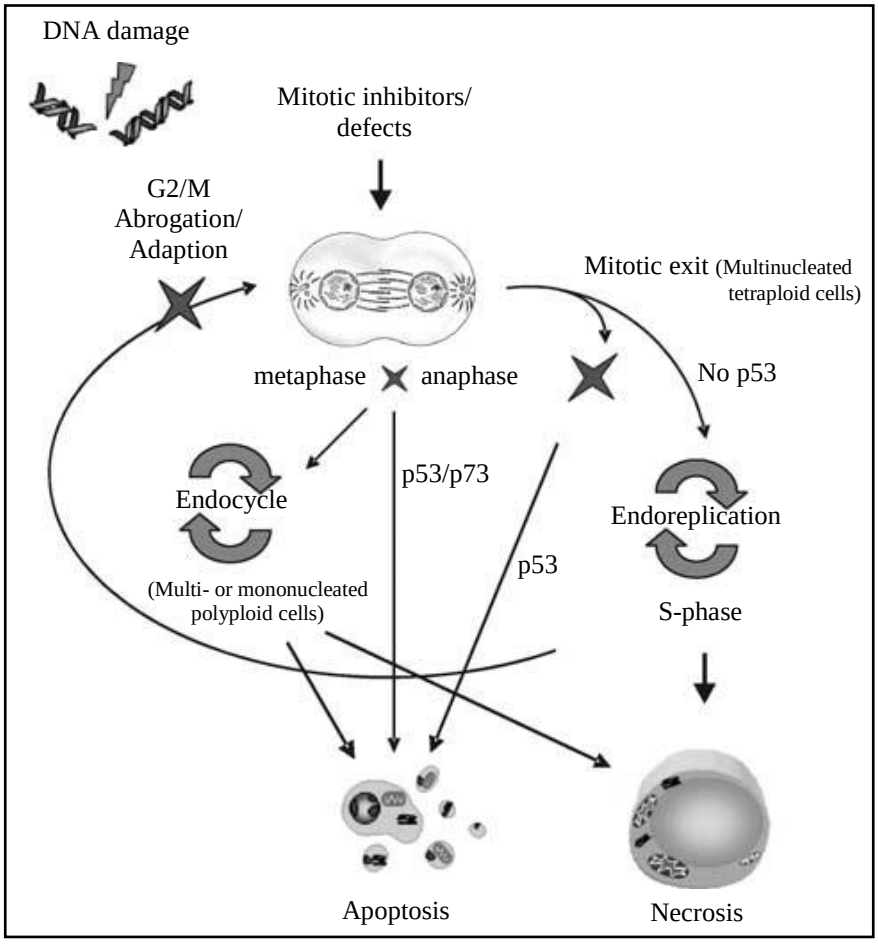

Figure 10. Schematic diagram of the pathways leading from MC to cell death *(Eriksson and Stigbrand, 2010).*

1.12.3 Senescence

Senescence has been demonstrated in HNSCC cells *(Bian et al., 2012, Gan et al., 2012)* and refers to a state of permanent cell cycle arrest, which acts as a growth retardation mechanism in response to radiotherapy, preventing the propagation of damaged DNA to the next cell generation *(Eriksson and Stigbrand, 2010)*. Replicative senescence occurs in normal cells that

have reached their proliferative limit as a consequence of telomere shortening *(Roninson et al., 2001)*, a factor which tumour cells can overcome by expressing the ribonucleoprotein telomerase, which reverses telomere shortening *(Wright and Shay, 2001).* Accelerated senescence occurs in response to DNA damage independently of telomere shortening *(Suzuki et al., 2001).* Both forms of senescence display similar cellular phenotypic characteristics: flattened and enlarged cells with increased granularity *(Hayflick and Moorhead, 1961, Stein and Dulic, 1995, Roninson et al., 2001).*

Senescence causes extensive alterations in gene expression, inhibiting several genes involved in cell proliferation and inducing several intra- and intercellular growth inhibitors *(Chang et al., 2002).* Both p53/p21 and p16/retinoblastoma protein (pRB) are responsible for the initiation and maintenance of senescence respectively *(Sugrue et al., 1997, Dai and Enders, 2000, Steiner et al., 2000, Zhang, 2007).* Gadhikar et al. *(Gadhikar et al., 2013)* and Skinner et al. *(Skinner et al., 2012)* demonstrated that senescence is p53-dependent. Gadhikar et al. demonstrated that a mutation in wild-type p53 leads to inhibition of the Chk1/2 kinases, which are necessary for the mediation of the DNA damage response to radiotherapy. Skinner et al. demonstrated a significant correlation between radiation-induced senescence and *in vitro* radiosensitivity and that senescence was inhibited by a disruptive p53 mutation in HNSCC cells. Accelerated senescence has, however, been reported to occur in the absence of p53, p21 or p16 indicating that other genes are involved in the process *(Shay and Roninson, 2004).*

Whilst senescent cells do not divide, they do remain metabolically active. It has been demonstrated that they overexpress and secrete tumour suppressing and promoting factors, including a number of cytokines that promote growth arrest and allow communication between senescent cells and their microenvironment *(Rodier et al., 2009, Coppe et al., 2010, Novakova et al., 2010)*, which is maintained by using microfluidic devices. This communication has been reported to promote angiogenesis, stimulate tumour cell growth and invasiveness and induce an inflammatory response *(Eriksson and Stigbrand, 2010).*

1.13 *In vitro* techniques to study HNSCC

1.13.1 Cell culture

HNSCC cell culture is important as it allows a population of HNSCC cells to be investigated and provides a preclinical model which can be used to search for novel and targeted therapies to treat HNSCC *(Lin et al., 2007).*

In 1981, three studies demonstrated that HNSCC cell lines could be reproducibly established in culture using the explant outgrowth and enzyme digestion methods *(Easty et al., 1981, Krause et al., 1981, Rheinwald and Beckett, 1981),* the former being the main method by which cell lines are established by current investigators *(Sacks, 1996).*

The primary explant method involves the outgrowth of cells from a small tissue fragment adherent to a growth surface such as a plasma clot or an extracellular matrix constituent e.g. collagen. Cells in the outgrowth are selected by their ability to migrate from the explant and those isolated in subculture because of their proliferative abilities. Disaggregation of the tissue, either by mechanical or enzymatic means, results in a suspension of cells and small aggregates, of which a proportion will attach to a solid substrate to form a monolayer. The cells within this monolayer, which are capable of proliferation, will be selected at the first subculture and may result in a cell line. Tissue disaggregation is capable of generating larger cultures more rapidly than explant culture, but explant is preferable if only small fragments of tissue are available or if the cells are fragile. As it is the precursor cells within a tissue that are capable of proliferation, they tend to make up the primary subculture; cell culture conditions must, therefore, by virtue of the process that produces them, favour both expansion and differentiation *(Freshney, 2010).*

It is well accepted that the major disadvantage of using cell lines to investigate HNSCC is that cell culture is a selective process and there is genetic drift due to long term culture *in vitro,* whereas HNSCC demonstrates a high level of heterogeneity. Only those cells which outgrow from an explant or attach following proteolytic dissociation of a primary tumour have the potential to grow in culture. Only those cells which survive and adapt to both the culture medium and culture techniques have the potential to grow *(Sacks, 1996).* Another disadvantage is that the cytological characterisation is lost during this process as a result of flattening of the explant with cell migration and some degree of central necrosis due to poor oxygenation *(Freshney, 2010).*

1.13.2 Organotypic culture

Organotypic culture involves growing cells in a three-dimensional environment as opposed to two-dimensional culture dishes and is a technique that has previously been used with HNSCC *(Robbins et al., 1991, Robbins et al., 1994, Eicher et al., 1996, Gutschalk et al., 2006, Chen et al., 2013, Dalley et al., 2013).* It enables the synthesis of a tissue equivalent or construct for studies of cell-cell and cell-matrix interaction and for *in vivo* implantation. In order to replicate tissue, all the cell types that present *in vivo* must be identified, cultured and recombined in the correct proportions and position, but this can be hard to verify.

Many methods of cell recombination exist ranging from allowing cells to multilayer by perfusing a monolayer *(Kruse et al., 1970)* to a highly complex perfused membrane *(Klement et al., 1987),* so called histotypic cultures. Using selective media, cloning or physical separation methods, it is possible to isolate purified cell strains from disaggregated tissue at primary culture or at first subculture. These purified cell cultures can then be combined in organotypic culture to recreate both the tissue density and cell interactions and matrix generation found in the tissue. To replicate the three-dimensional tissue structure, a scaffold is used to cultivate the cells, which promotes orderly regeneration by closely resembling the *in vivo* extracellular matrix *(Freshney, 2010).*

Organ culture involves the culture of small sized samples of tissue, normal or tumour, and enables maintenance of the normal *in vivo* histoarchitecture and diversity of cell types. Structural integrity is maintained with cells residing on *in vivo* produced extracellular matrix allowing for correct homologous and heterologous cellular interactions. Explant culture is able to overcome the problems associated with clonogenic-based assays i.e. difficulty in producing single cell suspensions and low cloning efficiencies *(Rupniak and Hill, 1980, Cobleigh et al., 1984).*

Organotypic culture methods have been used with HNSCC cells. Several of the most recent studies have used this culture technique to study the progression of normal cells to tumour cells and the behaviour of tumour cells and the factors promoting invasion. Yoo et al. *(Yoo et al., 2000)* used oral squamous cells and exposed them to a carcinogen to develop an *in vitro* HNSCC tumour progression model and were able to replicate similar angiogenic and cell cycle regulation properties of *in vitro* HNSCC. Gutschalk et al. *(Gutschalk et al., 2006)* used a three-dimensional organotypic model to demonstrate the role of granulocyte colony-stimulating factor in promoting tumour cell invasion in HNSCC. Dalley et al. *(Dalley et al.,*

2013) similarly investigated the progression of oral squamous cells from normal cells to dysplastic cells and onto malignant cells. Chen et al. *(Chen et al., 2013)* used this culture technique to demonstrate how carcinoma-associated fibroblasts promote tumour invasiveness.

This culture technique has also been used to investigate the effects of radiation on HNSCC. Tobita et al. *(Tobita et al., 2010)* used an organotypic culture system as an *in vitro* model to investigate the effects of radiation (0, 1, 3 and 8 Gy) on oral keratinocytes and demonstrated that the production of the pro-inflammatory cytokines IL-1alpha and IL-8 increased in a dose-dependent manner.

Whilst it has useful applications, organotypic culture also has its disadvantages. One of the main problems associated with organotypic culture is the diffusion of nutrients and gases into the tissue, a factor that limits specimen size. It does not incorporate physiological systems, such as vascular or nervous systems and cannot evaluate the therapeutic index of an intervention *(Benbrook, 2006)*. It has been stated also that there is an increased chance of experimental variability, given the use of different tissue fragments, which is not the case with cell lines *(De Gendt et al., 2009)*.

1.13.3 Three-dimensional culture system

Although organ/explant cultures have three-dimensional complexity, similar to *in vivo*, they lack the experimental reproducibility associated with cell culture. Three-dimensional culture systems have been developed to provide an organisational complexity that is intermediate to the culture of single cells and organ/explant cultures or *in vivo (Hoffman, 1991, Freshney, 2010)*. Three-dimensional systems offer an additional advantage in that histological-based assays can also be performed allowing structure-function studies to include cell biological, biochemical and molecular techniques, which enables the analysis of individual three-dimensional cultures at the molecular level.

Multicellular tumour spheroid (MTS) can be used as an organoid model in which tumour cells are seeded onto a membrane filter and cultured at the liquid-air interface. Cells aggregate into a three-dimensional structure, which has *in vivo*-like histoarchitecture *(Kopf-Maier, 1992)*. The culture of epithelial cells on a collagen matrix is then lifted to the liquid-air interface so that nutrients are obtained through the basal layer as *in vivo*, results in growth of a multi-layered three-dimensional skin-like epithelium, termed raft culture *(Asselineau et al.,*

1986). Physiologically, spheroids more closely resemble the *in vivo* environment compared to monolayer cells *(Mueller-Klieser, 1987, Sutherland, 1988).*

MTS have previously been used to study radiation biology, in particular, the testing of radiotherapy protocols, including dose rate and fractionation and the effects of combined therapies *(Stuschke et al., 1992, Stuschke et al., 1995).* Santini et al. *(Santini et al., 1999)* stated that future work should study radiation-induced apoptotic cell death, cell-cell interactions and cell-cycle events, which the current study will use microfluidic techniques to investigate.

Suit et al. *(Suit et al., 1990)* demonstrated an increased radiosensitivity of HNSCC spheroids compared to glioblastoma multiforme spheroids following irradiation with 6 Gy. Schwachofer et al. *(Schwachofer et al., 1991b)* subsequently demonstrated that HNSCC spheroids have a greater capacity to repair sublethal damage than neuroblastoma spheroids following irradiation with 4 Gy (75% repair cf 50%). The same group also investigated the influence of once or twice daily irradiation regimes on spheroid growth. They demonstrated that in small spheroids, growth delay was greater in twice daily regimens compared to once daily, whereas, in larger spheroids, there was no difference between the two regimens *(Schwachofer et al., 1991c).* Studies have been performed on hypoxia in HNSCC spheroids, a main causative factor of radioresistance. Schawachofer et al. *(Schwachofer et al., 1991a)* used MTS to investigate the oxygen tensions in HNSCC and neuroblastoma cells at one and five hours following irradiation with 5 and 10 Gy. No significant difference in oxygen tension was observed shortly after irradiation. More recently, Marushima et al. *(Marushima et al., 2011)* cultured HNSCC spheroids in a hypoxic microenvironment and demonstrated the key regulatory molecules that are responsible for activating the HIF-1α (hypoxia-inducible factor) pathway, which could elucidate targets for future therapies if radioresistance due to hypoxia is to be overcome.

Hirschhaeuser et al. *(Hirschhaeuser et al., 2010)* stated that spheroids generated from tumour or tissue biopsies are of growing interest in the area of individualised and patient-specific therapy. Kross et al. *(Kross et al., 2008)* used fragment spheroids of HNSCC and benign mucosa from the head and neck in a co-culture with monocytes. They demonstrated that increased cytokine levels in the supernatant were associated with tumour recurrence. A further advantage of using biopsy material is that the cultivated spheroids contain tumour progenitor stem cells, a major factor in radioresistance. Krishnamurty et al. *(Krishnamurthy et*

al., 2010) demonstrated an increased ability of self-renewal of cancer stem cells isolated from HNSCC cells, indicated by their propensity to form spheroids in suspension culture compared to controls, a characteristic that was also demonstrated by Harper et al. *(Harper et al., 2007)* and Lim et al. *(Lim et al., 2011)*. Recently, Liao et al. *(Liao et al., 2013)* used a HNSCC cancer stem cell MTS to demonstrate the susceptibility of CSC to cytotoxic T lymphocyte mediated lysis.

1.13.4 *In vitro* animal models

Animal models of HNSCC include chemically induced *de novo* cancer, syngenic animal tissue transplanted into an immunologically competent animal environment, xenogenic human tissue transplanted into an immunodeficient animal environment and transgenic models, each of which have their own advantages and disadvantages as shown in **Table 3**. There are two established systems for chemically induced *de novo* cancer: the hamster cheek pouch carcinogenesis induced by 7,12 dimethylbenz(a)anthracene (DMBA) *(Shklar, 1972)* and 4-nitroquinoline-N-oxide (4NQO) carcinogenesis of rat palate. The complete hamster carcinogenesis model (normal, premalignant and malignant buccal cells) has been established *in vitro* and characterised with respect to Polverini, Solt and colleagues *(Polverini and Solt, 1986, Polverini and Solt, 1988, Polverini et al., 1988, Solt et al., 1988, Moroco et al., 1990, Hussong et al., 1991).*

The tumorigenicity of HNSCC cell lines enables them to be used to create xenograft models, either by subcutaneous injection *(Baker, 1985)* or by direct injection into the oral cavity, which results in a tumour which is locally invasive and has metastatic potential *(Dinesman et al., 1990).*

Table 3. Summary of major advantages and disadvantages of HNSCC animal models *(Smith and Thomas, 2006).*

Classification	Advantages	Disadvantages
Chemical Carcinogenesis	Ability to study a lesion through all stages of carcinogenesis. Useful for testing carcinogenic promoters and inhibitors.	Increased time and expense until animal is testable. Lymph node metastasis uncommon.
Hamster cheek pouch First chemical carcinogenesis model for HNSCC DMBA painted onto the hamster cheek pouch	Tumour formation in 10-16 weeks.	Prolonged animal and carcinogen handling required may be hazardous to laboratory staff. Hamster cheek pouch has poor lymphatic drainage and no anatomic equivalent in human. Ectopic tumour formation in the oesophagus, stomach and lips.
Rat palate 4-NQO painted onto the rat palate *Rat tongue* 4-NQO added to rat drinking water	Evidence of field cancerisation. Histological and molecular progression of tumorigenesis is similar to human clinical disease. Decreased labour, carcinogenic exposure and animal husbandry compared with rat palate model.	Tumour formation in 20-26 weeks Tongue tumours are commonly observed concurrently. Aggressive features common to HNSCC are rarely seen in 4-NQO induced chemical carcinogenesis. Tumour formation in 20-28 weeks
Syngenic models Immortalised syngenic tumour cells transplanted into recipient animals *Subcutaneous transplantation* *Orthotopic transplantation*	Ready for study soon after transplantation Immunocompetent host allows for studies of tumour-host immune interactions Easy to follow tumour growth and monitor end points of study (e.g. tumour size) More closely resembles the local and regional aggressiveness of human clinical disease	Requires animal tumour tissue Model limited by benign growth pattern Subcutaneous tumour growth does not closely approximate human clinical disease Early tumour burden limits time period for study. Technically more difficult to measure and quantify tumour growth
Xenograft transplantation Human tumour tissue (immortalised cells or fresh tissue explants) is transplanted into recipient animals *Nude mouse – subcutaneous* *Nude mouse – orthotopic*	Allow for use of human tumour tissue Easy to follow tumour growth and monitor end points of study (e.g. tumour size) Orthotopic transplantation more closely recreates human disease with local tissue invasion and metastasis	No functional host immune system Human tumours do not metastasise and are not locally invasive when placed subcutaneously in nude mice

SCID mouse	Will accept engraftment of human lymphocytes. Cotransplantation of human tumour tissue with human lymphocytes allows study of interaction of tumour tissue with functional immune elements in an *in vivo* model	Early tumour burden limits time period of study. More difficult to quantify tumour burden and monitor efficacy of experimental manipulation if tumour burden is end-point. Low incidence of regional lymph node metastases.
Transgenic mouse models	Newer technologies may control gene expression at various stages of development through activation of mutant alleles at precise points in the developmental process	May not reflect human disease in terms of degree of gene expression during embryonic development and the expression levels of the antigen in normal tissues

1.14 Microfluidics

Earlier cell culture techniques were limited in that they were unable to accurately replicate the *in vivo* microenvironment. Conventional tissue culture methods typically supply nutrients and growth factors in batches, but as a result of cellular metabolism, nutrient levels diminish and waste products accumulate. This variation in the levels of nutrients and waste products does not imitate the tightly regulated homeostatic systems *in vivo (Walker et al., 2004, Warrick et al., 2007, Kim et al., 2007).* Given that the flow and spatial parameters which exist in tissue are very similar to those that can be achieved through microfluidic techniques, the opportunity to perform continuous perfusion of tissue samples *(Kim et al., 2006, Nevill et al., 2007)* offers a more attractive experimental approach than the turbulent fluidic conditions present in a standard batch culture system *(Yu et al., 2007).*

The benefits of microfluidic techniques for cell or tissue culture include laminar flow conditions, which enables predictable flow of fluids through the device, namely cell culture medium, small length scales, allowing for small tissue samples to be used, large surface to volume ratios, providing nutrients to a large surface area of tissue for a given volume of culture medium, in addition to portability, reusability and reduced material cost *(El-Ali et al., 2006, Meyvantsson and Beebe, 2008).* These factors, combined with unprecedented spatial and temporal control over materials entering and leaving the experimental system make the microfluidic device an extremely useful culture tool *(Takayama et al., 2003).* The ability to place a viable tissue biopsy in a microfluidic device offers the opportunity to control, probe and monitor complex cell functions in diseased and healthy tissue whilst maintaining the *in*

vivo architecture *(El-Ali et al., 2006, Weibel and Whitesides, 2006, Nakanishi et al., 2008, Puleo et al., 2007).*

The behaviour of HNSCC cells is governed by their microenvironment, which is a milieu of soluble factors, cell-matrix interactions and cell-cell contacts within an environment with specific physicochemical properties (pH, oxygen tension, temperature and osmolality). The factors present within this environment provide a set of extracellular cues that work in conjunction with each other to regulate cell structure, function, behaviour and ultimately growth, development and repair *(Young and Beebe, 2010).* Interactions between the cell and the extracellular matrix are mediated by cell surface integrins, which transduce mechanical signals to the cell's cytoskeleton, driving proliferation, differentiation and apoptosis *(Janmey and McCulloch, 2007).* The cell-matrix interactions are preserved in the current study by the use of tissue biopsy specimens, which enables maintenance of the tissue architecture. The maintenance of these cell-cell and cell-matrix interactions are imperative as they determine the fate of a cell in response to stresses such as radiotherapy *(Keenan and Folch, 2008).* Microfluidic techniques can maintain this cellular microenvironment and, by mimicking these parameters, maintain these cellular behaviours *(Kamotani et al., 2007).* Several other studies have used microfluidic techniques to study HNSCC tumour cell behaviour as shown in **Table 4**.

Various materials can be used to construct the microfluidic devices. Poly(dimethylsiloxane) (PDMS) was originally very popular due to its ease of construction, its non-toxicity to cells, its gas permeability and its excellent optical properties. However, recent work has highlighted problems with using it. It has been shown to sequester small hydrophobic molecules such as oestrogen *(Regehr et al., 2009)* and leach out uncrosslinked oligomers that bind to cell membranes. It has also been shown to interfere with cell metabolism and proliferation *(Paguirigan and Beebe, 2009).* The deformability property of PDMS has been shown to lead to undesirable sagging and bulging of microchannel walls *(Gervais et al., 2006).* By constructing the devices out of a more solid, inert substance such as glass, these problems can be overcome.

Table 4. A summary of the studies that have used microfluidic techniques to investigate HNSCC.

Author	HNSCC Tissue	Applications
Broche et al. *(Broche et al., 2007)*	Oral SCC cells compared to benign oral mucosal cells	Device for cancer cell biophysical property characterisation using dielectrophoresis. Compared to benign cells, the cytoplasmic conductivity is lower in malignant cells and a higher specific membrane capacitance.
Wen et al. *(Wen et al., 2007)*	Nasopharyngeal carcinoma cells	mRNA expressison changes in the tumour-associated genes p53, H-ras and NME1 in nasopharyngeal carcinoma cells before and after 5-FU treatment.
Gau et al. *(Gau and Wong, 2007)*	Oral SCC cells	Oral SCC diagnostics. Two salivary proteomic biomarkers (thioredoxin and IL-8) and four salivary mRNA biomarkers (SAT, ODZ, IL-8 and IL-1b) can detect oral cancer with high sensitivity and specificity.
Ziober et al. *(Ziober et al., 2008)*	Oral SCC	Biomarker based identification of oral cancer cells. 30-gene transcription profile in cancer cells isolated from oral fluid samples.
Zhang et al. *(Zhang et al., 2008)*	Nasopharyngeal carcinoma cells	On-chip oligonucleotide ligation using a series of functionalised beads to detect low-abundant point mutations in p53. Device capable of detecting one mutant p53 gene in 1000 wild-type sequences using the polymerase chain reaction.
Cho et al. *(Cho, 2009)*	HNSCC cells	Device for cancer cell biophysical property characterisation using impedance spectroscopy. Impedance differences demonstrated between HNSCC cells of different metastatic potential.
Yang et al. *(Yang et al., 2009)*	Nasopharyngeal carcinoma cells	mRNA expression changes of the tumour associated genes p53, c-myc and cyclin D1 in nasopharyngeal carcinoma cells before and after 5-FU treatment.
Tan et al. *(Tan et al., 2010)*	Tongue and pharynx cancer cells	Cell-sized based cancer cell separation device. PDMS based crescent shaped isolation wells. >80% cancer cell capture rate.
Hattersley et al *(Hattersley et al., 2012)*	HNSCC. Different primary sites and metastatic cervical lymph nodes	Glass microfluidic device used to investigate the cytotoxic effects of different chemotherapy regimens. A combination regimen containing cisplatin, 5-FU and docetaxel resulted in the greatest level of cytotoxicity compared to regimens containing 2 of the agents and a control.
Patel et al. *(Patel et al., 2013)*	HNSCC cell lines	The rapid detection of Desmolein 3 (DSG3) as a sensitive marker for lymph node metastasis using a microfluidic immunoarray platform

1.14.1 Scaling effects

Although a desirable feature of microfluidic systems is that it is scaled down to the sub-millimetre scale, it does mean that forces that were once deemed negligible become significant. Surface forces e.g. surface tension and electrostatic forces become dominant over body forces e.g. gravity, inertial forces. The ratio of surface area to volume, which is inversely proportionally to the characteristic length scale becomes significantly large, allowing a greater volume of fluid or sample molecules to interact with surfaces. The relationship between inertial and viscous forces in fluid transport is calculated by the Reynolds number:

Equation 2

Re = (inertial effect) / (viscous effect) = ρ*UL* / μ (ρ = density of fluid, *U* = average flow speed, *L* = characteristic length scale, μ = fluid viscosity)

In microfluidics, the viscosity of a fluid is the dominant force and determines flow behaviour, causing the Reynolds number to be much smaller than one, mainly due to small length scales and slow flow speeds. The most important consequence of a low Reynolds number flow is that fluid streams are driven parallel to the local orientation of microchannel walls without random fluctuations of the flow in time, so called laminar flow *(Sobek et al., 1993, Stone and Kim, 2001).*

1.14.2 Laminar flow

'This is the definitive feature of microfluidics and is characterised by a smooth, orderly motion of fluids without random temporal variations and strong dissipations of momentum and energy' *(Sato et al., 2003).*

A reduction in inertial forces allows for accurate prediction of flow fields, making it easy to control flow patterns and transport phenomena. Fluid motions in microfluidic systems operating at low Reynolds numbers are driven by externally applied pressure gradients *(Sato et al., 2003),* electro-osmosis *(Bharadwaj et al., 2002),* surface wetting *(Pollack et al., 2000, Lee et al., 2002, Hayes and Feenstra, 2003)* and interfacial tension gradients *(Bain, 2001).* In a microfluidic device, two or more miscible laminar streams are able to flow adjacent to each

other in the same direction, with only diffusive mixing occurring at the interface in the absence of transverse convective fluid motions. Each laminar stream is able to retain its chemical composition and physical contents over the short length of microchannels. This enables selective delivery of chemicals *(Delamarche et al., 1998, Takayama et al., 2001a, Takayama et al., 2001b),* proteins *(Delamarche et al., 1997, Zhao et al., 2002)* and cells *(Takayama et al., 1999)* to specific locations to form spatially directed patterns on channel surfaces. This technique is collectively known as 'laminar flow patterning' and has been utilised to study cell-cell, cell-surface and cell-medium interactions *(Folch and Toner, 2000).* Laminar flow is advantageous when investigating tumour biology as convective contributions can be negated and the supply of nutrients, gases and drugs, as well as the substances in the effluent from the device, such as soluble cytotoxicity markers as in the current study, can be controlled and understood *(Squires and Quake, 2005).*

The dimensions of the microfluidic environment are comparable to the intrinsic cellular and capillary dimensions (190μm wide and 70μm deep in the current study). Therefore, gas and drug diffusion rates, shear stress and even microscale cellular niches can be artificially recreated on chip, mimicking the physiological *in vivo* microenvironment *(Walsh et al., 2009).* Unlike other microfabricated technologies, which provide a snapshot of intermittent cellular reactions, microfluidics can provide real-time analysis *(Wlodkowic et al., 2010).*

1.14.3 Microfluidics and radiation

Previous work has addressed the administration of X-rays to microfluidic systems for X-ray diffraction and X-ray fluorescence chemical analysis. X-rays have been administered to microfluidic systems to assess the quality of crystals by X-ray diffraction *(Zheng et al., 2004a).* There have been various problems encountered during this process, especially with the material used to fabricate the microfluidic device as this can alter the amount of X-rays absorbed by the device. Glass and polydimethylsiloxane (PDMS) absorb the greatest amount of radiation, whereas polycarbonate of Bisphenol A absorbs the least *(Greaves and Manz, 2005).*

At low energy levels i.e. those within the kiloelectronvoltage spectrum, a photon can eject an electron from its host atom entirely, a process known as the photoelectric effect. This describes the emission of electrons from matter as a consequence of their absorption of the energy of the photon, electrons emitted in this manner are known as photoelectrons

(Richardson and Compton, 1912). At these energy levels, it has been stated that microfluidic chips made from borosilicate glass demonstrate such high radiation absorbance that they are inadequate for radiation analysis *(Greaves and Manz, 2005).* However, the energy levels of the radiation produced by a linac are in the megaelectronvoltage range and, therefore, the dominant effect is Compton scattering *(Compton 1925).* This describes the transference of part of the energy of an X-ray photon to an electron, which is subsequently ejected from its atom; the remaining energy being taken by the degraded photon. Therefore, at the radiation levels produced by the linac in this study, the absorbance of the glass is considered, but is not an issue.

To the best of the author’s knowledge, there are no previous studies investigating the response of HNSCC tissue biopsies to radiation in a microfluidic device.

Aims

The aim of this study was to develop a simple microfluidic device that can accurately detect the response of head and neck squamous cell carcinoma (HNSCC) biopsy samples to external beam radiotherapy. Ultimately, the aim will be to develop a tool that can be used to predict the response of an individual patient's tumour to radiotherapy prior to that patient starting radiotherapy treatment. This would offer potential benefits to both the patient and the National Health Service. For the patient it would avoid them undergoing an unnecessary treatment associated with significant morbidity and avoid the need for salvage surgery. Potentially there would be savings of time and money for the NHS.

The aim was to use rat liver to establish a tissue model, which could be used to investigate the effects of different doses of radiotherapy, administered as either a single or fractionated dose; the effects being analysed in two distinct ways. The measurement of soluble markers released by the tissue will assess cell death (lactate dehydrogenase – LDH) and hepatocyte synthetic function (albumin and urea). After being maintained in the device the tissue will be cryosectioned and haematoxylin and eosin analysis performed.

Once the tissue model has been established, the effects of different radiotherapy doses on HNSCC samples will be assessed. LDH and cytochrome-c will be measured in the effluent to assess cell death. H&E staining and immunohistochemistry will be performed on the tissue following maintenance in the device, assessing for apoptosis and DNA strand breaks in response to varying doses of radiotherapy.

Chapter 2

Materials and Methods

2.1 Design and fabrication of the microfluidic device

The microfluidic devices were fabricated in-house at Department of Chemistry, University of Hull, using photolithography techniques *(Broadwell et al., 2001, McCreedy, 2001).* AutoCAD LT software (computer-assisted design package) was used to design the microdevice from which a photomask was generated. The final device was generated in glass using standard photolithography and wet-etching techniques *(Broadwell et al., 2001).* The device consisted of two layers of glass: the top layer measuring 3mm in thickness had three holes drilled into it: one for inflow and two for outflow. A central chamber of 3mm diameter was also drilled in order to accommodate the tissue. The bottom glass layer, measuring 1mm in thickness, had a channel network etched into it to produce channels of 190µm wide and 70µm deep with one inflow channel and two divergent outflow channels. The holes drilled in the top layer married up with the channels in order to provide access to them. The two layers were then thermally bonded in a furnace at 590^{o}C for 3 h (**Figure 11**).

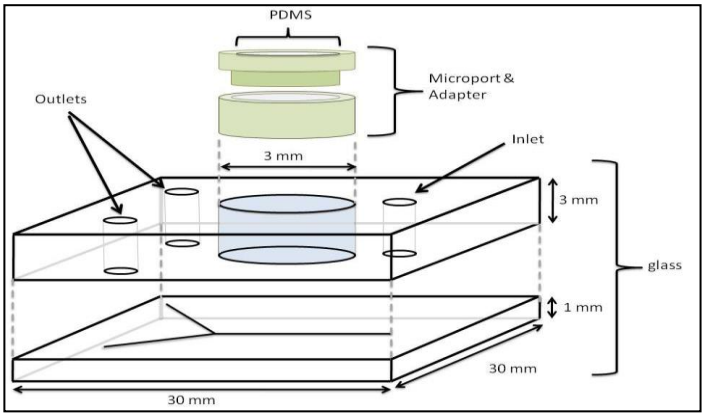

Figure 11. Schematic diagram of the microfluidic device *(Hattersley et al., 2008).*

2.2 Microfluidic system for maintaining tissue biopsies

2.2.1 Preparation of the microfluidic device

Prior to use, the glass microchips, tubing, 3-part adaptor and microport adaptor were sterilised by autoclaving at 121^{o}C for 20 minutes.

To assemble the tissue chamber, a microport (Anachem, UK) was glued to the surface of the top glass layer of the microfluidic device using Araldite Rapid Ceramic and Glass® glue (Bostik, UK) and positioned so that the drilled central chamber was at its centre. An English-threaded adaptor (Anachem) was then used to seal the tissue cavity. This adaptor was filled with poly-dimethylsiloxane (PDMS; Dow Corning, UK) to allow gaseous exchange. Polytetrafluroethylene (PTFE) tape (Draper, UK) was wound around the thread of the adaptor in order to form a watertight seal. The volume of the tissue chamber was approximately 20μL.

TFE Teflon® tubing (Anachem) with an internal diameter of 0.8mm and an external diameter of 1.58mm was used for both the inlets and outlets. The tubing was connected to the microfluidic device by gluing a trimmed yellow pipette tip to one end of it. The narrow part of the pipette tip was then pushed into the pre-drilled holes of the top glass layer so that it fitted securely. A 0.22μm syringe filter (Millipore, Watford, UK) was fitted in-line to a 20ml syringe (Becton, Dickson and Company) to remove any bacterial contamination and minimise any gas bubbles and the filter was connected to the inlet tubing via a 3-part adaptor (Upchurch Scientific, WA, USA) The syringe was then connected to a Harvard PhD 2000 syringe pump (Harvard, UK). The length of the tubing from the syringe to the device was 30cm, which allowed sufficient transit time for the medium to be heated to 37^{o}C before reaching the tissue. Outflow tubing measuring 8cm was used for the non-radiotherapy devices, whilst outflow tubing measuring 30cm was used for the radiotherapy devices as they had to pass through the drilled holes in the phantom (section 2.5). The microfluidic devices together with the outflow tubing and the majority of the inflow tubing were maintained at 37^{o}C by placing them in an egg incubator (Covatutto 24 Eco Automatic Incubator, Novital).

2.2.2 Running the microfluidic device

Once assembled the device was primed with 70% (v/v) ethanol/water by pumping through for 15 minutes at 10µl min^{-1} followed by a rinse with autoclaved, distilled water for 15 minutes at 10µl min^{-1}. Under aseptic conditions in a class II biological safety cabinet, appropriate medium was prepared as described previously (complete Williams Medium for rat liver tissue and complete DMEM for HNSCC tissue; sections 2.3 and 2.4 respectively), and added to a clean syringe before being pumped through the system for a minimum of 30 minutes at 20µl min^{-1}. Once primed, fresh tissue was divided into 5-10mg pieces using a scalpel and placed directly into the central well of the microfluidic devices under sterile conditions whereas frozen tissue samples were defrosted for two minutes and divided into 5-10mg pieces before being placed into the device. The threaded adaptor was used to seal the tissue in the culture chamber so that the ratio of chamber to tissue volume was approximately 1:0.8. The whole unit was then placed back into the 37^{o}C incubator.

The flow rate was set at 2µl min^{-1} and a visual check was made to ensure no bubbles were trapped in the chamber; any bubbles were removed using a sterile hypodermic needle. The effluent coming from the outflow tubing was collected at two hourly intervals throughout the day into a sterile 0.5ml polypropylene tube (Sarstedt, UK) with a hole fashioned in the lid. Parafilm was used to cover the hole to prevent bacterial contamination and leakage of the effluent. A single sample was collected overnight into a 1.5ml polypropylene tube and over the weekend a 15ml falcon tube was used. The two effluent samples from the outflow channels were combined and stored at 4^{o}C prior to the LDH, albumin and urea assays being performed. Cytochrome c samples were stored at -80^{o}C.

2.3 Rat liver collection and preparation

The liver was taken from Wistar rats (Wistar, B&K Universal Ltd, UK), which had been fed and watered *ad libitum* until anaesthetised (10ml kg^{-1} of 10mM sodium thiopentone, intraperitoneal) and killed under a Schedule 1 procedure prior to liver extraction. The liver was immediately sectioned into pieces approximately 1cm^3 in volume. Fresh samples were either divided into 3mm^3 pieces in a class II biological safety cabinet and placed directly into the microfluidic devices or stored in cryovials (Alpha Laboratories, UK) in Williams Media E (WME, Gibco, UK) with 18% (w/v) dimethyl-sulphoxide (DMSO), 10% (w/v) foetal bovine

serum (FBS) and penicillin/streptomycin 0.1U/ml and 0.1mg/ml respectively, before being cooled at 1^{o}C/min in a 'Mr Frosty' placed in a -80^{o}C freezer for 24 hours prior to storage in liquid nitrogen for future use.

2.4 Collection of HNSCC tissue samples

Samples were provided in an anonymous manner by patients undergoing surgery for T1-T3 head and neck squamous cell carcinoma, in accordance with Local Research Ethics Committee (LREC-10/H1304/6; AM01) and NHS Trust R&D approval (R0987), following written, informed consent, from newly presenting patients with HNSCC at the Head and Neck Surgery Dept. at Castle Hill Hospital, Hull. Tissue biopsies obtained were transported to the laboratory at 4^{o}C in Dulbecco's modified Eagle's media (DMEM, PAA Laboratories, Yeovil, Somerset, UK) supplemented with 10% (v/v) heat inactivated filtered (0.22μm filter, Millipore) foetal bovine serum (FBS), 3% (w/v) 4-(2-hydroxyethyl)-1-piperazineethanesulfonic acid (HEPES buffer, PAA), penicillin/streptomycin 0.1U/ml and 0.1mg/ml respectively (Sigma, UK), 1% (w/v) non-essential amino acids (PAA) and 0.4mM glutamine. Within 40 minutes of resection, the HNSCC tissue was cut into approximately 3mm^{3} sections under sterile conditions in a class II biological safety cabinet, each weighing between 5 and 10mg sections with minimal damage to the tissue. The weight of each individual sample was recorded. Fresh samples were either placed directly into the microfluidic devices or wrapped in aluminium foil and snap-frozen in liquid nitrogen followed by storage at -80^{o}C for future use.

2.5 Administration of radiation

Irradiation of the tissue took place at the Queen's Centre for Oncology, Castle Hill Hospital using a 6 MV photon beam from a Varian Linear Accelerator. A simple phantom was used which consisted of two perspex blocks, one placed on top of the other. An area was created in the lower block to accommodate the microfluidic device; the upper block had holes drilled in it to allow the inflow and outflow tubes to pass through. The phantom and a dummy container had previously been imaged on a Philips CT scanner to enable an accurate radiotherapy delivery to be planned based on the electron density variation within the phantom and using a pair of parallel opposed beams. Irradiation consisted of beams at gantry

angles of 90° and 270° with a 5cm x 5cm field size and each delivering 114 monitor units (MU) in order to produce a uniform dose to the centre of the specimen of 2 Gy. This delivery was incremented according to the specific dose required on each occasion. The microfluidic device, phantom, syringe driver and incubator were all transported to the radiotherapy suite in a metallic trolley with internal dimensions of 94 x 48 x 25cm with pneumatic tyres, which was padded with bubble wrap to ensure that all the equipment was secure on transfer. The transfer time from the laboratory to the radiotherapy suite was 10 minutes and it took approximately 15 minutes to administer the radiation. During the transfer the syringe driver and the incubator were powered by an uninterruptible power supply (UPS) (Riello UPS Net Dialog 1000, Riello UPS Ltd, UK).

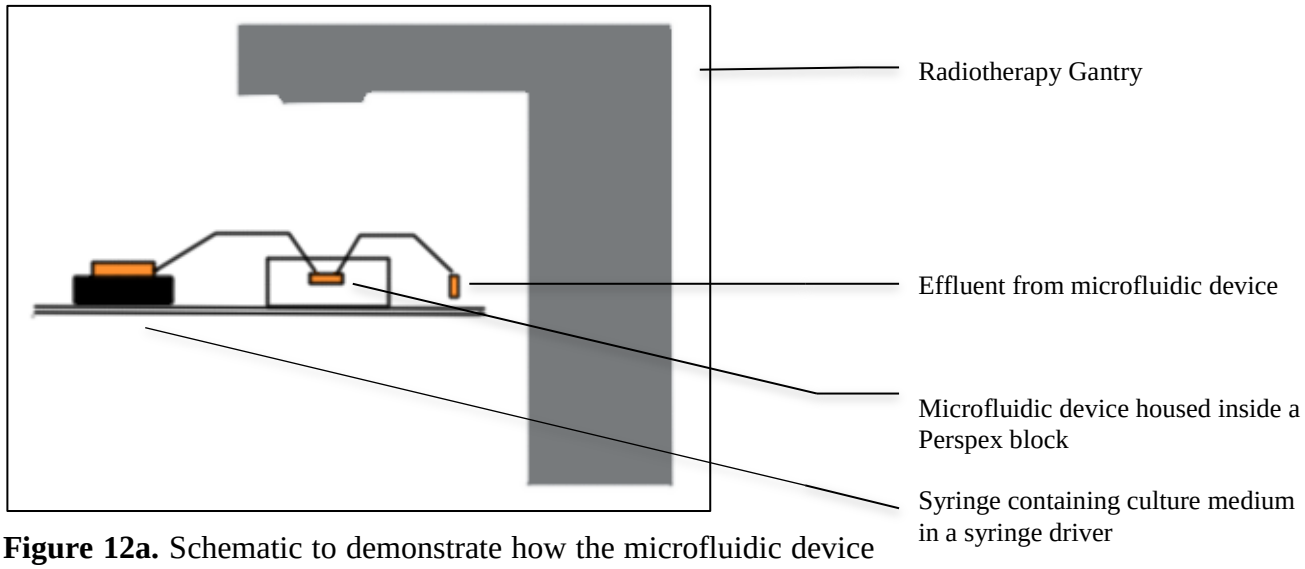

Figure 12a. Schematic to demonstrate how the microfluidic device was assembled to administer the radiation.

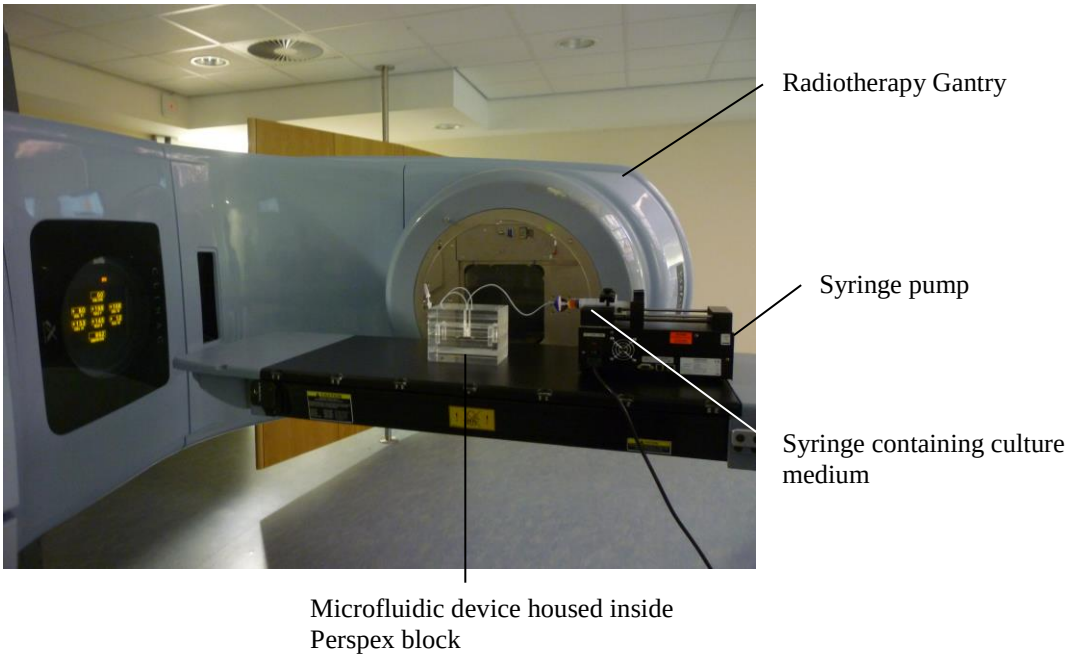

Figure 12b. Photograph demonstrating how the microfluidic device was assembled on the gantry for administration of radiation.

2.6 Measurement of cell death using lactate dehydrogenase (LDH) and cytochrome c release

2.6.1 LDH assay

LDH is an intracellular enzyme, present in the cytosol of all cells. It is a hydrogen transfer enzyme involved in the glycolysis pathway where, under anaerobic conditions, it causes the reoxidation of the coenzyme nicotinamide adenine dinucleotide (NADH) to NAD^+, which is necessary for adenosine tri-phosphate (ATP) synthesis. To enable this, NAD^+ acts as a cosubstrate in the conversion of pyruvate to lactate, which is catalysed by LDH (**Figure 13**) *(Rodwell, 1993)*. This mechanism is utilised in the cytotoxicity detection assay from Roche. In the first step NAD^+ is reduced to $NADH/H^+$ by the LDH-catalysed conversion of lactate to pyruvate. In the second step, the catalyst (diaphorase) transfers H/H^+ from $NADH/H^+$ to the tetrazolium salt INT (pale yellow) to formazan salt (red).

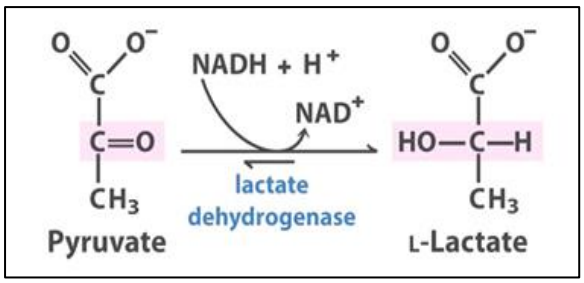

Figure 13. NAD^+ acts as a cosubstrate in the LDH reaction *(Rodwell, 1993).*

Cell lysis, as a result of cellular damage, causes cell membrane breakdown resulting in cytoplasmic enzymes, such as LDH, to be released into the extracellular space.

LDH levels in the effluent were measured using a colourimetric assay (LDH Cytotoxicity Detection Kit, Roche, UK). Following reconstitution of the catalyst (diaphorase/NAD^+ mixture) with 1.125ml of distilled water for each batch of 100 tests. An aliquot (125µl) of the reconstituted catalyst was added to 5.63ml of the dye solution (Iodotetrazolium chloride).

To a 96-well plate, 50µl of the effluent or control was added in duplicate to each well followed by 50µl of the prepared catalyst-dye mixture. The plate was incubated for 30 minutes at 37^{o}C after which 25µl of the stop solution (1N HCL) was added to each well. The absorbance of the wells was measured at 492nm with wavelength correction at 600nm using a Multiskan FC plate reader (Thermo Scientific). The absorbance values for medium alone were subtracted from each sample value and the values obtained were standardised per milligram of starting weight of tissue. In order to determine if the tissue was alive at the end of the experiment, in some cases lysis agent from the kit (10% (v/v) Triton-X) was added to the medium 4-6 hours prior to the end of the experiment to cause maximal cell membrane rupture in order to demonstrate the potential amount of LDH remaining in the tissue.

2.6.2 Cytochrome c ELISA

A Quantikine® human cytochrome c immunoassay ELISA kit (R&D Systems, UK) was used with the HNSCC tissue samples to measure the amount of cytochrome c present in the effluent.

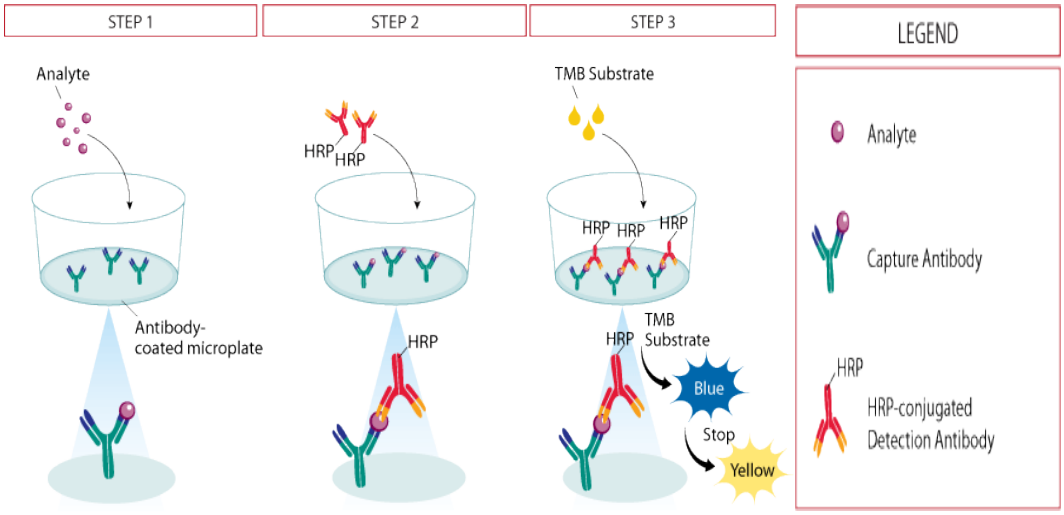

Figure 14. Quantikine human cytochrome c immunoassay ELISA *(R&D, 2013)*

A microplate pre-coated with capture antibody is provided with the kit. Samples or standards were added and any analyte present is bound by the immobilised antibody. Unbound materials were washed away. A second horseradish peroxidase (HRP)-labelled antibody (detection antibody) is added and binds to the captured analyte. Unbound antibody is washed away. Tetramethylbenzidine (TMB) substrate solution is added to the wells and a blue colour develops in proportion to the amount of analyte present in the sample. Colour development is stopped, turning the colour in the wells to yellow.

The effluent samples were stored as a batch at -80^{o}C following completion of the experiment. Prior to the assay, samples were defrosted and used undiluted; additional freeze/thaw cycles were avoided. The assay was carried out according to the manufacturer's protocol. Briefly, 100µl of calibrator diluent (provided) was added to a 96-well plate pre-coated with a monoclonal antibody against cytochrome c. The standards were prepared by adding 2ml of deionised water to the cytochrome c standard (provided), which produced a stock solution of 20ng ml^{-1}. Serial dilutions were performed with the calibrator diluent to produce concentrations of 10, 5, 2.5, 1.25 and 0.625ng ml^{-1}. Standard, control (medium alone) or sample (100µl) was added in duplicate. The plate was incubated for two hours at room temperature. The plate was washed four times with wash buffer (provided). HRP-conjugated

anti-cytochrome c conjugate (monoclonal antibody) (200µl) was added to each well and incubated for a further two hours. Following further washes, 200µl of substrate solution (hydrogen peroxide + TMB) was added to each well and incubated for 30 minutes. Sulphuric acid (50µl; 1M) was then added to each well to stop the reaction. The plate was read at 450nm with wavelength correction at 540nm.

The results were calculated by averaging the duplicate readings. The average zero standard optical standard was subtracted as was the reading for the medium alone. A standard curve was created by generating a four parameter logistic curve fit of the data from the standards.

2.7 Analysis of rat liver synthetic function

To assess the functionality of the liver tissue within the microfluidic device, albumin and urea production was investigated.

2.7.1 Albumin ELISA

To detect albumin levels in the effluent, a rat albumin enzyme-linked immunosorbant assay (ELISA) was used (Bethyl Laboratories Inc, TX, USA) according to the manufacturer's instructions. Briefly, each well of a 96-well flat bottom maxisorp ELISA plate (SLS, UK) was coated overnight with 100µl primary sheep anti-rat albumin antibody diluted in 0.05 M carbonate-bicarbonate buffer (Sigma-Aldrich, UK), pH 9.6 at 4°C. Following incubation, each well was washed five times with 200µl wash buffer (50 mM Tris, 0.14 M NaCl, and 0.05% (v/v) Tween 20, pH 8.0) using an automated plate washer (Wellwash Mk4 Thermo Scientific). Wells were subsequently blocked with 200µl of 50mM Tris, 0.14M NaCl, containing 1% (w/v) Bovine Serum Albumin (BSA) pH 8.0 for 30 min at ambient temperature followed by five washes. The rat albumin reference standards were prepared from an initial dilution of 10,000ng ml^{-1}, made by diluting 4µl rat reference serum (30mg ml^{-1} albumin) from the ELISA kit with 12ml of conjugate diluent (50mM Tris, 0.14M NaCl and 0.05% (v/v) Tween 20, pH 8.0). From this initial dilution, serial dilutions were performed to give eight standards at 125, 62.5, 31.25,15.6, 7.8, 3.9, 1.95 and 0ng ml^{-1}. An aliquot (100µl) of each dilution was incubated on the plate in duplicate alongside 100µl of effluent samples and 100µl of medium alone as a control for 1 h. The dilution factor was eight in conjugate. The plate was washed five times. The plates were subsequently incubated with 100µl HRP-

conjugated detection antibody diluted 1:5,000 in 50 mM Tris, 0.14 M NaCl and 0.05% (v/v) Tween 20, pH 8.0 for 1h. The plate was washed five times. Finally, a colorimetric reaction was carried out by the addition of 50µl undiluted TMB solution. The reaction was stopped with 25µl of 2M sulphuric acid and the absorbance of each well was measured at 450 nm.

The albumin levels were standardised per mg of rat liver tissue. A medium only control was used. A standard curve was plotted to determine the amount of rat albumin in an unknown sample with the average absorbance values, minus the blank values, for each standard concentration plotted against the corresponding rat albumin levels. The rat albumin concentrations obtained were multiplied by the dilution factor to determine the amount of rat albumin in the undiluted sample.

2.7.2 Urea assay

Urea concentrations in the effluent were determined using a colorimetric assay (QuantiChrom™ Urea Assay Kit, BioAssay Systems, USA) carried out according to the manufacturer's protocol. The improved Jung method with the kit utilises a chromogenic reagent that forms a coloured complex specifically with urea. The intensity of the colour, measured at 430nm, is directly proportional to the urea concentration in the sample.

The effluent samples were treated as low urea samples according to the manufacturer's instructions. They were stored at 2-8^{o}C prior to analysis and used within seven days. They were analysed as a batch after the completion of the microfluidic experiment.

The working reagent was prepared by adding equal volume of reagent A (<0.4% o-phthalaldehyde, <0.04% Brij 35 and 10% sulphuric acid) to reagent B (<0.08% primaquine diphosphate, <0.8% boric acid, 22% sulphuric acid and <0.04% brij 35). To each well of a 96-well plate, 50µl of 5mg urea/dl standard, control (medium alone) and samples were added in duplicate. Working reagent (200µl) was then added and incubated for 50 minutes at room temperature. The absorbance of each well was measured at 450nm. The urea levels were standardised per mg of rat liver tissue.

The urea concentration was calculated according to the equation:

Equation 3

$$[\text{urea (mg dl}^{-1}] = \frac{OD_{sample} - OD_{control}}{OD_{standard} - OD_{control}} \times 5$$

OD = optical density

2.8 Preparation of tissue for cryostat sectioning

To enable immunohistochemical and histological analysis, the tissue was embedded on a cork tile (approx. 1cm^2) covered with Tissue-Tek® (Sakura, Netherlands) and plunged immediately into liquid nitrogen-cooled 2-methyl butane solution (Sigma). This was then stored at -20^{o}C and sectioned using a cryostat within two weeks of fixing.

2.8.1 Cryostat sectioning

Prior to sectioning, each tissue specimen, embedded in Tissue-Tek® (Sakura) on a cork tile was fixed to a cryostat stage using Cryo-M Bed (A-M Systems, WA, USA). The cryostat was set at -15^{o}C and the cryostat adjusted so that it cut 5 micron thick sections. Each section was placed on Superfrost® Plus glass microscope slides (Merck UK) with 6 sections per slide. The slides were then stored at -20^{o}C for future analysis.

2.9 Histological analysis of tissue using Haematoxylin and Eosin

For histological analysis, the tissue sections were racked and fixed with 100% (v/v) cooled methanol (-20^{o}C). The slides were then placed in haematoxylin solution for one minute, after this slides were run under tap water for 10 minutes. The slides were dehydrated with 70%, then 95% ethanol for two minutes each, placed in eosin solution for 2 minutes followed by further dehydration with a quick (10 s) placement in 95%, then 100% ethanol. They were placed in three successive pots of Histo-clear (National Diagnostics, UK) for a total of five minutes and mounted in Histomount (National Diagnostics).

2.10 Immunohistochemical analysis

2.10.1 Pancytokeratin and M30 CytoDEATH™

Cytokeratins are proteins of keratin-containing intermediate filaments found in the intracytoplasmic cytoskeleton of epithelial tissue *(Franke et al., 1979)* and are used in the clinical diagnosis of HNSCC. The antibody used in this study labelled several different cytokeratin subtypes and is useful for the identification of tumours of epithelial origin.

A monoclonal mouse anti-human pancytokeratin (DAKOCytomation, DAKO, UK) was used to confirm the presence of squamous cell carcinoma within the tissue sample, particularly in the metastatic lymph node samples according to the following protocol. The sections used consisted of two sections from tissue that had not been maintained in the microfluidic device, which acted as the negative and positive controls, tissue that had been maintained in the device, but had not received radiotherapy and tissue that had been maintained in the device and received radiotherapy. The tissue sections were equilibrated to room temperature for five minutes before being racked up and fixed in pre-cooled (-20^{o}C) methanol (100% v/v) for 10 minutes at room temperature. They were fixed with the pre-cooled methanol for 10 minutes at room temperature. Following rinsing in Tris buffered saline (TBS) (Appendix 1) for five minutes the sections were placed in a Sequenza® rack and endogenous peroxidase was blocked by immersing the sections in 3% (v/v) H_2O_2 in 100% methanol for 15 minutes. The sections were then incubated for 20 minutes with normal horse blocking serum (Vectastain Elite kit) before nonspecific avidin/biotin binding was blocked by incubating each section with Avidin D (100µl; Vector Laboratories, UK) followed by 100µl Biotin (Vector Laboratories, UK) for 15 minutes each. The sections were incubated with 100µl of 1:100 diluted primary antibody except the negative control, which was incubated with 1:100 mouse IgG1 (DAKO Cytomation) for 1 hour at room temperature. The sections were then washed and incubated for 30 minutes with 100µl of biotinylated horse anti-mouse antibody (Vectastain Elite kit) during which time the avidin-biotin peroxidase complex was prepared by adding two drops of Avidin DH to 5ml of buffer solution followed by two drops of the paired biotinylated enzyme. The secondary antibody was washed off and replaced with 100µl avidin-biotin-peroxidase complex (Vectastain Elite kit) for 30 minutes. Peroxidase activity was detected using 3,3'- diaminobenzidine (DAB) (Sigma) prepared by dissolving one gold tablet and one silver tablet in 1ml of distilled water. The sections were then dehydrated through graded alcohols (70%, 90% and 100% v/v) and Histoclear (National Diagnostics, UK)

and were mounted in Histomount (National Diagnostics, UK) and visualisd under a light microscope.

The cells undergoing apoptosis were identified using the M30 CytoDEATH™ (Peviva, UK) antibody, which identifies apoptotic cell death by detecting a caspase-3 cleaved product of cytokeratin 18. The procedure was carried out according to the same protocol as the cytokeratin, except that 1:100 dilution of mouse IgG2 (DAKO Cytomation) was used as the isotype control.

2.10.2 Terminal deoxynucleotidyl transferase dUTP nick end labeling (TUNEL)

TUNEL was carried out according to the manufacturer's protocol (Roche, UK). Tissue sections were racked up and fixed in 4% (w/v) paraformaldehyde in PBS pH7.4 for 20 min at 15-25^{o}C before being washed for 30 min in PBS. The tissue was then treated with a permeabilisation solution (0.1% (v/v) Triton-X, 0.1% (w/v) sodium citrate) for 2 min on ice (4^{o}C). Both the positive and the negative controls were sections taken from HNSCC tissue prior to it being incubated in the microfluidic device. The positive control was treated with recombinant DNase I (3000U/ml - 3U/ml in 50 mM Tris-HCl, pH 7.5 1mg/ml BSA) for 10 min at 15-25^{o}C to induce DNA strand breaks prior to labelling procedures. The positive control was then rinsed with PBS. For each test, the TUNEL reaction mixture consisted of 5µl of TUNEL-Enzyme solution and 45µl of TUNEL-Label solution (Biotin-16-deoxyuridine-triphosphatase + terminal deoxynucleotidyl transferase reaction buffer). The reaction mixture was added directly to each section of the positive control and the sections of tissue that had been incubated in the microfluidic device with and without irradiation. The negative control was treated with TUNEL-Label solution (without terminal transferase). The sections were then covered with a glass cover slip to prevent evaporation and incubated for 60 minutes at 37^{o}C in a humidified atmosphere in the dark. The slides were rinsed with PBS and mounted using 4'6'-diamidino-2-phenylindole (DAPI) hard-set mountant. DNA strand breaks were visualised using fluorescence microscopy with an excitation wavelength in the range of 450-500nm and detection in the range of 515-565nm (green).

2.11 Calculation of the apoptotic and the DNA-strand break indices

The apoptotic (AI) and DNA-strand break indices were calculated by counting the number of cells that stained positive for M30 and TUNEL respectively in ten randomly chosen high-power fields (x400); only fields that contained positive cells were selected. A total of approximately 2-3000 cells were counted in the ten fields following the procedure outlined by Burcombe et al. *(Burcombe et al., 2006)*. The software package Image-Pro Premier® (MediaCybernetics, UK) was used to count the cells using the automatic counter facility. The number of positively stained cells was expressed as a percentage of the total number of cells within the field.

2.12 Statistical analysis

Statistical analysis was performed using SPSS (IBM, USA). Unpaired t-test was used to determine the statistical significance between treatments. *P*-values of less than 0.05 were considered significant.

Chapter 3:

The effect of radiation on rat liver tissue maintained in a microfluidic device

3.1 Introduction

The initial aim of this part of the study was to demonstrate that the microfluidic device could maintain tissue in a viable state over at least four days. A previous study had shown that rat liver tissue could be maintained in an identical microfluidic device to the one used in the current study *(Hattersley et al., 2008).* Rat liver tissue was used to demonstrate the ability of the microfluidic device to maintain the tissue in a viable state and subsequently to demonstrate the effects of radiation on the tissue. The results of the experiments with the rat liver tissue would enable optimisation of the technique for use with the HNSCC tissue. The rat liver tissue has certain similar qualities to HNSCC in that it is highly metabolically active and is moderately radiosensitive, which made it an ideal tissue to use to optimise the technique in preparation for the HNSCC tissue.

The viability of the rat liver tissue was assessed by measuring lactate dehydrogenase (LDH), an intracellular enzyme released from the tissue following cell death. To determine whether the rat liver tissue was alive at the end of the experiment, a lysis agent was added to the culture medium, which caused maximal cell rupture, which would cause an increase in LDH release, indicating that intact, viable cells remained in the tissue. To investigate whether the microfluidic device could maintain the synthetic functional ability of the rat liver tissue following extraction from the rat, albumin and urea were measured in the effluent from the device. This was performed initially under standard incubation conditions.

Radiation-induced cell death was assessed by measuring LDH, a marker of both apoptotic and necrotic cell death, in the effluent from the device. The effect of radiation on the rat liver's synthetic function was assessed by measuring albumin and urea in the effluent from the device.

To study the tissue architecture, the rat liver tissue was sectioned and analysed histologically using heamatoxylin and eosin. The initial experiments were performed to assess any architectural changes in the tissue caused by incubation in the microfluidic device, without

the tissue undergoing irradiation. Subsequent experiments assessed the tissue's architectural changes in response to radiation.

3.2 Materials and Methods

3.2.1 Design and fabrication of the microfluidic device

The glass microfluidic devices were fabricated in-house at the Department of Chemistry, University of Hull using photolithography techniques as described in section 2.1.

3.2.2 Preparation and running of the microfluidic device

The microfluidic device was prepared as described in section 2.2.1. Once assembled, the microfluidic device was run as in section 2.2.2. The effluent from the device was collected at two-hourly intervals, which provided enough effluent for analysis. The effluent was collected overnight, but these samples were not analysed. To establish whether the microfluidic device could maintain rat liver tissue in a viable state, three devices containing rat liver tissue were run together.

3.2.3 Rat liver collection and preparation

The liver was extracted from five Wistar rats as described in section 2.3. The liver was immediately sectioned into pieces approximately $1cm^3$ using a scalpel and either placed fresh in the microfluidic devices or frozen for future use.

3.2.4 Administration of radiation

The rat liver tissue was irradiated using a 6 MV photon beam from a Varian Linear Accelerator as described in section 2.5. The radiation doses consisted of a single dose of 20 Gy and fractionated doses, consisting of two fractions of 10 Gy, which were administered 24 h apart on days 2 and 3, and 5 daily fractions of 4 Gy. For each experiment in which the rat

liver was irradiated, there was one microfluidic device containing irradiated rat liver tissue and two control devices containing un-irradiated rat liver tissue.

3.2.5 LDH assay

LDH is an intracellular enzyme, which is involved in the glycolysis pathway. It is released from cells as a result of the cell membrane being compromised following cellular death due to irradiation. Therefore, the LDH assay was capable of detecting radiation-induced cell death. The assay was performed in duplicate on each sample of effluent as described in section 2.6.1. The absorbance value of the culture medium alone was used as a negative control and subtracted from the absorbance values of the effluent samples. To determine whether the tissue was alive at the end of the experiment, a lysis reagent was added near to the end of some of the experiments. This caused maximal cell membrane rupture, demonstrating the potential amount of LDH that could be released and, therefore, the presence of viable cells remaining in the tissue. The experiments were repeated three times, apart from the experiment in which the rat liver tissue was irradiated with two fractions of 10 Gy and maintained for 411h, which was performed once and the experiment in which the rat liver tissue was irradiated with five daily fractions of 4 Gy, which was performed twice. The mean absorbance values were calculated from the all of the experiments.

3.2.6 Albumin ELISA

The level of albumin produced by the rat liver tissue maintained in the microfluidic device was measured in the effluent from the device using the albumin ELISA as described in section 2.7.1. As in the LDH assay, the albumin was measured in duplicate from each two-hourly effluent sample. Each experiment was repeated three times and the mean albumin value was calculated.

3.2.7 Urea assay

The level of urea produced by the rat liver maintained in the microfluidic device was measured in the effluent from the device using the urea assay as described in section 2.7.2. As the urea levels in each two-hourly effluent collection were low, the two-hourly effluents were combined to give a measurement over 24 h.

3.2.8 Preparation of tissue for cryostat sectioning

The rat liver tissue was prepared as in section 2.8.

3.2.9 Cryostat sectioning

Prior to sectioning, each tissue specimen was prepared as in section 2.9 using a cryostat (Leica CM1100, Leica biosystems, UK). Sections were placed on Superfrost® Plus glass microscope slides (Merck, UK) with six sections per slide. The slides were stored at -20^{o}C for future analysis.

3.2.10 Histological analysis of tissue using Haematoxylin and Eosin

For histological analysis, the rat liver tissue sections were stained with Haematoxylin and Eosin as described in section 2.10. Sections were taken from the rat liver at each stage of the process and analysed histologically to determine the morphological changes caused by each of the following stages: rat liver tissue following extraction from the rat without incubation in the microfluidic device, tissue that had been incubated in the microfluidic device without irradiation and tissue that had been incubated in the microfluidic device and exposed to radiation.

3.3 Results

3.3.1 Assessment of viability of the rat liver tissue by determinining LDH release

The calculation of LDH levels was standardised per mg of tissue. A worked example of the calculation is shown in **Table 5**. LDH was measureable in the effluent from the microfluidic device as a result of cell death. **Figure 15** shows the levels of LDH released from rat liver (n=3), maintained in the microfluidic device without intervention over a period of 341 h (15 days). The initial elevated LDH levels decreased to minimally detectable levels 24-28 h after placement of the tissue into the microfluidic device. LDH levels remained low until the lysis reagent was added to the medium at 333 h, inducing a subsequent rise in LDH release 2-8 h after its addition.

Table 5. Calculation of LDH absorbance values for rat liver irradiated with a single dose of 20 Gy. This same calculation was performed for the control tissue in this experiment and for all other LDH results with the rat liver and HNSCC tissue.

Incubation time (hours)	LDH absorbance (a.u.)			LDH absorbance per mg of tissue (a.u.)			Mean LDH absorbance per mg of tissue (a.u.)
	Tissue 1	Tissue 2	Tissue 3	Tissue 1 (7.2mg)	Tissue 2 (7.6mg)	Tissue 3 (6.8mg)	
0-2	1.76	2.20	0.88	0.24	0.29	0.13	0.22
2-4	1.60	2.08	0.75	0.22	0.27	0.11	0.20
18-20	0.93	1.04	0.66	0.13	0.14	0.10	0.12
20-22	0.80	0.74	0.70	0.11	0.10	0.10	0.10
22-24	0.59	0.61	0.46	0.08	0.08	0.07	0.08
24-26	1.35	1.31	1.01	0.19	0.17	0.15	0.17
26-28	0.53	0.52	0.58	0.07	0.07	0.09	0.08
44-46	0.48	0.27	0.33	0.07	0.04	0.05	0.05
46-48	0.44	0.49	0.27	0.06	0.06	0.04	0.05
48-50	0.39	0.40	0.28	0.05	0.05	0.04	0.05
50-52	0.32	0.36	0.17	0.04	0.05	0.03	0.04
68-70	0.22	0.22	0.26	0.03	0.03	0.04	0.03
70-72	0.19	0.17	0.22	0.03	0.03	0.03	0.03
72-74	0.64	1.08	0.62	0.09	0.14	0.09	0.11
74-76	0.60	1.41	0.15	0.08	0.19	0.02	0.10

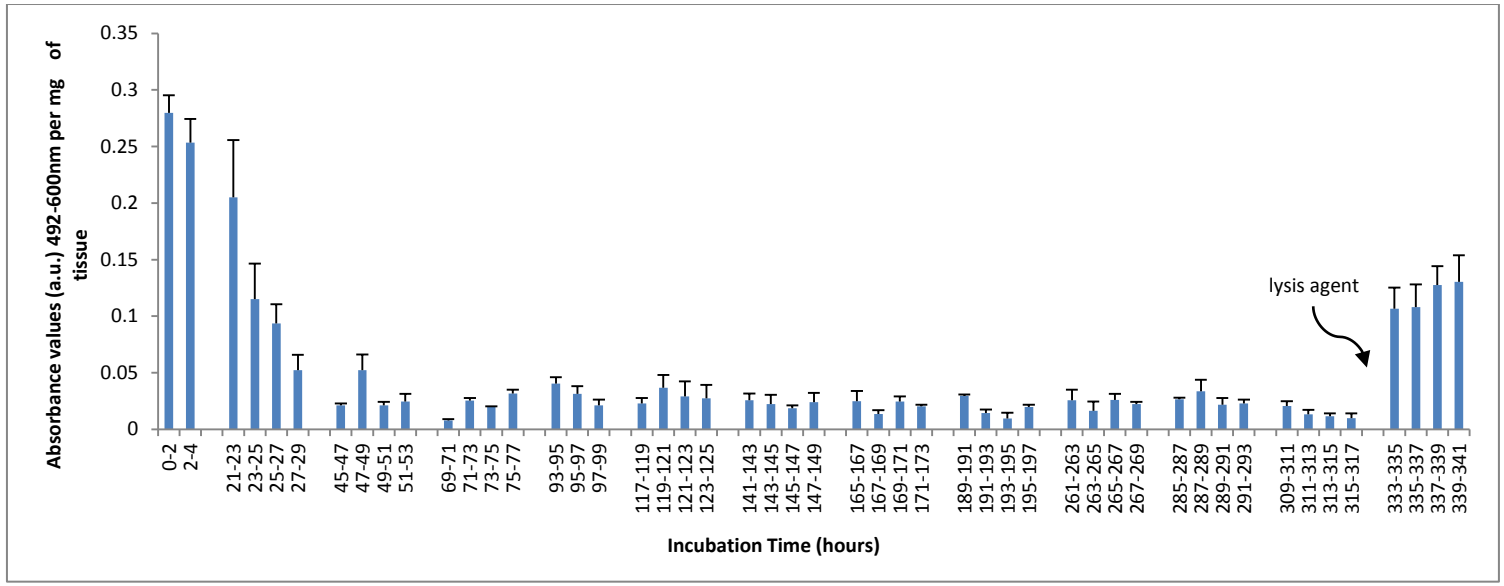

Figure 15. Absorbance measurements (492-600nm) following LDH assays on effluent from rat liver maintained in a microfluidic device for 341 h, standardised per mg of tissue (Mean of 3 separate experiments + SEM). Lysis agent was added at 333 h indicated by arrow. The effluent was collected overnight, but not analysed, as demonstrated by the gaps in the incubation time axis.

3.3.2 LDH release from rat liver following irradiation as a measure of cell death

Radiotherapy was administered to the rat liver as single doses of 10 Gy and 20 Gy and as a fractionated course, consisting of two fractions of 10 Gy and five fractions of 4 Gy. Treatment of the rat liver with a single dose of 10 Gy resulted in no significant increase in LDH release (n=3; data not shown). After administration of a single dose of 20 Gy (n=3) at 24 h (**Figure 16**), a significant surge in LDH release was observed 2 h post-irradiation compared to the control (p=0.028). The LDH levels subsequently dropped to levels comparable with the control, until the lysis agent was added at 70 h to the irradiated and control tissue, after which a significant rise in LDH was demonstrated (p=0.002). Interestingly, although not significant, the LDH levels following lysis reagent addition were lower in the irradiated group compared to the control. Other observations included partial degradation of the tissue subsequent to the LDH surge, which blocked the microfluidic device downstream of the tissue well, which resulted in the need to transfer the tissue to a new device for continuation of the experiment.

No significant increase in LDH release was demonstrated after the administration of radiotherapy doses of 10 Gy or less (n=20).

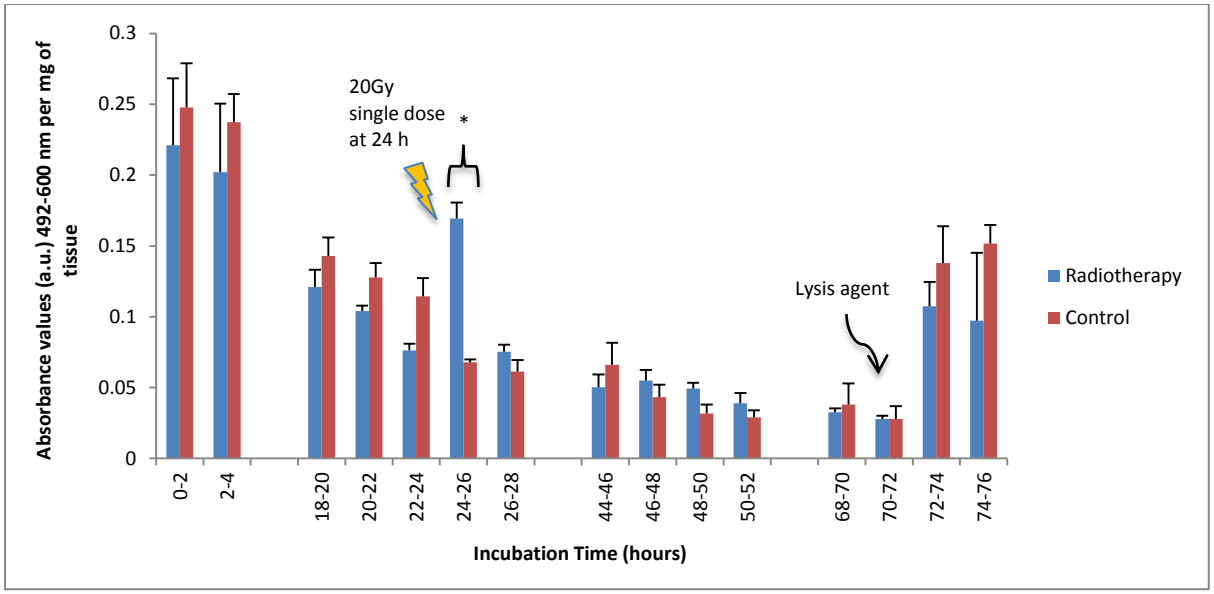

Figure 16. Absorbance measurements (492-600nm) following LDH assays on effluent released from rat liver maintained in a microfluidic device, standardised per mg of tissue (Mean of 3 separate experiments + SEM). Single dose of 20Gy administered at 24 h as shown by the yellow flash arrow. Control received no radiotherapy. Lysis agent added at 70 h to both the irradiated tissue and the control, indicated by arrow. Gaps indicate when effluent was not collected. A significant surge in LDH release was demonstrated after the administration of 20Gy radiotherapy compared to the control p=0.028* unpaired t-test. After addition of the lysis agent, there was an increase in both the irradiated and control tissue; the levels being higher in the control tissue, although this was not significant.

A fractionated course of radiotherapy consisting of two fractions of 10 Gy administered to the rat liver (n=3) at 26 and 52 h (**Figure 17**) caused a significant increase in LDH release in the 2 h post-irradiation time period after the second fraction (p=0.004), which then decreased to levels equivalent to that of the control, whereas no increase in LDH was observed after administration of the first 10 Gy dose. The tissue remained intact following the administration of the fractionated 2 x 10 Gy dose of radiotherapy and the microfluidic device remained. Following addition of the lysis agent, there was a subsequent increase in LDH release in both the irradiated and control tissue.

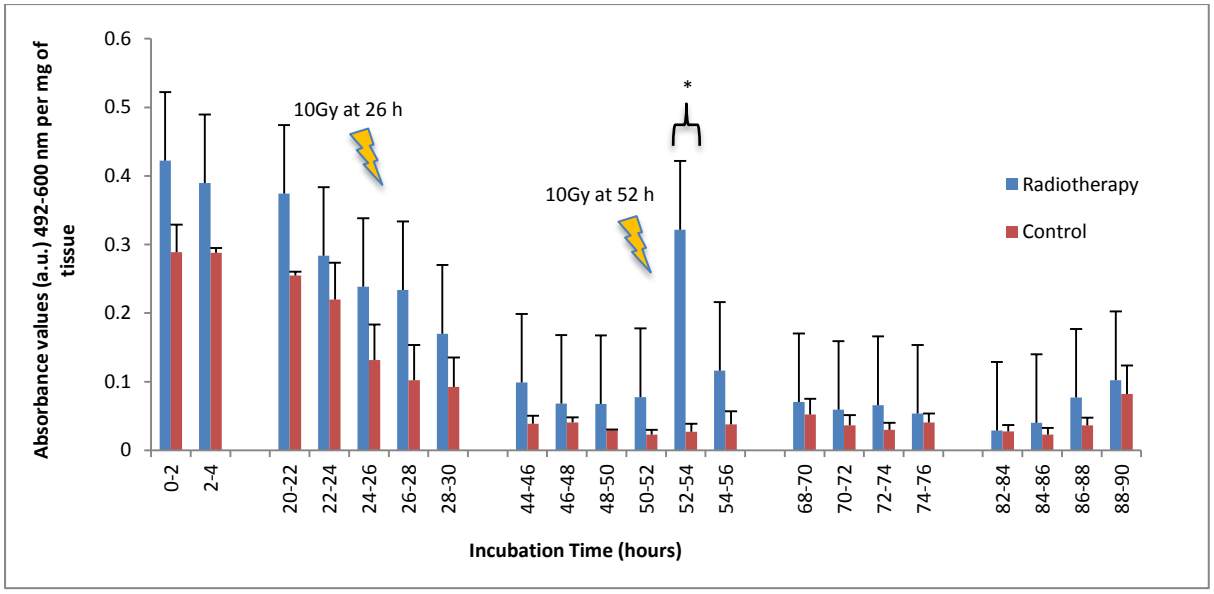

Figure 17. Absorbance measurements (492-600nm) following LDH assay on effluent released from rat liver standardised per mg of tissue (Mean of 3 separate experiments + SEM). 20Gy administered as two fractions of 10Gy at 26 and 52 h as shown by flash arrows. Lysis agent added at 82 h. Gaps indicate when effluent was not collected. Significant increase in LDH release demonstrated after the administration of the second 10Gy fraction compared to the control p=0.004* unpaired t-test.

To investigate whether any cellular death occurred over a longer time frame, an experiment was performed to maintain the tissue for 17 days post-irradiation, having received two fractions of 10 Gy at 27 and 52 h respectively (**Figure 18**). Again a surge in LDH release was demonstrated during the first two hours after the second fraction of radiotherapy with no such increase being observed following the first 10 Gy dose, as had occurred in the previous experiments. However, no further significant LDH release was seen detected after this point, until the lysis agent was added at 405 h.

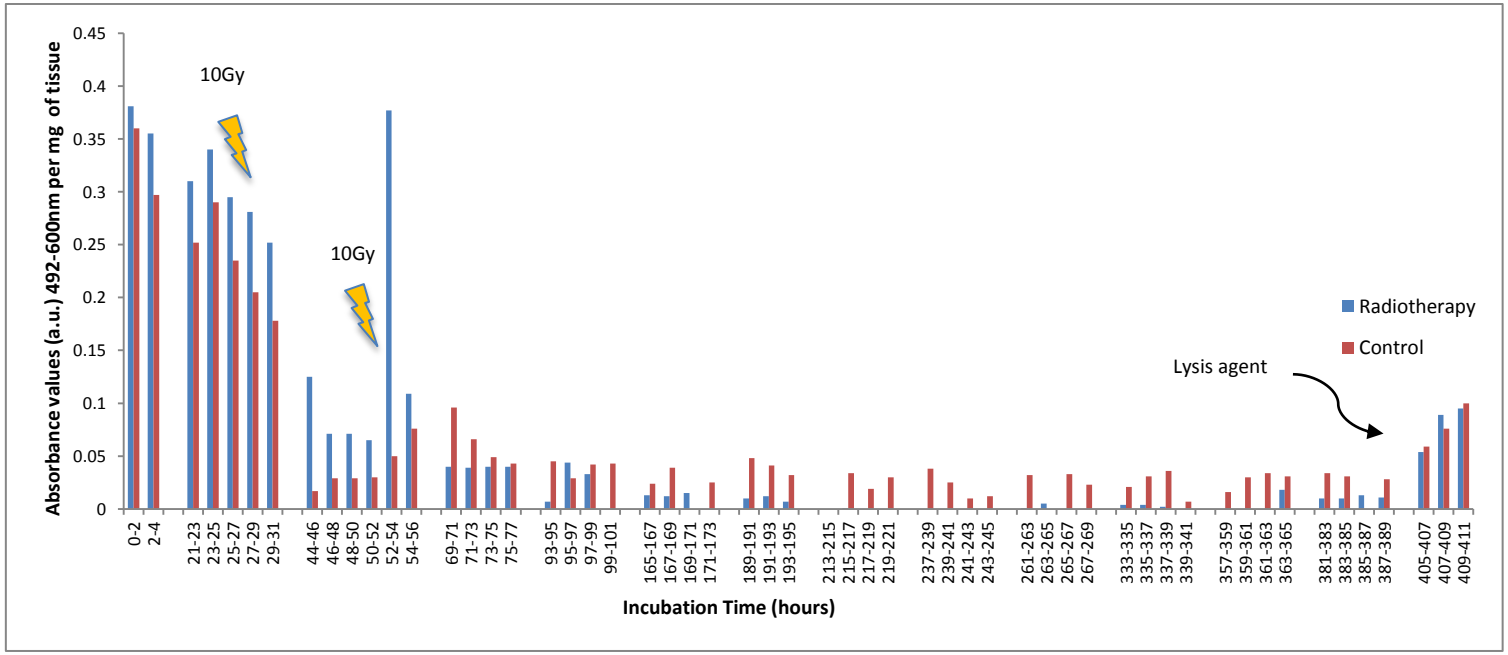

Figure 18. Absorbance measurement (492-600nm) following LDH assay on effluent released from rat liver standardised per mg of tissue. 20Gy administered as two fractions of 10Gy at 27 h and 52 h as shown by flash arrows. LDH standardised per mg of tissue. Lysis agent added at 405 h. Gaps indicate when effluent was not collected. A significant surge in LDH release was observed after the administration of the second fraction of 10Gy compared to the control.

The 20 Gy radiation dose was further divided into five fractions of 4 Gy. This dose regimen was chosen as the total administered dose remained at 20 Gy, which had demonstrated a significant increase in LDH release and the fraction dose more closely replicated a clinical radiotherapy dose (n=2; **Figure 19**). No significant increases in LDH release were observed following irradiation and there was no overall difference between the irradiated tissue and the control over the time period of incubation (p=0.996).

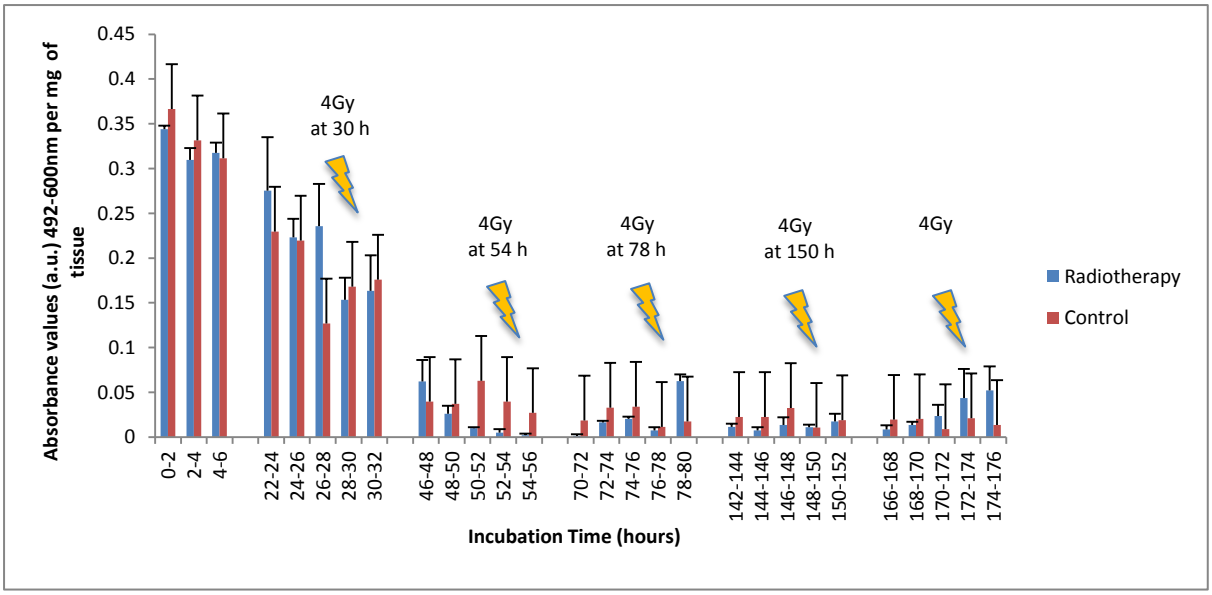

Figure 19. Absorbance measurements (492-600nm) following LDH assays on effluent released from rat liver standardised per mg of tissue (Mean of 2 separate experiments + SEM). 20Gy administered as five fractions of 4Gy at 30 h, 54 h, 78 h, 150 h and 174 h respectively as shown by flash arrows. No lysis agent was added. Gaps indicate when effluent was not collected. No significant difference between the irradiated and control tissues was observed p=0.996 unpaired t-test.

3.3.3 Albumin production as a measurement of rat liver function following irradiation

Albumin was detectable in the effluent from the device as a measure of rat liver function. **Table 6** shows a worked example of the calculation of albumin per mg of rat liver tissue for the tissue that was irradiated with a single dose of 20 Gy. Rat liver, incubated in the microfluidic device under standard conditions without radiotherapy treatment (n=3 chips) produced detectable albumin levels in the microfluidic effluent for 197 h (**Figure 20**). Levels observed fluctuated between 6 and 11ng ml^{-1} for the first 53 h, decreasing to between 1 and 4ng ml^{-1} from 53 to 197 h.

Table 6. Calculation of albumin levels in rat liver irradiated with a single 20 Gy dose. The same calculation was performed for the control tissue in this experiment and all other albumin results with the rat liver tissue.

Incubation time (hours)	Albumin (ng ml^{-1})			Albumin per mg of tissue (ng ml^{-1} mg^{-1})			Mean albumin per mg of tissue (ng ml^{-1} mg^{-1})
	Rat liver 1	Rat liver 2	Rat liver 3	Rat liver 1 (8.2mg)	Rat liver 2 (7.7mg)	Rat liver 3 (7.1mg)	
0-2	94.22	42.04	66.31	11.49	5.46	9.34	8.76
2-4	43.21	72.46	56.02	5.27	9.41	7.89	7.52
18-20	60.35	29.65	47.71	7.36	3.85	6.72	5.98
20-22	31.41	59.44	48.85	3.83	7.72	6.88	6.14
22-24	21.40	37.65	42.17	2.61	4.89	5.94	4.48
24-26	77.98	16.79	49.98	9.51	2.18	7.04	6.24
26-28	16.48	11.70	13.77	2.01	1.52	1.94	1.82
44-46	3.94	1.77	2.56	0.48	0.23	0.44	0.38
46-48	4.60	1.62	2.77	0.56	0.21	0.59	0.45
48-50	3.44	1.46	2.20	0.42	0.19	0.67	0.43
50-52	4.51	1.85	2.84	0.55	0.24	0.61	0.47
68-70	4.35	1.78	2.70	0.53	0.23	0.78	0.51
70-72	2.95	2.31	2.34	0.36	0.30	0.83	0.50
72-74	2.13	1.62	1.70	0.26	0.21	0.61	0.45
74-76	1.07	1.93	1.35	0.13	0.25	0.23	0.33
92-94	0.33	2.46	1.28	0.04	0.32	0.52	0.20
94-96	2.13	2.16	1.92	0.26	0.28	0.74	0.35
96-98	2.21	1.93	1.85	0.27	0.25	0.38	0.42
98-100	3.44	1.93	2.34	0.42	0.25	0.33	0.35

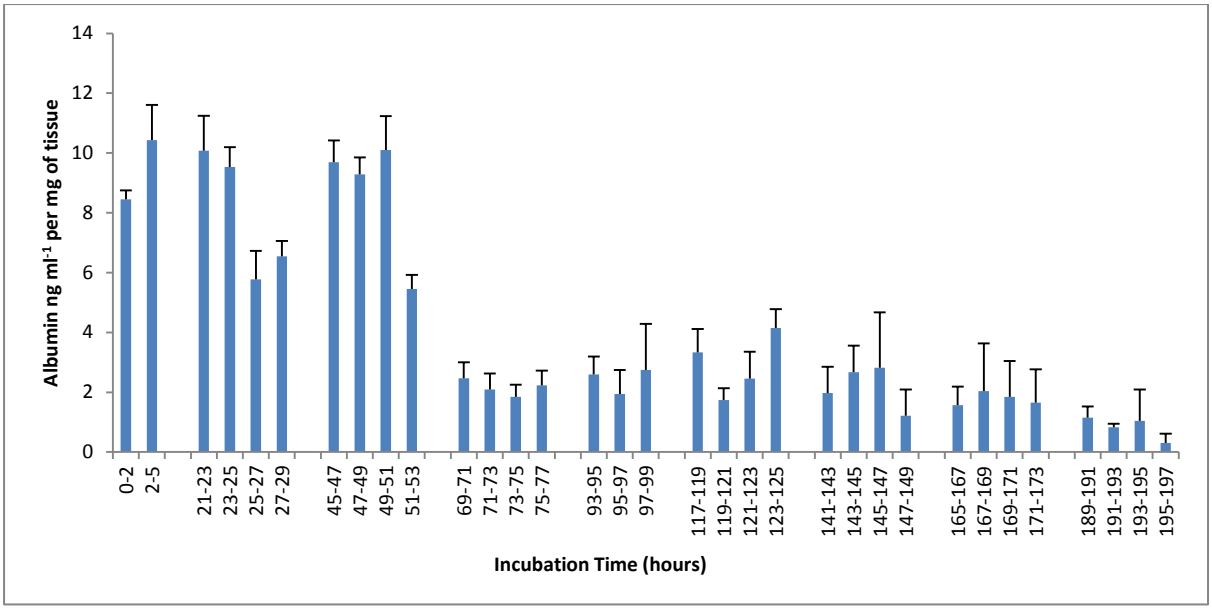

Figure 20. Albumin levels measured using ELISA standardised per mg of tissue (Mean of 3 separate experiments + SEM). No radiotherapy or lysis agent administered. Gaps indicate when effluent was not collected.

After the administration of 20 Gy of radiation as a single dose at 24 h (n=3), there was a significant decrease in the albumin produced by the rat liver in the irradiated group compared to the control (n=3; p=0.003) and compared to the previous time point (p=0.021) 4 h after the administration of radiotherapy, with levels dropping to minimally detectable levels 20-22 h after irradiation (**Figure 21**).

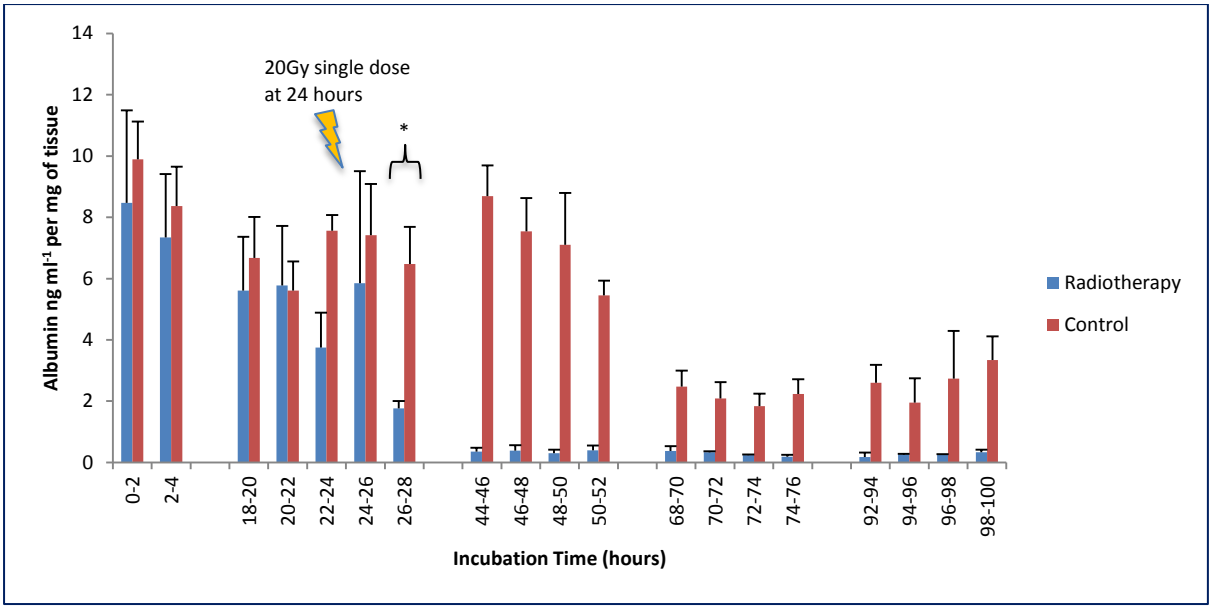

Figure 21. Albumin synthesis by rat liver maintained in a microfluidic device Levels detected using ELISA and standardised per mg of tissue. (Mean of 3 separate experiments + SEM). Single dose of 20Gy radiation administered at 24 h. A significant difference in albumin levels was observed between the irradiated and the control tissue p=0.003* unpaired t-test.

Following the administration of two fractions of 10Gy radiation at 26 h and 52 h, no significant difference was observed in albumin production, between the irradiated and non-irradiated groups (n=3; p=0.520). Levels of albumin were comparable between the two groups. However, the albumin levels in the irradiated group decreased to minimally detectable levels before the control tissue, although this was not significant (**Figure 22**).

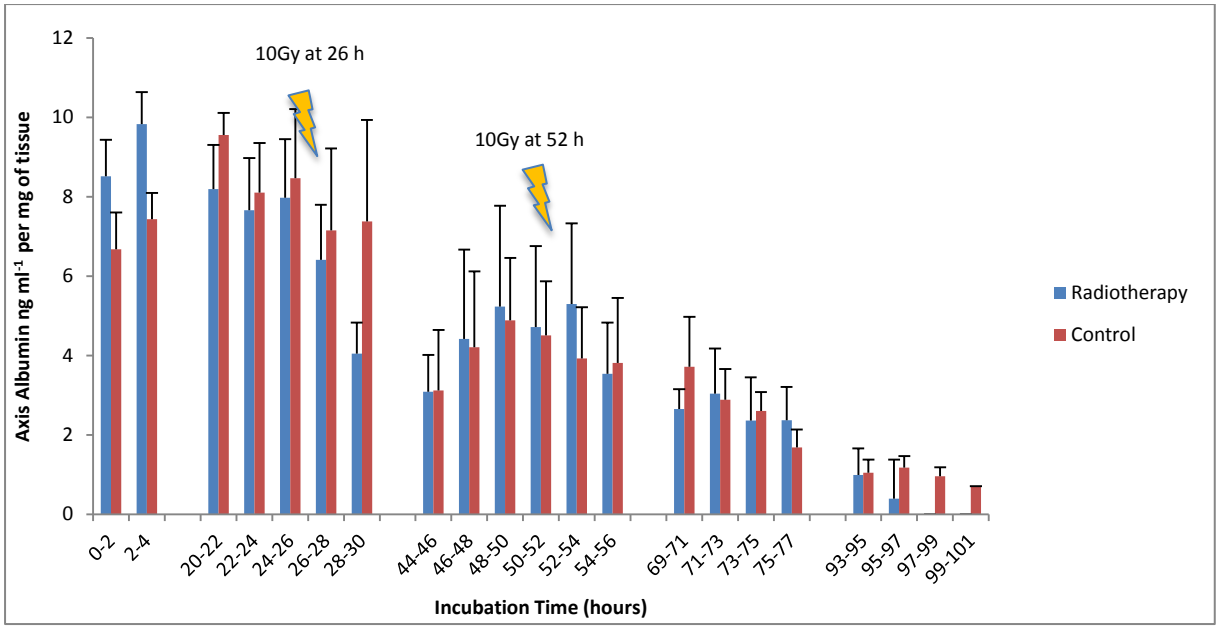

Figure 22. Albumin synthesis by rat liver maintained in a microfluidic cell. Levels device detected using ELISA and standardised per mg of tissue. (Mean of 3 separate experiments + SEM). 20Gy of radiotherapy administered as 2 fractions of 10Gy at 26 and 52 h. There was no significant difference between the irradiated and control tissue p=0.520 unpaired t-test.

3.3.4 Urea production as a measurement of rat liver function following irradiation

As the levels of urea in the effluent were low, the effluents were combined to give a measurement over 24 h. **Table 7** shows a worked example for the rat liver tissue that was irradiated with a single dose of 20 Gy. Under standard incubation conditions in the microfluidic device without radiotherapy treatment, rat liver continued urea production for 13 days (n=3; **Figure 23**). Levels were consistently between 5-8 µg ml^{-1} mg^{-1} for the first eight days, after which levels steadily decreased until minimally detectable levels were produced on day 13.

Table 7. Calculated values of urea concentration in the rat liver tissue that was irradiated with a single dose of 20 Gy. The same calculation was performed in the control tissue for this experiment and all other urea results with the rat liver tissue.

Incubation time (days)	Urea (μg ml^{-1})			Urea per mg of tissue (μg ml^{-1} mg^{-1})			[Urea] per mg of tissue (μg ml^{-1} mg^{-1})
	Rat liver 1	Rat liver 2	Rat liver 3	Rat liver 1 (7.2mg)	Rat liver 2 (8.4mg)	Rat liver 3 (6.7mg)	
1	56.45	70.64	54.34	7.84	8.41	8.11	8.12
2	38.88	51.24	21.71	5.40	6.1	3.24	4.91
3	1.92	7.48	3.69	0.27	0.89	0.55	0.57
4	1.63	4.45	3.15	0.23	0.53	0.47	0.41
5	1.56	4.03	3.75	0.22	0.48	0.56	0.42
6	2.41	3.44	3.62	0.34	0.41	0.54	0.43
7	1.49	2.77	3.08	0.21	0.33	0.46	0.33
8	1.35	2.60	2.08	0.19	0.31	0.31	0.27
9	1.28	3.11	2.21	0.18	0.37	0.33	0.29
10	1.42	2.02	1.68	0.20	0.24	0.25	0.23
11	2.06	2.10	1.41	0.29	0.25	0.21	0.25

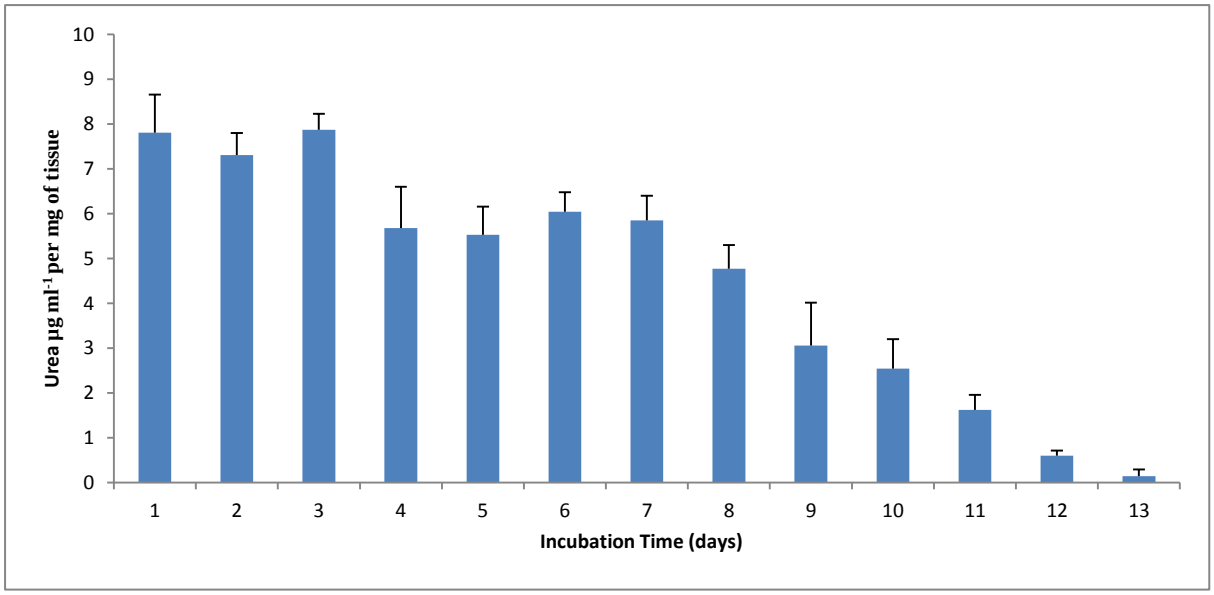

Figure 23. Urea synthesis by rat liver maintained in a microfluidic device. Levels detected using Quantichrom™ Urea Assay Kit and standardised per mg of tissue. (Mean of 3 separate experiments + SEM).

The administration of a single dose of 20 Gy at the end of day two, i.e. ≥24 h after the tissue was placed in the microfluidic device as in the other experiments, resulted in a significant decrease in urea production on day three (p=0.016) compared to the control tissue (n=3; **Figure 24**). The urea levels remained lower than that produced by the control tissue throughout the remainder of the experiment.

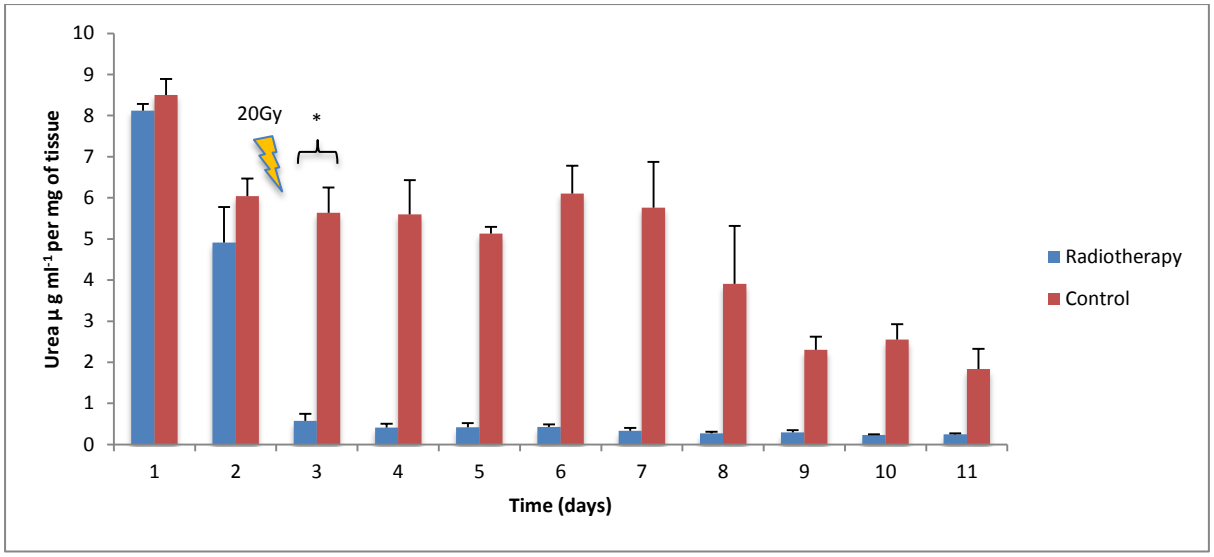

Figure 24. Urea synthesis by rat liver maintained in a microfluidic device. Levels detected using Quantichrom™ Urea Assay Kit and standardised per mg of tissue. (Mean of 3 separate experiments + SEM). 20Gy radiation administered as a single dose on day 2. p=0.016* between the irradiated tissue and the control. Unpaired t-test.

Following the administration of a course of 2 fractions of 10Gy of irradiation, administered at the end of day two and day three, no significant overall differences in urea production was observed between the control and the irradiated tissue (p=0.844) until day 10 when the levels produced by the irradiated group decreased to minimally detectable levels compared to the control (n=3; **Figure 25**).

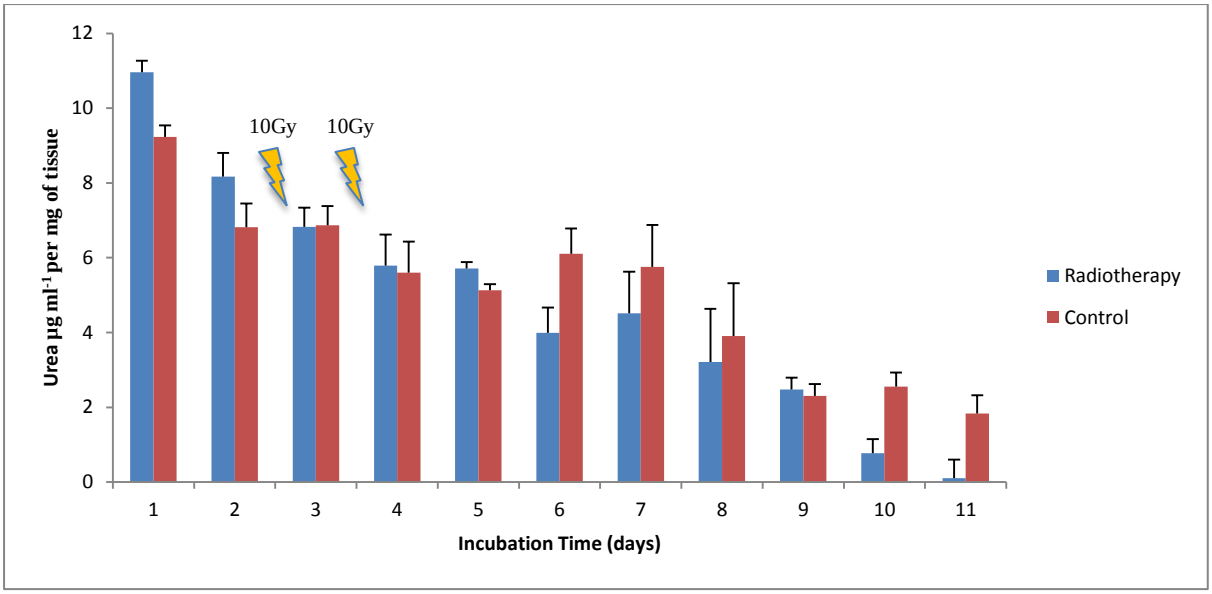

Figure 25. Urea synthesis by rat liver standardised per mg of tissue. Levels detected using Quantichrom™ Urea Assay Kit and standardised per mg of tissue (Mean of 3 separate experiments + SEM). Two fractions of 10Gy radiotherapy administered at the end of day 2 and day 3. *p*=0.844 unpaired t-test overall between the irradiated and control tissue.

3.3.5 Morphology of rat liver maintained in a microfluidic device and the effect of radiation

Prior to placement of the rat liver in the microfluidic device, the histological specimen displayed typical rat liver architecture with groups of hepatocytes divided by sinusoids (**Figure 26A**). Following four days of incubation of the rat liver in the microfluidic device without irradiation, the overall tissue architecture was maintained (**Figure 26B**) with some changes occurring by day six of incubation with evidence of vacuolar formation, indicative of hepatocellular death (**Figure 26C**). The morphology of the rat liver tissue following irradiation with a single dose of 20 Gy was not amenable to analysis due to the significant level of tissue degradation that it had undergone.

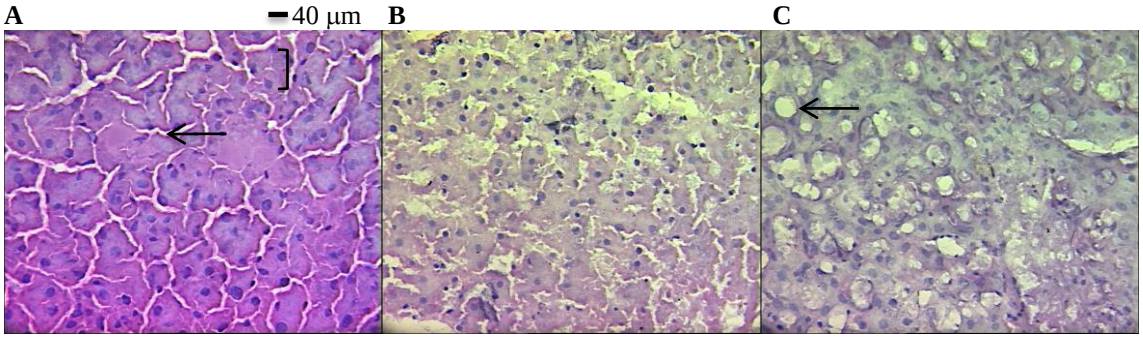

Figure 26. Haematoxylin (blue) and eosin (red) stained rat liver prepared using cryostat sectioning. **a)** Rat liver tissue prior to microfluidic incubation. Hepatocytes (bracket) and sinusoids (arrow) demonstrated, **b)** Rat liver following four days of incubation in the microfluidic device without radiotherapy and **c)** Rat liver following seven days of incubation in the microfluidic device. Vacuolation demonstrated by arrow. 400x magnification.

Significant architectural changes were demonstrated in the irradiated tissue when compared to the tissue that had been incubated in the microfluidic device for the same duration without radiotherapy treatment. These changes were indicative of hepatocellular death, characterised by the loss of nuclei and the formation of vacuoles. This was evident after treatment with two fractions of 10 Gy (**Figure 27b**) and to a greater extent following treatment with five fractions of 4 Gy (**Figure 27c**).

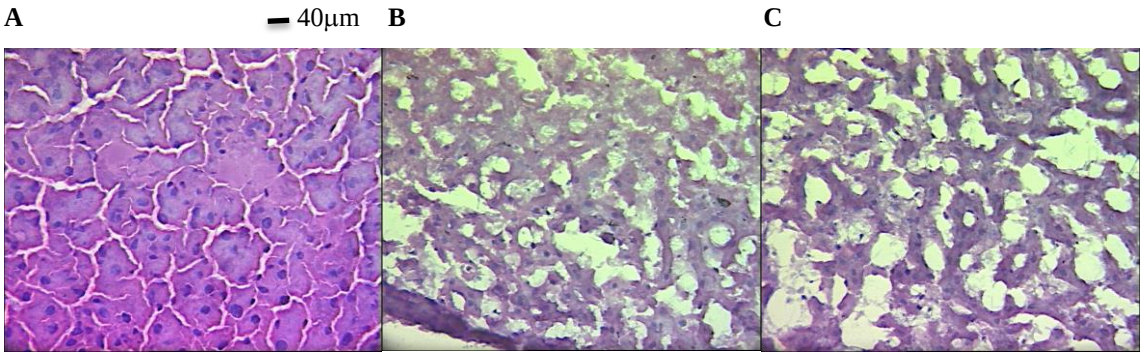

Figure 27. Haematoxylin (blue) and eosin (red) stained rat liver prepared using cryostat sectioning. **a)** Rat liver tissue prior to microfluidic incubation. **b)** Following seven days of incubation in the microfluidic device following with treatment using two fractions radiotherapy of 10Gy at day two and day three and **c)** seven days of incubation in the microfluidic device following treatment with five fractions of 4Gy on days two to six.

3.4 Discussion

3.4.1 Cytotoxicity measurement through detection of LDH

The release of LDH from a cell is a marker of both apoptotic and necrotic cell death *(Kroemer et al., 2009)* and is an established marker of radiation-induced cytotoxicity *(Ts'ao et al., 1996, Reddy and Lokesh, 1996, Cai et al., 2000).* Hattersley et al. *(Hattersley et al., 2012)* demonstrated how measurement of LDH in the effluent from the microfluidic device could detect chemotherapy-induced cytotoxicity in HNSCC tissue, which had been maintained in an identical microfluidic device to that used in the current study.

Under normal incubation conditions, without radiotherapy treatment, the rat liver tissue demonstrated raised levels of LDH during the first 24 h of incubation in the microfluidic device. The initial increased levels were consistently present and are thought to be caused by tissue handling and dissection during the tissue preparation stage, an observation that has been previously reported in HNSCC and rat liver *(Hattersley et al., 2011, Hattersley et al., 2012).* The LDH levels in the effluent subsequently decreased to minimally detectable levels following the first day of incubation suggesting either that the cells were no longer dying or that all of the tissue had died within the first day. To determine which of these was correct, lysis buffer was added to the tissue culture medium, which caused maximal cell membrane rupture, releasing LDH from any remaining live cells. In all experiments where lysis buffer was added, in both rat liver and HNSCC tissue, a rise in LDH levels was observed 2-8 h after addition, indicating intact viable cells within the tissue following maintenance in the microfluidic device. These findings were in agreement with Hattersley et al. who used an identical device with HNSCC and rat liver *(Hattersley et al., 2008, Hattersley et al., 2012).*

The microfluidic device was capable of maintaining both the irradiated and the non-irradiated control rat liver tissue in a viable state for up to 411 h, almost double the length of time that any tissue had previously been maintained using this microfluidic device *(Hattersley et al., 2008, Hattersley et al., 2012).* This demonstrated the potential of this technique for assessing tissue response to various interrogation methods, such as radiation and/or chemotherapy over a prolonged time period, which is more representative of the *in vivo* environment.

Administration of a single radiation dose of 20 Gy to the rat liver caused a significant increase in LDH release in the 2 h post-irradiation period, which subsequently decreased to levels comparable with the control tissue. The LDH levels remained low until the lysis agent

was added to the culture medium, after which a demonstrable increase in LDH release was observed in both the irradiated and control tissues, indicating viable cells remaining within the tissue. This demonstrates that cell death is induced by 20 Gy irradiation, but the existence of viable cells suggested that only a proportion of the cells had undergone radiation-induced cytotoxicity. A similar *in vitro* response to much lower doses of radiation (between 1 Gy and 4 Gy) was detected by Rao et al. *(Rao and Rao, 2010)* who demonstrated a significant increase in LDH release in the 2 h post-irradiation period followed by a subsequent decrease, however this was using a HeLa cell line irradiated in culture.

The method by which hepatocytes are affected by radiation was proposed by Castell et al. *(Castell JV, 1987)* who stated that radiation-induced alterations in non-parenchymal liver cells may be responsible for microvascular necrosis leading to the loss of hepatocytes as a result of a stimulation of a cascade of pathological events. Other studies have demonstrated severe hepatic injury after treatment with radiation doses similar to 20 Gy. Zhao et al. *(Zhao et al., 2009)* treated a section of rat liver *in vivo* with radiation and demonstrated severe hepatic injury after treatment with 25 Gy, as assessed by alanine aminotransferase (ALT) and aspartate aminotransferase (AST) activity and histopathological analysis. Through the irradiation of whole rat liver *in vivo,* Geraci et al. *(Geraci, 1985)* determined that the median lethal dose (LD50) for irradiation of the whole rat liver was 24 Gy. Considering that this was the LD50 for whole rat liver, it is not surprising that treatment of a biopsy-sized specimen of rat liver, as was used in the current study, caused a significant level of cellular death in the microfluidic device.

Senescence and apoptosis have both been demonstrated as modes of radiation-induced cytotoxicity in a variety of hepatocyte models, for example Koenig et al. *(Koenig S, 2008)* demonstrated that partial liver irradiation i.e. treatment of a section of the liver *in vivo* with 25 Gy caused a prolonged cell cycle block with increased levels of p53, p21 and cyclin D1, potentially leading to cell senescence. Shimura et al. *(Shimura T, 2010)* also demonstrated that treatment of the HepG2 and HeLa cell lines with a fractionated radiation course resulted in an overexpression of cyclin D1, which lead to the activation of DNA damage response mechanisms. Christiansen et al. *(Christiansen et al., 2004)* demonstrated that TNF-α-mediated apoptosis was the primary mode of radiotherapy-induced cytotoxicity in irradiated hepatocytes in culture following treatment with 2, 8 and 25 Gy. A dose-dependent relationship, with an increase in cell death for a given increase in radiation dose has previously been demonstrated when irradiating hepatocytes *in vitro* (**Table 8**).

Table 8. A summary of studies assessing the *in vitro* response of hepatocytes to radiation.

Authors	**Cell type**	**Radiation dose**	**Response**
Sakahara et al. *(Sakahara et al., 1992)*	Mice hepatocytes monolayer		Frequency of radiation-induced micronuclei increased in a dose-dependent manner.
Geraci et al. *(Geraci and Mariano, 1993)*	Hepatocytes	>10Gy	A dose-dependent decline in the number of hepatocytes with doses greater than 10Gy.
Nakajima et al. *(Nakajima and Yukawa, 1996)*	Monolayer hepatocytes	5Gy or 50Gy	Irradiation induced lipid peroxidation of hepatocytes in the range of 0-50Gy in a dose-dependent manner
Srinivasan et al. *(Srinivasan et al., 2008)*	Hepatocytes	1Gy to 4Gy	Increase in severity of DNA damage with an increase in radiation dose measured by the comet assay.
Maruko et al. *(Maruko et al., 2010)*	Rat hepatocytes		Difference in radioresponse between periportal and perivenous hepatocytes with a greater decline in DNA synthesis in the periportal hepatocytes with treatment <10Gy, but no difference ≥10Gy.
Jin et al. *(Jin et al., 2011)*	Hep G2 cells	0Gy to 6Gy	Dose-dependent decrease in survival fraction.
Zhang et al. *(Zhang et al., 2012)*	Human hepatoma cell line HepG2	0Gy to 10Gy	Dose-dependent decrease in survival fraction 5 days after irradiation with 80% following 2Gy cf 22% after 10Gy.

A dose-dependent relationship has also been demonstrated *in vivo* where whole rat liver irradiation treated with 15 Gy and 25 Gy demonstrated minimal histological change and showed no significant change in liver enzymatic function after 15 Gy. However, after irradiation with 25 Gy, there were demonstrable histological abnormalities, consisting of hepatic vein lesions and cellular necrosis, and liver injury, measured by the rose bengal test and plasma alkaline phosphatase concentrations, with a latent period of 35 to 42 days *(Geraci et al., 1991).* An advantage of the microfluidic system was that these tissue changes were demonstrated sooner, observable after only a few days following irradiation.

To investigate the effects of a fractionated course, which is closer to the radiation regimen used to treat patients, 20 Gy was divided into two fractions of 10 Gy, administered 24 h apart on days two and three of incubation. Using this method of irradiation the tissue maintained its integrity allowing the rat liver tissue to continue being cultured in the same microfluidic

device without the need for tissue transfer, thereby reducing the potential of tissue damage during transfer. A significant increase in LDH release was observed, however, only after the second fraction of 10 Gy in the 2 h post-irradiation period, similar to that recorded following treatment with a single dose of 20 Gy. No further LDH release was detected even up to 15 days of incubation until the addition of the lysis agent to the culture medium, indicating that no late stage cytotoxicity was caused by irradiation of the rat liver tissue. This is in contrast to the results observed following single radiotherapy doses of 10 Gy or less or a fractionated course, of five fractions of 4 Gy in which no significant increase in LDH release was observed.

In the experiment where the rat liver tissue was treated with a fractionated course of five fractions of 4 Gy. Although the total dose of the experiment in which the rat liver tissue was irradiated with five fractions of 4 Gy was 20 Gy, there was no significant increase in LDH release, which may indicate that the dose of each fraction was such that it allowed for DNA repair mechanisms to repair single-strand DNA breaks and that the number of double-strand DNA breaks caused was not sufficient to induce a significant level of cellular death. The premise of fractionation is that normal parenchymal cells are able to undergo repair between fractions, whilst the impaired repair mechanisms of tumour cells leads to cell death, which was reproduced by this technique.

3.4.2 Assessment of rat liver function by measurement of albumin and urea synthesis following irradiation.

Albumin and urea production are established markers of hepatic synthetic function *in vitro (Castell JV, 1987, Cheng Y, 2013)* and have previously been used to study the effects of irradiation on hepatocytes *(Lahiri S, 1995).* Both markers have previously been used to measure rat liver function in the effluent using an identical microfluidic technique *(Hattersley et al., 2008, Hattersley et al., 2012).*

Following incubation in the microfluidic device without radiotherapy treatment, the rat liver tissue continued to produce albumin for 197 h (eight days), although levels dropped after 53 h, and urea for 13 days, with a steady decline over seven days, indicating that the rat liver remained functional whilst being maintained using this technique. The levels of albumin and urea produced were comparable to other studies using microfluidic techniques *(Hattersley et al., 2008)*, however, the albumin and urea production in the current study was investigated

over a considerably longer period than previously reported, demonstrating the ability of this technique to maintain synthetic function and the potential for this technique to be utilised for tissue interrogation over a prolonged duration. This is the first study in which microfluidic techniques have been used to study hepatic synthetic function in response to radiotherapy.

Several other studies have investigated hepatocytes *in vitro* using three-dimensional culture techniques without radiation, with the majority using spheroids, and have demonstrated increased levels of albumin and urea production over monolayer culture *(Takahashi et al., 2010, Tostoes et al., 2011, Hsieh et al., 2010, Lee et al., 2013, Rossouw et al., 2012, Ng et al., 2005, Du et al., 2008, Mercey E, 2010, Cheng Y, 2013).* The advantage of the rat liver tissue used in this study over previous studies was that the tissue architecture was maintained, thereby preserving the intra- and intercellular relations and interactions which, as a result, enabled prolonged production of albumin and urea. Lee et al. *(Lee et al., 2013)* used spheroids on a liver-on-a-chip device to investigate the interactions between hepatocyte and hepatic stellate cells. They demonstrated that hepatic stellate cells have an important role in maintaining tight cell-cell contacts, which, in turn, improve liver-specific function. They demonstrated that spheroids derived from co-cultures i.e. hepatocytes and hepatic stellate cells exhibited improved albumin and urea synthesis over an eight day period compared to spheroids cultured solely from hepatocytes. Rossouw et al. *(Rossouw et al., 2012)* concluded that hepatocytes produced greater levels of albumin and urea in three-dimensional culture, because they were anchorage-dependent cells, which are sensitive to their microenvironment *(Ng et al., 2005)*, a statement which reinforced the importance of maintaining the intra- and intercellular interactions if the *in vivo* synthetic process is to be replicated.

Following the administration of a single dose of 20 Gy irradiation to the rat liver, there was a significant decrease in albumin production four hours post-treatment. This did not coincide with the point of maximum cellular damage, as demonstrated by the significant increase in LDH release, which occurred two hours after irradiation. The continued detection of albumin for four hours following irradiation was probably caused by the leaching of albumin from intracellular stores from hepatocytes with radiation-induced cell membrane damage. Albumin levels subsequently dropped to minimal detectable levels 22-24 h following irradiation. Geraci et al. *(Geraci and Mariano, 1993)* demonstrated that the treatment of rat hepatocytes with greater than 10 Gy radiation resulted in a dose-dependent decline in liver mass and hepatocytes. Interestingly, they also demonstrated that viable hepatocytes isolated from

irradiated dysfunctional livers were functionally normal when assessed with the rose bengal clearance test.

Following 20 Gy, there was a significant decrease in urea production during the 24 h following irradiation. There is a paucity of studies in the literature assessing the effects of ionising radiation on urea production by hepatocytes. Lahiri et al. *(Lahiri S, 1995)* assessed the effect of UV-B radiation of isolated rat hepatocytes in culture at various doses from 400-1000 Jm^{-2}. Urea production was not affected by any dose of UV-B, demonstrating that urea production depends on the type of radiation that the cells are exposed to.

Despite the fact that there was a significant increase in LDH release after treating the tissue with the second fraction of 10 Gy, albumin and urea production continued. This indicated that the level of cytotoxicity was enough to cause a significant release of LDH, but not enough to affect the synthetic function of all cells. The comparative preservation of tissue following the fractionated course was further confirmed by the lack of tissue degradation observed. The continued production of albumin in this current study is similar to two *in vivo* studies by Zamyatkina et al. *(Zamyatkina, 1962, Zamyatkina, 1965)* who reported a significant 75% decline in albumin synthesis by rat liver four to six days following whole-body irradiation with 900rads or 9 Gy and John et al. *(John and Miller, 1968)* who demonstrated a 25% reduction over the same time period under similar conditions.

3.4.3 Morphological changes in the rat liver in response to exposure to ionising radiation.

The histological appearance of the rat liver prior to being placed in the microfluidic device demonstrated that there was preservation of tissue architecture following retrieval of the liver from the rat and after the tissue had undergone tissue preparation including or excluding snap-freezing.

After incubation in the microfluidic device for four and six days without radiation, there were some mild changes in the tissue morphology, however, the majority of the tissue architecture was preserved.

After incubation in the microfluidic device for six days and with irradiation consisting of two fractions of 10 Gy or five fractions of 4 Gy, there were demonstrable histological changes in the irradiated tissue compared to the non-irradiated tissue with the primary finding being an increase in vacuolation and reduction in nuclei, both indicators of cellular death, findings that

were in keeping with those previously reported *(Rubaj, 1975, Geraci et al., 1991, Zavodnik LB, 2003).* However, even though there were changes in the morphology of the cells, this did not correlate with cell death or hepatocyte function as measured by LDH and albumin and urea respectively.

Chapter 4

The effect of radiation on head and neck squamous cell carcinoma (HNSCC) tissue maintained in a microfluidic device

4.1 Introduction

Radiotherapy is a well-established single modality therapy for the treatment of HNSCC. However, radioresistance is a major obstacle to a successful treatment with up to 25% of T2 laryngeal cancers being radioresistant *(Fernberg et al., 1989, Klintenberg et al., 1996, Johansen et al., 2002).* As well as early stage HNSCC, radioresistance is a major factor in the treatment of larger tumours. It is currently impossible to predict which tumours will respond to radiotherapy prior to a patient commencing treatment, which means that a patient will potentially undergo an unnecessary treatment with its associated morbidity.

The aim of this part of the study was to use microfluidic techniques to investigate the effects of radiation on HNSCC tissue with the ultimate goal being to develop a microfluidic device that is capable of predicting the response to radiotherapy of an individual's tumour prior to them commencing treatment.

It was important to establish initially whether this microfluidic device could maintain HNSCC tissue in a viable state over a number of days without any radiation as was successfully demonstrated with the rat liver tissue. This was determined by measuring the LDH in the effluent from the device. To determine whether the HNSCC was alive at the end of the experiment, a lysis agent was added to the culture medium, which caused maximal cell membrane rupture, releasing all the potential LDH into the effluent and demonstrating intact viable cells remaining in the tissue.

Several methods of analysis were used to study the effects of radiation on the HNSCC tissue. LDH was measured in the effluent from the microfluidic device to assess radiation-induced cell death as it had been in the rat liver. Cytochrome c is a specific marker of apoptosis and was measured in the effluent following irradiation of the HSNCC tissue. Hattersley et al *(Hattersley et al., 2012)* used it in an identical microfluidic device to demonstrate apoptosis induced by exposing the HSNCC tissue to chemotherapeutic agents. In the current study,

cytochrome c was used to identify whether a soluble marker could be measured in the effluent from the device to detect apoptosis following irradiation with 5 Gy or 10 Gy. These doses were chosen as they closely resembled radiotherapy doses that are used in the clinical treatment of HNSCC, with the replication of the clinical setting being the goal of the study.

In addition to LDH and cytochrome c, tissue analysis methods were used to investigate the effects of radiation on the HNSCC tissue. As with the rat liver tissue, Haematoxylin and Eosin staining was used to analyse changes in the architecture of the HNSCC tissue in response to incubation in the microfluidic device and exposure to radiation. Sections taken from the HNSCC at each stage of the process were analysed histologically for comparison to determine the morphological changes caused by each of the following stages: HNSCC tissue that had been excised from the patient, but had not been incubated in the microfluidic device, tissue that had been incubated in the device without irradiation and tissue that had been incubated in the device and irradiated.

Immunohistochemistry was performed with pancytokeratin and the M30 antibody. In order to confirm the presence of HNSCC cells in the tissue specimens that were incubated in the microfluidic device, a pancytokeratin antibody was used, which was capable of detecting HNSCC in a metastatic lymph node. Cytokeratins are proteins of keratin-containing intermediate filaments found in the intracytoplasmic cytoskeleton of epithelial tissue *(Franke et al., 1979)* and are used in the clinical diagnosis of HNSCC. The initial experiments studied the expression of pancytokeratin in the HNSCC tissue prior to it being incubated in the microfluidic device compared to the tissue that had been incubated for four and seven days respectively. The effect of radiation was assessed by studying its expression in the tissue following irradiation with a single dose of 2 Gy and five daily fractions of 2 Gy. These doses were used as they replicate a single fraction of a clinical course of radiotherapy and a weeklong radiotherapy course that a patient being treated for HNSCC would undergo.

The M30 antibody can show apoptosis by the detection of cytokeratin 18 that has been cleaved by caspase-3; its ability to demonstrate radiation-induced apoptosis has previously been demonstrated *(Allal et al., 2003, Gosens et al., 2008)*. This was used to demonstrate any apoptotic cell death that had been caused by irradiation of the HNSCC tissue. It was used in the HNSCC tissue prior to it being placed in the microfluidic device and following seven days of incubation in the device to determine whether there was any apoptosis caused by incubation of the tissue in the device. To demonstrate radiation-induced apoptosis, it was used

in the HNSCC tissue that had been irradiated with a single dose of 2 Gy and five daily fractions of 2 Gy.

Irradiation of HNSCC cells causes single and double strand DNA breaks, which, if unrepaired, lead to radiation-induced cell death *(Goodhead, 1994)*. The DNA-strand breaks were detectable using the terminal deoxynucleotidyl transferase dUTP nick end labelling (TUNEL) assay. TUNEL was used in the current study to detect the radiation-induced DNA-strand breaks and as an apoptotic marker to correlate with the results from using the M30 antibody.

4.2 Materials and Methods

4.2.1 Design and fabrication of the microfluidic device

The glass microfluidic devices were fabricated in-house at the Department of Chemistry, University of Hull using photolithography techniques as described in section 2.1, the same as those used with the rat liver tissue.

4.2.2 Preparation and running of the microfluidic device

The microfluidic device was prepared as in section 2.2.1. Once assembled the microfluidic device was run as per section 2.2.2. The effluent was collected at two-hourly intervals. The effluent was collected overnight, but these samples were not analysed.

4.2.3 Administration of radiation

The HNSCC tissue was irradiated using a 6MV photon beam from a Varian Linear Accelerator as in section 2.5. The tissue was exposed to single doses of 5 Gy, 10 Gy, 20 Gy and 40 Gy. The 5 Gy and 10 Gy radiation doses were administered to the same tissues at a 24 h interval, as were the 20 Gy and 40 Gy. The radiation had to be administered in this manner due to the logistics of irradiating the fresh tissue, given the clinical utility of the Linear Accelerator. In the second series of experiments, the HNSCC tissue was exposed to a single dose of 2 Gy and five daily fractions of 2 Gy. Each experiment was performed three times.

4.2.4 Collection of HNSCC tissue specimens

Samples were provided in an anonymous manner by patients undergoing surgery for T1-T3 head and neck squamous cell carcinoma, in accordance with Local Research Ethics Committee (LREC-10/H1304/6; AM01) and NHS Trust R&D approval (R0987) as described in section 2.4. Tissue specimens from different HNSCC primary and metastatic sites were used for analysis to ensure adequate variation.

4.2.5 LDH assay

The LDH assay was performed as described in section 2.6.1. The assay was performed on each two-hourly effluent sample in duplicate. The initial experiment to determine whether the microfluidic device could maintain the HNSCC tissue in a viable state was repeated with nine chips using tissue from different HNSCC tumours. The experiments in which the HNSCC tissue was irradiated were performed three times. The mean absorbance value was calculated. A negative control consisting of culture medium alone was subtracted.

4.2.6 Cytochrome c ELISA

Cytochrome c was analysed in the effluent from HNSCC tissue that had been treated with a single dose of 5 Gy or 10 Gy as in section 2.6.2. The experiment for each dose was repeated twice. Each sample was analysed in duplicate and a negative control consisting of culture medium alone was subtracted.

4.2.7 Preparation of tissue for cryostat sectioning

The HNSCC liver tissue was removed from the microfluidic device and prepared as in section 2.8.

4.2.8 Cryostat sectioning

Prior to sectioning, each tissue specimen was prepared as in section 2.9. A cryostat (Leica CM1100, Leica biosystems, UK) was used to ensure that the samples remained frozen whilst sectioning. Each section was placed on Superfrost® Plus glass microscope slides (Merck, UK) with six sections per slide. The slides were then stored at -20^{o}C for future analysis.

4.2.9 Histological analysis of tissue using Haematoxylin and Eosin

For histological analysis, the HNSCC tissue sections were stained with haematoxylin and eosin as described in section 2.10.

4.2.10 Pancytokeratin and M30 CytoDEATH™

Immunohistochemistry was performed on the HNSCC sections from three separate stages of the process: HNSCC tissue that had been removed from the patient, but not incubated in the microfluidic device, tissue that had been incubated in the device without irradiation and tissue that had been incubated in the device and irradiated as described in section 2.11. The mean apoptotic index was calculated from the M30 results as described in 2.12. Each experiment was carried out on a different HNSCC tumour and performed three times.

4.2.11 Terminal deoxynucleotidyl transferase dUTP nick end labelling (TUNEL)

The fluorescent-labelled TUNEL assay was carried out as described in section 2.11.2. The cells that had undergone radiation-induced DNA-strand breaks were stained with FITC and displayed green fluorescence. A DNA-strand break index was calculated in the same manner as the apoptotic index as described in section 2.12. Each experiment was carried on a different HNSCC tumour and performed three times.

4.3 Results

4.3.1 Assessment of viability of the HNSCC tissue by measuring LDH release

LDH was measureable in the effluent from the microfluidic device as a result of cell death. **Figure 28** shows the levels of LDH released from HNSCC tissue (n=9 experiments), maintained in the microfluidic device without intervention over a period of 149 h. The initial elevated LDH levels decreased to minimally detectable levels 24-28 h after placement of the tissue into the microfluidic device. LDH levels remained low in a similar manner to the rat liver, until the lysis reagent was added to the medium at 141 h, inducing a subsequent rise in LDH release 2-8 h after its addition in a similar manner to the rat liver tissue.

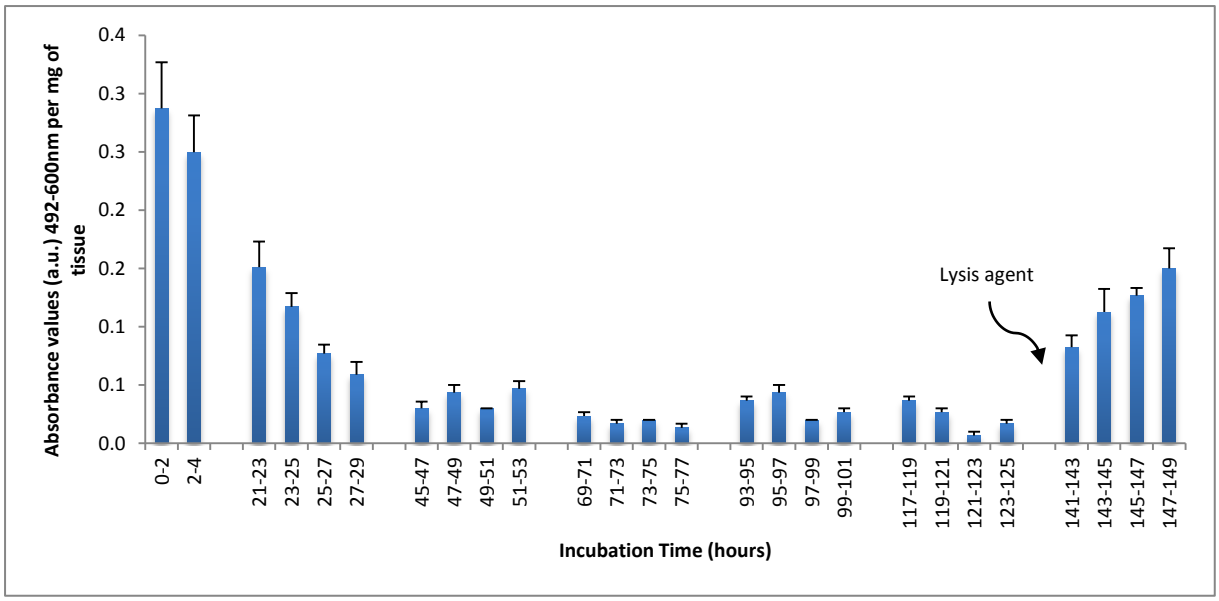

Figure 28. Absorbance measurements (492-600nm) following LDH assays on effluent from HNSCC tissue maintained in a microfluidic device for 149 h, standardised per mg of tissue (Mean of 9 separate experiments + SEM). Lysis agent was added at 141 hours as indicated by arrow. The effluent was not collected overnight, as demonstrated by the gaps in the incubation time axis.

4.3.2 LDH release from HNSCC tissue following irradiation as a measure of cell death

Single doses of 40 Gy and 20 Gy (n=3 for each dose: T1N2b tonsil, T3N2b larynx and T2N2b tonsil cervical metastases), 10 Gy and 5 Gy (n=3 for each dose: T1N2b tonsil, T0N2a cervical metastasis and T3 larynx) were administered to the HNSCC at different timepoints due to the logistics of irradiating the fresh HNSCC tissue (**Figure 29**). There was no

difference in LDH release between the individual tumours, therefore, an average of the three was used.

A significant increase in LDH (p=0.009) release into the effluent from the device was demonstrated after the HNSCC tissue was treated with 40 Gy. This surge in LDH occurred in the initial 2 h following irradiation, as in the rat liver. In a series of experiments, no significant LDH increase was demonstrated in the HNSCC tissue when less than 20 Gy was administered (n=8 experiments; data not shown).

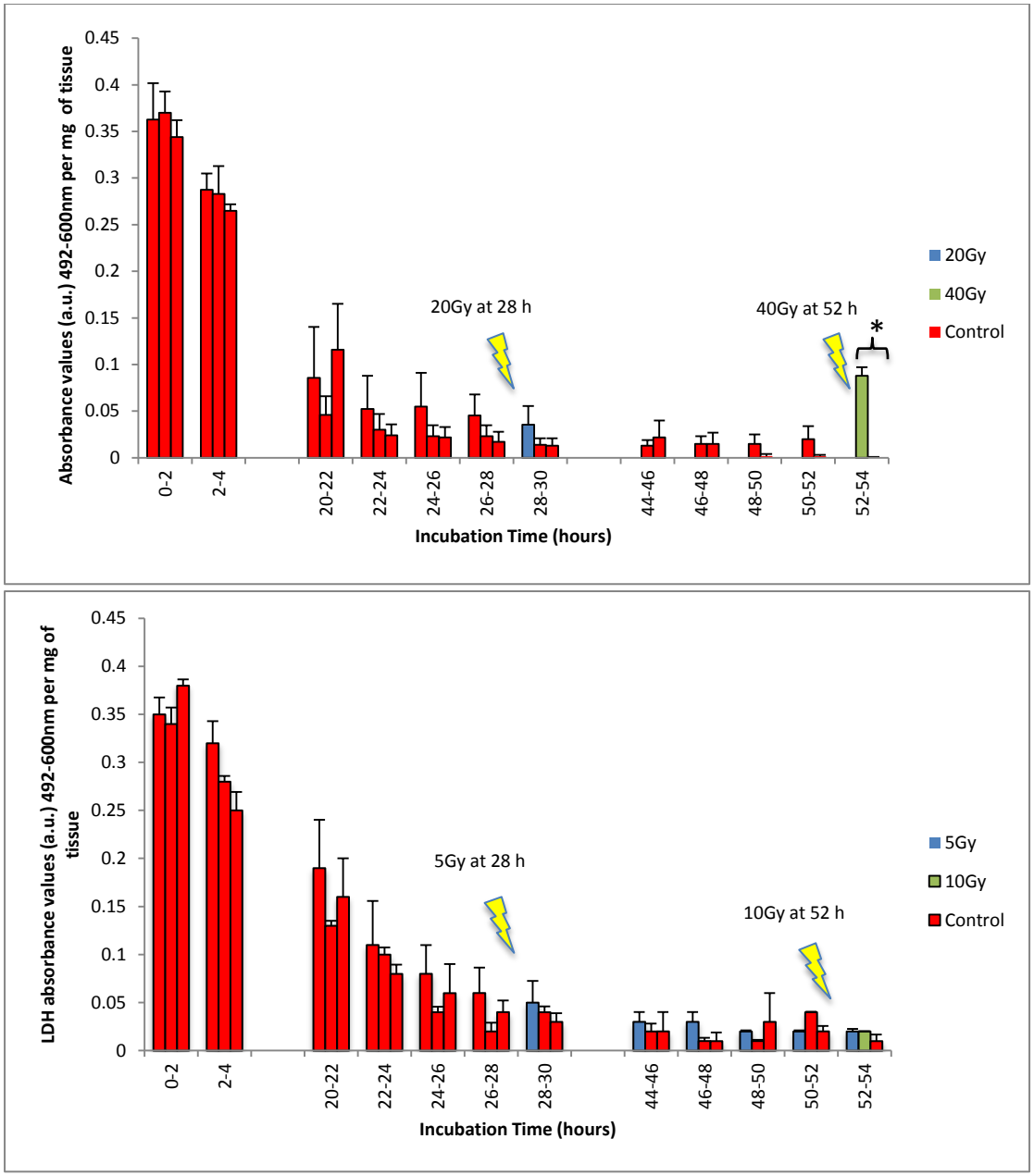

Figure 29. LDH absorbance in the effluent of HNSCC tissue maintained in a microfluidic device treated with a single dose of a) 20 Gy irradiation at 28 h and 40 Gy at 52 h (n=3: T1N2b tonsil, T3N2b larynx and T2N2b cervical metastases) and b) 5 Gy at 28 h (n=3) and 10 Gy at 52 h (n=3: T1N2b tonsil, T0N2a cervical metastasis and T3 larynx). No lysis agent added. Control received no radiotherapy. A significant LDH release was detected after administration of 40 Gy irradiation compared to control. p=0.009* unpaired t-test.

4.3.3 Cytochrome c release from HNSCC tissue following irradiation as a measure of apoptotic cell death

In order to determine whether apoptosis could be detected in the effluent following the administration of a lower, more clinically relevant dose of radiotherapy (5Gy and 10Gy) (n=2 for each dose; T2N2 oropharyngeal cervical lymph node metastases) the apoptotic-specific marker cytochrome c was measured. The pattern of release of cytochrome c was similar to that of LDH with initial high levels decreasing after 22 h. There was no overall significant increase in cytochrome c release observed in the group treated with radiation regardless of the dose administered compared with the control measured for at least 72 h following irradiation of the HNSCC tissue (p=0.895) (**Table 9**) (**Figure 30**).

Table 9. Cytochrome c levels with T2N2 orophrayngeal SCC metastatic cervical lymph nodes following irradiation with 5Gy and 10Gy at 28 h and 52 h respectively. The same calculation was performed for the control tissue.

Incubation time (hours)	Cytochrome c ($ng\ ml^{-1}$)		Cytochrome c per mg of tissue ($ng\ ml^{-1}\ mg^{-1}$)		Mean level of cytochrome c per mg of tissue ($ng\ ml^{-1}\ mg^{-1}$)
	T2N2 OPSCC LN	T2N2 OPSCC LN	T2N2 OPSCC LN (7.8mg)	T2N2 OPSCC LN (7.1mg)	
0-2	1.108	1.243	0.142	0.175	0.159
2-4	0.936	0.994	0.120	0.140	0.130
20-22	0.437	0.525	0.056	0.074	0.065
22-24	0.242	0.412	0.031	0.058	0.045
24-26	0.234	0.347	0.030	0.049	0.040
26-28	0.211	0.263	0.027	0.037	0.032
28-30	0.172	0.199	0.022	0.028	0.025
44-46	0.164	0.220	0.021	0.031	0.026
46-48	0.109	0.185	0.014	0.026	0.020
48-50	0.094	0.206	0.012	0.029	0.021
50-52	0.070	0.107	0.009	0.015	0.012
52-54	0.078	0.078	0.010	0.011	0.011
68-70	0.016	0.083	0.002	0.011	0.007
70-72	0.025	0.072	0.003	0.010	0.007
72-74	0.031	0.066	0.004	0.009	0.008
74-76	0.080	0.057	0.010	0.008	0.011
76-78	0.076	0.074	0.005	0.010	0.008
92-94	0.016	0.077	0.002	0.011	0.007
94-96	0.031	0.081	0.004	0.010	0.007
96-98	0.047	0.086	0.006	0.012	0.009
98-100	0.027	0.100	0.003	0.014	0.009
100-102	0.082	0.135	0.011	0.019	0.015
116-118	0.019	0.070	0.002	0.010	0.007
118-120	0.028	0.050	0.004	0.007	0.007
120-122	0.015	0.081	0.002	0.010	0.006
122-124	0.037	0.079	0.005	0.011	0.008
124-126	0.042	0.021	0.005	0.003	0.004

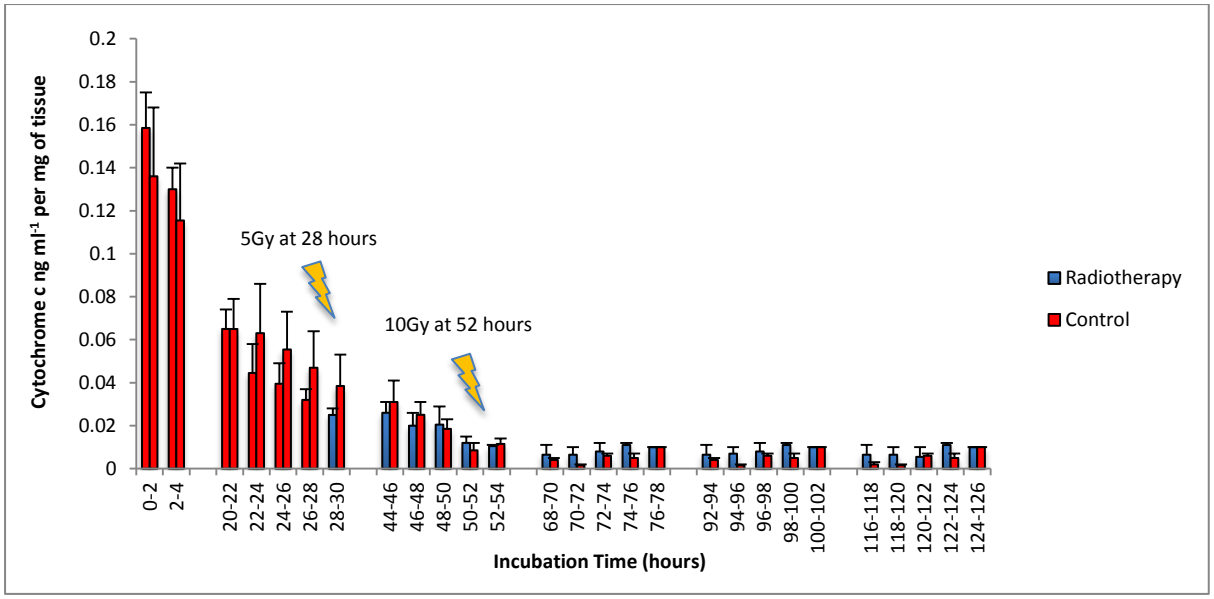

Figure 30. Cytochrome c release from HNSCC tissue maintained in a microfluidic device (n=2: T2N2 oropharyngeal cervical metastases). Single doses of 5 Gy and 10 Gy of radiation were administered at 28 h and 52 h respectively, indicated by the yellow flash arrows. Cytochrome c standardised per mg of tissue (+SEM). Mean of two separate experiments + SEM. *p*=0.895 overall between the irradiated and the control tissue. Unpaired t-test.

4.3.4 Morphology of the HNSCC tissue maintained in a microfluidic device and the effect of irradiation

Histological analysis of cryostat prepared sections, using standard haematoxylin and eosin staining, demonstrated that the structure of the HNSCC tissue was maintained during incubation in the microfluidic device for four days. This can be observed by comparison of the sections in **Figures 31a** & **31b**, **Figures 32a** & **32b** and **Figures 33a** & **33b**. Sections were prepared from an oropharyngeal metastatic cervical lymph node (T2N2a), prior to placement in the microfluidic device (**31a** & **31b**), following four days of incubation (**32a** & **32b**) and following seven days of incubation (**33a** & **33b**). There were no discernible differences in the architecture between the sections without microfluidic incubation and those following four days of incubation with no loss of nuclei or intercellular cohesion. However, following seven days of incubation in the microfluidic device, there were some architectural changes with evidence of mild loss of intercellular cohesion, although this was minimal.

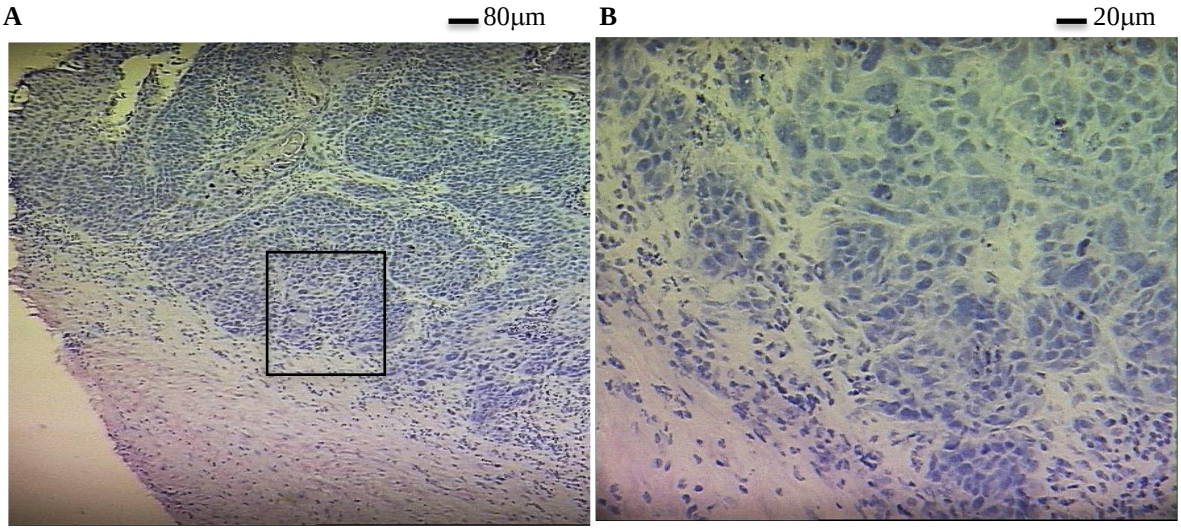

Figure 31. Haematoxylin (blue) and eosin (red) stained HNSCC cryostat sections prepared from tissue before incubation in the microfluidic device (T2N2 oropharyngeal cervical lymph node metastasis). **a)** 50x magnification and **b)** 200x magnification – area of magnification demarcated by square.

No discernible difference was observed in the architecture between the HNSCC tissue incubated in the microfluidic device for four days without irradiation (**Figure 32a & b**) compared with the HNSCC tissue that had been irradiated with 2 Gy on day two and incubated for the same duration (**Figure 33c & d**).

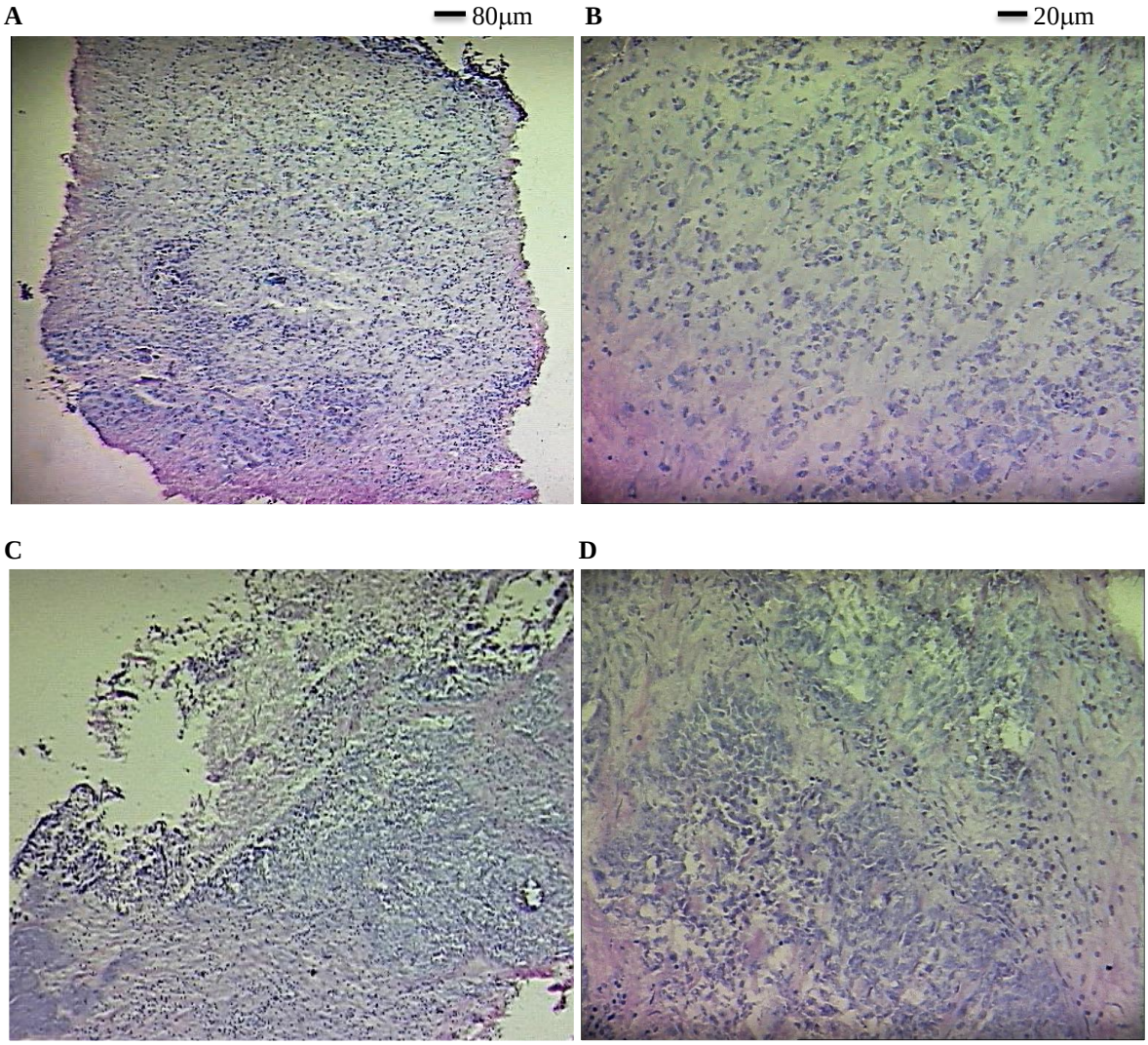

Figure 32. Haematoxylin (blue) and eosin (red) stained HNSCC cryostat prepared tissue (T2N2 oropharyngeal cervical lymph node metastasis) following 4 days of incubation in the microfluidic device. Non-irradiated tissue: **a)** 50x magnification and **b)** 200x magnification. Tissue prepared 72 h after receiving 2 Gy of radiotherapy: **c)** 50x magnification and **d)** 200x magnification.

There was a demonstrable difference in the HNSCC (T2N2a oropharyngeal cervical lymph node metastases) tissue architecture following seven days of incubation between the irradiated and the non-irradiated tissue following five fractions of 2 Gy (**Figure 33**). The irradiated tissue demonstrated characteristics of cellular death with loss of nuclei and intercellular cohesion. A 'keratin pearl' can clearly be seen in the irradiated tissue (arrow), a pathognomic feature of SCC, with a paucity of viable cells surrounding it and distinct loss of intercellular cohesion.

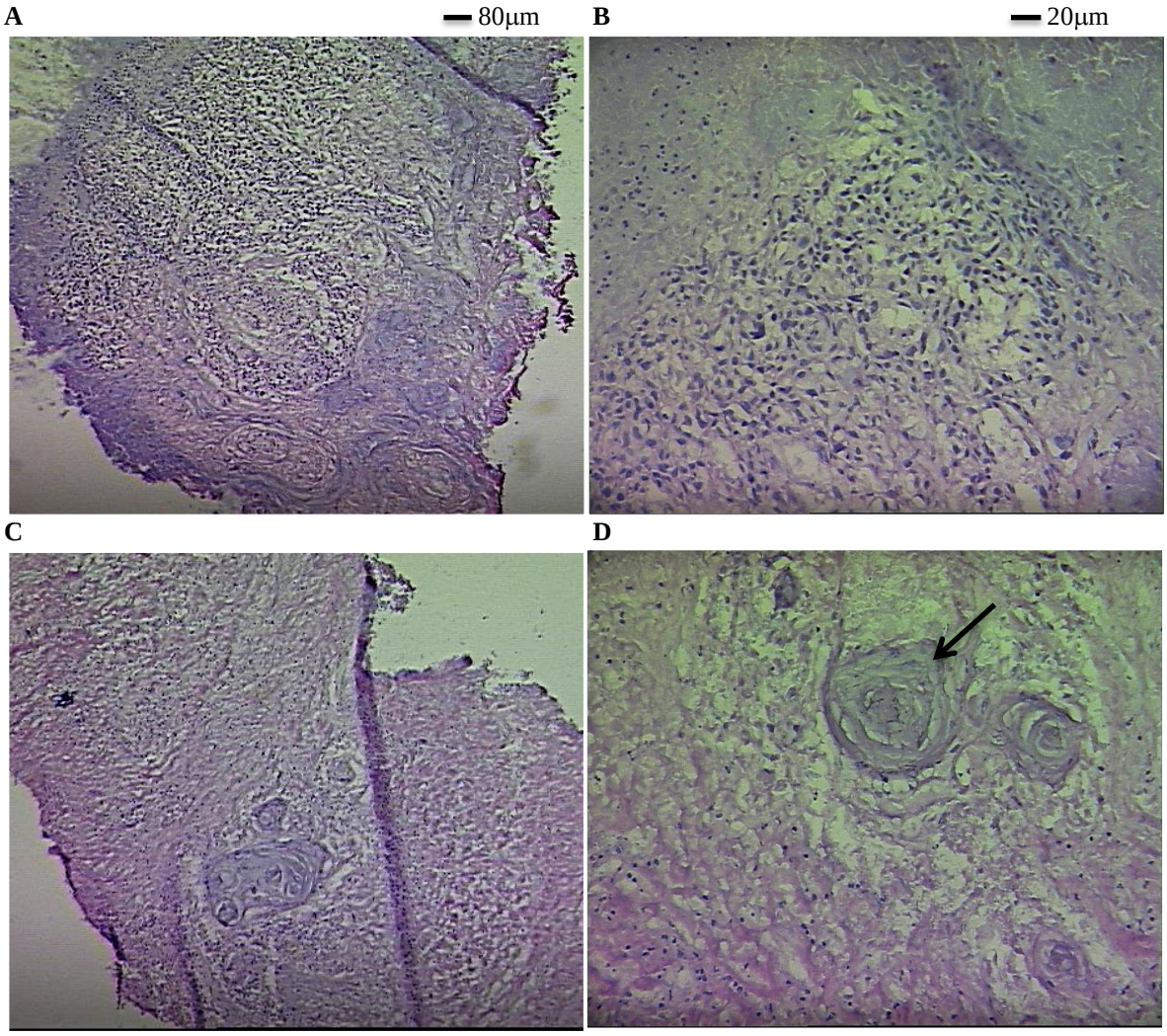

Figure 33. Haematoxylin (blue) and eosin (red) stained HNSCC cryostat prepared tissue (T2N2 oropharyngeal cervical lymph node metastasis). Non-irradiated tissue following 7 days of incubation in the microfluidic device: **a)** 50x magnification and **b)** 200x magnification. HNSCC tissue irradiated with 5 fractions of 2 Gy at 24 h and incubated for a further 6 days: **c)** 50x magnification and **d)** 200x magnification. Keratin pearl demonstrated by arrow.

4.3.5 Detection of the presence of HNSCC cells within the HNSCC sections using pancytokeratin and the effect of radiation on its expression

Pancytokeratin was used to confirm the presence of SCC cells within the HNSCC tissue (T2N2 oropharyngeal cervical lymph node metastases), a process that enabled delineation of areas of SCC within metastatic cervical lymph nodes as demonstrated in **Figures 34a** & **34b,** which show HNSCC tissue prior to being incubated in the microfluidic device.

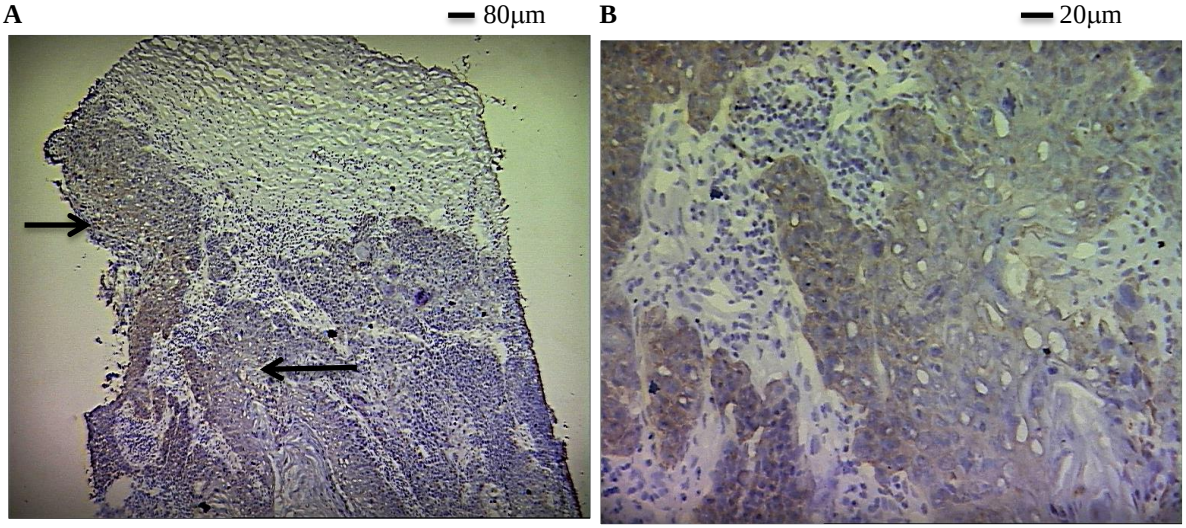

Figure 34. Immunohistochemical staining of cryopreserved HNSCC tissue (T2N2 oropharyngeal cervical lymph node metastasis) with pancytokeratin (1:100 dilution, brown nuclei; blue haematoxylin counterstain) prior to incubation in the microfluidic device as shown by arrows. **a)** 50x magnification. **b)** 200x magnification.

No discernible difference in the expression of cytokeratin was observed between the HNSCC tissue prior to incubation in the microfluidic device (**Figures 34a** & **34b**), at day four of incubation (**Figures 35a** & **35b**) and day seven of incubation (**Figures 36a** & **36b**). Treatment of the tissue with radiotherapy also demonstrated no discernible difference in cytokeratin expression, either after 2 Gy at 24 h (**Figures 35c** & **35d**) or five daily fractions of 2 Gy (**Figures 36c** & **36d**).

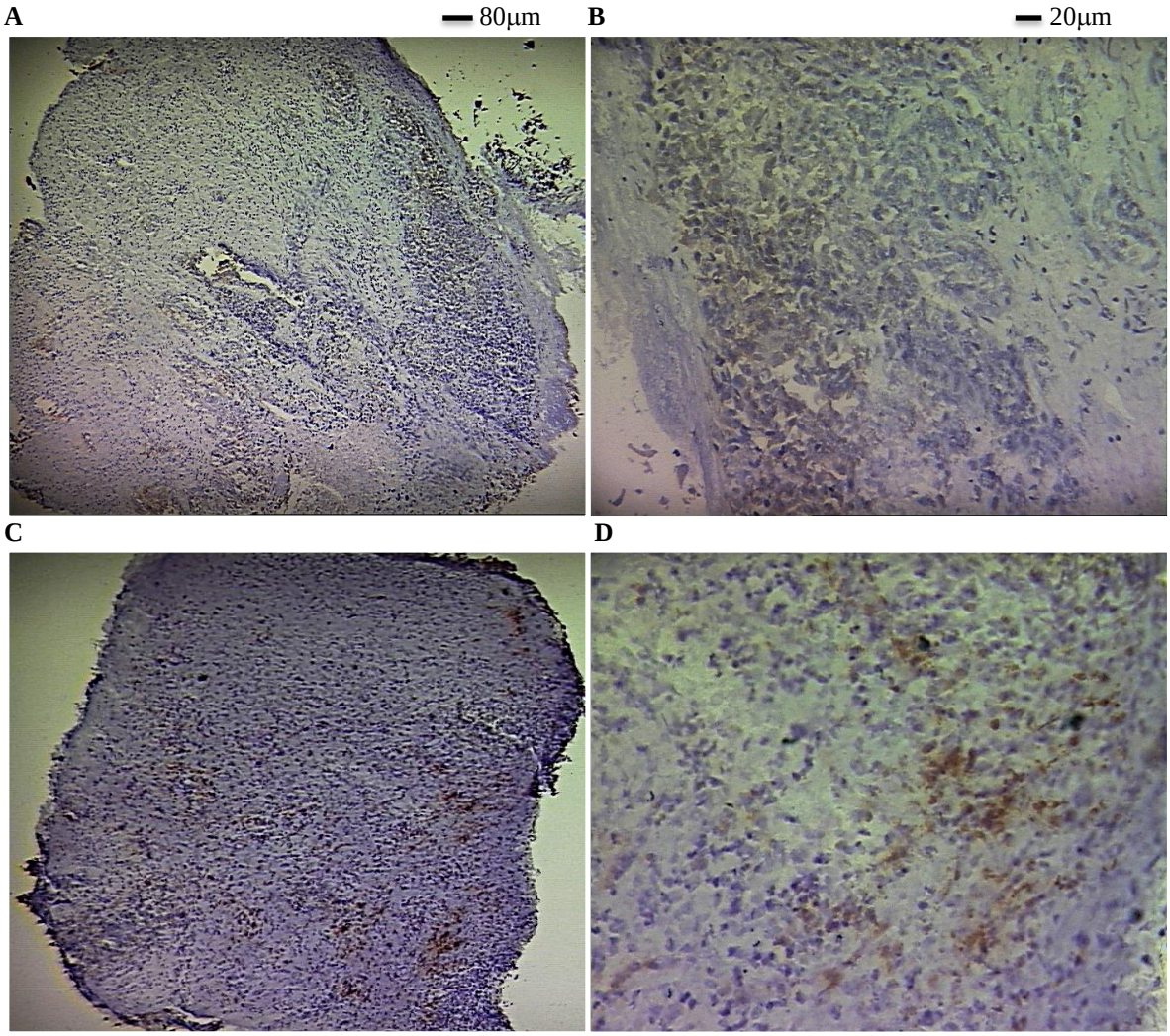

Figure 35. Immunohistochemical staining of cryostat sectioned HNSCC tissue (T2N2 oropharyngeal cervical lymph node metastasis) with pancytokeratin (1:100 dilution, brown nuclei; blue haematoxylin counterstain) following 4 days of incubation in a microfluidic device. Non-irradiated tissue: **a)** 50x magnification. **b)** 200x magnification. HNSCC tissue 72 h after treatment with a single dose of 2 Gy radiotherapy: **c)** 50x magnification. **d)** 200x magnification.

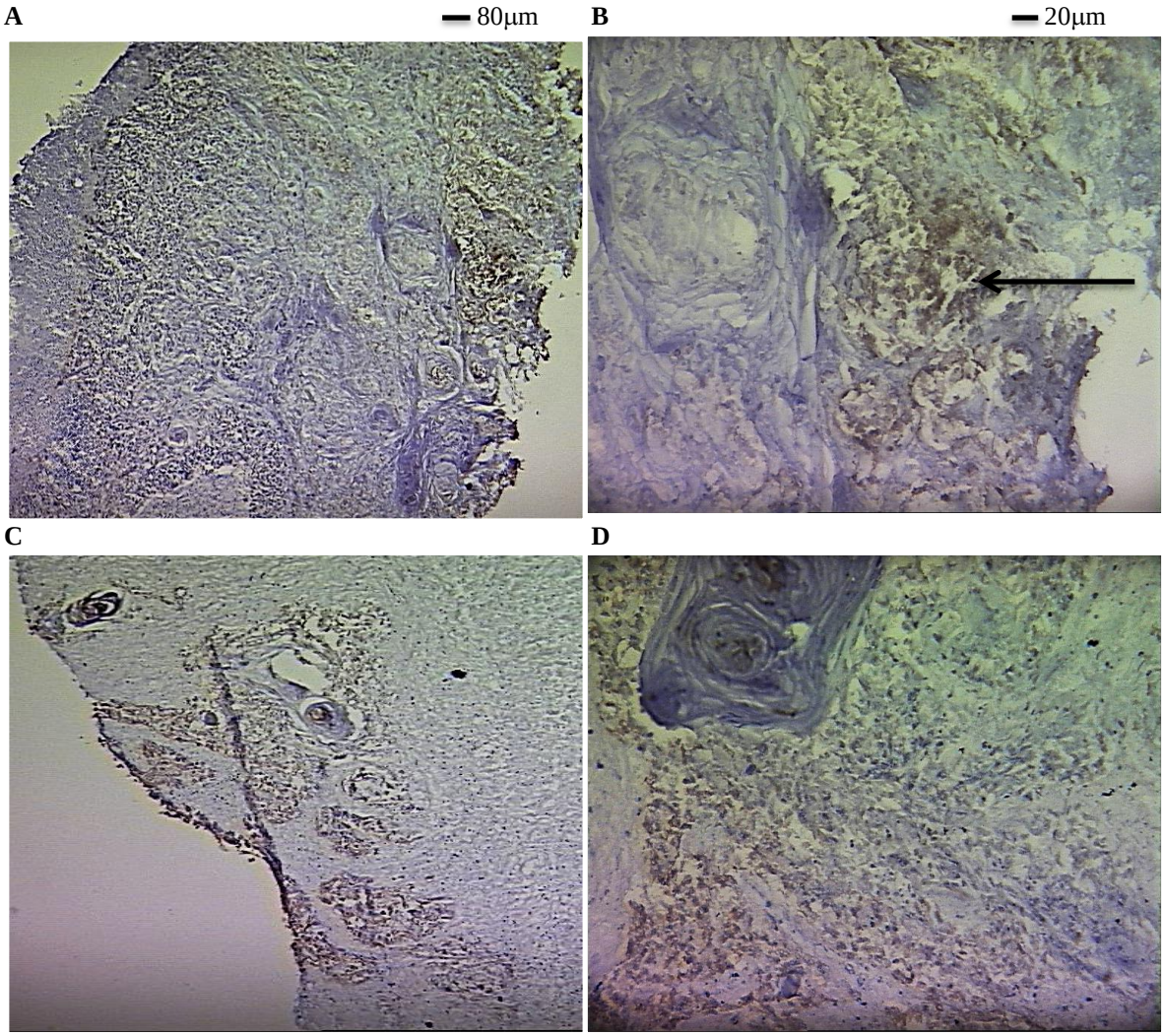

Figure 36. Immunohistochemical staining of cryosectioned HNSCC tissue (T2N2 oropharyngeal cervical lymph node metastasis) with pancytokeratin (1:100 dilution, brown nuclei; blue haematoxylin counterstain) following 7 days of incubation in the microfluidic device. Non-irradiated tissue: **a)** 50x magnification. **b)** 200x magnification. Tissue treated with 5 daily fractions of 2 Gy radiotherapy: **c)** 50x magnification. **d)** 200x magnification.

4.3.6 Detection of radiation-induced apoptotic cell death in the HNSCC tissue using caspase-3 cleaved cytokeratin 18

M30 CytoDEATH™ is a marker of apoptosis as it detects caspase-3 cleaved cytokeratin 18, part of the cytoskeleton in HNSCC cells. A small number of cells had undergone spontaneous apoptosis prior to the tissue being placed in the microfluidic device and in the tissue that had been incubated in the device. No statistically significant difference was found in the number of apoptotic cells in the tissue that was not incubated in the microfluidic device and the tissue that had been incubated for up to seven days in the device, but had received no radiotherapy, the maximum length of time that the tissue was maintained in the device during these experiments (**Figures 37a & b** and **Figures 38a** & **b** and **Figures 39a & b**).

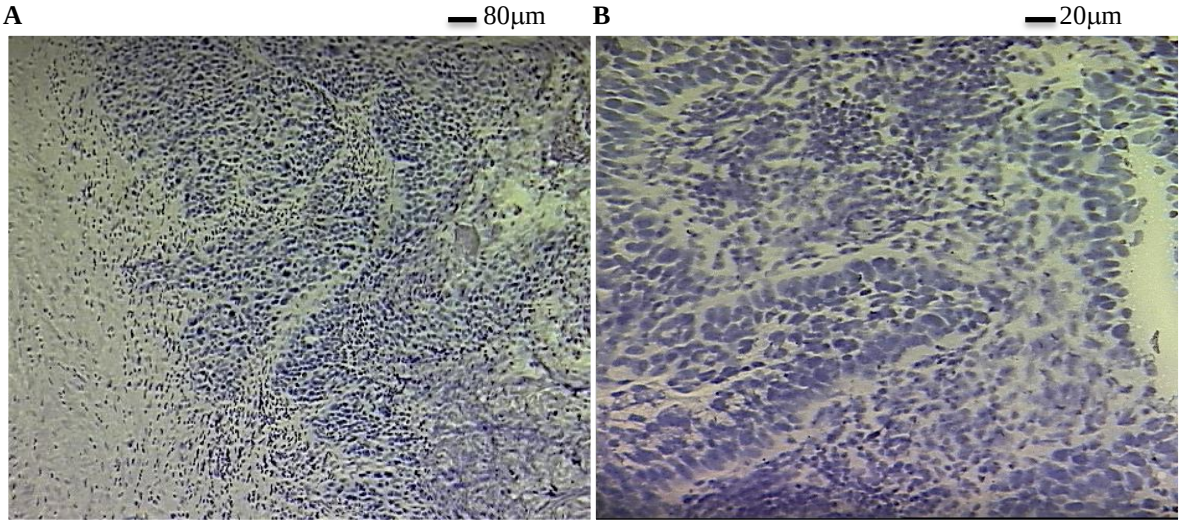

Figure 37. Immunohistochemical staining of cryostat sectioned HNSCC tissue (T2N2 metastatic cervical lymph node metastasis) with M30 (1:100 dilution: brown nuclei; haematoxylin counterstain) prior to incubation in the microfluidic device. **a)** 50x magnification. **b)** 200x magnification.

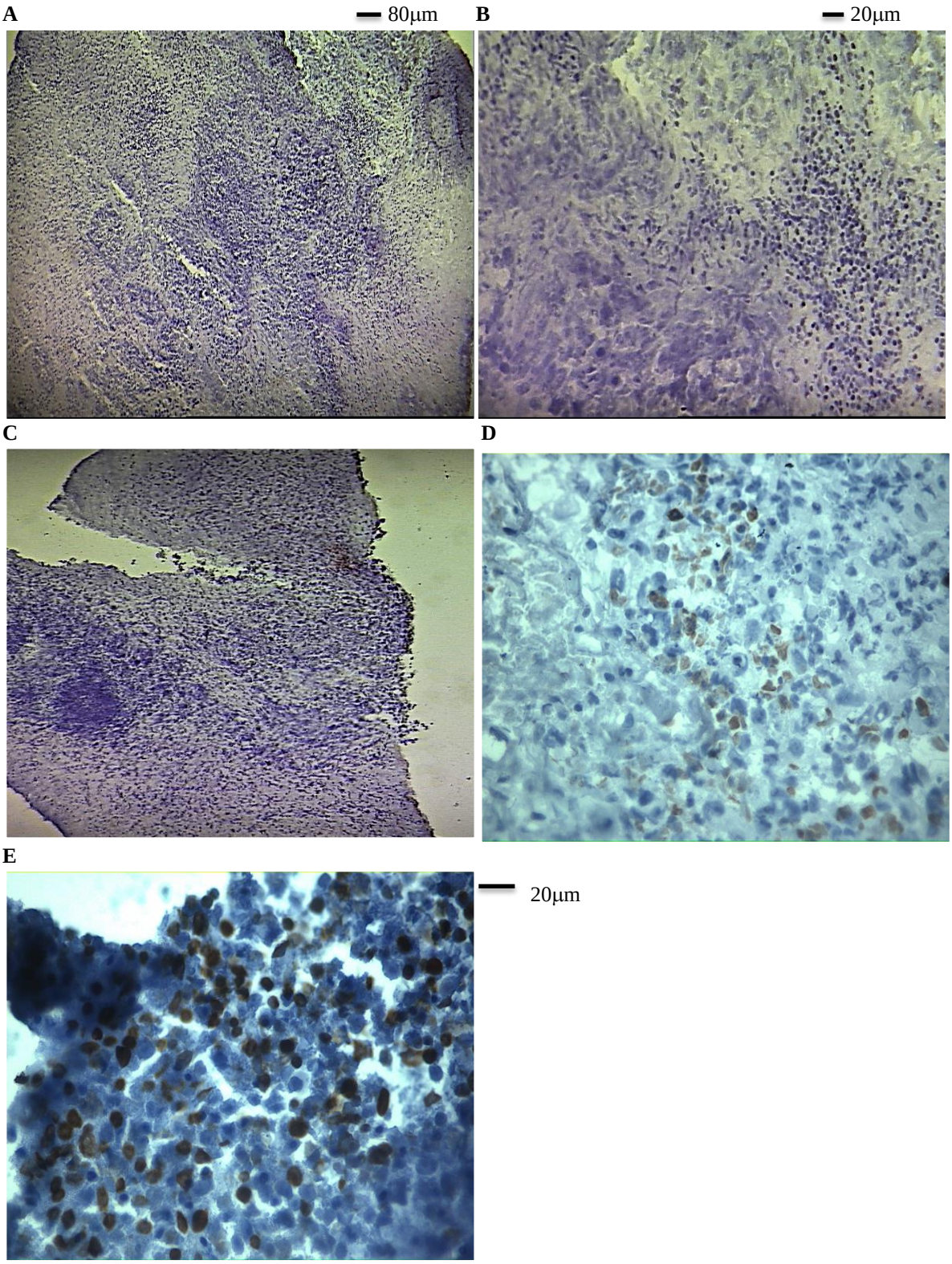

Figure 38. Immunohistochemical staining of cryostat sectioned HNSCC tissue (T2N2 oropharyngeal cervical lymph node metastasis) with M30 (1:100 dilution: brown nuclei; blue haematoxylin counterstain) following 4 days of incubation. Non-irradiated tissue: **a)** 50x magnification. **b)** 200x magnification. HNSCC tissue 72 h following treatment with a single dose of 2 Gy radiation: **c)** 50x magnification. **d)** 200x magnification. **e)** HNSCC tissue 72 h following treatment with a single dose of 40 Gy. 400x magnification

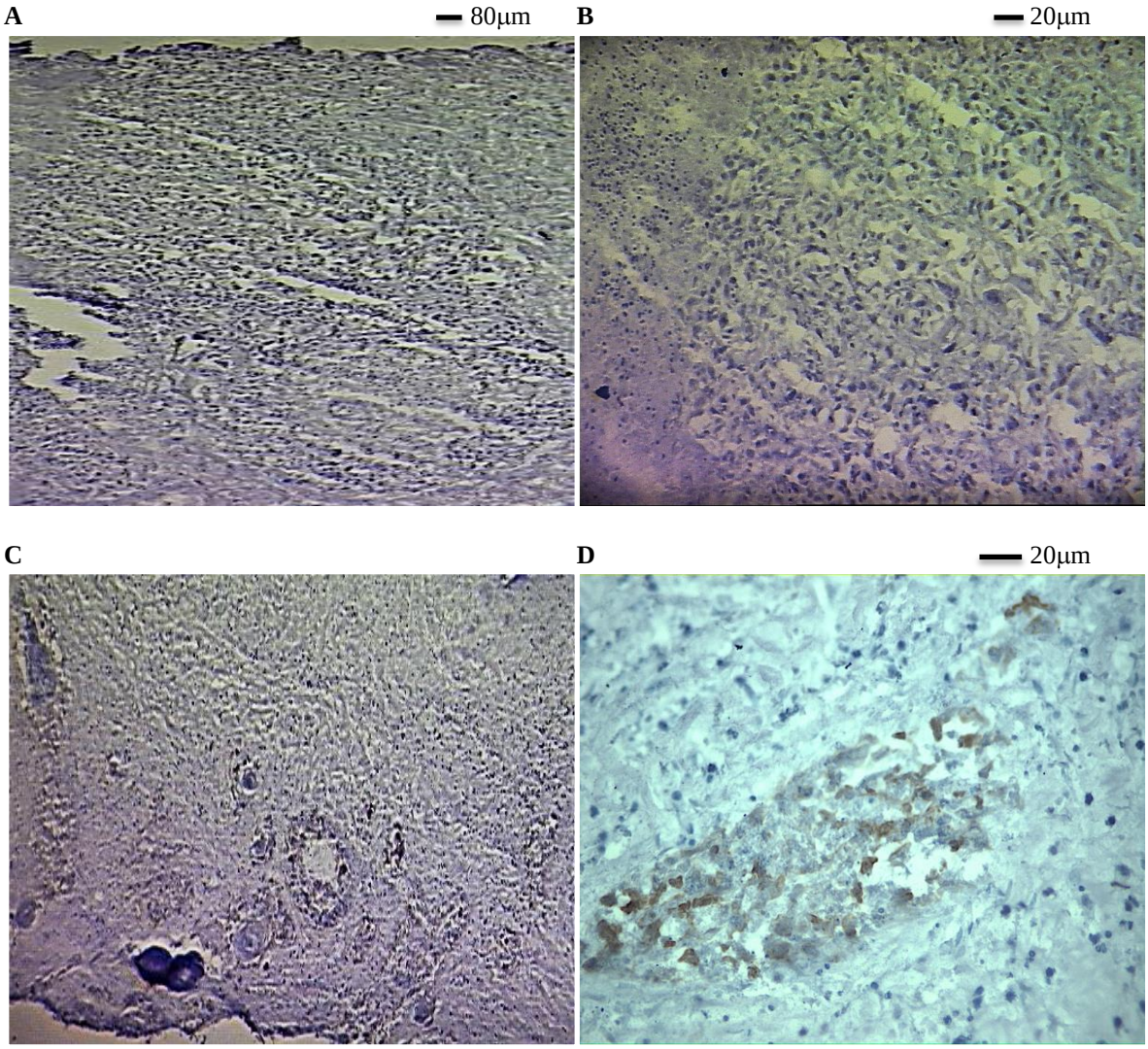

Figure 39. Immunohistochemical staining of cryostat sectioned HNSCC tissue (T2N2 oropharyngeal cervical lymph node metastasis) with M30 (1:100 dilution: brown nuclei; blue haematoxylin counterstain) following 7 days of incubation in the microfluidic device. Non-irradiated tissue: **a)** 50x magnification. **b)** 200x magnification. Following treatment with 5 daily fractions of 2 Gy radiation: **c)** 50x magnification. **d)** 400x magnification.

Apoptosis in the HNSCC tissue was expressed as the apoptotic index (AI), which was derived by calculating the number of cells that stained positively for M30 as a percentage of the total number of cells in 10 randomly selected high-power fields.

No significant difference was observed in the AI in the HNSCC tissue prior to being incubated in the microfluidic device compared to the tissue that had been incubated in the device for seven days, but had received no radiotherapy (**Figures 37a & b** and **Figures 39a & b**) (0.5% cf 0.6%; p=0.29). The AI of the treatment group was significantly different to the non-irradiated tissue for all doses (7% cf 0.6%; p=0.001) (**Figure 38e and Figures 39a & b**). A dose-dependent relationship was observed between the dose of radiotherapy administered

and the AI with an increase in radiotherapy dose resulting in an increase in apoptosis (**Figure 40**). For each dose increment, there was a significant increase in AI, except for the increment from10 Gy to 20 Gy (**Table 11**).

Table 10. Calculation of apoptotic index for the HNSCC tissue irradiated with single doses. The same calculation was performed for the HNSCC tissue that was irradiated with a fractionated course.

Radiation dose (Gy)	Number of M30 positive cells			Total number of cells counted			(M30 +ve cells/total cells counted) x 100 Apoptotic index (%)
	T2N2 OPSCC LN 1	T2N2 OPSCC LN 2	T2N2 OPSCC LN 3	T2N2 OPSCC LN 1	T2N2 OPSCC LN 2	T2N2 OPSCC LN 3	
Pre-MF	24	21	16	3041	2954	2671	0.5
No RT	27	22	20	3004	2749	2837	0.6
5	167	156	231	2384	3127	2572	7.0
10	362	350	509	2415	2690	3183	14.7
20	500	380	505	2379	2712	2195	19.3
40	1367	1010	1218	2847	2244	3124	44.0

Table 11. Apoptotic index for single radiotherapy dose increments.

Radiotherapy Dose Increment (Gy)	Apoptotic Index (%)	*p*-value
0 – 5	0.6 - 7	0.006
5 – 10	7 – 14.7	0.006
10 - 20	14.7 – 19.3	0.128
20 – 40	19.3 - 44	0.003

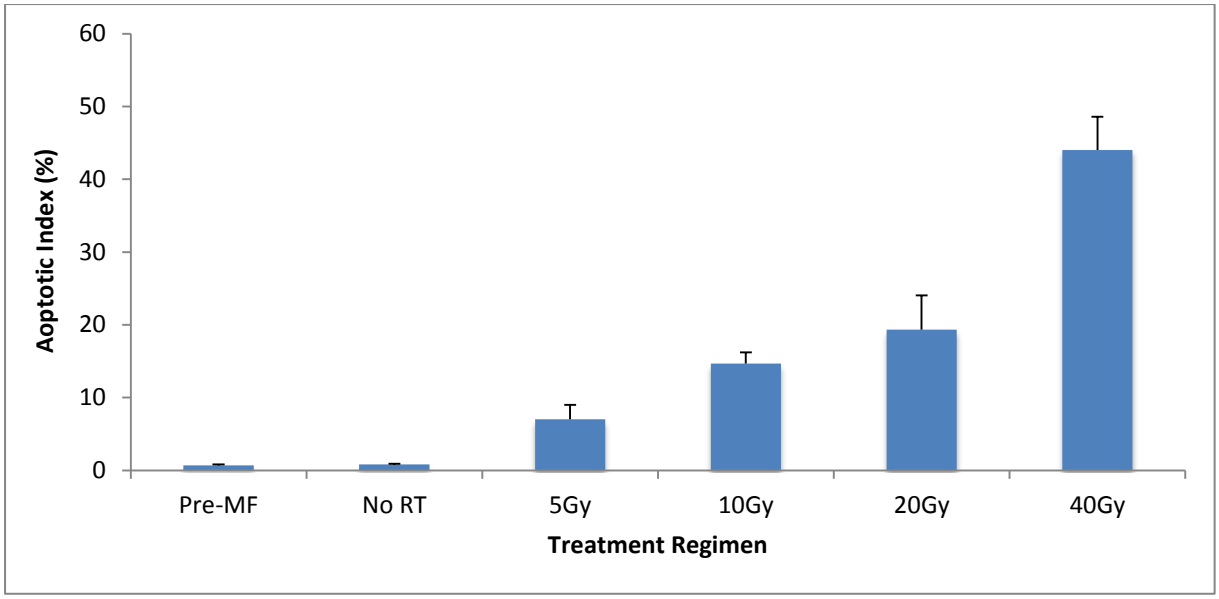

Figure 40. Apoptotic index for different radiation doses of HNSCC tissue maintained in a microfluidic device (T2N2 oropharyngeal cervical lymph node metastasis) and treated with single doses of radiotherapy. (Mean of 3 separate experiments + SEM). 'Pre-MF' refers to the tissue that was not incubated in the microfluidic device or treated with radiotherapy, 'No RT' refers to the tissue that was incubated in the device for the same duration as the irradiated tissue, but itself did not receive radiotherapy treatment.

In the HNSCC tissue that was treated with five daily fractions of 2 Gy, there was no significant difference in the AI between the tissue prior to being incubated in the device i.e. time 0 and the tissue that had been incubated for seven days, but not treated with radiotherapy (p=0.101) (**Figures 37a & b** and **Figures 39a & b**). A significant difference in AI was, however, demonstrated between the non-irradiated tissue and the tissue that had received radiotherapy (p=0.001) (**Figures 39a & b** and **Figures 38c & d** and **39c & d**) and also within the treatment group, with the tissue treated with five fractions of 2 Gy demonstrating a significant increase in apoptosis compared to the tissue treated with a single 2 Gy radiation fraction (p=0.01; **Figure 41**) (**Figures 38c & d** and **39c & d**).

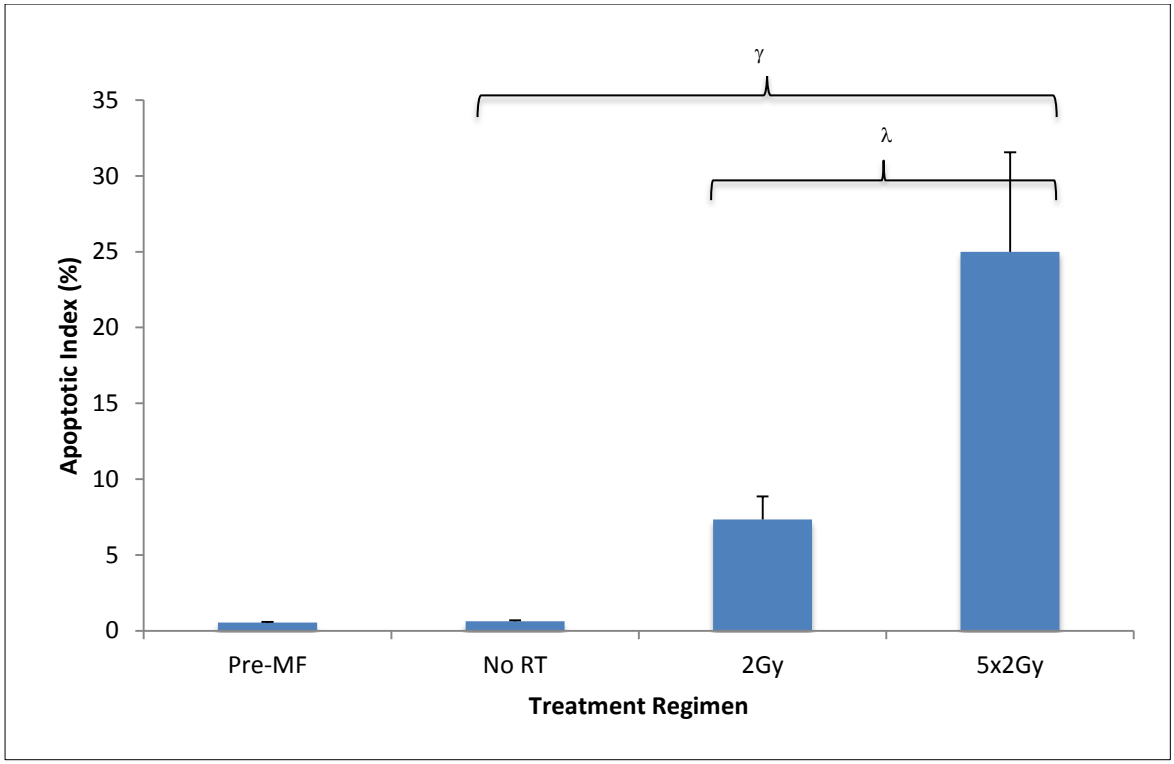

Figure 41. Apoptotic index for different radiation regimens of an HNSCC metastatic cervical lymph node (Mean of 3 separate experiments +SEM**)**. 'Pre-MF' refers to the tissue that was not incubated in the microfluidic device or treated with radiation, 'No RT' refers to the tissue that was incubated in the device for the same duration (seven days) as the treated tissue, but did not receive radiotherapy treatment. The treatment group consists of the tissue that received a single radiation fraction of 2 Gy and 5 daily fractions of 2 Gy '5x2Gy'. p=0.001γ; p=0.01λ unpaired t-test.

4.3.7 Detection of radiation-induced DNA-strand breaks in the HNSCC tissue using terminal deoxynucleotidyl transferase dUTP nick end labelling (TUNEL)

Fluorescence-labelled TUNEL was used to detect radiation-induced DNA-strand breaks in the HNSCC tissue that had been treated with a fractionated course of radiation to investigate the effects of a course of radiation which closely resembled that which would be used in the clinical treatment of HNSCC. There was no significant difference in the number of cells with DNA-strand breaks in the tissue prior to being incubated in the microfluidic device compared to the tissue that had been incubated for the same length of time (seven days), but not treated with radiation (**Figure 42;** p=0.349).

In order to calculate a difference in DNA-strand breaks between the different treatments, a DNA-strand break index was calculated (**Figure 43**), which was calculated in the same manner as the apoptotic index. A significant increase in DNA-strand breaks was observed in the tissue that had been irradiated, with both 2 Gy and five daily fractions of 2 Gy radiation, compared to the non-irradiated tissue (**Figure 42;** p=0.001). In addition the treatment of the tissue with five fractions of 2 Gy caused an increased number of DNA-strand breaks compared to the tissue that had been treated with a single fraction of 2 Gy (p=0.008).

A

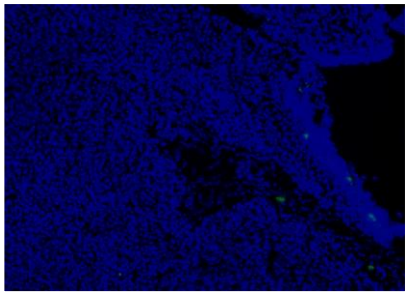

B

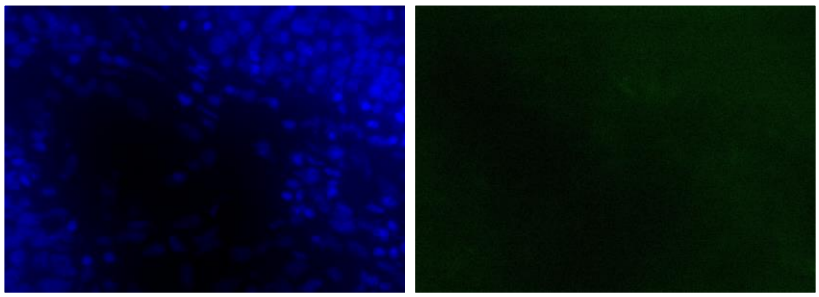

C

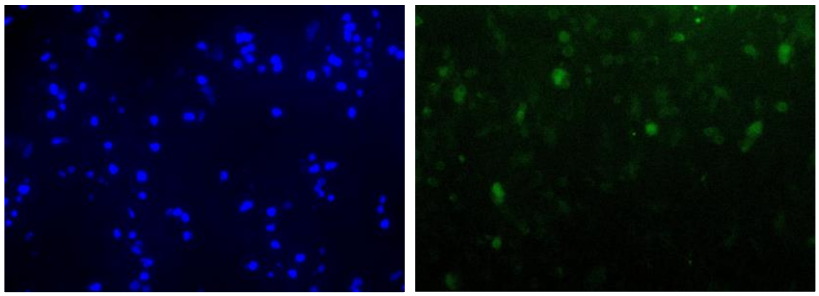

D

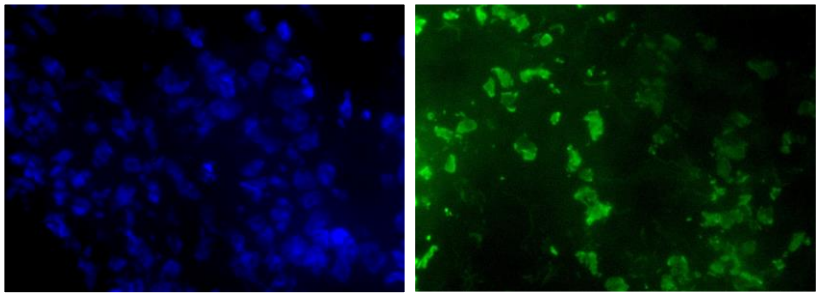

Figure 42. HNSCC cryosectioned tissue (T2N2 oropharyngeal cervical lymph node metastasis) following fluorescent detection of DNA strand breaks using TUNEL. **a)** Prior to incubation. 100x magnification. **b)** Following seven days of incubation in the microfluidic device without radiotherapy, **c)** 72 h following treatment with a single dose of 2 Gy radiation and **d)** Tissue treated with five daily fractions of 2 Gy radiation. DNA-strand break indicated by green fluorescence (FITC right hand panel) with blue fluorescence (DAPI left hand panel) counterstain. Images **b)**, **c)** and **d)** x400 magnification.

Table 12. Table to show data for DNA-strand break index calculation.

Radiation dose (Gy)	Number of TUNEL positive cells			Total number of cells counted			(TUNEL +ve cells/total cells counted) x 100 DSB index (%)
	T2N2 OPSCC LN 1	T2N2 OPSCC LN 2	T2N2 OPSCC LN 3	T2N2 OPSCC LN 1	T2N2 OPSCC LN 2	T2N2 OPSCC LN 3	
Pre-MF	7	6	13	2416	1859	2691	0.4
No RT	11	10	9	2783	2618	1577	0.5
2	114	179	50	2843	2236	1679	5.0
5x2	221	453	523	1579	2515	2490	17.7

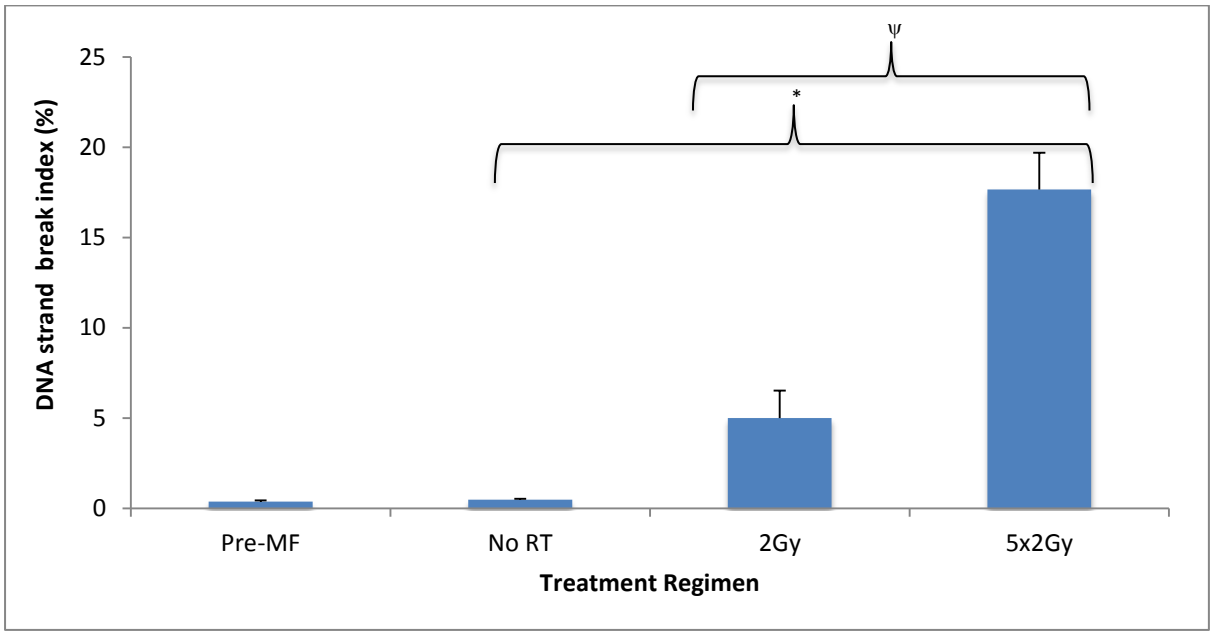

Figure 43. Index of DNA-strand breaks following TUNEL following different radiation treatment regimens of HNSCC (n=3; T2 larynx; 2xT2N2 oropharyngeal cervical lymph node metastases) (Mean of three experiments + SEM). 'Pre-MF' refers to the tissue that was not incubated in the microfluidic device or treated with radiotherapy, 'No RT' refers to the tissue that was incubated in the device for the same duration as the treated tissue (seven days), but did not receive radiotherapy. p=0.001*; p=0.008ψ unpaired t test.

4.4 Discussion

4.4.1 Cytotoxicity detection through the measurement of LDH and cytochrome c

LDH was used as a marker of cell death following radiation as it has previously been demonstrated as a reliable marker of cell death in an identical microfluidic device with HNSCC in response to chemotoxic agents *(Hattersley et al., 2012).*

Incubating HNSCC tissue in the microfluidic device without radiation resulted in LDH being released in a similar manner to that observed in the rat liver. It was possible to maintain the HNSCC tissue in a viable state for seven days without significant LDH release following the initial high LDH levels observed during the first 24 h, which were most probably due to tissue handling and preparation. Addition of the lysis agent to the culture medium, again induced an increase in LDH levels, indicating the presence of viable cells within the tissue following prolonged incubation in the microfluidic device.

The dose required for HNSCC to produce a significant detectable increase in LDH release was 40Gy, double that of the rat liver. Lower doses or fractionated doses did not produce any response. This dose was surprisingly high, considering that the total dose of a course of radiotherapy for the treatment of early stage laryngeal cancer is 60 Gy. It would be expected that the HNSCC tissue would have a similar threshold dose to the rat liver. Alati et al *(Alati et al., 1988)* compared the radiosensitivity of rat hepatocytes and human hepatocytes by measuring DNA repair following irradiation. They demonstrated that there was no significant difference in the radiosensitivity in the two groups. Therefore, it was reasonable to assume that the threshold radiation dose for human hepatocytes maintained in the microfluidic device would be similar to 20 Gy. By the same argument, considering that both liver and HNSCC cells are deemed to be moderately radiosensitive *(Kasten-Pisula U, 2009)*, the radiation threshold dose of the HNSCC tissue should have been at a similar level also.

The higher threshold dose in the HNSCC may have been due to a difference in the intrinsic radiosensitivity of the HNSCC and rat liver tissues, despite both being reported as being moderately radiosensitive. At this dose, it is likely that the LDH produced is due either to very high levels of apoptosis or, more likely, due to necrosis. The results of the current study were in agreement with Cai et al. *(Cai et al., 2000)* who looked at the effects of radiation on central nervous system cells in culture and demonstrated a significant increase in LDH release

only after 60 Gy, not 30 Gy and concluded that the LDH must have been detecting necrosis, rather than apoptosis.

Cytochrome c is an established soluble marker of apoptosis in HNSCC cells *(Macha et al., 2010)* and tissue *(Hattersley et al., 2012)*. Its release was used as a measure of apoptosis in the effluent from the microfluidic device as has previously been shown following microfluidic culture of HNSCC tissue in response to cytotoxic agents *(Hattersley et al., 2012)*. However, in the current study, no significant increases were observed following irradiation with either 5 Gy or 10 Gy; these doses being closer to those used in the clinical treatment of HNSCC. This highlights how radiation and chemotherapy differ in causing cell lysis in the microfluidic device.

These results are in contrast to other studies in which cytochrome c has been used to detect apoptosis in HNSCC cells in response to radiation, however these experiments were performed with cell lines rather than intact tissue. For example, Spring et al. *(Spring et al., 2004)* demonstrated an increase in apoptosis by measuring cytochrome c in the cytosol of the HNSCC cell lines in response to 2 Gy irradiation. A reason for this difference may be due to the preservation of the tissue architecture in the microfluidic device.

4.4.2 Morphology of HNSCC tissue maintained in a microfluidic device and the effect of radiation

In accordance with the results from the rat liver experiment, the histological appearance of the HNSCC tissue prior to being placed in the microfluidic device demonstrated that there was preservation of tissue architecture following excision and tissue preparation including or excluding snap-freezing. After four days of incubation in the device, there were again no discernible differences in the architecture compared to the pre-incubation section, which had not been incubated in the microfluidic device, however, after seven days of incubation, there were apparent architectural changes with mild loss of intercellular cohesion. Shinomiya *(Shinomiya, 2001)* described three characteristic histological features of radiation-induced apoptosis: pyknosis, cell shrinkage and internucleosomal breakage of chromatin and stated that these occur within the first few hours following irradiation.

The results of the current study are in agreement with a previous study by Kellokumpu-Lehtinen *(Kellokumpu-Lehtinen, 1990)* where HNSCC tissue samples were taken from

patients before and after radical treatment and the morphology assessed using H&E staining. The authors stated that radiotherapy caused several cellular changes with cellular atypia due to cellular death being the most prominent and suggested that changes in cytoskeleton and desmosomes might be important in the anchorage of tumour cells and might have a predictive value for the tumour's response to radiotherapy.

4.4.3 Detection of pancytokeratin and caspase-3 cleaved cytokeratin 18 (M30) as a marker of apoptosis

Calculation of the apoptotic index demonstrated no significant difference in apoptosis between the HNSCC tissue prior to it being placed in the microfluidic device and the HNSCC tissue that had been incubated in the device for seven days without irradiation. This indicated that the microfluidic device was able to maintain the HNSCC tissue in a viable state and that the level of apoptosis demonstrated was comparable to that occurring spontaneously in the tissue, agreeing with minimal histological changes and slow loss of function.

A significant increase in apoptosis was demonstrated following irradiation of the HNSCC tissue compared with the non-irradiated control tissue for both the single dose and the fractionated treatment regimens. In the single dose treatment regimen, there was a dose-dependent relationship with an increase in apoptosis for a given increase in radiation. This dose-dependent relationship between HNSCC and radiotherapy has been demonstrated both *in vitro (Artman et al., 2010, Riesterer et al., 2011, Yadav et al., 2011, Pickhard et al., 2011, Vermeer et al., 2013)* and *in vivo* by Hoebers et al. *(Hoebers et al., 2008)* who demonstrated a dose-dependent increase in uptake in the range of 0-8 Gy in patients with HNSCC. Although it could be argued that the dose-dependent relationship between radiotherapy dose and apoptosis is an expected result, the experiment presented here demonstrates the capability of this microfluidic technique to reproduce this relationship and, further, to reproduce the clinical response of a patient's individual tumour to radiation.

In the HNSCC tissue treated with a fractionated course, consisting of a single fraction of 2 Gy compared to five fractions of 2 Gy, there was no significant difference in apoptosis between the tissue prior to being placed in the microfluidic device and the tissue that was incubated in the device without irradiation, which was the same as in the experiments involving irradiating the tissue with single doses of radiation. There was a significant increase in apoptosis following irradiation of the tissue with 2 Gy of irradiation compared to the control.

Considering that 2 Gy is the dose of a single fraction used in the treatment of HNSCC, the ability of this technique to detect apoptosis following treatment with this dose demonstrated its superior sensitivity compared to both LDH and cytochrome c. The apoptotic index of a single dose of 10 Gy was lower than that of five fractions of 2 Gy, although the total dose was the same. This demonstrates the increased efficacy of a fractionated course in causing radiation-induced cell death. Drahos et al. *(Drahos et al., 2004)* treated two melanoma cell lines with eight fractions of 0.5 Gy or a single dose of 4 Gy *in vitro*. They demonstrated a significant increase in apoptosis in the cells that were treated with the fractionated course compared to the single dose, which is in agreement with the current study.

Stausbol-Gron et al. *(Stausbol-Gron et al., 1999)* assessed the radiosensitivity of HNSCC cells and fibroblasts by determining the surviving fraction after the administration of 2 Gy. However, the problem they encountered was that it proved difficult to differentiate between fibroblasts and HNSCC cancer cells. The use of pancytokeratin and the M30 antibody in the current study demonstrated the presence of HNSCC cells within the metastatic lymph node tissue samples and those HNSCC cells which were apoptotic respectively. Through the detection of pancytokeratin, it was demonstrated that all the tissue samples that were sectioned contained HNSCC cells and that there was no demonstrable change in the expression of cytokeratin after treatment with different irradiation doses, which the current study is the first to demonstrate.

The M30 antibody has previously been used to detect apoptosis in rat liver *(Topaloglu et al., 2003, Schleimer et al., 2008, Boncompagni et al., 2011)* and HNSCC tissue, in both *in vitro* and *in vivo* studies *(Thurnher et al., 2001, Eder-Czembirek et al., 2005, Vormittag et al., 2005, Ozturk et al., 2009, Macha et al., 2010, Cheng et al., 2012).* It is a sensitive marker of early apoptosis *(Cheng et al., 2012)* and was capable of detecting radiation-induced cell death in the HNSCC tissue after the administration of as little as 2 Gy irradiation *(Aravindan et al., 2011)*, the same dose as a single fraction used in the clinical treatment of HNSCC. In addition to apoptosis, caspases are involved in cellular death following mitotic catastrophe and, therefore, it could be proposed that M30 is also capable of detecting those cells that undergo caspase-dependent cell death as a consequence of mitotic catastrophe.

Previous studies using HeLa-Hep2 adenocarcinoma cells have demonstrated the use of M30 as a marker of radiation-induced apoptosis after low-dose radiotherapy. Mirzaie-Joniani et al. *(Mirzaie-Joniani et al., 2002)* used it in their study to show a significant increase in apoptosis

after 2 Gy irradiation with approximately 20% of the remaining population displaying apoptotic staining at 24 h, whilst Eriksson et al. *(Eriksson et al., 2003)* used it to demonstrate increased apoptotic cell death after the combination of low-dose radiation and radioimmunotherapy.

Treatment of the HNSCC tissue with five fractions of 2 Gy on consecutive days replicated a weeklong radiotherapy course comparable to treating a patient in the clinical setting. As might be expected, a significant increase in the apoptotic index was demonstrated between the HNSCC tissue that was treated with five fractions of 2 Gy compared to a single fraction of 2 Gy suggesting that the effect was additive. An *in vivo* study by Le et al. *(Le, 1997)* demonstrated that total dose, fraction size and overall treatment time were all significant factors for local control in T1 and T2 laryngeal cancers. This demonstrates that this microfluidic technique is able to reproduce the results that would be expected clinically.

Using caspase-3 detection as a measure of apoptosis in HNSCC cells, Roberg et al. *(Roberg et al., 2007)* treated three different oral SCC cell lines with radiotherapy and found that apoptotic morphology and caspase-3 activity were only detected in cell lines that exhibited high or moderate radiosensitivity. They concluded that apoptotic cell death and the balance between pro- and anti-apoptotic proteins determine the outcome to radiotherapy. Ohnisihi et al. *(Ohnishi et al., 2002)* demonstrated that the radiosensitivity of HNSCC cells is tightly correlated with the induction of apoptosis through caspase-3 activation by demonstrating that radiation-induced cell death is caspase-dependent and, therefore, p53 mediated in HNSCC cells at doses of 2Gy or greater. Yasumoto et al. *(Yasumoto et al., 2003)* used two HNSCC cell lines, one with mutated p53 and one with wild-type p53 and demonstrated that the expression of apoptosis-inductive genes, such as caspases-3, 8, 9 and 10 were increased by X-ray irradiation only in those cells containing wild-type p53 suggesting that the lack of p53 observed in the majority of HNSCC tumours could be responsible for the radioresistance seen in a lot of tumours *(Bristow et al., 1994, Sandulache et al., 2012)*. Treatment of HNSCC with low-dose fractionated radiotherapy treatments (<1Gy) have demonstrated p53-independent cell death *(Shareef et al., 2008)*. Dey et al. *(Dey et al., 2003)* treated HNSCC cell lines with a single fraction of 2 Gy or four fractions of 0.5 Gy and demonstrated that radiation-induced cell death in the HNSCC cells treated with four fractions of 0.5 Gy occurred in a p53-independent manner *in vitro,* a phenomenon known as hyper-radiosensitivity, which is most prominent when cells are in the G2 phase of the cell cycle. Shareef et al. *(Shareef et al., 2008)* treated oral cancer cell lines with a single dose of 2 Gy or a course of low dose fractionated

radiotherapy consisting of four fractions of 0.5 Gy. They demonstrated a significant increase in apoptosis in the fractionated course, which is in agreement with the studies that have reported on low-dose hyper-radiosensitivity. Krueger et al. *(Krueger et al., 2007)* proposed that the enhanced sensitivity of cells to low doses of radiotherapy is due to the failure of ATM-dependent repair processes to fully arrest the progression of damaged G2-phase cells harbouring unrepaired DNA breaks entering mitosis.

4.4.4 TUNEL analysis to detect radiation-induced DNA-strand breaks in HNSCC tissue following irradiation in a microfluidic device

The TUNEL assay is capable of detecting both single-strand and double-strand DNA breaks caused by ionising radiation *(Ribeiro et al., 2006).* It is a well-established marker of apoptosis in various tissues including HNSCC, having been used in several recent studies *(Heath et al., 2012, Sweeny et al., 2012, Li et al., 2012, Khan et al., 2012, Adhim et al., 2013)* and has been used to demonstrate radiation-induced DNA-strand breaks in HNSCC cell lines *(Uno et al., 2001, Masunaga et al., 2002, Dey et al., 2003, Spring et al., 2004, Zou et al., 2008, Park et al., 2009, Dean et al., 2009, Feng et al., 2011).*

TUNEL analysis demonstrated no significant difference in DNA-strand breaks between the HNSCC tissue prior to it being placed in the microfluidic device and the tissue, which was incubated in the device for 6 days, but received no radiation. This indicated that incubation of the tissue in the microfluidic device caused no significant increase in DNA-strand breaks, which further confirmed the capability of this microfluidic device to maintain the viability of the tissue for a time period that allows for investigation of the tissue's response to radiation. There was a significant overall increase in DNA-strand breaks between the HNSCC tissue that received irradiation (2 Gy and five fractions of 2 Gy) and the HNSCC tissue that had been incubated in the device without radiation, indicating that the increase in DNA-strandbreaks was caused by exposure to radiotherapy and not due to incubation in the device. A significant increase in DNA-strand breaks was demonstrated between the HNSCC tissue that had been irradiated with a single 2 Gy fraction compared to the tissue that had been incubated in the microfluidic device without irradiation. These results are in agreement with Lee et al. *(Lee et al., 2007)* who demonstrated a significant increase in DNA fragmentation, using the TUNEL assay, and apoptosis, using the annexin V system, following irradiation of human leukemic lymphoma cells with 2 Gy radiation and also with Su et al. *(Su, 2009)* in

their study of irradiation with a three-dimensional skin cell model. They demonstrated an increased percentage of TUNEL-positive cells after exposure to 2 Gy radiation compared to 0 Gy after 24 h following irradiation. After 48 h following irradiation with 2 Gy, there was no increase in TUNEL-positive cells compared to 24 h post-irradiation. This demonstrated the sensitivity of this technique, which was capable of detecting DNA-strand breaks after irradiation of the tissue with as little as 2 Gy as was seen with the current microfluidic method. In addition, there was a significant increase in the number of DNA-strand breaks in the HNSCC tissue that had been irradiated with five fractions of 2 Gy compared to a single 2 Gy fraction, demonstrating that an increase in the number of radiation fractions caused an increase in the number of DNA-strand breaks, which is in agreement with the results of Bradley et al. *(Bradley et al., 1982)* who used a filter elution technique to measure the number of DNA double-strand breaks in rat hepatocytes, which had been cultured in monolayer, after treatment with increasing radiation doses of 5-20 kilorads i.e. 0.5-2 Gy. They demonstrated an increased number of double-strand breaks after treatment for a given increase in radiation dose with 2 Gy producing significantly more than 1 Gy or 0.5 Gy. Similar results were observed by Ohno et al. *(Ohno et al., 1998)* who excised cervical cancer cells from patients before and after treatment with 9 Gy irradiation and demonstrated a significant increase in the apoptotic index calculated using in situ nick end labelling from 0.22% before treatment to 1.2% after treatment. The increase in DNA-strand breaks in the tissue with an increase in the number of radiation fractions is an important result as it demonstrates that the microfluidic device can reproduce the expected clinical result, which is imperative if this device is to be developed further into a predictive tool.

Similar to this study, other studies have used the survival fraction of cells after the administration of 2 Gy, known as SF2. Bhosle et al. *(Bhosle et al., 2005)* took biopsies from patients with stage III cervical carcinoma before and 24 h after the first fractionated radiation dose of 2 Gy. The TUNEL assay was used to measure radiation-induced cervical apoptosis. They demonstrated that the apoptotic sensitivity of these cells significantly correlated with the radiation treatment outcome in these patients after completion of their radiotherapy course with a total dose of 70 Gy. They suggested that the apoptotic index might form a basis for prognosis in radiotherapy in stage III cervical cancer patients. West et al. *(West et al., 1997)* demonstrated this in patients with uterine cervical carcinoma using the modified Courtenay-Mills soft agar clonogenic assay. In their study of patients with HNSCC undergoing radiotherapy treatment, Bjork-Eriksson et al. *(Bjork-Eriksson et al., 2000)* took biopsies and treated the tissue with 2 Gy, whilst the patients were treated with a full course of radiotherapy.

They demonstrated that there was a significant correlation between the survival fraction after 2 Gy (SF2) and local tumour control and patient survival.

4.5 Conclusions and future work

The current study has demonstrated that this microfluidic technique is an excellent platform for maintaining both normal and malignant tissue in a viable state in a pseudo *in vivo* environment over several days, without it undergoing significant levels of apoptosis or DNA-strand breaks, which allowed the effects of radiation to be investigated. The results gained with the M30 antibody and TUNEL have demonstrated that this technique can reproduce the expected clinical result, which is a crucial step if it is to be developed into a tool, capable of predicting an individual tumour's response to radiation. This study is a significant step in the development of a device capable of predicting the response of an individual's tumour to radiotherapy.

Tissue-based markers of apoptosis and DNA-strand breaks proved to be a superior method of detecting radiation-induced cell death in the HNSCC tissue maintained in the microfluidic device compared to soluble markers. The tissue-based markers of apoptosis and DNA-strand breaks were able to detect radiation-induced cell damage or death at clinically relevant radiation doses. As a marker of apoptosis, the TUNEL results reinforced those gained with M30 and those that might be expected with an increase in the number of fractions of 2 Gy causing an increase in the number of cells undergoing apoptosis. The precursor event to all modes of radiation-induced cell death: apoptosis, mitotic catastrophe and senescence, is radiation-induced DNA damage. As the TUNEL assay detects breaks in the DNA strands, it could be argued that it is capable of detecting the antecedent event to apoptosis, mitotic catastrophe and senescence i.e. radiation-induced DNA damage. Therefore, TUNEL may be a more useful and accurate marker of radiation-induced cell death than all the other markers used in this study.

A major advantage of this microfluidic technique is its versatility, which has meant that there is great potential for its future use. There are several interesting areas where this device could prove ideal. The first of these would be in combination therapies, such as chemoradiotherapy regimens. The current study has proved its capability in the investigation of the effects of radiation on HNSCC tissue. Previous work by Hattersley et al. *(Hattersley et al., 2012)* has demonstrated its use in interrogating HNSCC tissue with the chemotherapy agents cisplatin,

5-FU and docetaxel. As concurrent chemoradiotherapy is now widely accepted as the definitve treatment for locoregionally advanced HNSCC *(Schoder, 2009),* it would prove of great clinical benefit if this technique could be expanded to incorporate both treatment modalities. Other combination therapies, such as radiotherapy and cetuximab may prove equally interesting.

As well as other treatment modalities, the device could be adapted so that it is capable of detecting biomarkers that are associated with radioresistance. Silva et al. *(Silva et al., 2007)* described several biomarkers, which could be used to predict the response of an HNSCC tumour to radiotherapy, such as hypoxic markers e.g. HIF1α, proliferation markers e.g. EGFR, radioresistant genes e.g. KU70, DNA-PK, ATM and XRCC3. There is potential for detectors of these markers to be added to the current microfluidic device, potentially increasing the robustness of the device as a predictive tool.

As was previously discussed in section 4.23, the ability of this technique to demonstrate a significant level of radiation-induced apoptosis or DNA-strand break after treatment with 2Gy would potentially mean that this technique could be used to investigate the SF2 of an individual's tumour and this may lead to its development as a tool capable of predicting outcome to radiotherapy treatment as SF2 has previosuly been correlated with outcome *(Bjork-Eriksson et al., 2000).*

The outcome following a course of radiotherapy in HNSCC is dependent on treatment parameters such as total dose, dose per fraction and overall treatment time. In addition to this, there are several tumour and patient related factors, which influence the outcome, such as tumour site and size, stage and histology as well as patient age, sex and pre-morbid state. However, Stausbol-Gron et al. *(Stausbol-Gron et al., 1999)* argued that there is such variation in the outcome that it cannot be explained by these factors alone. This is understandable given the significant heterogeneity of HNSCC *(Mroz et al., 2013).* This provides the ideal platform for the advent of personalised cancer treatment in order to improve the outcome both in the individual and at the patient population level. Over the past few years, personalised cancer treatment has generated a significant amount of interest. In 2007, Senator Barack Obama stated that: 'We are in a new era of the life sciences, but in no area of research is the promise greater than in personalised medicine'. In the USA the Genomics and Personalised Medicine Act was passed the same year *(Dikenson, 2012).* However, there have been warnings that the NHS will not be able to cope financially with the provision of personalised medicine. Sir

John Bell, Academy President of The Academy of Medical Sciences, stated that the NHS will struggle to cope with the advent of personalised medicine due to the financial strains that it is already under *(Bryon-Dodd, 2011)*.

This microfluidic technique could provide the ultimate cost-effective tool in personalised medicine, capable of predicting the response of an individual's tumour to radiotherapy prior to the commencement of treatment.

References

Larygneal Squamous Cell Carcinoma at 10x Magnification [Online]. Available: http://www.microscopyu.com/staticgallery/pathology/squamouscellcarcinomaoflarynx10x0.4.html [Accessed 10 November 2011].

ADHIM, Z., OTSUKI, N., KITAMOTO, J., MORISHITA, N., KAWABATA, M., SHIRAKAWA, T. & NIBU, K. 2013. Gene silencing with siRNA targeting E6/E7 as a therapeutic intervention against head and neck cancer-containing HPV16 cell lines. *Acta Otolaryngol,* 133**,** 761-71.

AH-SEE, K. W., COOKE, T. G., PICKFORD, I. R., SOUTAR, D. & BALMAIN, A. 1994. An allelotype of squamous carcinoma of the head and neck using microsatellite markers. *Cancer Res,* 54**,** 1617-21.

AISNER, J., JACOBS, M., SINABALDI, V., GRAY, W. & EISENBERGER, M. 1994. Chemoradiotherapy for the treatment of regionally advanced head and neck cancers. *Semin Oncol,* 21**,** 35-44.

AL-ASSAR, O., MUSCHEL, R. J., MANTONI, T. S., MCKENNA, W. G. & BRUNNER, T. B. 2009. Radiation response of cancer stem-like cells from established human cell lines after sorting for surface markers. *Int J Radiat Oncol Biol Phys,* 75**,** 1216-25.

ALATI, T., VAN CLEEFF, M., STROM, S. C. & JIRTLE, R. L. 1988. Radiation sensitivity of adult human parenchymal hepatocytes. *Radiat Res,* 115**,** 152-60.

ALLAL, A. S., WAELCHLI, L. & BRUNDLER, M. A. 2003. Prognostic value of apoptosis-regulating protein expression in anal squamous cell carcinoma. *Clin Cancer Res,* 9**,** 6489-96.

ALVAREZ, S., DRANE, P., MEILLER, A., BRAS, M., DEGUIN-CHAMBON, V., BOUVARD, V. & MAY, E. 2006. A comprehensive study of p53 transcriptional activity in thymus and spleen of gamma irradiated mouse: high sensitivity of genes involved in the two main apoptotic pathways. *Int J Radiat Biol,* 82**,** 761-70.

AMBROSCH, P., KRON, M. & FREUDENBERG, L. S. 1998. Clinical staging of oropharyngeal carcinoma: a critical evaluation of a new stage grouping proposal. *Cancer,* 82**,** 1613-20.

ANG, K. K., BERKEY, B. A., TU, X., ZHANG, H. Z., KATZ, R., HAMMOND, E. H., FU, K. K. & MILAS, L. 2002. Impact of epidermal growth factor receptor expression on survival and pattern of relapse in patients with advanced head and neck carcinoma. *Cancer Res,* 62**,** 7350-6.

ANWAR, K., NAKAKUKI, K., NAIKI, H. & INUZUKA, M. 1993. ras gene mutations and HPV infection are common in human laryngeal carcinoma. *Int J Cancer,* 53**,** 22-8.

ARAVINDAN, N., THOMAS, C. R., JR., ARAVINDAN, S., MOHAN, A. S., VEERARAGHAVAN, J. & NATARAJAN, M. 2011. Irreversible EGFR inhibitor EKB-569 targets low-LET gamma-radiation-triggered rel orchestration and potentiates cell death in squamous cell carcinoma. *PLoS One,* 6**,** e29705.

ARTMAN, T., SCHILLING, D., GNANN, J., MOLLS, M., MULTHOFF, G. & BAYER, C. 2010. Irradiation-induced regulation of plasminogen activator inhibitor type-1 and vascular endothelial growth factor in six human squamous cell carcinoma lines of the head and neck. *Int J Radiat Oncol Biol Phys,* 76**,** 574-82.

ASSELINEAU, D., BERNARD, B. A., BAILLY, C., DARMON, M. & PRUNIERAS, M. 1986. Human epidermis reconstructed by culture: is it "normal"? *J Invest Dermatol,* 86**,** 181-6.

BAIN, C. D. 2001. Motion of Liquids on Surfaces. *ChemPhysChem,* 2**,** 580-582.

BAKER, S. R. 1985. An in vivo model for squamous cell carcinoma of the head and neck. *Laryngoscope,* 95**,** 43-56.

BAO, S., WU, Q., MCLENDON, R. E., HAO, Y., SHI, Q., HJELMELAND, A. B., DEWHIRST, M. W., BIGNER, D. D. & RICH, J. N. 2006. Glioma stem cells promote radioresistance by preferential activation of the DNA damage response. *Nature,* 444**,** 756-60.

BARTKOWIAK, D., HOGNER, S., NOTHDURFT, W. & ROTTINGER, E. M. 2001. Cell cycle and growth response of CHO cells to X-irradiation: threshold-free repair at low doses. *Int J Radiat Oncol Biol Phys,* 50**,** 221-7.

BAUMANN, M., KRAUSE, M. & HILL, R. 2008. Exploring the role of cancer stem cells in radioresistance. *Nat Rev Cancer,* 8**,** 545-54.

BEASLEY, N. 2008a. Anatomy of the Larynx and Tracheobronchial Tree. *In:* GLEESON, M., BROWNING, G.G., BURTON, M.J., CLARKE, R., HIBBERT, J., JONES, N.S., LUND, V.J., LUXON, L.M., WATKINSON, J.C. (ed.) *Scott-Brown's Otorhinolaryngology, Head and Neck Surgery.* 7th ed. London: Hodder Arnold.

BEASLEY, N. 2008b. Anatomy of the Pharynx and Oesophagus. *In:* GLEESON, M., BROWNING, G.G., BURTON, M.J., CLARKE, R., HIBBERT, J., JONES, N.S., LUND, V.J., LUXON, L.M., WATKINSON, J.C. (ed.) *Scott-Brown's Otorhinolaryngology, Head and Neck Surgery.* London: Hodder Arnold.

BEGG, A. C., HAUSTERMANS, K., HART, A. A., DISCHE, S., SAUNDERS, M., ZACKRISSON, B., GUSTAFFSON, H., COUCKE, P., PASCHOUD, N., HOYER, M., OVERGAARD, J., ANTOGNONI, P., RICHETTI, A., BOURHIS, J., BARTELINK, H., HORIOT, J. C., CORVO, R., GIARETTI, W., AWWAD, H., SHOUMAN, T., JOUFFROY, T., MACIOROWSKI, Z., DOBROWSKY, W., STRUIKMANS, H., WILSON, G. D. & ET AL. 1999. The value of pretreatment cell kinetic parameters as predictors for radiotherapy outcome in head and neck cancer: a multicenter analysis. *Radiother Oncol,* 50**,** 13-23.

BEGG AC, S. G. 2002. *Basic Clinical Radiobiology,* London, Arnold.

BENBROOK, D. M. 2006. Organotypic cultures represent tumor microenvironment for dug testing. *Drug Discovery Today: Disease Models,* 3**,** 143-148.

BENTZEN, S. M. & THAMES, H. D. 1991. Clinical evidence for tumor clonogen regeneration: interpretations of the data. *Radiother Oncol,* 22**,** 161-6.

BERNIER, J., COOPER, J. S., PAJAK, T. F., VAN GLABBEKE, M., BOURHIS, J., FORASTIERE, A., OZSAHIN, E. M., JACOBS, J. R., JASSEM, J., ANG, K. K. & LEFEBVRE, J. L. 2005. Defining risk levels in locally advanced head and neck cancers: a comparative analysis of concurrent postoperative radiation plus chemotherapy trials of the EORTC (#22931) and RTOG (# 9501). *Head Neck,* 27**,** 843-50.

BERNIER, J., DOMENGE, C., OZSAHIN, M., MATUSZEWSKA, K., LEFEBVRE, J. L., GREINER, R. H., GIRALT, J., MAINGON, P., ROLLAND, F., BOLLA, M., COGNETTI, F., BOURHIS, J., KIRKPATRICK, A. & VAN GLABBEKE, M. 2004. Postoperative irradiation with or without concomitant chemotherapy for locally advanced head and neck cancer. *N Engl J Med,* 350**,** 1945-52.

BHARADWAJ, R., SANTIAGO, J. G. & MOHAMMADI, B. 2002. Design and optimization of on-chip capillary electrophoresis. *Electrophoresis,* 23**,** 2729-44.

BHIDE, S. A., NEWBOLD, K. L., HARRINGTON, K. J. & NUTTING, C. M. 2012. Clinical evaluation of intensity-modulated radiotherapy for head and neck cancers. *Br J Radiol,* 85**,** 487-94.

BHOSLE, S. M., HUILGOL, N. G. & MISHRA, K. P. 2005. Apoptotic index as predictive marker for radiosensitivity of cervical carcinoma: evaluation of membrane fluidity, biochemical parameters and apoptosis after the first dose of fractionated radiotherapy to patients. *Cancer Detect Prev,* 29**,** 369-75.

BIAN, Y., HALL, B., SUN, Z. J., MOLINOLO, A., CHEN, W., GUTKIND, J. S., WAES, C. V. & KULKARNI, A. B. 2012. Loss of TGF-beta signaling and PTEN promotes head and neck squamous cell carcinoma through cellular senescence evasion and cancer-related inflammation. *Oncogene,* 31**,** 3322-32.

BIANCHINI, C., CIORBA, A., STOMEO, F., PELUCCHI, S. & PASTORE, A. 2012. Immunonutrition in head and neck cancer: have a look before surgery! *Eur Arch Otorhinolaryngol,* 269**,** 5-8.

BIRCHALL, M. A., POPE, L. 2008. Tumours of the Larynx. *In:* GLEESON, M., BROWNING, G.G., BURTON, M.J., CLARKE, R., HIBBERT, J., JONES, N.S., LUND, V.J., LUXON, L.M., WATKINSON, J.C. (ed.) *Scott-Brown's Otorhinolaryngology, Head and Neck Surgery.* Seventh ed. London: Hodder-Arnold.

BJORK-ERIKSSON, T., WEST, C., KARLSSON, E. & MERCKE, C. 2000. Tumor radiosensitivity (SF2) is a prognostic factor for local control in head and neck cancers. *Int J Radiat Oncol Biol Phys,* 46**,** 13-9.

BLAGOSKLONNY, M. V., DEMIDENKO, Z. N., GIOVINO, M., SZYNAL, C., DONSKOY, E., HERRMANN, R. A., BARRY, J. J. & WHALEN, A. M. 2006. Cytostatic activity of paclitaxel in coronary artery smooth muscle cells is mediated through transient mitotic arrest followed by permanent post-mitotic arrest: comparison with cancer cells. *Cell Cycle,* 5**,** 1574-9.

BONCOMPAGNI, E., GINI, E., FERRIGNO, A., MILANESI, G., GRINGERI, E., BARNI, S., CILLO, U., VAIRETTI, M. & FREITAS, I. 2011. Decreased apoptosis in fatty livers submitted to subnormothermic machine-perfusion respect to cold storage. *Eur J Histochem,* 55**,** e40.

BONNER, J. A., HARARI, P. M., GIRALT, J., AZARNIA, N., SHIN, D. M., COHEN, R. B., JONES, C. U., SUR, R., RABEN, D., JASSEM, J., OVE, R., KIES, M. S., BASELGA, J., YOUSSOUFIAN, H., AMELLAL, N., ROWINSKY, E. K. & ANG, K. K. 2006. Radiotherapy plus cetuximab for squamous-cell carcinoma of the head and neck. *N Engl J Med,* 354**,** 567-78.

BOSETTI, C., LA VECCHIA, C., TALAMINI, R., NEGRI, E., LEVI, F., DAL MASO, L. & FRANCESCHI, S. 2002. Food groups and laryngeal cancer risk: a case-control study from Italy and Switzerland. *Int J Cancer,* 100**,** 355-60.

BOSETTI, C., LA VECCHIA, C., TALAMINI, R., NEGRI, E., LEVI, F., FRYZEK, J., MCLAUGHLIN, J. K., GARAVELLO, W. & FRANCESCHI, S. 2003. Energy, macronutrients and laryngeal cancer risk. *Ann Oncol,* 14**,** 907-12.

BOURKE, E., DODSON, H., MERDES, A., CUFFE, L., ZACHOS, G., WALKER, M., GILLESPIE, D. & MORRISON, C. G. 2007. DNA damage induces Chk1-dependent centrosome amplification. *EMBO Rep,* 8**,** 603-9.

BOYLE, J. O., HAKIM, J., KOCH, W., VAN DER RIET, P., HRUBAN, R. H., ROA, R. A., CORREO, R., EBY, Y. J., RUPPERT, J. M. & SIDRANSKY, D. 1993. The incidence of p53 mutations increases with progression of head and neck cancer. *Cancer Res,* 53**,** 4477-80.

BOZEC, A., PEYRADE, F. & MILANO, G. 2013. Molecular targeted therapies in the management of head and neck squamous cell carcinoma: recent developments and perspectives. *Anticancer Agents Med Chem,* 13**,** 389-402.

BRADLEY, M. O., DYSART, G., FITZSIMMONS, K., HARBACH, P., LEWIN, J. & WOLF, G. 1982. Measurements by filter elution of DNA single- and double-strand breaks in rat hepatocytes: effects of nitrosamines and gamma-irradiation. *Cancer Res,* 42**,** 2592-7.

BRADLEY, P. J. 2008. Oropharyngeal Tumours. *In:* GLEESON, M., BROWNING, G.G., BURTON, M.J., CLARKE, R., HIBBERT, J., JONES, N.S., LUND, V.J., LUXON,

L.M., WATKINSON, J.C. (ed.) *Scott-Brown's Otorhinolaryngology, Head and Neck Surgery.* 7th ed. London: Hodder Arnold.
BRISTOW, R. G., JANG, A., PEACOCK, J., CHUNG, S., BENCHIMOL, S. & HILL, R. P. 1994. Mutant p53 increases radioresistance in rat embryo fibroblasts simultaneously transfected with HPV16-E7 and/or activated H-ras. *Oncogene,* 9**,** 1527-36.
BRIZEL, D. M., SIBLEY, G. S., PROSNITZ, L. R., SCHER, R. L. & DEWHIRST, M. W. 1997. Tumor hypoxia adversely affects the prognosis of carcinoma of the head and neck. *Int J Radiat Oncol Biol Phys,* 38**,** 285-9.
BROADWELL, I., FLETCHER, P. D., HASWELL, S. J., MCCREEDY, T. & ZHANG, X. 2001. Quantitative 3-dimensional profiling of channel networks within transparent lab-on-a-chip microreactors using a digital imaging method. *Lab Chip,* 1**,** 66-71.
BROCHE, L. M., BHADAL, N., LEWIS, M. P., PORTER, S., HUGHES, M. P. & LABEED, F. H. 2007. Early detection of oral cancer - Is dielectrophoresis the answer? *Oral Oncol,* 43**,** 199-203.
BROWMAN, G. P., MOHIDE, E. A., WILLAN, A., HODSON, I., WONG, G., GRIMARD, L., MACKENZIE, R. G., EL-SAYED, S., DUNN, E. & FARRELL, S. 2002. Association between smoking during radiotherapy and prognosis in head and neck cancer: a follow-up study. *Head Neck,* 24**,** 1031-7.
BROWMAN, G. P., WONG, G., HODSON, I., SATHYA, J., RUSSELL, R., MCALPINE, L., SKINGLEY, P. & LEVINE, M. N. 1993. Influence of cigarette smoking on the efficacy of radiation therapy in head and neck cancer. *N Engl J Med,* 328**,** 159-63.
BRYON-DODD, K. 2011. *NHS may struggle to cope with personalised medicine* [Online]. BioNews. Available: http://www.bionews.org.uk/page_104104 [Accessed 23.9.13 2013].
BURCOMBE, R., WILSON, G. D., DOWSETT, M., KHAN, I., RICHMAN, P. I., DALEY, F., DETRE, S. & MAKRIS, A. 2006. Evaluation of Ki-67 proliferation and apoptotic index before, during and after neoadjuvant chemotherapy for primary breast cancer. *Breast Cancer Res,* 8**,** R31.
BURNS, T. F., BERNHARD, E. J. & EL-DEIRY, W. S. 2001. Tissue specific expression of p53 target genes suggests a key role for KILLER/DR5 in p53-dependent apoptosis in vivo. *Oncogene,* 20**,** 4601-12.
BUSSINK, J., VAN DER KOGEL, A. J. & KAANDERS, J. H. 2008. Activation of the PI3-K/AKT pathway and implications for radioresistance mechanisms in head and neck cancer. *Lancet Oncol,* 9**,** 288-96.
CAI, L., CHERIAN, M. G., ISKANDER, S., LEBLANC, M. & HAMMOND, R. R. 2000. Metallothionein induction in human CNS in vitro: neuroprotection from ionizing radiation. *Int J Radiat Biol,* 76**,** 1009-17.
CALAIS, G., ALFONSI, M., BARDET, E., SIRE, C., GERMAIN, T., BERGEROT, P., RHEIN, B., TORTOCHAUX, J., OUDINOT, P. & BERTRAND, P. 1999. Randomized trial of radiation therapy versus concomitant chemotherapy and radiation therapy for advanced-stage oropharynx carcinoma. *J Natl Cancer Inst,* 91**,** 2081-6.
CALIFANO, J., VAN DER RIET, P., WESTRA, W., NAWROZ, H., CLAYMAN, G., PIANTADOSI, S., CORIO, R., LEE, D., GREENBERG, B., KOCH, W. & SIDRANSKY, D. 1996. Genetic progression model for head and neck cancer: implications for field cancerization. *Cancer Res,* 56**,** 2488-92.
CALIFANO, J., WESTRA, W. H., MEININGER, G., CORIO, R., KOCH, W. M. & SIDRANSKY, D. 2000. Genetic progression and clonal relationship of recurrent premalignant head and neck lesions. *Clin Cancer Res,* 6**,** 347-52.
CAMP, A. A., FUNDAKOWSKI, C., PETRUZZELLI, G. J. & EMAMI, B. 2009. Functional and oncologic results following transoral laser microsurgical excision of base of tongue carcinoma. *Otolaryngol Head Neck Surg,* 141**,** 66-9.

CASENGHI, M., MANGIACASALE, R., TUYNDER, M., CAILLET-FAUQUET, P., ELHAJOUJI, A., LAVIA, P., MOUSSET, S., KIRSCH-VOLDERS, M. & CUNDARI, E. 1999. p53-independent apoptosis and p53-dependent block of DNA rereplication following mitotic spindle inhibition in human cells. *Exp Cell Res,* 250**,** 339-50.

CASTEDO, M., COQUELLE, A., VIVET, S., VITALE, I., KAUFFMANN, A., DESSEN, P., PEQUIGNOT, M. O., CASARES, N., VALENT, A., MOUHAMAD, S., SCHMITT, E., MODJTAHEDI, N., VAINCHENKER, W., ZITVOGEL, L., LAZAR, V., GARRIDO, C. & KROEMER, G. 2006. Apoptosis regulation in tetraploid cancer cells. *EMBO J,* 25**,** 2584-95.

CASTEDO, M. & KROEMER, G. 2004. [Mitotic catastrophe: a special case of apoptosis]. *J Soc Biol,* 198**,** 97-103.

CASTEDO, M., PERFETTINI, J. L., ROUMIER, T., ANDREAU, K., MEDEMA, R. & KROEMER, G. 2004. Cell death by mitotic catastrophe: a molecular definition. *Oncogene,* 23**,** 2825-37.

CASTELL JV, G.-L. M., MIRANDA MA, MORERA IM 1987. Toxic effects of the photoproducts of chlorpromazine on cultured hepatocytes. *Hepatology,* 7**,** 349-54.

CEKIN, E., OZYURT, M., ERKUL, E., ERGUNAY, K., CINCIK, H., KAPUCU, B. & GUNGOR, A. 2012. The association between Helicobacter pylori and laryngopharyngeal reflux in laryngeal pathologies. *Ear Nose Throat J,* 91**,** E6-9.

CHANG, B. D., SWIFT, M. E., SHEN, M., FANG, J., BROUDE, E. V. & RONINSON, I. B. 2002. Molecular determinants of terminal growth arrest induced in tumor cells by a chemotherapeutic agent. *Proc Natl Acad Sci U S A,* 99**,** 389-94.

CHEN, A. Y., SCHRAG, N., HAO, Y., STEWART, A. & WARD, E. 2007. Changes in treatment of advanced oropharyngeal cancer, 1985-2001. *Laryngoscope,* 117**,** 16-21.

CHEN, S. F., NIEH, S., JAO, S. W., WU, M. Z., LIU, C. L., CHANG, Y. C. & LIN, Y. S. 2013. The paracrine effect of cancer-associated fibroblast-induced interleukin-33 regulates the invasiveness of head and neck squamous cell carcinoma. *J Pathol*.

CHEN, Z. G. 2009. The cancer stem cell concept in progression of head and neck cancer. *J Oncol,* 2009**,** 894064.

CHENG, Q., LU, L., GRAFSTROM, J., OLOFSSON, M. H., THORELL, J. O., SAMEN, E., JOHANSSON, K., AHLZEN, H. S., STONE-ELANDER, S., LINDER, S. & ARNER, E. S. 2012. Combining [11C]-AnxA5 PET imaging with serum biomarkers for improved detection in live mice of modest cell death in human solid tumor xenografts. *PLoS One,* 7**,** e42151.

CHENG Y, W. Y., KANG YZ, HU PY, GAO Y, PAN MX. 2013. In vitro culture of tumour-derived hepatocytes in decellularised whole-liver biological scaffolds. *Digestion,* 87**,** 189-195.

CHIOU, S. H., YU, C. C., HUANG, C. Y., LIN, S. C., LIU, C. J., TSAI, T. H., CHOU, S. H., CHIEN, C. S., KU, H. H. & LO, J. F. 2008. Positive correlations of Oct-4 and Nanog in oral cancer stem-like cells and high-grade oral squamous cell carcinoma. *Clin Cancer Res,* 14**,** 4085-95.

CHO, Y., KIM, H.S., FRAZIER, A.B., CHEN, Z.G., SHIN, D.M., HAN, A. 2009. Whole-cell impedance analysis for highly and poorly metastatic cancer cells. *J. Microelectromech. Syst.,* 18**,** 808-817.

CHRISTIANSEN, H., SAILE, B., NEUBAUER-SAILE, K., TIPPELT, S., RAVE-FRANK, M., HERMANN, R. M., DUDAS, J., HESS, C. F., SCHMIDBERGER, H. & RAMADORI, G. 2004. Irradiation leads to susceptibility of hepatocytes to TNF-alpha mediated apoptosis. *Radiother Oncol,* 72**,** 291-6.

CLARKE, M. F., DICK, J. E., DIRKS, P. B., EAVES, C. J., JAMIESON, C. H., JONES, D. L., VISVADER, J., WEISSMAN, I. L. & WAHL, G. M. 2006. Cancer stem cells--

perspectives on current status and future directions: AACR Workshop on cancer stem cells. *Cancer Res,* 66**,** 9339-44.
CLAYMAN, G. L., JOHNSON, C. J., 2ND, MORRISON, W., GINSBERG, L. & LIPPMAN, S. M. 2001. The role of neck dissection after chemoradiotherapy for oropharyngeal cancer with advanced nodal disease. *Arch Otolaryngol Head Neck Surg,* 127**,** 135-9.
CLAYMAN, G. L., STEWART, M. G., WEBER, R. S., EL-NAGGAR, A. K. & GRIMM, E. A. 1994. Human papillomavirus in laryngeal and hypopharyngeal carcinomas. Relationship to survival. *Arch Otolaryngol Head Neck Surg,* 120**,** 743-8.
COBLEIGH, M. A., GALLAGHER, P. A., HILL, J. H., APPLEBAUM, E. L. & MCGUIRE, W. P. 1984. Growth of human squamous head and neck cancer in vitro. *Am J Pathol,* 115**,** 397-402.
CONWAY, D. I., STOCKTON, D. L., WARNAKULASURIYA, K. A., OGDEN, G. & MACPHERSON, L. M. 2006. Incidence of oral and oropharyngeal cancer in United Kingdom (1990-1999) -- recent trends and regional variation. *Oral Oncol,* 42**,** 586-92.
COOPER, J. S., PAJAK, T. F., FORASTIERE, A. A., JACOBS, J., CAMPBELL, B. H., SAXMAN, S. B., KISH, J. A., KIM, H. E., CMELAK, A. J., ROTMAN, M., MACHTAY, M., ENSLEY, J. F., CHAO, K. S., SCHULTZ, C. J., LEE, N. & FU, K. K. 2004. Postoperative concurrent radiotherapy and chemotherapy for high-risk squamous-cell carcinoma of the head and neck. *N Engl J Med,* 350**,** 1937-44.
COPPE, J. P., DESPREZ, P. Y., KRTOLICA, A. & CAMPISI, J. 2010. The senescence-associated secretory phenotype: the dark side of tumor suppression. *Annu Rev Pathol,* 5**,** 99-118.
COTRAN RS, K. V., COLLINS T. 1997. Neoplasia. *In:* KUMAR V, C. R., ROBBINS SL (ed.) *Basic Pathology.* Philadelphia: WB Saunders.
COUPLAND, V. H., CHAPMAN, P., LINKLATER, K. M., SEHGAL, A., MOLLER, H. & DAVIES, E. A. 2009. Trends in the epidemiology of larynx and lung cancer in south-east England, 1985-2004. *Br J Cancer,* 100**,** 167-9.
CRUK. 2009. *Laryngeal cancer - survival statistics* [Online]. Available: http://www.info.cancerresearch.org/cancerstats/types/larynx/survival [Accessed 15 October 2011].
CRUK. 2010. *Oral Cancer - UK Mortality Statistics* [Online]. Available: http://info.cancerresearchuk.org/cancerstats/types/oral/mortality/ [Accessed 2 April 2012].
CRUK. 2011. *Human Papillomaviruses* [Online]. Available: http://info.cancerresearchuk.org/cancerstats/causes/infectiousagents/humanpapillomaviruses/ - source9 [Accessed 2 April 2012].
CRUK. 2012. *Oral Cancer - UK Incidence Statistics* [Online]. Available: http://info.cancerresearchuk.org/cancerstats/types/oral/incidence/uk-oral-cancer-incidence-statistics [Accessed 2 April 2012].
CUMMINGS, C. W., FLINT, P.W., HARKER, L.A., HAUGHEY, B.H., RICHARDSON, M.A., ROBBINS, K.T., SCHULLER, D.E., THOMAS, J.R. 2005. *Otolaryngology Head and Neck Surgery,* Philadelphia, Elsevier.
DAI, C. Y. & ENDERS, G. H. 2000. p16 INK4a can initiate an autonomous senescence program. *Oncogene,* 19**,** 1613-22.
DALERBA, P., CHO, R. W. & CLARKE, M. F. 2007. Cancer stem cells: models and concepts. *Annu Rev Med,* 58**,** 267-84.
DALLEY, A. J., ABDULMAJEED, A. A., UPTON, Z. & FARAH, C. S. 2013. Organotypic culture of normal, dysplastic and squamous cell carcinoma-derived oral cell lines reveals loss of spatial regulation of CD44 and p75 NTR in malignancy. *J Oral Pathol Med,* 42**,** 37-46.
DALLOL, A., AGATHANGGELOU, A., FENTON, S. L., AHMED-CHOUDHURY, J., HESSON, L., VOS, M. D., CLARK, G. J., DOWNWARD, J., MAHER, E. R. &

LATIF, F. 2004. RASSF1A interacts with microtubule-associated proteins and modulates microtubule dynamics. *Cancer Res,* 64**,** 4112-6.
DAMEK-POPRAWA, M., VOLGINA, A., KOROSTOFF, J., SOLLECITO, T. P., BROSE, M. S., O'MALLEY, B. W., JR., AKINTOYE, S. O. & DIRIENZO, J. M. 2011. Targeted inhibition of CD133+ cells in oral cancer cell lines. *J Dent Res,* 90**,** 638-45.
DAS, S., BOSWELL, S. A., AARONSON, S. A. & LEE, S. W. 2008. P53 promoter selection: choosing between life and death. *Cell Cycle,* 7**,** 154-7.
DAS, S., RAJ, L., ZHAO, B., KIMURA, Y., BERNSTEIN, A., AARONSON, S. A. & LEE, S. W. 2007. Hzf Determines cell survival upon genotoxic stress by modulating p53 transactivation. *Cell,* 130**,** 624-37.
DE GENDT, K., MCKINNELL, C., WILLEMS, A., SAUNDERS, P. T., SHARPE, R. M., ATANASSOVA, N., SWINNEN, J. V. & VERHOEVEN, G. 2009. Organotypic cultures of prepubertal mouse testes: a method to study androgen action in sertoli cells while preserving their natural environment. *Biol Reprod,* 81**,** 1083-92.
DE STEFANI, E., BOFFETTA, P., OREGGIA, F., BRENNAN, P., RONCO, A., DENEO-PELLEGRINI, H. & MENDILAHARSU, M. 2000. Plant foods and risk of laryngeal cancer: A case-control study in Uruguay. *Int J Cancer,* 87**,** 129-32.
DE STEFANI, E., BOFFETTA, P., RONCO, A. L., DENEO-PELLEGRINI, H., ACOSTA, G. & MENDILAHARSU, M. 2007. Dietary patterns and risk of laryngeal cancer: an exploratory factor analysis in Uruguayan men. *Int J Cancer,* 121**,** 1086-91.
DE VILLIERS, E. M. 1994. Human pathogenic papillomavirus types: an update. *Curr Top Microbiol Immunol,* 186**,** 1-12.
DEAN, N. R., NEWMAN, J. R., HELMAN, E. E., ZHANG, W., SAFAVY, S., WEEKS, D. M., CUNNINGHAM, M., SNYDER, L. A., TANG, Y., YAN, L., MCNALLY, L. R., BUCHSBAUM, D. J. & ROSENTHAL, E. L. 2009. Anti-EMMPRIN monoclonal antibody as a novel agent for therapy of head and neck cancer. *Clin Cancer Res,* 15**,** 4058-65.
DELAMARCHE, E., BERNARD, A., SCHMID, H., BIETSCH, A., MICHEL, B. & BIEBUYCK, H. 1998. Microfluidic Networks for Chemical Patterning of Substrates: Design and Application to Bioassays. *Journal of the American Chemical Society,* 120**,** 500-508.
DELAMARCHE, E., BERNARD, A., SCHMID, H., MICHEL, B. & BIEBUYCK, H. 1997. Patterned Delivery of Immunoglobulins to Surfaces Using Microfluidic Networks. *Science,* 276**,** 779-781.
DENIS, F., GARAUD, P., BARDET, E., ALFONSI, M., SIRE, C., GERMAIN, T., BERGEROT, P., RHEIN, B., TORTOCHAUX, J. & CALAIS, G. 2004. Final results of the 94-01 French Head and Neck Oncology and Radiotherapy Group randomized trial comparing radiotherapy alone with concomitant radiochemotherapy in advanced-stage oropharynx carcinoma. *J Clin Oncol,* 22**,** 69-76.
DEY, P., ARNOLD, D., WIGHT, R., MACKENZIE, K., KELLY, C. & WILSON, J. 2002. Radiotherapy versus open surgery versus endolaryngeal surgery (with or without laser) for early laryngeal squamous cell cancer. *Cochrane Database Syst Rev***,** CD002027.
DEY, S., SPRING, P. M., ARNOLD, S., VALENTINO, J., CHENDIL, D., REGINE, W. F., MOHIUDDIN, M. & AHMED, M. M. 2003. Low-dose fractionated radiation potentiates the effects of Paclitaxel in wild-type and mutant p53 head and neck tumor cell lines. *Clin Cancer Res,* 9**,** 1557-65.
DHILLON, N. 2004. Anatomy. *In:* LALWANI, A. K. (ed.) *Current Diagnosis & Treatment in Otolaryngology - Head and Neck Surgery.* USA: Lange Medical Books / McGraw-Hill.

DIEHN, M. & CLARKE, M. F. 2006. Cancer stem cells and radiotherapy: new insights into tumor radioresistance. *J Natl Cancer Inst,* 98**,** 1755-7.
DIKENSON, D. 2012. *Personalised medicine: a reality check* [Online]. Available: http://www.bionews.org.uk/page_205094 [Accessed 23.9.13 2013].
DINESMAN, A., HAUGHEY, B., GATES, G. A., AUFDEMORTE, T. & VON HOFF, D. D. 1990. Development of a new in vivo model for head and neck cancer. *Otolaryngol Head Neck Surg,* 103**,** 766-74.
DINSHAW, K. A., AGARWAL, J. P., GHOSH-LASKAR, S., GUPTA, T. & SHRIVASTAVA, S. K. 2006. Radical radiotherapy in head and neck squamous cell carcinoma: an analysis of prognostic and therapeutic factors. *Clin Oncol (R Coll Radiol),* 18**,** 383-9.
DISCHE, S., SAUNDERS, M.I. 2002. Clinical Radiobiology. *In:* PRICE, P., SIKORA, K. (ed.) *Treatment of Cancer.* 4th ed. London Hodder Arnold.
DODSON, H., WHEATLEY, S. P. & MORRISON, C. G. 2007. Involvement of centrosome amplification in radiation-induced mitotic catastrophe. *Cell Cycle,* 6**,** 364-70.
DONG, S. M., SUN, D. I., BENOIT, N. E., KUZMIN, I., LERMAN, M. I. & SIDRANSKY, D. 2003. Epigenetic inactivation of RASSF1A in head and neck cancer. *Clin Cancer Res,* 9**,** 3635-40.
DORR, W., HAMILTON, C. S., BOYD, T., REED, B. & DENHAM, J. W. 2002. Radiation-induced changes in cellularity and proliferation in human oral mucosa. *Int J Radiat Oncol Biol Phys,* 52**,** 911-7.
DRAHOS, A., DAM, A. & OREG, Z. 2004. [Radiosensitizing effect of hyperfractionated radiation]. *Magy Onkol,* 48**,** 323-31.
DU, Y., HAN, R., WEN, F., NG SAN SAN, S., XIA, L., WOHLAND, T., LEO, H. L. & YU, H. 2008. Synthetic sandwich culture of 3D hepatocyte monolayer. *Biomaterials,* 29**,** 290-301.
DUBRAY, B., MOSSERI, V., BRUNIN, F., JAULERRY, C., PONCET, P., RODRIGUEZ, J., BRUGERE, J., POINT, D., GIRAUD, P. & COSSET, J. M. 1996. Anemia is associated with lower local-regional control and survival after radiation therapy for head and neck cancer: a prospective study. *Radiology,* 201**,** 553-8.
EASTY, D. M., EASTY, G. C., CARTER, R. L., MONAGHAN, P. & BUTLER, L. J. 1981. Ten human carcinoma cell lines derived from squamous carcinomas of the head and neck. *Br J Cancer,* 43**,** 772-85.
EDER-CZEMBIREK, C., CZEMBIREK, C., EROVIC, B. M., SELZER, E., TURHANI, D., VORMITTAG, L. & THURNHER, D. 2005. Combination of betulinic acid with cisplatin--different cytotoxic effects in two head and neck cancer cell lines. *Oncol Rep,* 14**,** 667-71.
EIBAND, J. D., ELIAS, E. G., SUTER, C. M., GRAY, W. C. & DIDOLKAR, M. S. 1989. Prognostic factors in squamous cell carcinoma of the larynx. *Am J Surg,* 158**,** 314-7.
EICHER, S. A., CLAYMAN, G. L., LIU, T. J., SHILLITOE, E. J., STORTHZ, K. A., ROTH, J. A. & LOTAN, R. 1996. Evaluation of topical gene therapy for head and neck squamous cell carcinoma in an organotypic model. *Clin Cancer Res,* 2**,** 1659-64.
EL-ALI, J., SORGER, P. K. & JENSEN, K. F. 2006. Cells on chips. *Nature,* 442**,** 403-11.
ELLIS, L., RACHET, B., BIRCHALL, M. & COLEMAN, M. P. 2011. Trends and inequalities in laryngeal cancer survival in men and women: England and Wales 1991-2006. *Oral Oncol.*
EMBREE-KU, M., VENTURINI, D. & BOEKELHEIDE, K. 2002. Fas is involved in the p53-dependent apoptotic response to ionizing radiation in mouse testis. *Biol Reprod,* 66**,** 1456-61.

ERENPREISA, J. & CRAGG, M. S. 2007. Cancer: a matter of life cycle? *Cell Biol Int,* 31**,** 1507-10.
ERENPREISA, J., KALEJS, M., IANZINI, F., KOSMACEK, E. A., MACKEY, M. A., EMZINSH, D., CRAGG, M. S., IVANOV, A. & ILLIDGE, T. M. 2005. Segregation of genomes in polyploid tumour cells following mitotic catastrophe. *Cell Biol Int,* 29**,** 1005-11.
ERIKSEN, J. G., LASSEN, P. & OVERGAARD, J. 2010. Do all patients with head and neck cancer benefit from radiotherapy and concurrent cetuximab? *Lancet Oncol,* 11**,** 312-3.
ERIKSEN, J. G., STEINICHE, T., ASKAA, J., ALSNER, J. & OVERGAARD, J. 2004. The prognostic value of epidermal growth factor receptor is related to tumor differentiation and the overall treatment time of radiotherapy in squamous cell carcinomas of the head and neck. *Int J Radiat Oncol Biol Phys,* 58**,** 561-6.
ERIKSSON, D., BLOMBERG, J., LINDGREN, T., LOFROTH, P. O., JOHANSSON, L., RIKLUND, K. & STIGBRAND, T. 2008. Iodine-131 induces mitotic catastrophes and activates apoptotic pathways in HeLa Hep2 cells. *Cancer Biother Radiopharm,* 23**,** 541-9.
ERIKSSON, D., JONIANI, H. M., SHEIKHOLVAEZIN, A., LOFROTH, P. O., JOHANSSON, L., RIKLUND AHLSTROM, K. & STIGBRAND, T. 2003. Combined low dose radio- and radioimmunotherapy of experimental HeLa Hep 2 tumours. *Eur J Nucl Med Mol Imaging,* 30**,** 895-906.
ERIKSSON, D., LOFROTH, P. O., JOHANSSON, L., RIKLUND, K. A. & STIGBRAND, T. 2007. Cell cycle disturbances and mitotic catastrophes in HeLa Hep2 cells following 2.5 to 10 Gy of ionizing radiation. *Clin Cancer Res,* 13**,** 5501s-5508s.
ERIKSSON, D. & STIGBRAND, T. 2010. Radiation-induced cell death mechanisms. *Tumour Biol,* 31**,** 363-72.
ESTEVE, J., RIBOLI, E., PEQUIGNOT, G., TERRACINI, B., MERLETTI, F., CROSIGNANI, P., ASCUNCE, N., ZUBIRI, L., BLANCHET, F., RAYMOND, L., REPETTO, F. & TUYNS, A. J. 1996. Diet and cancers of the larynx and hypopharynx: the IARC multi-center study in southwestern Europe. *Cancer Causes Control,* 7**,** 240-52.
EUSTACE, A., MANI, N., SPAN, P. N., IRLAM, J. J., TAYLOR, J., BETTS, G. N., DENLEY, H., MILLER, C. J., HOMER, J. J., ROJAS, A. M., HOSKIN, P. J., BUFFA, F. M., HARRIS, A. L., KAANDERS, J. H. & WEST, C. M. 2013. A 26-Gene Hypoxia Signature Predicts Benefit from Hypoxia-Modifying Therapy in Laryngeal Cancer but Not Bladder Cancer. *Clin Cancer Res,* 19**,** 4879-4888.
FAKHRY, C., WESTRA, W. H., LI, S., CMELAK, A., RIDGE, J. A., PINTO, H., FORASTIERE, A. & GILLISON, M. L. 2008. Improved survival of patients with human papillomavirus-positive head and neck squamous cell carcinoma in a prospective clinical trial. *J Natl Cancer Inst,* 100**,** 261-9.
FEI, P. & EL-DEIRY, W. S. 2003. P53 and radiation responses. *Oncogene,* 22**,** 5774-83.
FENG, J., ZOU, J., LI, L., ZHAO, Y. & LIU, S. 2011. Antisense oligodeoxynucleotides targeting ATM strengthen apoptosis of laryngeal squamous cell carcinoma grown in nude mice. *J Exp Clin Cancer Res,* 30**,** 43.
FERNBERG, J. O., RINGBORG, U., SILFVERSWARD, C., EWERT, G., HAGLUND, S., SCHIRATZKI, H. & STRANDER, H. 1989. Radiation therapy in early glottic cancer. Analysis of 177 consecutive cases. *Acta Otolaryngol,* 108**,** 478-81.
FINDLEY, H. W., GU, L., YEAGER, A. M. & ZHOU, M. 1997. Expression and regulation of Bcl-2, Bcl-xl, and Bax correlate with p53 status and sensitivity to apoptosis in childhood acute lymphoblastic leukemia. *Blood,* 89**,** 2986-93.

FOLCH, A. & TONER, M. 2000. MICROENGINEERING OF CELLULAR INTERACTIONS. *Annual Review of Biomedical Engineering,* 2**,** 227-256.
FORASTIERE, A. A., GOEPFERT, H., MAOR, M., PAJAK, T. F., WEBER, R., MORRISON, W., GLISSON, B., TROTTI, A., RIDGE, J. A., CHAO, C., PETERS, G., LEE, D. J., LEAF, A., ENSLEY, J. & COOPER, J. 2003. Concurrent chemotherapy and radiotherapy for organ preservation in advanced laryngeal cancer. *N Engl J Med,* 349**,** 2091-8.
FRANK, N. Y., SCHATTON, T. & FRANK, M. H. 2010. The therapeutic promise of the cancer stem cell concept. *J Clin Invest,* 120**,** 41-50.
FRANKE, W. W., SCHMID, E., OSBORN, M. & WEBER, K. 1979. Intermediate-sized filaments of human endothelial cells. *J Cell Biol,* 81**,** 570-80.
FRESHNEY, R. I. 2010. Basic Principles of Cell Culture. *In:* VUNJAK-NOVAKOVIC, G., FRESHNEY, R.I. (ed.) *Culture of Cells for Tissue Engineering.* London: John Wiley & Sons.
FUERTES, M. A., CASTILLA, J., ALONSO, C. & PEREZ, J. M. 2003. Cisplatin biochemical mechanism of action: from cytotoxicity to induction of cell death through interconnections between apoptotic and necrotic pathways. *Curr Med Chem,* 10**,** 257-66.
GADHIKAR, M. A., SCIUTO, M. R., ORTEGA ALVES, M. V., PICKERING, C. R., OSMAN, A. A., NESKEY, D. M., ZHAO, M., FITZGERALD, A. L., MYERS, J. N. & FREDERICK, M. J. 2013. Chk1/2 inhibition overcomes the cisplatin resistance of head and neck cancer cells secondary to the loss of functional p53. *Mol Cancer Ther*.
GAN, C. P., HAMID, S., HOR, S. Y., ZAIN, R. B., ISMAIL, S. M., WAN MUSTAFA, W. M., TEO, S. H., SAUNDERS, N. & CHEONG, S. C. 2012. Valproic acid: growth inhibition of head and neck cancer by induction of terminal differentiation and senescence. *Head Neck,* 34**,** 344-53.
GANEM, N. J. & PELLMAN, D. 2007. Limiting the proliferation of polyploid cells. *Cell,* 131**,** 437-40.
GANEM, N. J., STORCHOVA, Z. & PELLMAN, D. 2007. Tetraploidy, aneuploidy and cancer. *Curr Opin Genet Dev,* 17**,** 157-62.
GARNIS, C., BALDWIN, C., ZHANG, L., ROSIN, M. P. & LAM, W. L. 2003. Use of complete coverage array comparative genomic hybridization to define copy number alterations on chromosome 3p in oral squamous cell carcinomas. *Cancer Res,* 63**,** 8582-5.
GAU, V. & WONG, D. 2007. Oral fluid nanosensor test (OFNASET) with advanced electrochemical-based molecular analysis platform. *Ann N Y Acad Sci,* 1098**,** 401-10.
GENUTH, S. 1998. Whole Body Metabolism. *In:* BERNE, R., LEVY, MN (ed.) *Physiology.* 4th ed. St. Louis: Mosby.
GERACI, J. P., JACKSON, K.L., MARIANO, M.S., LEITCH, J.M. 1985. Hepatic injury after whole-liver irradiation in the rat. *Radiat Res,* 101**,** 508-18.
GERACI, J. P. & MARIANO, M. S. 1993. Radiation hepatology of the rat: parenchymal and nonparenchymal cell injury. *Radiat Res,* 136**,** 205-13.
GERACI, J. P., MARIANO, M. S. & JACKSON, K. L. 1991. Hepatic radiation injury in the rat. *Radiat Res,* 125**,** 65-72.
GERVAIS, T., EL-ALI, J., GUNTHER, A. & JENSEN, K. F. 2006. Flow-induced deformation of shallow microfluidic channels. *Lab Chip,* 6**,** 500-7.
GOODHEAD, D. T. 1994. Initial events in the cellular effects of ionizing radiations: clustered damage in DNA. *Int J Radiat Biol,* 65**,** 7-17.

GOODMAN, M., MORGAN, R. W., RAY, R., MALLOY, C. D. & ZHAO, K. 1999. Cancer in asbestos-exposed occupational cohorts: a meta-analysis. *Cancer Causes Control,* 10**,** 453-65.

GOSENS, M. J., DRESEN, R. C., RUTTEN, H. J., NIEUWENHUIJZEN, G. A., VAN DER LAAK, J. A., MARTIJN, H., TAN-GO, I., NAGTEGAAL, I. D., VAN DEN BRULE, A. J. & VAN KRIEKEN, J. H. 2008. Preoperative radiochemotherapy is successful also in patients with locally advanced rectal cancer who have intrinsically high apoptotic tumours. *Ann Oncol,* 19**,** 2026-32.

GRANDIS, J. R. & TWEARDY, D. J. 1993. Elevated levels of transforming growth factor alpha and epidermal growth factor receptor messenger RNA are early markers of carcinogenesis in head and neck cancer. *Cancer Res,* 53**,** 3579-84.

GREAVES, E. D. & MANZ, A. 2005. Toward on-chip X-ray analysis. *Lab Chip,* 5**,** 382-91.

GRONBAEK, M., BECKER, U., JOHANSEN, D., TONNESEN, H., JENSEN, G. & SORENSEN, T. I. 1998. Population based cohort study of the association between alcohol intake and cancer of the upper digestive tract. *BMJ,* 317**,** 844-7.

GUPTA, A. K., MCKENNA, W. G., WEBER, C. N., FELDMAN, M. D., GOLDSMITH, J. D., MICK, R., MACHTAY, M., ROSENTHAL, D. I., BAKANAUSKAS, V. J., CERNIGLIA, G. J., BERNHARD, E. J., WEBER, R. S. & MUSCHEL, R. J. 2002. Local recurrence in head and neck cancer: relationship to radiation resistance and signal transduction. *Clin Cancer Res,* 8**,** 885-92.

GUTSCHALK, C. M., HEROLD-MENDE, C. C., FUSENIG, N. E. & MUELLER, M. M. 2006. Granulocyte colony-stimulating factor and granulocyte-macrophage colony-stimulating factor promote malignant growth of cells from head and neck squamous cell carcinomas in vivo. *Cancer Res,* 66**,** 8026-36.

HAGER, G., FORMANEK, M., GEDLICKA, C., KNERER, B. & KORNFEHL, J. 2001. Ethanol decreases expression of p21 and increases hyperphosphorylated pRb in cell lines of squamous cell carcinomas of the head and neck. *Alcohol Clin Exp Res,* 25**,** 496-501.

HALDAR, S., NEGRINI, M., MONNE, M., SABBIONI, S. & CROCE, C. M. 1994. Down-regulation of bcl-2 by p53 in breast cancer cells. *Cancer Res,* 54**,** 2095-7.

HANSEN, O., OVERGAARD, J., HANSEN, H. S., OVERGAARD, M., HOYER, M., JORGENSEN, K. E., BASTHOLT, L. & BERTHELSEN, A. 1997. Importance of overall treatment time for the outcome of radiotherapy of advanced head and neck carcinoma: dependency on tumor differentiation. *Radiother Oncol,* 43**,** 47-51.

HARPER, L. J., PIPER, K., COMMON, J., FORTUNE, F. & MACKENZIE, I. C. 2007. Stem cell patterns in cell lines derived from head and neck squamous cell carcinoma. *J Oral Pathol Med,* 36**,** 594-603.

HARRIS, A. L. 2002. Hypoxia--a key regulatory factor in tumour growth. *Nat Rev Cancer,* 2**,** 38-47.

HARRISON, L. B., CHADHA, M., HILL, R. J., HU, K. & SHASHA, D. 2002. Impact of tumor hypoxia and anemia on radiation therapy outcomes. *Oncologist,* 7**,** 492-508.

HART, A. A., MAK-KREGAR, S., HILGERS, F. J., LEVENDAG, P. C., MANNI, J. J., SPOELSTRA, H. A., BRUASET, I. A., VAN DER LAAN, B. F., ANNYAS, A. A., VAN DER BEEK, J. M. & ET AL. 1995. The importance of correct stage grouping in oncology. Results of a nationwide study of oropharyngeal carcinoma in The Netherlands. *Cancer,* 75**,** 2656-62.

HATTERSLEY, S. M., DYER, C. E., GREENMAN, J. & HASWELL, S. J. 2008. Development of a microfluidic device for the maintenance and interrogation of viable tissue biopsies. *Lab Chip,* 8**,** 1842-6.

HATTERSLEY, S. M., GREENMAN, J. & HASWELL, S. J. 2011. Study of ethanol induced toxicity in liver explants using microfluidic devices. *Biomed Microdevices,* 13**,** 1005-14.

HATTERSLEY, S. M., SYLVESTER, D. C., DYER, C. E., STAFFORD, N. D., HASWELL, S. J. & GREENMAN, J. 2012. A microfluidic system for testing the responses of head and neck squamous cell carcinoma tissue biopsies to treatment with chemotherapy drugs. *Ann Biomed Eng,* 40**,** 1277-88.

HAYES, R. A. & FEENSTRA, B. J. 2003. Video-speed electronic paper based on electrowetting. *Nature,* 425**,** 383-5.

HAYFLICK, L. & MOORHEAD, P. S. 1961. The serial cultivation of human diploid cell strains. *Exp Cell Res,* 25**,** 585-621.

HEATH, C. H., SORACE, A., KNOWLES, J., ROSENTHAL, E. & HOYT, K. 2012. Microbubble therapy enhances anti-tumor properties of cisplatin and cetuximab in vitro and in vivo. *Otolaryngol Head Neck Surg,* 146**,** 938-45.

HELTON, E. S. & CHEN, X. 2007. p53 modulation of the DNA damage response. *J Cell Biochem,* 100**,** 883-96.

HIRSCHHAEUSER, F., MENNE, H., DITTFELD, C., WEST, J., MUELLER-KLIESER, W. & KUNZ-SCHUGHART, L. A. 2010. Multicellular tumor spheroids: an underestimated tool is catching up again. *J Biotechnol,* 148**,** 3-15.

HOEBERS, F. J., KARTACHOVA, M., DE BOIS, J., VAN DEN BREKEL, M. W., VAN TINTEREN, H., VAN HERK, M., RASCH, C. R., VALDES OLMOS, R. A. & VERHEIJ, M. 2008. 99mTc Hynic-rh-Annexin V scintigraphy for in vivo imaging of apoptosis in patients with head and neck cancer treated with chemoradiotherapy. *Eur J Nucl Med Mol Imaging,* 35**,** 509-18.

HOFFMAN, R. M. 1991. Three-dimensional histoculture: origins and applications in cancer research. *Cancer Cells,* 3**,** 86-92.

HOFFMAN, W. H., BIADE, S., ZILFOU, J. T., CHEN, J. & MURPHY, M. 2002. Transcriptional repression of the anti-apoptotic survivin gene by wild type p53. *J Biol Chem,* 277**,** 3247-57.

HOGG, R. P., HONORIO, S., MARTINEZ, A., AGATHANGGELOU, A., DALLOL, A., FULLWOOD, P., WEICHSELBAUM, R., KUO, M. J., MAHER, E. R. & LATIF, F. 2002. Frequent 3p allele loss and epigenetic inactivation of the RASSF1A tumour suppressor gene from region 3p21.3 in head and neck squamous cell carcinoma. *Eur J Cancer,* 38**,** 1585-92.

HOLLSTEIN, M., SIDRANSKY, D., VOGELSTEIN, B. & HARRIS, C. C. 1991. p53 mutations in human cancers. *Science,* 253**,** 49-53.

HOMER J, R. G. 2012. Pharynx: oropharynx. *In:* WATKINSON JC, G. R. (ed.) *Stell and Maran's Textbook of Head and Neck Surgery and Oncology.* Fifth ed. London: Hodder Arnold.

HOOGSTEEN, I. J., MARRES, H. A., WIJFFELS, K. I., RIJKEN, P. F., PETERS, J. P., VAN DEN HOOGEN, F. J., OOSTERWIJK, E., VAN DER KOGEL, A. J. & KAANDERS, J. H. 2005. Colocalization of carbonic anhydrase 9 expression and cell proliferation in human head and neck squamous cell carcinoma. *Clin Cancer Res,* 11**,** 97-106.

HOU, Y. T., IJIMA, H., MATSUMOTO, S., KUBO, T., TAKEI, T., SAKAI, S. & KAWAKAMI, K. 2010. Effect of a hepatocyte growth factor/heparin-immobilized collagen system on albumin synthesis and spheroid formation by hepatocytes. *J Biosci Bioeng,* 110**,** 208-16.

HSIEH, T. M., NG, C. W., NARAYANAN, K., WAN, A. C. & YING, J. Y. 2010. Three-dimensional microstructured tissue scaffolds fabricated by two-photon laser scanning photolithography. *Biomaterials,* 31**,** 7648-52.
HUSSONG, J. W., POLVERINI, P. J. & SOLT, D. B. 1991. Resistant keratinocytes in 7,12-dimethylbenz[a]anthracene-initiated hamster buccal pouch epithelium. *Carcinogenesis,* 12**,** 617-22.
IANZINI, F., BERTOLDO, A., KOSMACEK, E. A., PHILLIPS, S. L. & MACKEY, M. A. 2006. Lack of p53 function promotes radiation-induced mitotic catastrophe in mouse embryonic fibroblast cells. *Cancer Cell Int,* 6**,** 11.
IGNEY, F. H. & KRAMMER, P. H. 2002. Death and anti-death: tumour resistance to apoptosis. *Nat Rev Cancer,* 2**,** 277-88.
INDOVINA, P., RAINALDI, G. & SANTINI, M. T. 2007. Three-dimensional cell organization leads to a different type of ionizing radiation-induced cell death: MG-63 monolayer cells undergo mitotic catastrophe while spheroids die of apoptosis. *Int J Oncol,* 31**,** 1473-83.
ISLES, M. G., MCCONKEY, C. & MEHANNA, H. M. 2008. A systematic review and meta-analysis of the role of positron emission tomography in the follow up of head and neck squamous cell carcinoma following radiotherapy or chemoradiotherapy. *Clin Otolaryngol,* 33**,** 210-22.
JALLEPALLI, P. V. & LENGAUER, C. 2001. Chromosome segregation and cancer: cutting through the mystery. *Nat Rev Cancer,* 1**,** 109-17.
JANMEY, P. A. & MCCULLOCH, C. A. 2007. Cell mechanics: integrating cell responses to mechanical stimuli. *Annu Rev Biomed Eng,* 9**,** 1-34.
JEMAL, A., BRAY, F., CENTER, M. M., FERLAY, J., WARD, E. & FORMAN, D. 2011. Global cancer statistics. *CA Cancer J Clin,* 61**,** 69-90.
JI, Y. B., TAE, K., AHN, T. H., LEE, S. H., KIM, K. R., PARK, C. W., PARK, B. L. & SHIN, H. D. 2011. ADH1B and ALDH2 polymorphisms and their associations with increased risk of squamous cell carcinoma of the head and neck in the Korean population. *Oral Oncol,* 47**,** 583-7.
JIANG, X. & WANG, X. 2000. Cytochrome c promotes caspase-9 activation by inducing nucleotide binding to Apaf-1. *J Biol Chem,* 275**,** 31199-203.
JIN, X., LI, Q., WU, Q., LI, P., MATSUMOTO, Y., FURUSAWA, Y., GONG, L., HAO, J. & DAI, Z. 2011. Radiosensitization by inhibiting survivin in human hepatoma HepG2 cells to high-LET radiation. *J Radiat Res,* 52**,** 335-41.
JIN, Z. & EL-DEIRY, W. S. 2005. Overview of cell death signaling pathways. *Cancer Biol Ther,* 4**,** 139-63.
JOHANSEN, L. V., GRAU, C. & OVERGAARD, J. 2002. Supraglottic carcinoma: patterns of failure and salvage treatment after curatively intended radiotherapy in 410 consecutive patients. *Int J Radiat Oncol Biol Phys,* 53**,** 948-58.
JOHN, D. W. & MILLER, L. L. 1968. Effect of whole x-irradiation of rats on net synthesis of albumin, fibrinogen, alpha-1-acid glycoprotein, and alpha-2-globulin (acute phase globulin) by the isolated, perfused rat liver. *J Biol Chem,* 243**,** 268-73.
JOHNSTON, N., YAN, J. C., HOEKZEMA, C. R., SAMUELS, T. L., STONER, G. D., BLUMIN, J. H. & BOCK, J. M. 2012. Pepsin promotes proliferation of laryngeal and pharyngeal epithelial cells. *Laryngoscope,* 122**,** 1317-25.
JONATHAN, E. C., BERNHARD, E. J. & MCKENNA, W. G. 1999. How does radiation kill cells? *Curr Opin Chem Biol,* 3**,** 77-83.
KAANDERS, J. H., WIJFFELS, K. I., MARRES, H. A., LJUNGKVIST, A. S., POP, L. A., VAN DEN HOOGEN, F. J., DE WILDE, P. C., BUSSINK, J., RALEIGH, J. A. &

VAN DER KOGEL, A. J. 2002. Pimonidazole binding and tumor vascularity predict for treatment outcome in head and neck cancer. *Cancer Res,* 62**,** 7066-74.
KALYANKRISHNA, S. & GRANDIS, J. R. 2006. Epidermal growth factor receptor biology in head and neck cancer. *J Clin Oncol,* 24**,** 2666-72.
KAMOTANI, Y., HUH, D., FUTAI, N. & TAKAYAMA, S. 2007. At the Interface: Advanced Microfluidic Assays for Study of Cell Function
BioMEMS and Biomedical Nanotechnology. *In:* FERRARI, M., DESAI, T. & BHATIA, S. (eds.). Springer US.
KARIN, M., YAMAMOTO, Y. & WANG, Q. M. 2004. The IKK NF-kappa B system: a treasure trove for drug development. *Nat Rev Drug Discov,* 3**,** 17-26.
KASTAN, M. 1997. On the TRAIL from p53 to apoptosis? *Nat Genet,* 17**,** 130-1.
KASTEN-PISULA U, M. A., BRAMMER I, BORGMANN K, MANSOUR WY, DEGENHARDT S, KRAUSE M, SCHREIBER A, DAHM-DAPHI J, PETERSEN C, DIKOMEY E, BAUMANN M. 2009. The extreme radiosensitivity of the squamous cell carcinoma SKX is due to a defect in double-strand break repair. *Radiother Oncol,* 90**,** 257-64.
KAWAMURA, K., FUJIKAWA-YAMAMOTO, K., OZAKI, M., IWABUCHI, K., NAKASHIMA, H., DOMIKI, C., MORITA, N., INOUE, M., TOKUNAGA, K., SHIBA, N., IKEDA, R. & SUZUKI, K. 2004. Centrosome hyperamplification and chromosomal damage after exposure to radiation. *Oncology,* 67**,** 460-470.
KAWAMURA, K., MORITA, N., DOMIKI, C., FUJIKAWA-YAMAMOTO, K., HASHIMOTO, M., IWABUCHI, K. & SUZUKI, K. 2006. Induction of centrosome amplification in p53 siRNA-treated human fibroblast cells by radiation exposure. *Cancer Sci,* 97**,** 252-8.
KEENAN, T. M. & FOLCH, A. 2008. Biomolecular gradients in cell culture systems. *Lab Chip,* 8**,** 34-57.
KELLOKUMPU-LEHTINEN, P., SODERSTROM, K.O., KORTEKANGAS, A., NORDMAN, E. 1990. Radiation-induced morphological changes and radiocurability in squamous cell carcinoma of the head and neck region. A preliminary report. . *Acta Oncol,* 29**,** 517-20.
KELLY, C., PALERI, V., DOWNS, C. & SHAH, R. 2007. Deterioration in quality of life and depressive symptoms during radiation therapy for head and neck cancer. *Otolaryngol Head Neck Surg,* 136**,** 108-11.
KETCHAM, A. S., WEXLER, H. & MANTEL, N. 1963. Effects of alcohol in mouse neoplasia. *Cancer Res,* 23**,** 667-70.
KHAN, Z., TIWARI, R. P., KHAN, N., PRASAD, G. B. & BISEN, P. S. 2012. Induction of apoptosis and sensitization of head and neck squamous carcinoma cells to cisplatin by targeting survivin gene expression. *Curr Gene Ther,* 12**,** 444-53.
KIM, L., TOH, Y. C., VOLDMAN, J. & YU, H. 2007. A practical guide to microfluidic perfusion culture of adherent mammalian cells. *Lab Chip,* 7**,** 681-94.
KIM, L., VAHEY, M. D., LEE, H. Y. & VOLDMAN, J. 2006. Microfluidic arrays for logarithmically perfused embryonic stem cell culture. *Lab Chip,* 6**,** 394-406.
KISIELEWSKI, A. E., XIAO, G. H., LIU, S. C., KLEIN-SZANTO, A. J., NOVARA, M., SINA, J., BLEICHER, K., YEUNG, R. S. & GOODROW, T. L. 1998. Analysis of the FHIT gene and its product in squamous cell carcinomas of the head and neck. *Oncogene,* 17**,** 83-91.
KLEIN, L. E., FREEZE, B. S., SMITH, A. B., 3RD & HORWITZ, S. B. 2005. The microtubule stabilizing agent discodermolide is a potent inducer of accelerated cell senescence. *Cell Cycle,* 4**,** 501-7.

KLEMENT, G., SCHEIRER, W. & KATINGER, H. W. 1987. Construction of a large scale membrane reactor system with different compartments for cells, medium and product. *Dev Biol Stand,* 66**,** 221-6.
KLINTENBERG, C., LUNDGREN, J., ADELL, G., TYTOR, M., NORBERG-SPAAK, L., EDELMAN, R. & CARSTENSEN, J. M. 1996. Primary radiotherapy of T1 and T2 glottic carcinoma--analysis of treatment results and prognostic factors in 223 patients. *Acta Oncol,* 35 Suppl 8**,** 81-6.
KOBAYASHI, T., RUAN, S., JABBUR, J. R., CONSOLI, U., CLODI, K., SHIKU, H., OWEN-SCHAUB, L. B., ANDREEFF, M., REED, J. C. & ZHANG, W. 1998. Differential p53 phosphorylation and activation of apoptosis-promoting genes Bax and Fas/APO-1 by irradiation and ara-C treatment. *Cell Death Differ,* 5**,** 584-91.
KOENIG S, K. P., SCHMIDT TK, RAVE-FRAENK M, ROTHE H, HERMANN RM, BECKER H, HESS CF, CHRISTIANSEN H 2008. Irradiation as preparitive regimen for hepatocyte transplantation causes prolonged cell cycle block. *Int J Radiat Biol,* 84**,** 285-98.
KOOPER, D. P., VAN DEN BROEK, P., MANNI, J. J., TIWARI, R. M. & SNOW, G. B. 1995. Partial vertical laryngectomy for recurrent glottic carcinoma. *Clin Otolaryngol Allied Sci,* 20**,** 167-70.
KOPF-MAIER, P. 1992. A new approach for realizing the "antioncogram". *Life Sci,* 50**,** 1711-8.
KOUMENIS, C. 2006. ER stress, hypoxia tolerance and tumor progression. *Curr Mol Med,* 6**,** 55-69.
KRAUSE, C. J., CAREY, T. E., OTT, R. W., HURBIS, C., MCCLATCHEY, K. D. & REGEZI, J. A. 1981. Human squamous cell carcinoma. Establishment and characterization of new permanent cell lines. *Arch Otolaryngol,* 107**,** 703-10.
KREIMER, A. R., CLIFFORD, G. M., BOYLE, P. & FRANCESCHI, S. 2005. Human papillomavirus types in head and neck squamous cell carcinomas worldwide: a systematic review. *Cancer Epidemiol Biomarkers Prev,* 14**,** 467-75.
KRISHNAMURTHY, S., DONG, Z., VODOPYANOV, D., IMAI, A., HELMAN, J. I., PRINCE, M. E., WICHA, M. S. & NOR, J. E. 2010. Endothelial cell-initiated signaling promotes the survival and self-renewal of cancer stem cells. *Cancer Res,* 70**,** 9969-78.
KROEMER, G., GALLUZZI, L., VANDENABEELE, P., ABRAMS, J., ALNEMRI, E. S., BAEHRECKE, E. H., BLAGOSKLONNY, M. V., EL-DEIRY, W. S., GOLSTEIN, P., GREEN, D. R., HENGARTNER, M., KNIGHT, R. A., KUMAR, S., LIPTON, S. A., MALORNI, W., NUNEZ, G., PETER, M. E., TSCHOPP, J., YUAN, J., PIACENTINI, M., ZHIVOTOVSKY, B. & MELINO, G. 2009. Classification of cell death: recommendations of the Nomenclature Committee on Cell Death 2009. *Cell Death Differ,* 16**,** 3-11.
KROSS, K. W., HEIMDAL, J. H., OLSNES, C., OLOFSSON, J. & AARSTAD, H. J. 2008. Co-culture of head and neck squamous cell carcinoma spheroids with autologous monocytes predicts prognosis. *Scand J Immunol,* 67**,** 392-9.
KRUEGER, S. A., JOINER, M. C., WEINFELD, M., PIASENTIN, E. & MARPLES, B. 2007. Role of apoptosis in low-dose hyper-radiosensitivity. *Radiat Res,* 167**,** 260-7.
KRUSE, P. F., JR., KEEN, L. N. & WHITTLE, W. L. 1970. Some distinctive characteristics of high density perfusion cultures of diverse cell types. *In Vitro,* 6**,** 75-88.
KUJATH, M., KERR, P., MYERS, C., BAMMEKE, F., LAMBERT, P., COOKE, A. & SUTHERLAND, D. 2011. Functional outcomes and laryngectomy-free survival after transoral CO laser microsurgery for stage 1 and 2 glottic carcinoma. *J Otolaryngol Head Neck Surg,* 40 Suppl 1**,** S49-58.

KUTCHAI, H. 1998. Gastrointestinal Secretions. *In:* BERNE RM, L. M. (ed.) *Physiology.* 4th ed. St. Louis: Mosby.

LA VECCHIA, C., NEGRI, E., D'AVANZO, B., FRANCESCHI, S., DECARLI, A. & BOYLE, P. 1990. Dietary indicators of laryngeal cancer risk. *Cancer Res,* 50**,** 4497-500.

LA VECCHIA, C., TAVANI, A., FRANCESCHI, S., LEVI, F., CORRAO, G. & NEGRI, E. 1997. Epidemiology and prevention of oral cancer. *Oral Oncol,* 33**,** 302-12.

LAHIRI S, H. C., AYESHA Q, KHAN AA, SRINIVAS VK, NAITHANI R. 1995. Effect of UV-B (302nm) irradiation on isolated rat hepatocytes. *Liver,* 15**,** 149-52.

LAKHANI SR, D. S., FINLAYSON CJ 2003. Cell Growth and its Disorders. *Basic Pathology: an Introduction to the Mechanisms of Disease.* London: Edward Arnold.

LAM, L., LOGAN, R. M., LUKE, C. & REES, G. L. 2007. Retrospective study of survival and treatment pattern in a cohort of patients with oral and oropharyngeal tongue cancers from 1987 to 2004. *Oral Oncol,* 43**,** 150-8.

LAVAF, A., GENDEN, E. M., CESARETTI, J. A., PACKER, S. & KAO, J. 2008. Adjuvant radiotherapy improves overall survival for patients with lymph node-positive head and neck squamous cell carcinoma. *Cancer,* 112**,** 535-43.

LE, Q. T., FU, K.K., KROLL, S., RYU, J.K., QUIVEY, J.M., MEYLER, T.S., KRIEG, R.M., PHILLIPS, T.L. 1997. Influence of fraction size, total dose, and overall time on local control of T1-T2 glottic carcinoma. *Int J Radiat Oncol Biol Phys,* 39**,** 115-26.

LEE, J., MOON, H., FOWLER, J., SCHOELLHAMMER, T. & KIM, C.-J. 2002. Electrowetting and electrowetting-on-dielectric for microscale liquid handling. *Sensors and Actuators A: Physical,* 95**,** 259-268.

LEE, J. H., KIM, S. Y., KIL, I. S. & PARK, J. W. 2007. Regulation of ionizing radiation-induced apoptosis by mitochondrial NADP+-dependent isocitrate dehydrogenase. *J Biol Chem,* 282**,** 13385-94.

LEE, J. H. & PAULL, T. T. 2004. Direct activation of the ATM protein kinase by the Mre11/Rad50/Nbs1 complex. *Science,* 304**,** 93-6.

LEE, S. A., NO, D. Y., KANG, E., JU, J., KIM, D. S. & LEE, S. H. 2013. Spheroid-based three-dimensional liver-on-a-chip to investigate hepatocyte-hepatic stellate cell interactions and flow effects. *Lab Chip*.

LEE, Y. C., MARRON, M., BENHAMOU, S., BOUCHARDY, C., AHRENS, W., POHLABELN, H., LAGIOU, P., TRICHOPOULOS, D., AGUDO, A., CASTELLSAGUE, X., BENCKO, V., HOLCATOVA, I., KJAERHEIM, K., MERLETTI, F., RICHIARDI, L., MACFARLANE, G. J., MACFARLANE, T. V., TALAMINI, R., BARZAN, L., CANOVA, C., SIMONATO, L., CONWAY, D. I., MCKINNEY, P. A., LOWRY, R. J., SNEDDON, L., ZNAOR, A., HEALY, C. M., MCCARTAN, B. E., BRENNAN, P. & HASHIBE, M. 2009. Active and involuntary tobacco smoking and upper aerodigestive tract cancer risks in a multicenter case-control study. *Cancer Epidemiol Biomarkers Prev,* 18**,** 3353-61.

LESLIE, P., MCHANWELL, S. 2008. Physiology of Swallowing *In:* GLEESON, M., BROWNING, G.G., BURTON, M.J., CLARKE, R., HIBBERT, J., JONES, N.S., LUND, V.J., LUXON, L.M., WATKINSON, J.C. (ed.) *Scott-Brown's Otorhinolaryngology, Head and Neck Surgery.* 7th ed. London: Hodder Arnold.

LEVI, F., PASCHE, C., LUCCHINI, F., BOSETTI, C. & LA VECCHIA, C. 2004. Processed meat and the risk of selected digestive tract and laryngeal neoplasms in Switzerland. *Ann Oncol,* 15**,** 346-9.

LEWIN, J. S., GILLENWATER, A. M., GARRETT, J. D., BISHOP-LEONE, J. K., NGUYEN, D. D., CALLENDER, D. L., AYERS, G. D. & MYERS, J. N. 2003.

Characterization of laryngopharyngeal reflux in patients with premalignant or early carcinomas of the larynx. *Cancer,* 97**,** 1010-4.
LI, D. W., SUN, Y. J., SUN, Z. F. & DONG, P. 2012. Involvement of focal adhesion kinase in cellular proliferation, apoptosis and prognosis of laryngeal squamous cell carcinoma. *J Laryngol Otol,* 126**,** 1127-33.
LI, P., NIJHAWAN, D., BUDIHARDJO, I., SRINIVASULA, S. M., AHMAD, M., ALNEMRI, E. S. & WANG, X. 1997. Cytochrome c and dATP-dependent formation of Apaf-1/caspase-9 complex initiates an apoptotic protease cascade. *Cell,* 91**,** 479-89.
LIAO, T., KAUFMANN, A. M., QIAN, X., SANGVATANAKUL, V., CHEN, C., KUBE, T., ZHANG, G. & ALBERS, A. E. 2013. Susceptibility to cytotoxic T cell lysis of cancer stem cells derived from cervical and head and neck tumor cell lines. *J Cancer Res Clin Oncol,* 139**,** 159-70.
LIEBERTZ, D. J., LECHNER, M. G., MASOOD, R., SINHA, U. K., HAN, J., PURI, R. K., CORREA, A. J. & EPSTEIN, A. L. 2010. Establishment and characterization of a novel head and neck squamous cell carcinoma cell line USC-HN1. *Head Neck Oncol,* 2**,** 5.
LIM, Y. C., KOO, B. S., LEE, J. S., LIM, J. Y. & CHOI, E. C. 2006. Distributions of cervical lymph node metastases in oropharyngeal carcinoma: therapeutic implications for the N0 neck. *Laryngoscope,* 116**,** 1148-52.
LIM, Y. C., OH, S. Y., CHA, Y. Y., KIM, S. H., JIN, X. & KIM, H. 2011. Cancer stem cell traits in squamospheres derived from primary head and neck squamous cell carcinomas. *Oral Oncol,* 47**,** 83-91.
LIN, C. J., GRANDIS, J. R., CAREY, T. E., GOLLIN, S. M., WHITESIDE, T. L., KOCH, W. M., FERRIS, R. L. & LAI, S. Y. 2007. Head and neck squamous cell carcinoma cell lines: established models and rationale for selection. *Head Neck,* 29**,** 163-88.
LIN, T. Y., CHANG, J. T., WANG, H. M., CHAN, S. H., CHIU, C. C., LIN, C. Y., FAN, K. H., LIAO, C. T., CHEN, I. H., LIU, T. Z., LI, H. F. & CHENG, A. J. 2010. Proteomics of the radioresistant phenotype in head-and-neck cancer: Gp96 as a novel prediction marker and sensitizing target for radiotherapy. *Int J Radiat Oncol Biol Phys,* 78**,** 246-56.
LIN, Y., MA, W. & BENCHIMOL, S. 2000. Pidd, a new death-domain-containing protein, is induced by p53 and promotes apoptosis. *Nat Genet,* 26**,** 122-7.
LINDAHL, T., SATOH, M. S., POIRIER, G. G. & KLUNGLAND, A. 1995. Post-translational modification of poly(ADP-ribose) polymerase induced by DNA strand breaks. *Trends Biochem Sci,* 20**,** 405-11.
LLEWELLYN, C. D., JOHNSON, N. W. & WARNAKULASURIYA, K. A. 2001. Risk factors for squamous cell carcinoma of the oral cavity in young people--a comprehensive literature review. *Oral Oncol,* 37**,** 401-18.
LONGLEY, D. B., HARKIN, D. P. & JOHNSTON, P. G. 2003. 5-fluorouracil: mechanisms of action and clinical strategies. *Nat Rev Cancer,* 3**,** 330-8.
LUO, X., BUDIHARDJO, I., ZOU, H., SLAUGHTER, C. & WANG, X. 1998. Bid, a Bcl2 interacting protein, mediates cytochrome c release from mitochondria in response to activation of cell surface death receptors. *Cell,* 94**,** 481-90.
LYSENG-WILLIAMSON, K. A. & FENTON, C. 2005. Docetaxel: a review of its use in metastatic breast cancer. *Drugs,* 65**,** 2513-31.
MAALOUF, M., ALPHONSE, G., COLLIAUX, A., BEUVE, M., TRAJKOVIC-BODENNEC, S., BATTISTON-MONTAGNE, P., TESTARD, I., CHAPET, O., BAJARD, M., TAUCHER-SCHOLZ, G., FOURNIER, C. & RODRIGUEZ-LAFRASSE, C. 2009. Different mechanisms of cell death in radiosensitive and

radioresistant p53 mutated head and neck squamous cell carcinoma cell lines exposed to carbon ions and x-rays. *Int J Radiat Oncol Biol Phys,* 74**,** 200-9.
MACHA, M. A., MATTA, A., CHAUHAN, S., SIU, K. M. & RALHAN, R. 2010. 14-3-3 zeta is a molecular target in guggulsterone induced apoptosis in head and neck cancer cells. *BMC Cancer,* 10**,** 655.
MACKENZIE K, M. M. 2012. Larynx. *In:* WATKINSON JC, G. R. (ed.) *Stell and Maran's Textbook of Head and Neck Surgery and Oncology.* Fifth ed. London: Hodder Arnold.
MACKINNON, P., MORRIS, J. 2005. *Head and Neck,* Oxford, Oxford University Press.
MACKLE, T. & O'DWYER, T. 2006. A comparative analysis of anterior versus posterior squamous cell carcinoma of the tongue: a 10-year review. *J Laryngol Otol,* 120**,** 393-6.
MAGNANI, C., FERRANTE, D., BARONE-ADESI, F., BERTOLOTTI, M., TODESCO, A., MIRABELLI, D. & TERRACINI, B. 2008. Cancer risk after cessation of asbestos exposure: a cohort study of Italian asbestos cement workers. *Occup Environ Med,* 65**,** 164-70.
MAIER, H., BORN, I. A., VEITH, S., ADLER, D. & SEITZ, H. K. 1986. The effect of chronic ethanol consumption on salivary gland morphology and function in the rat. *Alcohol Clin Exp Res,* 10**,** 425-7.
MAJOR, A. G., PITTY, L. P. & FARAH, C. S. 2013. Cancer stem cell markers in head and neck squamous cell carcinoma. *Stem Cells Int,* 2013**,** 319489.
MAO, L., FAN, Y. H., LOTAN, R. & HONG, W. K. 1996a. Frequent abnormalities of FHIT, a candidate tumor suppressor gene, in head and neck cancer cell lines. *Cancer Res,* 56**,** 5128-31.
MAO, L., LEE, J. S., FAN, Y. H., RO, J. Y., BATSAKIS, J. G., LIPPMAN, S., HITTELMAN, W. & HONG, W. K. 1996b. Frequent microsatellite alterations at chromosomes 9p21 and 3p14 in oral premalignant lesions and their value in cancer risk assessment. *Nat Med,* 2**,** 682-5.
MARCHAND, J. L., LUCE, D., LECLERC, A., GOLDBERG, P., ORLOWSKI, E., BUGEL, I. & BRUGERE, J. 2000. Laryngeal and hypopharyngeal cancer and occupational exposure to asbestos and man-made vitreous fibers: results of a case-control study. *Am J Ind Med,* 37**,** 581-9.
MARUKO, A., OHTAKE, Y., KAWAGUCHI, M., KOBAYASHI, T., BABA, T., KUWAHARA, Y., NAKAGAWA, H., SHIMURA, T., FUKUMOTO, M. & OHKUBO, Y. 2010. X-radiation-induced down-regulation of the EGF receptor in primary cultured rat hepatocytes. *Radiat Res,* 173**,** 620-8.
MARUR, S., D'SOUZA, G., WESTRA, W. H. & FORASTIERE, A. A. 2010. HPV-associated head and neck cancer: a virus-related cancer epidemic. *Lancet Oncol,* 11**,** 781-9.
MARUSHIMA, H., SHIBATA, S., ASAKURA, T., MATSUURA, T., MAEHASHI, H., ISHII, Y., EDA, H., AOKI, K., IIDA, Y., MORIKAWA, T. & OHKAWA, K. 2011. Three-dimensional culture promotes reconstitution of the tumor-specific hypoxic microenvironment under TGFbeta stimulation. *Int J Oncol,* 39**,** 1327-36.
MARUYA, S., ISSA, J. P., WEBER, R. S., ROSENTHAL, D. I., HAVILAND, J. C., LOTAN, R. & EL-NAGGAR, A. K. 2004. Differential methylation status of tumor-associated genes in head and neck squamous carcinoma: incidence and potential implications. *Clin Cancer Res,* 10**,** 3825-30.
MASUNAGA, S., ONO, K., TAKAHASHI, A., OHNISHI, T., KINASHI, Y. & TAKAGAKI, M. 2002. Radiobiological characteristics of solid tumours depending on the p53 status of the tumour cells, with emphasis on the response of intratumour quiescent cells. *Eur J Cancer,* 38**,** 718-27.

MCCORD, A. M., JAMAL, M., WILLIAMS, E. S., CAMPHAUSEN, K. & TOFILON, P. J. 2009. CD133+ glioblastoma stem-like cells are radiosensitive with a defective DNA damage response compared with established cell lines. *Clin Cancer Res,* 15**,** 5145-53.

MCCREEDY, T. 2001. Rapid prototyping of glass and PDMS microstructures for micro total analytical systems and micro chemical reactors by microfabrication in the general laboratory. *Anal. Chim. Acta,* 427**,** 39-43.

MCKENNA, W. G., WEISS, M. C., BAKANAUSKAS, V. J., SANDLER, H., KELSTEN, M. L., BIAGLOW, J., TUTTLE, S. W., ENDLICH, B., LING, C. C. & MUSCHEL, R. J. 1990a. The role of the H-ras oncogene in radiation resistance and metastasis. *Int J Radiat Oncol Biol Phys,* 18**,** 849-59.

MCKENNA, W. G., WEISS, M. C., ENDLICH, B., LING, C. C., BAKANAUSKAS, V. J., KELSTEN, M. L. & MUSCHEL, R. J. 1990b. Synergistic effect of the v-myc oncogene with H-ras on radioresistance. *Cancer Res,* 50**,** 97-102.

MCLAUGHLIN, J. K., GRIDLEY, G., BLOCK, G., WINN, D. M., PRESTON-MARTIN, S., SCHOENBERG, J. B., GREENBERG, R. S., STEMHAGEN, A., AUSTIN, D. F., ERSHOW, A. G. & ET AL. 1988. Dietary factors in oral and pharyngeal cancer. *J Natl Cancer Inst,* 80**,** 1237-43.

MCLAUGHLIN, M. P., PARSONS, J. T., FEIN, D. A., STRINGER, S. P., CASSISI, N. J., MENDENHALL, W. M. & MILLION, R. R. 1996. Salvage surgery after radiotherapy failure in T1-T2 squamous cell carcinoma of the glottic larynx. *Head Neck,* 18**,** 229-35.

MCMILLAN, T. J. 2002. Molecular Radiobiology. *In:* PRICE, P., SIKORA, K. (ed.) *Treatment of Cancer.* London: Hodder Arnold.

MELLIN, H., FRIESLAND, S., LEWENSOHN, R., DALIANIS, T. & MUNCK-WIKLAND, E. 2000. Human papillomavirus (HPV) DNA in tonsillar cancer: clinical correlates, risk of relapse, and survival. *Int J Cancer,* 89**,** 300-4.

MENDELSOHN, J. & BASELGA, J. 2003. Status of epidermal growth factor receptor antagonists in the biology and treatment of cancer. *J Clin Oncol,* 21**,** 2787-99.

MENDENHALL, W. M. 2004. Mandibular osteoradionecrosis. *J Clin Oncol,* 22**,** 4867-8.

MENDENHALL, W. M., AMDUR, R. J., STRINGER, S. P., VILLARET, D. B. & CASSISI, N. J. 2000. Radiation therapy for squamous cell carcinoma of the tonsillar region: a preferred alternative to surgery? *J Clin Oncol,* 18**,** 2219-25.

MENDENHALL, W. M., HINERMAN, R. W., AMDUR, R. J., MALYAPA, R. S., LANSFORD, C. D., WERNING, J. W. & VILLARET, D. B. 2006. Postoperative radiotherapy for squamous cell carcinoma of the head and neck. *Clin Med Res,* 4**,** 200-8.

MERCEY E, O. P., GLAISE D, CALVO-MUNOZ ML, GUGUEN-GUILLOUZO C, FOUQUE B 2010. The application of 3D micropatterning of agarose substrate for cell culture and in situ comet assays. *Biomaterials,* 31**,** 3156-65.

MEREDITH, S. D., LEVINE, P. A., BURNS, J. A., GAFFEY, M. J., BOYD, J. C., WEISS, L. M., ERICKSON, N. L. & WILLIAMS, M. E. 1995. Chromosome 11q13 amplification in head and neck squamous cell carcinoma. Association with poor prognosis. *Arch Otolaryngol Head Neck Surg,* 121**,** 790-4.

MEYVANTSSON, I. & BEEBE, D. J. 2008. Cell culture models in microfluidic systems. *Annu Rev Anal Chem (Palo Alto Calif),* 1**,** 423-49.

MICHALIDES, R., VAN VEELEN, N., HART, A., LOFTUS, B., WIENTJENS, E. & BALM, A. 1995. Overexpression of cyclin D1 correlates with recurrence in a group of forty-seven operable squamous cell carcinomas of the head and neck. *Cancer Res,* 55**,** 975-8.

MIRZAIE-JONIANI, H., ERIKSSON, D., SHEIKHOLVAEZIN, A., JOHANSSON, A., LOFROTH, P. O., JOHANSSON, L. & STIGBRAND, T. 2002. Apoptosis induced by low-dose and low-dose-rate radiation. *Cancer,* 94**,** 1210-4.
MIYASHITA, T., HARIGAI, M., HANADA, M. & REED, J. C. 1994. Identification of a p53-dependent negative response element in the bcl-2 gene. *Cancer Res,* 54**,** 3131-5.
MONROE, M. M., ANDERSON, E. C., CLAYBURGH, D. R. & WONG, M. H. 2011. Cancer stem cells in head and neck squamous cell carcinoma. *J Oncol,* 2011**,** 762780.
MOORTHY, R., WARFIELD, A.T. 2012. Head and Neck Pathology. *In:* WATKINSON, J. C., GILBERT, R.W. (ed.) *Stell and Maran's Textbook of Head and Neck Surgery and Oncology.* 5th ed. London: Hodder Arnold.
MOROCO, J. R., SOLT, D. B. & POLVERINI, P. J. 1990. Sequential loss of suppressor genes for three specific functions during in vivo carcinogenesis. *Lab Invest,* 63**,** 298-306.
MROZ, E. A., TWARD, A. D., PICKERING, C. R., MYERS, J. N., FERRIS, R. L. & ROCCO, J. W. 2013. High intratumor genetic heterogeneity is related to worse outcome in patients with head and neck squamous cell carcinoma. *Cancer,* 119**,** 3034-42.
MUELLER-KLIESER, W. 1987. Multicellular spheroids. A review on cellular aggregates in cancer research. *J Cancer Res Clin Oncol,* 113**,** 101-22.
MUNRO AJ, S. N. 2008. Head and Neck Cancer. *In:* PRICE P, S. K., ILLIDGE T (ed.) *Treatment of Cancer.* 5th ed. London Hodder Arnold.
NAKAJIMA, T. & YUKAWA, O. 1996. Radiation-induced translocation of protein kinase C through membrane lipid peroxidation in primary cultured rat hepatocytes. *Int J Radiat Biol,* 70**,** 473-80.
NAKANISHI, J., TAKARADA, T., YAMAGUCHI, K. & MAEDA, M. 2008. Recent advances in cell micropatterning techniques for bioanalytical and biomedical sciences. *Anal Sci,* 24**,** 67-72.
NAUDO, P., LACCOURREYE, O., WEINSTEIN, G., JOUFFRE, V., LACCOURREYE, H. & BRASNU, D. 1998. Complications and functional outcome after supracricoid partial laryngectomy with cricohyoidoepiglottopexy. *Otolaryngol Head Neck Surg,* 118**,** 124-9.
NAWROZ, H., VAN DER RIET, P., HRUBAN, R. H., KOCH, W., RUPPERT, J. M. & SIDRANSKY, D. 1994. Allelotype of head and neck squamous cell carcinoma. *Cancer Res,* 54**,** 1152-5.
NEVILL, J. T., COOPER, R., DUECK, M., BRESLAUER, D. N. & LEE, L. P. 2007. Integrated microfluidic cell culture and lysis on a chip. *Lab Chip,* 7**,** 1689-95.
NG, S., WU, Y. N., ZHOU, Y., TOH, Y. E., HO, Z. Z., CHIA, S. M., ZHU, J. H., MAO, H. Q. & YU, H. 2005. Optimization of 3-D hepatocyte culture by controlling the physical and chemical properties of the extra-cellular matrices. *Biomaterials,* 26**,** 3153-63.
NGUYEN, N. P., VOS, P., SMITH, H. J., NGUYEN, P. D., ALFIERI, A., KARLSSON, U., DUTTA, S., LEMANSKI, C., NGUYEN, L. M. & SALLAH, S. 2007. Concurrent chemoradiation for locally advanced oropharyngeal cancer. *Am J Otolaryngol,* 28**,** 3-8.
NIKITAKIS, N. G., SAUK, J.J., PAPANICOLAOU, S.I. 2004. The role of apoptosis in oral diseases: mechanisms; aberrations in neoplastic, autoimmune; infectious; haematologic and developmental diseases; and therapeutic options. *Oral Surgery, Oral Medicine, Oral Pathology, Oral Radiology and Endodontics,* 97**,** 476-490.
NIX, P., CAWKWELL, L., PATMORE, H., GREENMAN, J. & STAFFORD, N. 2005. Bcl-2 expression predicts radiotherapy failure in laryngeal cancer. *Br J Cancer,* 92**,** 2185-9.
NORDSMARK, M., BENTZEN, S. M., RUDAT, V., BRIZEL, D., LARTIGAU, E., STADLER, P., BECKER, A., ADAM, M., MOLLS, M., DUNST, J., TERRIS, D. J.

& OVERGAARD, J. 2005. Prognostic value of tumor oxygenation in 397 head and neck tumors after primary radiation therapy. An international multi-center study. *Radiother Oncol,* 77**,** 18-24.
NOVAKOVA, Z., HUBACKOVA, S., KOSAR, M., JANDEROVA-ROSSMEISLOVA, L., DOBROVOLNA, J., VASICOVA, P., VANCUROVA, M., HOREJSI, Z., HOZAK, P., BARTEK, J. & HODNY, Z. 2010. Cytokine expression and signaling in drug-induced cellular senescence. *Oncogene,* 29**,** 273-84.
NURGALIEVA, Z. Z., GRAHAM, D. Y., DAHLSTROM, K. R., WEI, Q. & STURGIS, E. M. 2005. A pilot study of Helicobacter pylori infection and risk of laryngopharyngeal cancer. *Head Neck,* 27**,** 22-7.
OHNISHI, K., OTA, I., TAKAHASHI, A., YANE, K., MATSUMOTO, H. & OHNISHI, T. 2002. Transfection of mutant p53 gene depresses X-ray- or CDDP-induced apoptosis in a human squamous cell carcinoma of the head and neck. *Apoptosis,* 7**,** 367-72.
OHNO, T., NAKANO, T., NIIBE, Y., TSUJII, H. & OKA, K. 1998. Bax protein expression correlates with radiation-induced apoptosis in radiation therapy for cervical carcinoma. *Cancer,* 83**,** 103-10.
OKAMOTO, A., CHIKAMATSU, K., SAKAKURA, K., HATSUSHIKA, K., TAKAHASHI, G. & MASUYAMA, K. 2009. Expansion and characterization of cancer stem-like cells in squamous cell carcinoma of the head and neck. *Oral Oncol,* 45**,** 633-9.
OVERGAARD, J., HANSEN, H. S., JORGENSEN, K. & HJELM HANSEN, M. 1986. Primary radiotherapy of larynx and pharynx carcinoma--an analysis of some factors influencing local control and survival. *Int J Radiat Oncol Biol Phys,* 12**,** 515-21.
OZLUGEDIK, S., YORULMAZ, I. & GOKCAN, K. 2006. Is laryngopharyngeal reflux an important risk factor in the development of laryngeal carcinoma? *Eur Arch Otorhinolaryngol,* 263**,** 339-43.
OZTURK, B., COSKUN, U., SANCAK, B., YAMAN, E., BUYUKBERBER, S. & BENEKLI, M. 2009. Elevated serum levels of M30 and M65 in patients with locally advanced head and neck tumors. *Int Immunopharmacol,* 9**,** 645-8.
PAGUIRIGAN, A. L. & BEEBE, D. J. 2009. From the cellular perspective: exploring differences in the cellular baseline in macroscale and microfluidic cultures. *Integr Biol (Camb),* 1**,** 182-95.
PALERI, V., THOMAS, L., BASAVAIAH, N., DRINNAN, M., MEHANNA, H. & JONES, T. 2011. Oncologic outcomes of open conservation laryngectomy for radiorecurrent laryngeal carcinoma: a systematic review and meta-analysis of English-language literature. *Cancer,* 117**,** 2668-76.
PALERI V, W. J. 2012. Metastatic Neck Disease. *In:* WATKINSON JC, G. R. (ed.) *Stell and Maran's Textbook of Head and Neck Surgery and Oncology.* 5th ed. London: Hodder & Stoughton.
PAMEIIJER, F. A., BALM, A.J., HILGERS, F.J. 1997. Variability of tumour volumes in T3-staged head and neck tumours. . *Head Neck,* 19**,** 6-13.
PARK, J. J., CHANG, H. W., JEONG, E. J., ROH, J. L., CHOI, S. H., JEON, S. Y., KO, G. H. & KIM, S. Y. 2009. Peroxiredoxin IV protects cells from radiation-induced apoptosis in head-and-neck squamous cell carcinoma. *Int J Radiat Oncol Biol Phys,* 73**,** 1196-202.
PARKIN, D. M. 2011. 11. Cancers attributable to infection in the UK in 2010. *Br J Cancer,* 105 Suppl 2**,** S49-56.
PARKIN, D. M., BRAY, F., FERLAY, J. & PISANI, P. 2001. Estimating the world cancer burden: Globocan 2000. *Int J Cancer,* 94**,** 153-6.
PARSONS, J. T., MENDENHALL, W. M., STRINGER, S. P., AMDUR, R. J., HINERMAN, R. W., VILLARET, D. B., MOORE-HIGGS, G. J., GREENE, B. D., SPEER, T. W.,

CASSISI, N. J. & MILLION, R. R. 2002. Squamous cell carcinoma of the oropharynx: surgery, radiation therapy, or both. *Cancer,* 94**,** 2967-80.
PATEL, V., MARTIN, D., MALHOTRA, R., MARSH, C. A., DOCI, C. L., VEENSTRA, T. D., NATHAN, C. A., SINHA, U. K., SINGH, B., MOLINOLO, A. A., RUSLING, J. F. & GUTKIND, J. S. 2013. DSG3 as a biomarker for the ultrasensitive detection of occult lymph node metastasis in oral cancer using nanostructured immunoarrays. *Oral Oncol,* 49**,** 93-101.
PEDRERO, J. M., CARRACEDO, D. G., PINTO, C. M., ZAPATERO, A. H., RODRIGO, J. P., NIETO, C. S. & GONZALEZ, M. V. 2005. Frequent genetic and biochemical alterations of the PI 3-K/AKT/PTEN pathway in head and neck squamous cell carcinoma. *Int J Cancer,* 114**,** 242-8.
PEREZ-ORDONEZ, B., BEAUCHEMIN, M. & JORDAN, R. C. 2006. Molecular biology of squamous cell carcinoma of the head and neck. *J Clin Pathol,* 59**,** 445-53.
PICKHARD, A. C., MARGRAF, J., KNOPF, A., STARK, T., PIONTEK, G., BECK, C., BOULESTEIX, A. L., SCHERER, E. Q., PIGORSCH, S., SCHLEGEL, J., ARNOLD, W. & REITER, R. 2011. Inhibition of radiation induced migration of human head and neck squamous cell carcinoma cells by blocking of EGF receptor pathways. *BMC Cancer,* 11**,** 388.
PIGNON, J. P., LE MAITRE, A., MAILLARD, E. & BOURHIS, J. 2009. Meta-analysis of chemotherapy in head and neck cancer (MACH-NC): an update on 93 randomised trials and 17,346 patients. *Radiother Oncol,* 92**,** 4-14.
PODGORSAK, E. B. 2005. Treatment Machines for External Beam Radiotherapy. *In:* E.B., P. (ed.) *Radiation Oncology Physics: A Handbook for Teachers and Students.* Austria: IAEA.
POLLACK, M. G., FAIR, R. B. & SHENDEROV, A. D. 2000. Electrowetting-based actuation of liquid droplets for microfluidic applications. *Applied Physics Letters,* 77**,** 1725-1726.
POLVERINI, P. J., SHIMIZU, K. & SOLT, D. B. 1988. Control of angiogenic activity in carcinogen-initiated and neoplastic hamster pouch keratinocytes and their hybrid cells. *J Oral Pathol,* 17**,** 522-7.
POLVERINI, P. J. & SOLT, D. B. 1986. Effect of in vivo carcinogen exposure on colony formation and growth of hamster buccal pouch keratinocytes in culture. *Lab Invest,* 54**,** 432-41.
POLVERINI, P. J. & SOLT, D. B. 1988. Expression of the angiogenic phenotype by a subpopulation of keratinocytes derived from 7,12-dimethylbenz[a]anthracene-initiated hamster buccal pouch epithelium. *Carcinogenesis,* 9**,** 117-22.
PORCEDDU, S. V., JARMOLOWSKI, E., HICKS, R. J., WARE, R., WEIH, L., RISCHIN, D., CORRY, J. & PETERS, L. J. 2005. Utility of positron emission tomography for the detection of disease in residual neck nodes after (chemo)radiotherapy in head and neck cancer. *Head Neck,* 27**,** 175-81.
POSCHL, G. & SEITZ, H. K. 2004. Alcohol and cancer. *Alcohol Alcohol,* 39**,** 155-65.
POSNER, M. R., HERSHOCK, D. M., BLAJMAN, C. R., MICKIEWICZ, E., WINQUIST, E., GORBOUNOVA, V., TJULANDIN, S., SHIN, D. M., CULLEN, K., ERVIN, T. J., MURPHY, B. A., RAEZ, L. E., COHEN, R. B., SPAULDING, M., TISHLER, R. B., ROTH, B., VIROGLIO RDEL, C., VENKATESAN, V., ROMANOV, I., AGARWALA, S., HARTER, K. W., DUGAN, M., CMELAK, A., MARKOE, A. M., READ, P. W., STEINBRENNER, L., COLEVAS, A. D., NORRIS, C. M., JR. & HADDAD, R. I. 2007. Cisplatin and fluorouracil alone or with docetaxel in head and neck cancer. *N Engl J Med,* 357**,** 1705-15.

PRINCE, M. E., SIVANANDAN, R., KACZOROWSKI, A., WOLF, G. T., KAPLAN, M. J., DALERBA, P., WEISSMAN, I. L., CLARKE, M. F. & AILLES, L. E. 2007. Identification of a subpopulation of cells with cancer stem cell properties in head and neck squamous cell carcinoma. *Proc Natl Acad Sci U S A,* 104**,** 973-8.

PRINCE, M. E. P., AILLES, L.E. 2008. Cancer Stem cells in head and neck squamous cell cancer. *J Clin Oncol,* 26**,** 2871-5.

PULEO, C. M., YEH, H. C. & WANG, T. H. 2007. Applications of MEMS technologies in tissue engineering. *Tissue Eng,* 13**,** 2839-54.

QADEER, M. A., COLABIANCHI, N. & VAEZI, M. F. 2005. Is GERD a risk factor for laryngeal cancer? *Laryngoscope,* 115**,** 486-91.

R&D. 2013. *Quantikine ELISA Assay Principle* [Online]. Available: wwwrndsystems.com//product_detail_objectname_quantikineelisaassayprinciple.aspx 2013].

RADFORD, I. R., MURPHY, T. K., RADLEY, J. M. & ELLIS, S. L. 1994. Radiation response of mouse lymphoid and myeloid cell lines. Part II. Apoptotic death is shown by all lines examined. *Int J Radiat Biol,* 65**,** 217-27.

RAGIN, C. C. & TAIOLI, E. 2007. Survival of squamous cell carcinoma of the head and neck in relation to human papillomavirus infection: review and meta-analysis. *Int J Cancer,* 121**,** 1813-20.

RAO, S. K. & RAO, P. S. 2010. Alteration in the radiosensitivity of HeLa cells by dichloromethane extract of guduchi (Tinospora cordifolia). *Integr Cancer Ther,* 9**,** 378-84.

RASAMNY, J. J., ALLAK, A., KROOK, K. A., JO, V. Y., POLICARPIO-NICOLAS, M. L., SUMNER, H. M., MOSKALUK, C. A., FRIERSON, H. F., JR. & JAMESON, M. J. 2012. Cyclin D1 and FADD as biomarkers in head and neck squamous cell carcinoma. *Otolaryngol Head Neck Surg,* 146**,** 923-31.

RASHEED, Z. A., KOWALSKI, J., SMITH, B. D. & MATSUI, W. 2011. Concise review: Emerging concepts in clinical targeting of cancer stem cells. *Stem Cells,* 29**,** 883-7.

REDDY, A. C. & LOKESH, B. R. 1996. Effect of curcumin and eugenol on iron-induced hepatic toxicity in rats. *Toxicology,* 107**,** 39-45.

REGEHR, K. J., DOMENECH, M., KOEPSEL, J. T., CARVER, K. C., ELLISON-ZELSKI, S. J., MURPHY, W. L., SCHULER, L. A., ALARID, E. T. & BEEBE, D. J. 2009. Biological implications of polydimethylsiloxane-based microfluidic cell culture. *Lab Chip,* 9**,** 2132-9.

RHEINWALD, J. G. & BECKETT, M. A. 1981. Tumorigenic keratinocyte lines requiring anchorage and fibroblast support cultures from human squamous cell carcinomas. *Cancer Res,* 41**,** 1657-63.

RIBEIRO, G. F., CORTE-REAL, M. & JOHANSSON, B. 2006. Characterization of DNA damage in yeast apoptosis induced by hydrogen peroxide, acetic acid, and hyperosmotic shock. *Mol Biol Cell,* 17**,** 4584-91.

RICH, J. T., MILOV, S., LEWIS, J. S., JR., THORSTAD, W. L., ADKINS, D. R. & HAUGHEY, B. H. 2009. Transoral laser microsurgery (TLM) +/- adjuvant therapy for advanced stage oropharyngeal cancer: outcomes and prognostic factors. *Laryngoscope,* 119**,** 1709-19.

RICHARDSON, O. W. & COMPTON, K. T. 1912. The Photoelectric Effect. *Science,* 35**,** 783-4.

RIEDER, C. L. & MAIATO, H. 2004. Stuck in division or passing through: what happens when cells cannot satisfy the spindle assembly checkpoint. *Dev Cell,* 7**,** 637-51.

RIEDL, S. J. & SHI, Y. 2004. Molecular mechanisms of caspase regulation during apoptosis. *Nat Rev Mol Cell Biol,* 5**,** 897-907.

RIESTERER, O., YANG, Q., RAJU, U., TORRES, M., MOLKENTINE, D., PATEL, N., VALDECANAS, D., MILAS, L. & ANG, K. K. 2011. Combination of anti-IGF-1R antibody A12 and ionizing radiation in upper respiratory tract cancers. *Int J Radiat Oncol Biol Phys,* 79**,** 1179-87.

ROBBINS, K. T., CONNORS, K. M., STORNIOLO, A. M., HANCHETT, C. & HOFFMAN, R. M. 1994. Sponge-gel-supported histoculture drug-response assay for head and neck cancer. Correlations with clinical response to cisplatin. *Arch Otolaryngol Head Neck Surg,* 120**,** 288-92.

ROBBINS, K. T., VARKI, N. M., STORNIOLO, A. M., HOFFMAN, H. & HOFFMAN, R. M. 1991. Drug response of head and neck tumors in native-state histoculture. *Arch Otolaryngol Head Neck Surg,* 117**,** 83-6.

ROBERG, K., JONSSON, A. C., GRENMAN, R. & NORBERG-SPAAK, L. 2007. Radiotherapy response in oral squamous carcinoma cell lines: evaluation of apoptotic proteins as prognostic factors. *Head Neck,* 29**,** 325-34.

RODIER, F., COPPE, J. P., PATIL, C. K., HOEIJMAKERS, W. A., MUNOZ, D. P., RAZA, S. R., FREUND, A., CAMPEAU, E., DAVALOS, A. R. & CAMPISI, J. 2009. Persistent DNA damage signalling triggers senescence-associated inflammatory cytokine secretion. *Nat Cell Biol,* 11**,** 973-9.

RODRIGUEZ, J. & LAZEBNIK, Y. 1999. Caspase-9 and APAF-1 form an active holoenzyme. *Genes Dev,* 13**,** 3179-84.

RODWELL, V. W. 1993. Enzymes: General Properties. *In:* MURRAY, R. K., MAYES. P.A., RODWELL, V.W. (ed.) *Harper's Biochemistry.* London: Appleton & LAnge.

RONINSON, I. B., BROUDE, E. V. & CHANG, B. D. 2001. If not apoptosis, then what? Treatment-induced senescence and mitotic catastrophe in tumor cells. *Drug Resist Updat,* 4**,** 303-13.

ROSSOUW, C. L., CHETTY, A., MOOLMAN, F. S., BIRKHOLTZ, L. M., HOPPE, H. & MANCAMA, D. T. 2012. Thermo-responsive non-woven scaffolds for "smart" 3D cell culture. *Biotechnol Bioeng,* 109**,** 2147-58.

ROWELL, N. 2012. Principles of Radiotherapy. *In:* WATKINSON, J. C., GILBERT, R.W. (ed.) *Stell and Maran's Textbook of Head and Neck Surgery and Oncology.* London: Hodder Arnold.

ROWLEY, H., JONES, A., SPANDIDOS, D. & FIELD, J. 1996. Definition of a tumor suppressor gene locus on the short arm of chromosome 3 in squamous cell carcinoma of the head and neck by means of microsatellite markers. *Arch Otolaryngol Head Neck Surg,* 122**,** 497-501.

RUBAJ, B. 1975. Pathomorphological and histochemical changes in the liver of rabbits following fractional irradiation with Co-60. *Pol Arch Weter,* 18**,** 107-15.

RUDAT, V., DIETZ, A., SCHRAMM, O., CONRADT, C., MAIER, H., FLENTJE, M. & WANNENMACHER, M. 1999. Prognostic impact of total tumor volume and hemoglobin concentration on the outcome of patients with advanced head and neck cancer after concomitant boost radiochemotherapy. *Radiother Oncol,* 53**,** 119-25.

RUPNIAK, H. T. & HILL, B. T. 1980. The poor cloning ability in agar of human tumour cells from biopsies of primary tumours. *Cell Biol Int Rep,* 4**,** 479-86.

RUTH, A. C. & RONINSON, I. B. 2000. Effects of the multidrug transporter P-glycoprotein on cellular responses to ionizing radiation. *Cancer Res,* 60**,** 2576-8.

SACKS, P. G. 1996. Cell, tissue and organ culture as in vitro models to study the biology of squamous cell carcinomas of the head and neck. *Cancer Metastasis Rev,* 15**,** 27-51.

SAKAHARA, H., ONO, K., SAGA, T., AKUTA, K., ENDO, K., KONISHI, J. & ABE, M. 1992. Hepatocyte response to continuous low dose-rate radiation in radioimmunotherapy assessed by micronucleus assay. *Int J Radiat Biol,* 62**,** 443-8.

SALASPURO, M. P. 2003. Acetaldehyde, microbes, and cancer of the digestive tract. *Crit Rev Clin Lab Sci,* 40**,** 183-208.
SANDULACHE, V. C., SKINNER, H. D., OW, T. J., ZHANG, A., XIA, X., LUCHAK, J. M., WONG, L. J., PICKERING, C. R., ZHOU, G. & MYERS, J. N. 2012. Individualizing antimetabolic treatment strategies for head and neck squamous cell carcinoma based on TP53 mutational status. *Cancer,* 118**,** 711-21.
SANTINI, M. T., RAINALDI, G. & INDOVINA, P. L. 1999. Multicellular tumour spheroids in radiation biology. *Int J Radiat Biol,* 75**,** 787-99.
SAPKOTA, A., GAJALAKSHMI, V., JETLY, D. H., ROYCHOWDHURY, S., DIKSHIT, R. P., BRENNAN, P., HASHIBE, M. & BOFFETTA, P. 2008. Indoor air pollution from solid fuels and risk of hypopharyngeal/laryngeal and lung cancers: a multicentric case-control study from India. *Int J Epidemiol,* 37**,** 321-8.
SATO, K., HIBARA, A., TOKESHI, M., HISAMOTO, H. & KITAMORI, T. 2003. Integration of chemical and biochemical analysis systems into a glass microchip. *Anal Sci,* 19**,** 15-22.
SATO, N., MIZUMOTO, K., NAKAMURA, M. & TANAKA, M. 2000. Radiation-induced centrosome overduplication and multiple mitotic spindles in human tumor cells. *Exp Cell Res,* 255**,** 321-6.
SAYED, S. I., DWIVEDI, R. C., KATNA, R., GARG, A., PATHAK, K. A., NUTTING, C. M., RHYS-EVANS, P., HARRINGTON, K. J. & KAZI, R. 2011. Implications of understanding cancer stem cell (CSC) biology in head and neck squamous cell cancer. *Oral Oncol,* 47**,** 237-43.
SCAFFIDI, C., FULDA, S., SRINIVASAN, A., FRIESEN, C., LI, F., TOMASELLI, K. J., DEBATIN, K. M., KRAMMER, P. H. & PETER, M. E. 1998. Two CD95 (APO-1/Fas) signaling pathways. *EMBO J,* 17**,** 1675-87.
SCHLEIMER, K., STIPPEL, D. L., KASPER, H. U., ALLWISSNER, R., YAVUZYASAR, S., HOLSCHER, A. H. & BECKURTS, K. T. 2008. Competition between native liver and graft in auxiliary liver transplantation in a rat model. *Transplant Proc,* 40**,** 967-70.
SCHODER, H., FURY, M., LEE, N., KRAUS, D. 2009. PET monitoring of therapy response in head and neck squamous cell carcinoma. *J Nucl Med,* 50**,** 74S-88S.
SCHWACHOFER, J. H., ACKER, H., CROOIJMANS, R. P., VAN GASTEREN, J. J., HOLTERMANN, G., HOOGENHOUT, J., JERUSALEM, C. R. & KAL, H. B. 1991a. Oxygen tensions in two human tumor cell lines grown and irradiated as multicellular spheroids. *Anticancer Res,* 11**,** 273-9.
SCHWACHOFER, J. H., CROOIJMANS, R. P., HOOGENHOUT, H., KAL, H. B., SCHAAPVELD, R. Q. & WESSELS, J. 1991b. Differences in repair of radiation induced damage in two human tumor cell lines as measured by cell survival and alkaline DNA unwinding. *Strahlenther Onkol,* 167**,** 35-40.
SCHWACHOFER, J. H., CROOIJMANS, R. P., HOOGENHOUT, J. & KAL, H. B. 1991c. The influence of once or twice daily irradiation regimens on growth of squamous cell carcinoma spheroids of different diameters. *Anticancer Res,* 11**,** 1369-72.
SEITZ, H. K., MATSUZAKI, S., YOKOYAMA, A., HOMANN, N., VAKEVAINEN, S. & WANG, X. D. 2001. Alcohol and cancer. *Alcohol Clin Exp Res,* 25**,** 137S-143S.
SEIWERT, T. Y., SALAMA, J. K. & VOKES, E. E. 2007. The chemoradiation paradigm in head and neck cancer. *Nat Clin Pract Oncol,* 4**,** 156-71.
SEMENZA, G. L. 2003. Targeting HIF-1 for cancer therapy. *Nat Rev Cancer,* 3**,** 721-32.
SEWALL, G. K., PALAZZI-CHURAS, K. L., RICHARDS, G. M., HARTIG, G. K. & HARARI, P. M. 2007. Planned postradiotherapy neck dissection: Rationale and clinical outcomes. *Laryngoscope,* 117**,** 121-8.

SHAH, J. P. 1990. Patterns of cervical lymph node metastasis from squamous carcinomas of the upper aerodigestive tract. *Am J Surg,* 160**,** 405-9.
SHAHNAVAZ, S. A., REGEZI, J. A., BRADLEY, G., DUBE, I. D. & JORDAN, R. C. 2000. p53 gene mutations in sequential oral epithelial dysplasias and squamous cell carcinomas. *J Pathol,* 190**,** 417-22.
SHAPIRO, J. A., JACOBS, E. J. & THUN, M. J. 2000. Cigar smoking in men and risk of death from tobacco-related cancers. *J Natl Cancer Inst,* 92**,** 333-7.
SHAREEF, M. M., BROWN, B., SHAJAHAN, S., SATHISHKUMAR, S., ARNOLD, S. M., MOHIUDDIN, M., AHMED, M. M. & SPRING, P. M. 2008. Lack of P-glycoprotein expression by low-dose fractionated radiation results from loss of nuclear factor-kappaB and NF-Y activation in oral carcinoma cells. *Mol Cancer Res,* 6**,** 89-98.
SHAY, J. W. & RONINSON, I. B. 2004. Hallmarks of senescence in carcinogenesis and cancer therapy. *Oncogene,* 23**,** 2919-33.
SHEARD, M. A., ULDRIJAN, S. & VOJTESEK, B. 2003. Role of p53 in regulating constitutive and X-radiation-inducible CD95 expression and function in carcinoma cells. *Cancer Res,* 63**,** 7176-84.
SHEARD, M. A., VOJTESEK, B., JANAKOVA, L., KOVARIK, J. & ZALOUDIK, J. 1997. Up-regulation of Fas (CD95) in human p53wild-type cancer cells treated with ionizing radiation. *Int J Cancer,* 73**,** 757-62.
SHEIKH, M. S., BURNS, T. F., HUANG, Y., WU, G. S., AMUNDSON, S., BROOKS, K. S., FORNACE, A. J., JR. & EL-DEIRY, W. S. 1998. p53-dependent and -independent regulation of the death receptor KILLER/DR5 gene expression in response to genotoxic stress and tumor necrosis factor alpha. *Cancer Res,* 58**,** 1593-8.
SHIMIZU, K., INOUE, H., SAITOH, M., OHTSUKI, N., ISHIDA, H., MAKINO, K., AMATSU, M. & NIBU, K. 2006. Distribution and impact of lymph node metastases in oropharyngeal cancer. *Acta Otolaryngol,* 126**,** 872-7.
SHIMURA T, K. S., OCHIAI Y, NAKAGAWA H, KUWAHARA Y, TAKAI Y, KOBAYASHI J, KOMATSU K, FUKUMOTO M. 2010. Acquired radioresistance of human tumor cells by DNA-PK/AKT/GSK3beta-mediated cyclin D1 overexpression. *Oncogene,* 29**,** 4826-37.
SHINOMIYA, N. 2001. New concepts in radiation-induced apoptosis: 'premitotic apoptosis' and 'postmitotic apoptosis'. *J Cell Mol Med,* 5**,** 240-53.
SHKLAR, G. 1972. Experimental oral pathology in the Syrian hamster. *Prog Exp Tumor Res,* 16**,** 518-38.
SILVA, P., HOMER, J. J., SLEVIN, N. J., MUSGROVE, B. T., SLOAN, P., PRICE, P. & WEST, C. M. 2007. Clinical and biological factors affecting response to radiotherapy in patients with head and neck cancer: a review. *Clin Otolaryngol,* 32**,** 337-45.
SILVER, C. E., BEITLER, J. J., SHAHA, A. R., RINALDO, A. & FERLITO, A. 2009. Current trends in initial management of laryngeal cancer: the declining use of open surgery. *Eur Arch Otorhinolaryngol,* 266**,** 1333-52.
SINGH, H. P., KUMAR, P., AGGARWAL, P., GOEL, R. 2012. *De-novo* squamous cell carcinoma of an edentulous ridge. *Clinical Cancer Investigation Journal,* 1**,** 83-85.
SKINNER, H. D., SANDULACHE, V. C., OW, T. J., MEYN, R. E., YORDY, J. S., BEADLE, B. M., FITZGERALD, A. L., GIRI, U., ANG, K. K. & MYERS, J. N. 2012. TP53 disruptive mutations lead to head and neck cancer treatment failure through inhibition of radiation-induced senescence. *Clin Cancer Res,* 18**,** 290-300.
SMEETS, S. J., VAN DER PLAS, M., SCHAAIJ-VISSER, T. B., VAN VEEN, E. A., VAN MEERLOO, J., BRAAKHUIS, B. J., STEENBERGEN, R. D. & BRAKENHOFF, R. H. 2011. Immortalization of oral keratinocytes by functional inactivation of the p53 and pRb pathways. *Int J Cancer,* 128**,** 1596-605.

SMITH, L. P. & THOMAS, G. R. 2006. Animal models for the study of squamous cell carcinoma of the upper aerodigestive tract: a historical perspective with review of their utility and limitations. Part A. Chemically-induced de novo cancer, syngeneic animal models of HNSCC, animal models of transplanted xenogeneic human tumors. *Int J Cancer,* 118**,** 2111-22.

SNOW, G. B., ANNYAS, A. A., VAN SLOOTEN, E. A., BARTELINK, H. & HART, A. A. 1982. Prognostic factors of neck node metastasis. *Clin Otolaryngol Allied Sci,* 7**,** 185-92.

SOBEK, D., YOUNG, A. M., GRAY, M. L. & SENTURIA, S. D. A microfabricated flow chamber for optical measurements in fluids. Micro Electro Mechanical Systems, 1993, MEMS '93, Proceedings An Investigation of Micro Structures, Sensors, Actuators, Machines and Systems. IEEE., 7-10 Feb 1993 1993. 219-224.

SOBIN, L., GOSPODAROWICZ, M., WITTEKIND, C. 2010. *TNM Classification of Malignant Tumours,* Oxford, Blackwell.

SOLT, D. B., POLVERINI, P. J., RAY, S., FEI, Y. & BISWAS, D. K. 1988. Early neoplastic commitment of hamster buccal pouch epithelium exposed biweekly to 7,12-dimethylbenz[a]anthracene. *Carcinogenesis,* 9**,** 2173-7.

SOUSSI, T. & BEROUD, C. 2001. Assessing TP53 status in human tumours to evaluate clinical outcome. *Nat Rev Cancer,* 1**,** 233-40.

SOUSSI, T. & LOZANO, G. 2005. p53 mutation heterogeneity in cancer. *Biochem Biophys Res Commun,* 331**,** 834-42.

SPRING, P. M., ARNOLD, S. M., SHAJAHAN, S., BROWN, B., DEY, S., LELE, S. M., VALENTINO, J., JONES, R., MOHIUDDIN, M. & AHMED, M. M. 2004. Low dose fractionated radiation potentiates the effects of taxotere in nude mice xenografts of squamous cell carcinoma of head and neck. *Cell Cycle,* 3**,** 479-85.

SQUIRES, T. M. & QUAKE, S. R. 2005. Microfluidics: Fluid physics at the nanoliter scale. *Reviews of Modern Physics,* 77**,** 977-1026.

SRINIVASAN, M., SUDHEER, A. R., RAJASEKARAN, K. N. & MENON, V. P. 2008. Effect of curcumin analog on gamma-radiation-induced cellular changes in primary culture of isolated rat hepatocytes in vitro. *Chem Biol Interact,* 176**,** 1-8.

STAFFORD, N. D. 2008. Aetiology of Head and Neck Cancer. *In:* GLEESON, M., BROWNING, G.G., BURTON, M.J., CLARKE, R., HIBBERT, J., JONES, N.S., LUND, V.J., LUXON, L.M., WATKINSON, J.C. (ed.) *Scott-Brown's Otorhinolaryngology, Head and Neck Surgery.* London: Hodder Arnold.

STAUSBOL-GRON, B., BENTZEN, S. M., JORGENSEN, K. E., NIELSEN, O. S., BUNDGAARD, T. & OVERGAARD, J. 1999. In vitro radiosensitivity of tumour cells and fibroblasts derived from head and neck carcinomas: mutual relationship and correlation with clinical data. *Br J Cancer,* 79**,** 1074-84.

STEIN, G. H. & DULIC, V. 1995. Origins of G1 arrest in senescent human fibroblasts. *Bioessays,* 17**,** 537-43.

STEINER, M. S., WANG, Y., ZHANG, Y., ZHANG, X. & LU, Y. 2000. p16/MTS1/INK4A suppresses prostate cancer by both pRb dependent and independent pathways. *Oncogene,* 19**,** 1297-306.

STENSON, K. M., HUO, D., BLAIR, E., COHEN, E. E., ARGIRIS, A., HARAF, D. J. & VOKES, E. E. 2006. Planned post-chemoradiation neck dissection: significance of radiation dose. *Laryngoscope,* 116**,** 33-6.

STONE, H. A. & KIM, S. 2001. Microfluidics: Basic issues, applications, and challenges. *AIChE Journal,* 47**,** 1250-1254.

STORCHOVA, Z. & PELLMAN, D. 2004. From polyploidy to aneuploidy, genome instability and cancer. *Nat Rev Mol Cell Biol,* 5**,** 45-54.

STRYKER, J. A. 2007. Science to practice: why is the liver a radiosensitive organ? *Radiology,* 242**,** 1-2.
STUSCHKE, M., BUDACH, V., BUDACH, W., FELDMANN, H. J. & SACK, H. 1992. Radioresponsiveness, sublethal damage repair and stem cell rate in spheroids from three human tumor lines: comparison with xenograft data. *Int J Radiat Oncol Biol Phys,* 24**,** 119-26.
STUSCHKE, M., BUDACH, V., STUBEN, G., STREFFER, C. & SACK, H. 1995. Heterogeneity in the fractionation sensitivities of human tumor cell lines: studies in a three-dimensional model system. *Int J Radiat Oncol Biol Phys,* 32**,** 395-408.
SU, Y., MEADOR, J.A., GEARD, C.R., BALAJEE, A.S. 2009. Analysis of ionizing radiation-induced DNA damage and repair in three-dimensional human skin model system. *Exp Dermatol,* 19**,** 16-22.
SUGRUE, M. M., SHIN, D. Y., LEE, S. W. & AARONSON, S. A. 1997. Wild-type p53 triggers a rapid senescence program in human tumor cells lacking functional p53. *Proc Natl Acad Sci U S A,* 94**,** 9648-53.
SUIT, H. D., ZIETMAN, A., TOMKINSON, K., RAMSAY, J., GERWECK, L. & SEDLACEK, R. 1990. Radiation response of xenografts of a human squamous cell carcinoma and a glioblastoma multiforme: a progress report. *Int J Radiat Oncol Biol Phys,* 18**,** 365-73.
SUTHERLAND, R. M. 1988. Cell and environment interactions in tumor microregions: the multicell spheroid model. *Science,* 240**,** 177-84.
SUZUKI, K., MORI, I., NAKAYAMA, Y., MIYAKODA, M., KODAMA, S. & WATANABE, M. 2001. Radiation-induced senescence-like growth arrest requires TP53 function but not telomere shortening. *Radiat Res,* 155**,** 248-253.
SWEENY, L., LIU, Z., LANCASTER, W., HART, J., HARTMAN, Y. E. & ROSENTHAL, E. L. 2012. Inhibition of fibroblasts reduced head and neck cancer growth by targeting fibroblast growth factor receptor. *Laryngoscope,* 122**,** 1539-44.
TAE, K., JIN, B. J., JI, Y. B., JEONG, J. H., CHO, S. H. & LEE, S. H. 2011. The role of laryngopharyngeal reflux as a risk factor in laryngeal cancer: a preliminary report. *Clin Exp Otorhinolaryngol,* 4**,** 101-4.
TAKAHASHI, R., SONODA, H., TABATA, Y. & HISADA, A. 2010. Formation of hepatocyte spheroids with structural polarity and functional bile canaliculi using nanopillar sheets. *Tissue Eng Part A,* 16**,** 1983-95.
TAKAYAMA, S., MCDONALD, J. C., OSTUNI, E., LIANG, M. N., KENIS, P. J. A., ISMAGILOV, R. F. & WHITESIDES, G. M. 1999. Patterning cells and their environments using multiple laminar fluid flows in capillary networks. *Proceedings of the National Academy of Sciences,* 96**,** 5545-5548.
TAKAYAMA, S., OSTUNI, E., LEDUC, P., NARUSE, K., INGBER, D. E. & WHITESIDES, G. M. 2001a. Laminar flows: Subcellular positioning of small molecules. *Nature,* 411**,** 1016-1016.
TAKAYAMA, S., OSTUNI, E., LEDUC, P., NARUSE, K., INGBER, D. E. & WHITESIDES, G. M. 2003. Selective chemical treatment of cellular microdomains using multiple laminar streams. *Chem Biol,* 10**,** 123-30.
TAKAYAMA, S., OSTUNI, E., QIAN, X., MCDONALD, J. C., JIANG, X., LEDUC, P., WU, M. H., INGBER, D. E. & WHITESIDES, G. M. 2001b. Topographical Micropatterning of Poly(dimethylsiloxane) Using Laminar Flows of Liquids in Capillaries. *Advanced Materials,* 13**,** 570-574.
TAN, S. J., LAKSHMI, R. L., CHEN, P., LIM, W. T., YOBAS, L. & LIM, C. T. 2010. Versatile label free biochip for the detection of circulating tumor cells from peripheral blood in cancer patients. *Biosens Bioelectron,* 26**,** 1701-5.

TANAKA, T., OHKUBO, S., TATSUNO, I. & PRIVES, C. 2007. hCAS/CSE1L associates with chromatin and regulates expression of select p53 target genes. *Cell,* 130**,** 638-50.
TANG, K., LI, Y., ZHANG, Z., GU, Y., XIONG, Y., FENG, G., HE, L. & QIN, S. 2010. The PstI/RsaI and DraI polymorphisms of CYP2E1 and head and neck cancer risk: a meta-analysis based on 21 case-control studies. *BMC Cancer,* 10**,** 575.
TAYLOR, R. C., CULLEN, S. P. & MARTIN, S. J. 2008. Apoptosis: controlled demolition at the cellular level. *Nat Rev Mol Cell Biol,* 9**,** 231-241.
TERHAARD, C. H., HORDIJK, G. J. & RAVASZ, L. A. 1992. Treatment of advanced laryngeal cancer (T3-4). *Acta Otorhinolaryngol Belg,* 46**,** 197-212.
THOMPSON, L. D. R. 2006. Head and Neck Pathology. *In:* THOMPSON, L. D. R. (ed.) *Foundations in Diagnostic Pathology Series.* Philadelphia: Churchill Livingstone Elsevier.
THURNHER, D., BAKROEVA, M., SCHUTZ, G., PELZMANN, M., FORMANEK, M., KNERER, B. & KORNFEHL, J. 2001. Non-steroidal anti-inflammatory drugs induce apoptosis in head and neck cancer cell lines. *Acta Otolaryngol,* 121**,** 957-62.
TIMMER, J. C. & SALVESEN, G. S. 2007. Caspase substrates. *Cell Death Differ,* 14**,** 66-72.
TOBITA, T., IZUMI, K. & FEINBERG, S. E. 2010. Development of an in vitro model for radiation-induced effects on oral keratinocytes. *Int J Oral Maxillofac Surg,* 39**,** 364-70.
TOPALOGLU, S., ABBASOGLU, O., AYHAN, A., SOKMENSUER, C. & KILINC, K. 2003. Antiapoptotic and protective effects of roscovitine on ischemia-reperfusion injury of the rat liver. *Liver Int,* 23**,** 300-7.
TORRENTE, M. C., RODRIGO, J. P., HAIGENTZ, M., JR., DIKKERS, F. G., RINALDO, A., TAKES, R. P., OLOFSSON, J. & FERLITO, A. 2011. Human papillomavirus infections in laryngeal cancer. *Head Neck,* 33**,** 581-6.
TOSTOES, R. M., LEITE, S. B., MIRANDA, J. P., SOUSA, M., WANG, D. I., CARRONDO, M. J. & ALVES, P. M. 2011. Perfusion of 3D encapsulated hepatocytes--a synergistic effect enhancing long-term functionality in bioreactors. *Biotechnol Bioeng,* 108**,** 41-9.
TOUSTRUP, K., SORENSEN, B. S., NORDSMARK, M., BUSK, M., WIUF, C., ALSNER, J. & OVERGAARD, J. 2011. Development of a hypoxia gene expression classifier with predictive impact for hypoxic modification of radiotherapy in head and neck cancer. *Cancer Res,* 71**,** 5923-31.
TS'AO, C., MOLTENI, A. & TAYLOR, J. M. 1996. Injury-specific cytotoxic response of tumor cells and endothelial cells. *Pathol Res Pract,* 192**,** 1-9.
TUBIANA, M. 1988. Repopulation in human tumors. A biological background for fractionation in radiotherapy. *Acta Oncol,* 27**,** 83-8.
TUYNS, A. J., ESTEVE, J., RAYMOND, L., BERRINO, F., BENHAMOU, E., BLANCHET, F., BOFFETTA, P., CROSIGNANI, P., DEL MORAL, A., LEHMANN, W. & ET AL. 1988. Cancer of the larynx/hypopharynx, tobacco and alcohol: IARC international case-control study in Turin and Varese (Italy), Zaragoza and Navarra (Spain), Geneva (Switzerland) and Calvados (France). *Int J Cancer,* 41**,** 483-91.
UNO, M., OTSUKI, T., KUREBAYASHI, J., SAKAGUCHI, H., ISOZAKI, Y., UEKI, A., YATA, K., FUJII, T., HIRATSUKA, J., AKISADA, T., HARADA, T. & IMAJO, Y. 2001. Anti-HER2-antibody enhances irradiation-induced growth inhibition in head and neck carcinoma. *Int J Cancer,* 94**,** 474-9.
VAKEVAINEN, S., TILLONEN, J., AGARWAL, D. P., SRIVASTAVA, N. & SALASPURO, M. 2000. High salivary acetaldehyde after a moderate dose of alcohol in ALDH2-deficient subjects: strong evidence for the local carcinogenic action of acetaldehyde. *Alcohol Clin Exp Res,* 24**,** 873-7.

VAKIFAHMETOGLU, H., OLSSON, M. & ZHIVOTOVSKY, B. 2008. Death through a tragedy: mitotic catastrophe. *Cell Death Differ,* 15**,** 1153-62.
VAN DER RIET, P., NAWROZ, H., HRUBAN, R. H., CORIO, R., TOKINO, K., KOCH, W. & SIDRANSKY, D. 1994. Frequent loss of chromosome 9p21-22 early in head and neck cancer progression. *Cancer Res,* 54**,** 1156-8.
VAN DYCK, E., STASIAK, A. Z., STASIAK, A. & WEST, S. C. 1999. Binding of double-strand breaks in DNA by human Rad52 protein. *Nature,* 398**,** 728-31.
VERMEER, D. W., SPANOS, W. C., VERMEER, P. D., BRUNS, A. M., LEE, K. M. & LEE, J. H. 2013. Radiation-induced loss of cell surface CD47 enhances immune-mediated clearance of human papillomavirus-positive cancer. *Int J Cancer,* 133**,** 120-9.
VISAPAA, J. P., GOTTE, K., BENESOVA, M., LI, J., HOMANN, N., CONRADT, C., INOUE, H., TISCH, M., HORRMANN, K., VAKEVAINEN, S., SALASPURO, M. & SEITZ, H. K. 2004. Increased cancer risk in heavy drinkers with the alcohol dehydrogenase 1C*1 allele, possibly due to salivary acetaldehyde. *Gut,* 53**,** 871-6.
VORMITTAG, L., LAMM, W., EROVIC, B. M., CZEMBIREK, C., KORNEK, G. & THURNHER, D. 2005. Expression levels of Akt in nimesulide-treated squamous carcinoma cell lines of the head and neck. *Oncol Rep,* 13**,** 207-10.
VOS, M. D., MARTINEZ, A., ELAM, C., DALLOL, A., TAYLOR, B. J., LATIF, F. & CLARK, G. J. 2004. A role for the RASSF1A tumor suppressor in the regulation of tubulin polymerization and genomic stability. *Cancer Res,* 64**,** 4244-50.
WALKER, G. M., ZERINGUE, H. C. & BEEBE, D. J. 2004. Microenvironment design considerations for cellular scale studies. *Lab Chip,* 4**,** 91-7.
WALSH, C. L., BABIN, B. M., KASINSKAS, R. W., FOSTER, J. A., MCGARRY, M. J. & FORBES, N. S. 2009. A multipurpose microfluidic device designed to mimic microenvironment gradients and develop targeted cancer therapeutics. *Lab Chip,* 9**,** 545-54.
WANG, X. 2001. The expanding role of mitochondria in apoptosis. *Genes Dev,* 15**,** 2922-33.
WANG, Y., JI, P., LIU, J., BROADDUS, R. R., XUE, F. & ZHANG, W. 2009. Centrosome-associated regulators of the G(2)/M checkpoint as targets for cancer therapy. *Mol Cancer,* 8**,** 8.
WARD, R. J. & DIRKS, P. B. 2007. Cancer stem cells: at the headwaters of tumor development. *Annu Rev Pathol,* 2**,** 175-89.
WARRICK, J., MEYVANTSSON, I., JU, J. & BEEBE, D. J. 2007. High-throughput microfluidics: improved sample treatment and washing over standard wells. *Lab Chip,* 7**,** 316-21.
WEAVER, B. A. & CLEVELAND, D. W. 2005. Decoding the links between mitosis, cancer, and chemotherapy: The mitotic checkpoint, adaptation, and cell death. *Cancer Cell,* 8**,** 7-12.
WEIBEL, D. B. & WHITESIDES, G. M. 2006. Applications of microfluidics in chemical biology. *Curr Opin Chem Biol,* 10**,** 584-91.
WEISS, M. H., HARRISON, L. B. & ISAACS, R. S. 1994. Use of decision analysis in planning a management strategy for the stage N0 neck. *Arch Otolaryngol Head Neck Surg,* 120**,** 699-702.
WEN, J., YANG, X., WANG, K., TAN, W., ZHOU, L., ZUO, X., ZHANG, H. & CHEN, Y. 2007. One-dimensional microfluidic beads array for multiple mRNAs expression detection. *Biosens Bioelectron,* 22**,** 2759-62.
WEST, C. M., DAVIDSON, S. E., ROBERTS, S. A. & HUNTER, R. D. 1997. The independence of intrinsic radiosensitivity as a prognostic factor for patient response to radiotherapy of carcinoma of the cervix. *Br J Cancer,* 76**,** 1184-90.

WIJERS, O. B., LEVENDAG, P. C., BRAAKSMA, M. M., BOONZAAIJER, M., VISCH, L. L. & SCHMITZ, P. I. 2002. Patients with head and neck cancer cured by radiation therapy: a survey of the dry mouth syndrome in long-term survivors. *Head Neck,* 24**,** 737-47.

WILLIAMS, P. D., OWENS, C. R., DZIEGIELEWSKI, J., MOSKALUK, C. A., READ, P. W., LARNER, J. M., STORY, M. D., BROCK, W. A., AMUNDSON, S. A., LEE, J. K. & THEODORESCU, D. 2011. Cyclophilin B expression is associated with in vitro radioresistance and clinical outcome after radiotherapy. *Neoplasia,* 13**,** 1122-31.

WITHERS, H. R., TAYLOR, J. M. & MACIEJEWSKI, B. 1988. The hazard of accelerated tumor clonogen repopulation during radiotherapy. *Acta Oncol,* 27**,** 131-46.

WLODKOWIC, D., SKOMMER, J. & DARZYNKIEWICZ, Z. 2010. Cytometry in cell necrobiology revisited. Recent advances and new vistas. *Cytometry A,* 77**,** 591-606.

WOUTERSEN, R. A., APPELMAN, L. M., VAN GARDEREN-HOETMER, A. & FERON, V. J. 1986. Inhalation toxicity of acetaldehyde in rats. III. Carcinogenicity study. *Toxicology,* 41**,** 213-31.

WRIGHT, W. E. & SHAY, J. W. 2001. Cellular senescence as a tumor-protection mechanism: the essential role of counting. *Curr Opin Genet Dev,* 11**,** 98-103.

WU, G. S., BURNS, T. F., MCDONALD, E. R., 3RD, JIANG, W., MENG, R., KRANTZ, I. D., KAO, G., GAN, D. D., ZHOU, J. Y., MUSCHEL, R., HAMILTON, S. R., SPINNER, N. B., MARKOWITZ, S., WU, G. & EL-DEIRY, W. S. 1997. KILLER/DR5 is a DNA damage-inducible p53-regulated death receptor gene. *Nat Genet,* 17**,** 141-3.

WYNDER, E. L., COVEY, L. S., MABUCHI, K. & MUSHINSKI, M. 1976. Environmental factors in cancer of the larynx: a second look. *Cancer,* 38**,** 1591-601.

YADAV, A., KUMAR, B., TEKNOS, T. N. & KUMAR, P. 2011. Sorafenib enhances the antitumor effects of chemoradiation treatment by downregulating ERCC-1 and XRCC-1 DNA repair proteins. *Mol Cancer Ther,* 10**,** 1241-51.

YAMADA, H. Y. & GORBSKY, G. J. 2006. Spindle checkpoint function and cellular sensitivity to antimitotic drugs. *Mol Cancer Ther,* 5**,** 2963-9.

YANG, X., ZHAO, X., ZUO, X., WANG, K., WEN, J. & ZHANG, H. 2009. Nucleic acids detection using cationic fluorescent polymer based on one-dimensional microfluidic beads array. *Talanta,* 77**,** 1027-31.

YAO, M., GRAHAM, M. M., HOFFMAN, H. T., SMITH, R. B., FUNK, G. F., GRAHAM, S. M., DORNFELD, K. J., SKWARCHUK, M., MENDA, Y. & BUATTI, J. M. 2004. The role of post-radiation therapy FDG PET in prediction of necessity for post-radiation therapy neck dissection in locally advanced head-and-neck squamous cell carcinoma. *Int J Radiat Oncol Biol Phys,* 59**,** 1001-10.

YASUMOTO, J., IMAI, Y., TAKAHASHI, A., OHNISHI, K., YUKI, K., KIRITA, T. & OHNISHI, T. 2003. Analysis of apoptosis-related gene expression after X-ray irradiation in human tongue squamous cell carcinoma cells harboring wild-type or mutated p53 gene. *J Radiat Res,* 44**,** 41-5.

YOKOYAMA, A., MURAMATSU, T., OHMORI, T., YOKOYAMA, T., OKUYAMA, K., TAKAHASHI, H., HASEGAWA, Y., HIGUCHI, S., MARUYAMA, K., SHIRAKURA, K. & ISHII, H. 1998. Alcohol-related cancers and aldehyde dehydrogenase-2 in Japanese alcoholics. *Carcinogenesis,* 19**,** 1383-7.

YOUNG, E. W. & BEEBE, D. J. 2010. Fundamentals of microfluidic cell culture in controlled microenvironments. *Chem Soc Rev,* 39**,** 1036-48.

YU, H., ALEXANDER, C. M. & BEEBE, D. J. 2007. Understanding microchannel culture: parameters involved in soluble factor signaling. *Lab Chip,* 7**,** 726-730.

ZAMYATKINA, O. G. 1962. Biosynthesis of serum albumin in rats in radiation sickness. *Radiobiologiia,* 2**,** 685.
ZAMYATKINA, O. G. 1965. Causes of liver serum albumin synthesis in rats with acute radiation sickness. *Fed Proc Transl Suppl.,* 24**,** 693-5.
ZAVODNIK LB, K. R., ARTSUKEVICH AN, CHUMACHENKO SS, SHEIBAK VM, OVCHINNIKOV VA, BUKO VU. 2003. Dynamics of structural changes in rat liver after single dose of gamma-irradiation. *Radiats Biol Radioecol,* 43**,** 618-24.
ZHAN, Q., FAN, S., BAE, I., GUILLOUF, C., LIEBERMANN, D. A., O'CONNOR, P. M. & FORNACE, A. J., JR. 1994. Induction of bax by genotoxic stress in human cells correlates with normal p53 status and apoptosis. *Oncogene,* 9**,** 3743-51.
ZHANG, H. 2007. Molecular signaling and genetic pathways of senescence: Its role in tumorigenesis and aging. *J Cell Physiol,* 210**,** 567-74.
ZHANG, H., YANG, X., WANG, K., TAN, W., LI, H., ZUO, X. & WEN, J. 2008. On-chip oligonucleotide ligation assay using one-dimensional microfluidic beads array for the detection of low-abundant DNA point mutations. *Biosens Bioelectron,* 23**,** 945-51.
ZHANG, Q., SHI, S., YEN, Y., BROWN, J., TA, J. Q. & LE, A. D. 2010. A subpopulation of CD133(+) cancer stem-like cells characterized in human oral squamous cell carcinoma confer resistance to chemotherapy. *Cancer Lett,* 289**,** 151-60.
ZHANG, X., ZHOU, X., CHEN, R. & ZHANG, H. 2012. Radiosensitization by inhibiting complex I activity in human hepatoma HepG2 cells to X-ray radiation. *J Radiat Res,* 53**,** 257-63.
ZHAO, B., MOORE, J. S. & BEEBE, D. J. 2002. Principles of Surface-Directed Liquid Flow in Microfluidic Channels. *Analytical Chemistry,* 74**,** 4259-4268.
ZHAO, J. D., JIANG, G. L., HU, W. G., XU, Z. Y. & WANG, C. F. 2009. Hepatocyte regeneration after partial liver irradiation in rats. *Exp Toxicol Pathol,* 61**,** 511-8.
ZHEN, W., KARNELL, L. H., HOFFMAN, H. T., FUNK, G. F., BUATTI, J. M. & MENCK, H. R. 2004. The National Cancer Data Base report on squamous cell carcinoma of the base of tongue. *Head Neck,* 26**,** 660-74.
ZHENG, B., TICE, J. D., ROACH, L. S. & ISMAGILOV, R. F. 2004a. A droplet-based, composite PDMS/glass capillary microfluidic system for evaluating protein crystallization conditions by microbatch and vapor-diffusion methods with on-chip X-ray diffraction. *Angew Chem Int Ed Engl,* 43**,** 2508-11.
ZHENG, S., MA, X., ZHANG, L., GUNN, L., SMITH, M. T., WIEMELS, J. L., LEUNG, K., BUFFLER, P. A. & WIENCKE, J. K. 2004b. Hypermethylation of the 5' CpG island of the FHIT gene is associated with hyperdiploid and translocation-negative subtypes of pediatric leukemia. *Cancer Res,* 64**,** 2000-6.
ZHOU, M., GU, L., LI, F., ZHU, Y., WOODS, W. G. & FINDLEY, H. W. 2002. DNA damage induces a novel p53-survivin signaling pathway regulating cell cycle and apoptosis in acute lymphoblastic leukemia cells. *J Pharmacol Exp Ther,* 303**,** 124-31.
ZIOBER, B. L., MAUK, M. G., FALLS, E. M., CHEN, Z., ZIOBER, A. F. & BAU, H. H. 2008. Lab-on-a-chip for oral cancer screening and diagnosis. *Head Neck,* 30**,** 111-21.
ZOU, J., QIAO, X., YE, H., YANG, Y., ZHENG, X., ZHAO, H. & LIU, S. 2008. Antisense inhibition of ATM gene enhances the radiosensitivity of head and neck squamous cell carcinoma in mice. *J Exp Clin Cancer Res,* 27**,** 56.